“ROLE OF SOX9 TRANSCRIPTION FACTOR IN HUMAN BREAST EPITHELIAL CELLS, BREAST CANCER STEM CELLS AND TAMOXIFEN RESISTANCE”

Doctoral thesis

Giacomo Domenici

This work was carried out in the Cell Biology and Stem Cell Unit at the Centre for Cooperative Researches (CIC bioGUNE)

2017

Supervisor: Dr MdM Vivanco

Supported by:

Index

ACKNOWLEDGEMENTS

First of all, I would like to thank Dr. María Vivanco for giving me the opportunity to pursue my PhD thesis in her lab as well as for help, guidance and for letting me to freely explore scientific questions.

A special thanks also goes to Dr. Miriam Rábano, for her excellent technical assistance and friendship.

A thank to all the women who have donated their tissues (both healthy and tumorous) for my scientific experiments.

I would like to thank also the amazing women from ACAMBI (Asociación de cancer de mama de Bilbao) for their helpful activities towards breast cancer patients and for supporting our laboratory.

Thanks also to all my labmates too! It was a pleasure for me to spend time together at CICbioGUNE!(More or less in chronological order!!). Bruno, Oihana, Valentine, Marco, Lucia, Nora, Amelie, Irantzu, Virginia, Esti, Eder, Inma, So Young, Iskander, Teresa and Onintza.

Special thanks also to Dr. Kypta for his critical and constructive help and guidance. A special thanks also goes to other people working at CICbioGUNE such as Cora, Encarni, Nuria, Monica, Vidal, Itziar, Edurne, Veronica, Georgina, Natalia, Lorea, Leire and Arkaitz. A special mention is for my lovely friend Patri!!

I would like to acknowledge here all the Italian (Sofia, Carola, Natascia, Jessica, Francesca, Imma, Michele, Pierluigi, Elvira and Marilena) and Spanish (Cristina, Sandra and Julia) students I had in my lab! (Hopefully I didn't forget anyone…!).

A special thanks also to great people that have contributed in different manners to support and help me during these years: my parents, grandparents, brothers, Aitor, Galder, Phillip, Lucia, Margherita, Sergio and Arminda.

Special thanks to my friend Francesco for letting me to use his painting "Afròs" as Thesis cover and my brother Angelo for cover design.

Abbreviations

ABCG-2 – ATP-binding cassette, sub-family G2
ALDH – Aldehyde Dehydrogenase
APS – Ammonium Persulfate
AREG – Anphiregulin
BAA – BODIPY amino acetate
bFGF – basic Fibroblast Growth Factor
BSA – Bovine Serum Albumin
CALLA – Common Acute Lymphoblastic Leukaemia Antigen
CD – Cluster of Differentiation
cDNA – complementary Deoxyribonucleic Acid
ChIP Chromatin Immunoprecipitation
CRD – Cistein Rich Domain
CSCs – Cancer Stem Cells
DAB – 3,3'-diaminobenzidine
DAPI – 4',6-diamidino-2-phenylindole
DBD – DNA Binding Domain
DCIS – Ductal Carcinoma *In Situ*
DEAB – Diethylaminobenzaldehyde
DNA – Deoxyribonucleic Acid
dNTP – Deoxynucleoside triphosphate
DTT -– Dithiothreitol
DVL - Dishevelled
ECL – Enhanced Chemiluminescence
EGF – Epidermal Growth Factor
EGFR – Epidermal Growth Factor Receptor
EMA – Epithelial Membrane Antigen
EMT – Epithelial-Mesenchymal Transition
EpCAM – Epithelial Cell Adhedion Molecule
ER – Estrogen Receptor
ERE – Estrogen-Responsive Element
ES – Embryonic Stem
ESA – Epithelial Specific Antigen
FACS – Fluorescence-Activated Cell Sorting
FBS – Fetal Bovine Serum
FITC – Fluorescein Isothiocyanate
FWD – Forward
FZ – Frizzled
GFP – Green Fluorescent Protein
GSEA – Gene Set Enrichment Analysis
GSK3 – Glicogen Syntase Kinase 3
HBMECs – Human MammaryBreast Epithelial Cells
HDAC – Histone deacetylase
HEPES – 4-(2-hydroxyethyl)-1-piperazineethansulfonic acid

HER2 – Receptor tyrosine-protein kinase erbB-2
HRT – Hormone Replacement Therapy
HSC Hematopoietic Stem Cells
IGF-R1 Insulin Growth Factor Receptor 1
IgGg – Immunoglobulin G
kDa – kilodalton
Ki67 – Antigen Ki67
Lin – Lineage
MAPKs Mitogen associated protein Kinases
MDR-1 Multidrug Resistance 1
MMTV-LTR – Mouse Mammary Tumour Virus
mRNA – Messenger Ribonucleic Acid
NLS – Nuclear localization sequence
P4 – Progesterone
PBS – Phosphate-Buffered Saline
PCR – Polymerase Chain Reaction
PDGF – Plateled derived Growth Factor
PDX – Patient Derived Xenograft
PE – Phycoerythrin
PKA – Protein Kinase A
PR – Progesterone Receptor
RANK – Receptor Activator of Nuclear Factor κ B
RANKL – Receptor Activator of Nuclear Factor κ B Ligand
REV – Reverse
RNA – Ribonucleic Acid
RPM – Revolution Per Minute
SC – Stem Cell
SD – Standard Deviation
SDS – Sodium Dodecyl Sulphate
SERMs – Selective ER Modulators
SHH – Sonic Hedgehog
shRNA – short hairpin RNA
siRNA – small interference RNA
SP – Side Population
TBS – Tris Buffered Saline
TBST– Tris Buffered Saline with Tween 20
TDLU – Terminal Duct Lobular Unit
TEMED – Tetramethylethylenediamine
TF – Transcription Factors
TNBCs – Triple Negative Breast Cancer Cells
Tris – Tris(hydroxymethyl)aminomethane
Tween 20 – Polyxyethylene (20) sorbitan monolaurate
Wnt - Wingless-type MMTV integration site family - Long Terminal Repeat

Summary

The human mammary gland is a dynamic organ that undergoes cycles of proliferation and involution. The ability of being such a plastic organ is due to the presence of adult stem cells that are able to self-renew and differentiate, giving rise to the whole mammary gland lineage.

According to the Breast Cancer Stem Cells hypothesis (CSCs), breast cancer arises from normal stem cells that undergo oncogenic transformation. There are also increasing evidences that indicate the presence of cells with cancer stem cells features in other solid tumors as colon, lung and prostate as well as in leukemia. Solid tumors are then characterized by strong heterogeneity, in which there are cells with stem/progenitor cells features (able to self-renew and differentiate as well as quiescent and resistant to pharmacological treatment and radiotherapy) and proliferating differentiated cells that are easily targeted by current therapies. Then, when a cancer is exposed to radio and chemotherapy, the first ones survive and give rise to recurrence of the primary tumors, while the latter are eliminated.

As a consequence, it is very important to study and identify molecular targets and pathways that are up-regulated in these cells and that maintain them, hoping to definitely eradicate cancers.

SOXs are transcription factors implicated in the maintenance of stem/progenitor cells in different tissues. Our lab identified Sox2 as a key player of tamoxifen resistance in breast cancer cells and in the maintenance of breast cancer stem cells. One of the Sox factor that resulted induced in Sox2 overexpressing cells was Sox9, that recently it has been associated with mammary stem cells state in the mouse mammary gland. So we sought to determine whether Sox9 was relevant in normal human mammary epithelial stem/progenitor cells as well as in CSCs

In normal mammary epithelial cells context, our studies demonstrated that Sox9 is a marker of $CD49f^+/EpCAM^+/ALDEFLUOR^+$ (aldehyde-dehydrogenase positive) luminal progenitor cells and that silencing of Sox9 is able to reduce progenitor markers and $ALDEFLUOR^+$ cells as well as cell proliferation, luminal differentiation and growth in matrigel.

In breast cancer cells, Sox9 resulted to be important for cell clonogenicity and growth in anchorage-independent condition as well as for cell invasion. Sox9 depletion in luminal breast cancer cells caused a reduction in ALDEFLUOR+ cells as well as mammospheres formation. Sox9 is induced in ER^- primary breast cancers and in ER^- breast cancer cell lines. Estrogen treatment reduced Sox9 expression, which may explain, in part, the increased Sox9 expression os in ER^- breast cancer over ER^+.

In addition, in an *in vitro* model of tamoxifen resistance we observed an increased Sox9 expression compared to control cells and, interestingly, these cells are enriched in cytoplasmic Sox9. We found similar result in a cohort of primary and recurrent breast cancer patient tissues after tamoxifen treatment. Finally, we showed also evidences for a Sox2-Sox9 positive activation loop that turn into the stimulation of the Wnt pathway in breast cancer cells.

In conclusion, Sox9 marks both normal progenitor cells in the human mammary gland and $ALDEFLUOR^+$ in luminal breast cancer cells, and Sox2/Sox9/Wnt axis may represents a useful target for breast cancer treatment.

Resumen

La glándula mamaria humana es un órgano dinámico que durante su desarrollo post natal es capaz de hacer ciclos de proliferación e involución. Dicha plasticidad es debida a la presencia de células madre adultas que son capaces de auto-renovarse y diferenciarse, generando todas las células presentes en la glándula mamaria.

Según la teoría de las células madre tumorales (CSCs), el cáncer de mama se desarrollaría de células madre normales que se transforman oncógenicamente. Hay también muchas evidencias experimentales que indican como células con estas características sean presentes también en otros tumores sólidos como colon, pulmón y próstata, así como en leucemias. Los tumores sólidos son entonces caracterizados de una alta hetereogeneidad, en la cual, hay tanto células con características de células madre y progenidoras (que tienen capacidad de auto-renovarse y diferenciarse, así como ser quiescentes y resistir a tratamientos farmacológicos y radioterápico) y células diferenciadas que son rápidamente eliminadas a través de las terapias. Entonces, cuando un cáncer es expuesto a radio y quimioterapia, las primeras sobreviven y causan recurrencia del tumor primario, mientras las segundas se eliminan

Como consecuencia, es muy importante estudiar e identificar dianas y rutas moleculares que son expresadas e incrementadas en estas células para mantenerlas, con la esperanza de erradicar el cáncer.

Los factores de transcripción SOXs son implicados en el mantenimiento de celulas madre/progenidoras en diferentes tejidos. Nuestro laboratorio ha identificado Sox2 como factor importante en el mantenimiento de la resistencia al tamoxifeno en células de cáncer de mama y en el mantenimiento de células madre de cáncer. Uno de los factores Sox que estaba incrementado en células que expresan altos niveles de Sox2 era Sox9, que recientemente ha sido implicado en el mantenimiento de las células madre de epitelio mamario de ratón. Entonces hemos pensado de investigar la posible implicación de Sox9 en células madre/progenitoras de epitelio mamario humano, así como en células de cáncer de mama.

En el contexto de células epiteliales mamaria humana, nuestros estudios demuestran que Sox9 es un marcador de células progenitoras luminales $CD49f^{+}/EpCAM^{+}/ALDEFLUOR^{+}$ (aldehído-dehydrogenasa positivas) y que el silenciamiento de Sox9 es capaz de reducir la expresión de marcadores de células progenitoras, así como las células $ALDEFLUOR^{+}$ y la proliferación celular, diferenciamiento luminal y crecimiento en matriz extracelular.

En células de cáncer de mama, Sox9 resulta ser importante por la clonogenicidad celular y por el crecimiento en condiciones de falta de adherencia al substrado así como por la invasividad celular. La reducción de Sox9 en células de cáncer de mama luminales causaba una reducción de las células $ALDEFLUOR^{+}$, así como la formación de mamoesferas. Hemos observado que Sox9 está más expresado en tumores y en líneas celulares ER^{-}; el estrógeno es capaz de reducir la expresión de Sox9, lo que podría explicar, en parte, el aumento de expresión de Sox9 en cáncer de mama ER^{-}.

En nuestros modelos en vitro de resistencia al tamoxifeno hemos observado un aumento de expresión de Sox9 en comparación con las células de control y, muy interesante, estas células eran enriquecidas en Sox9 citosólico. Hemos observado un aumento de tinción citosólica en cortes inmunoistoquimico en tejido de pacientes después de tratamiento endocrino. También tenemos evidencias de una regulación positiva entre Sox2 y Sox9 que inducía la estimulación del pathway Wnt en células de cáncer de mama.

En conclusión, Sox9 es un marcador de células progenidoras luminales en la glándula mamaria humana y de las células $ALDEFLUOR^{+}$ en células luminales de mama humana, y el axis Sox2/Sox9/Wnt puede ser una diana interesante en el tratamiento de cáncer de mama

.

Chapter 1: Introduction

1. The human breast

1.1 Structure and cellular composition of the human breast

The mammary gland is a very interesting structure that distinguishes mammals from other animals and its function is milk production to nourish offspring (Inman et al., 2015).

The mammary gland is a complex secretory organ composed of a branching structure of ducts and lobules. These structures present ectodermally derived cells, such as luminal, myoepithelial cells, and mesodermal-derived stromal cells. The ducts are bilayered structures composed of luminal cells, which form organized ducts, surrounded by myoepithelial cells (Parmar and Cunha, 2004).

During lactation, luminal cells from lobules produce milk, which is secreted thanks to the contraction of myoepithelial cells that surround the luminal ducts. It is important to point out that the mammary gland is not only composed of epithelium, but also of different kinds of cells, including macrophages, endothelial cells and fibroblasts. Fibroblasts, in particular, have been identified as important cells in the biology of the mammary gland, because they support mammary gland development *in vitro* and *in vivo* (Parmar and Cunha, 2004). In addition, lobules and ducts in the mammary gland are embedded in adipose tissue, which encloses the mammary epithelial structures.

1.2 Mammary gland development

In all mammals, the mammary gland arises from localized areas of the ventral thick structures of the ventral ectoderm or epidermis. Human and mouse mammary gland structure and development show important differences (Parmar and Cunha, 2004). In mice, mammary buds form by elevation of a structure called “mammary crest” that give rise to the “milk line”, that is a thickening of the epidermis in the midventral area of the embryo. In mouse, there is an elongation of the primary duct, which grows through the mammary fat pad and subsequently form a small-branched ductal tree, which at birth is composed by 15-20 branching ducts. In humans, mammary gland development start at day 35 of embryonal development (4th week) with the proliferation of an epidermal area

in the thoracic region, which extends in two region called “mammary ridges”. At week 6, these areas are mainly present in two thoracic regions that start to proliferate inwards in the surrounding mesenchyme. Between 10 and 12 weeks, during the “budding stage”, epithelial buds sprout from the invading placode, and the buds become lobular and rounded, while the nipple start to form on the superficial epidermis. In this period, these primordial ducts start being surrounded by mesenchymal cells, which differentiate into fibroblasts, smooth muscle cells, endothelial cells and adipocytes.

Subsequently, epithelial and myoepithelial cells start to give rise to main morphological differences, and after 6 months of pregnancy, the structure of the fetal gland is established. This structure remains quiescent until puberty, when hormonal stimuli induce further development and make the mammary gland a functional structure (Parmar and Cunha, 2004).

During puberty, in female, branching become very prominent, with segmental ducts being formed from the primary duct, while in males there is no further development (Howard and Gusterson, 2000). The mammary gland undergoes different cycles of development, growth and involution, and intriguingly, it reaches full development only after birth. In fact, during puberty, under the control of hormones and other stimuli, the ductal epithelium invades the mammary fat pad and gives rise to complex branching morphogenesis (Brisken and O’Malley, 2010). After several rounds of branching and elongation, structures called acini are formed. Structures formed by acini arising from one terminal duct and embedded in surrounding stroma are referred as terminal duct lobular unit (TDLU).

These structures are very different during various stages, being branched during puberty, fully developed during pregnancy and lactation, showing duct dilatation and atrophy during the menopausal stage. Old women show marked atrophy of both ducts and TDLU (Parmar and Cunha, 2004).

Interestingly, in humans, the mammary gland is formed embriologically similarly in male and female, while in male rodent testosterone induces breast bud destruction at E14 (Kratochwil and Schwartz, 1976) while in humans develop similarly between male and female embryological development (Howard and Gusterson, 2000).

During pregnancy, luminal epithelial cells proliferate rapidly in response to circulating hormones, including progesterone and prolactin. After birthchild, the developing secretory alveoli produce milk, which is released in response to the suckling infant. Oxytocin in turn induces the contraction of the myoepithelial cells that surround the ducts, thus moving the milk through the ductal tree and to the nipple (Crowley, 2015).

During the lactation period the breast reaches its maximum developmental stage; during weaning, the lack of milk production stimuli triggers a process of regression of the mammary gland tree, called “involution”, which includes apoptosis and remodelation by proteases (Watson and Kreuzaler, 2011).

2. Ovarian hormones in the mammary gland development

Ovarian hormones, estrogen and progesterone, play an important role in mammary gland development and breast cancer (Stingl, 2011). In premenopausal women, estrogen is produced in the ovaries, while after the menopause these hormones can be produced in brain, bones and adipose tissues, and are called collectively “extragonadal estrogens” (Labrie, 2015).

Ovarian estrogens act on distant organs since they are released in the blood stream, while extragonadal estrogens act mostly in a paracrine manner. The estrogen receptor (ER) is a ligand-activated transcription factor that belongs to the superfamily of steroid hormone and nuclear receptors, and it regulates the expression of a particular subset of target genes through the binding to a specific palindromic sequence called the estrogen-responsive-element (ERE). Using breast cancer cell lines, several ER target genes have been described, for example: PR (Jacobsen and Horwitz, 2012) and PS2 (Jakowlew et al., 1984) and, recently, using whole genome chromatin immunoprecipitation (ChIP) genomic regions bound by ER have been identified (Carroll et al., 2005).

Two different isoforms of ER have been described and cloned: ERα (Green et al., 1986) and ERβ (Kuiper et al., 1996). ERα is expressed in brain, bone, the cardiovascular system, uterus, liver and breast (Nilsson and Gustafsson, 2011). ERβ is also expressed

in many tissues, including kidney, lung, the central nervous system, the cardiovascular system, the immune system, the urogenital tract and the gastrointestinal tract (from now to on, ER refers to ERα, unless stated otherwise).

Both ERs share high homology in the DNA-binding domain and can recognize the same EREs, however, the amino acid conservation is not more than 55% in the ligand-binding domain. As a result, ERβ has lower affinity for 17-β-estradiol, the physiological form of estrogen, than ER (Kuiper et al., 1997).

The ER gene (ESR1) encodes a protein of 595 amino acid residues with a molecular mass of 66 KDa, and it is composed of 6 different structural domains (Fig.1.1) (Kumar et al., 1987). The A/B domain is involved in hormone-independent transcriptional activation (Lees et al., 1989). The C domain is the DNA binding domain (DBD), composed of two zinc-finger domains are responsible for interaction with the DNA. The consensus ERE consists of two AGGTCA inverted repeats separated by three nucleotides (Druege et al., 1986). The D domain contains a 39 aminoacids linker that joins the DBD domain with the ligand binding region (LBD) and, in addition, it contains the nuclear localisation sequence (NLS). The last domain, F, appears to be involved in the interaction with selective estrogen receptor modulators (SERMs) (Goodsell, 2002; Jordan and O'Malley, 2007).

Fig. 1.1 ERα structural domain

ER is expressed by 15-25% of breast luminal cells, and strong immunohistochemical staining can be found in epithelial cells lining ducts and lobules, while stromal and myoepithelial cells are ER negative. Conversely, ERβ shows a more ubiquitous distribution in the human mammary gland; in fact, it is expressed by all luminal, myoepithelial and stromal cells (Speirs et al., 2002).

Surprisingly, despite its wide expression in the mammary gland (Brisken and O'Malley, 2010), ERβ-knockout mice showed only a mild delay in side branching (Antal et al., 2008), while ER knock-out mice (ERα-KO) lack ductal morphogenesis or alveolar development (Bocchinfuso et al., 2000), indicating that the prominent player in mammary gland development is ER and not ERβ.

In the mouse, it has been shown that estrogen can work through the induction of the paracrine factor amphiregulin (AREG), that stimulates cell proliferation, terminal end bud formation and ductal elongation (Ciarloni et al., 2007). In addition, the importance of AREG during mammary gland formation has been highlighted by the fact that $AREG^{-/-}$ epithelial cells transplanted in the mammary fat pad of recipient mice failed to develop a proper mammary gland. AREG is induced by estrogen in breast cancer cell lines and positively contributes to MCF-7 breast cancer cells tumorigenicity *in vivo* (Peterson et al., 2015).

Progesterone (P4) is a key cycling ovarian steroid hormone and has a major role in promoting glandular differentiation of the endometrium. P4 is also sustained at high levels during pregnancy and is required for maintenance of pregnancy (Obr and Edwards, 2012). Progesterone receptor knock-out mice (PR-KO) lack mammary gland development, especially mammary gland branching and alveologenesis (Soyal et al., 2002). Progesterone receptors (PRs) include two proteins (A and B) that are expressed from a single gene, as a result of transcription from two alternative promoters (Kastner et al., 1990). Using mice strains that lack PR-A or PR-B, it has been shown that the receptor involved in mammary gland alveologenesis is PR-B (Mulac-Jericevic et al., 2000).

Jane Visvader laboratory showed that mammary stem cells derived from ovariectomized mice and implanted into cleared fat pad leaded to a remarkable reduced mammary repopulating ability *in vivo* compared to control cells (Asselin-Labat et al., 2010), suggesting that ovarian hormones are very important for mammary stem cells function. Furthermore, when they treated mice with E2, P4 or combination of both, they found that only combination of the hormones was able to expand mammary stem cells.

Nevertheless, letrozol (which reduces estrogen synthesis by aromatase inhibition) did not altered the amount of mammary stem cells in treated mice versus the controls but

their ability to induce mouse fat-pat filling was impaired. Finally, they observed that in mice, during pregnancy, there is an increase in mammary stem cells mostly due to the increased expression of RANKL by luminal cells, which expands stem cells, signaling through RANK, which is expressed by mammary stem cells (Asselin-Labat et al., 2010). RANKL is strongly induced by P4, as well as Wnt4 (Fernandez-Valdivia and Lydon, 2012).

In the human mammary gland, it has been shown that P4 increases cell proliferation of breast progenitor cells (Graham et al., 2009). Collectively, these results claim for a P4 role in mammary stem cells expansion through the RANKL-RANK axis.

3. Breast cancer: epidemiology and risk factors

Breast cancer is the most common cancer in women followed by colorectum and lung cancer, both in developing and developed countries (Ferlay et al., 2010). It is especially common in western and subsaharian countries (Akarolo-Anthony et al., 2010).

Different breast cancer risk factors can be collectively classified as non-preventable and preventable. Non-preventable risk factors are age, sex and hereditary genetic traits (Howell et al., 2014). Breast cancer risk increases with age and, of course, being a woman increases dramatically the possibility of develop a breast cancer. In fact, 99% of breast cancers are diagnosed in women, while the rest account for breast cancers in male (Giordano et al., 2004). Hereditary traits account for 10% of the cases and the 2 most studied genes involved in breast cancer genetic predisposition are BRCA1 and BRCA2 (Engel and Fischer, 2015). The risk of developing breast cancer in patients carrying BRCA1 or BRCA2 mutations is considered to be up to 80% (Narod, 2006).

Early menarche and late menopause are associated with enhanced breast cancer risk, likely due to the increased cycles of exposure to ovarian hormones (Cuzick, 2008). Conversely, early first birth and breast-feeding appeared as protective factors (Manrique Tejedor et al., 2015).

Preventable risk factors are represented by the lack of physical exercise and obesity (Protani et al., 2010). Exposure to hormone replacement therapy (HRT, estrogen plus progestin) in post-menopausal women has been shown to increase breast cancer

risk (Stevenson et al., 2011), Alcohol intake is considered also a risk factor in breast cancer (Parkin et al., 2011) and a study conducted in Denmark predicts a reduction in breast cancer risk under reduced alcohol consumption (Soerjomataram et al., 2010).

Finally, it is still debated whether smoking represents a preventable risk factor (Kispert and McHowat, 2017), but studies demonstrated that smoking increases breast cancer risk, correlating with years of smoking and number of cigarettes smoked (Xue et al., 2011) as well as smoking before first birth (Gaudet et al., 2016).

3.1 Breast cancer classification

Breast cancer is a very heterogeneous disease, characterized by a vast array of molecular profiles. Breakthrough work from Perou and collaborators shed light on this issue, by characterizing breast cancer in 5 main different molecular clusters: Luminal A, Luminal B, HER2 overexpressing, basal and normal-like (Table 1.1) (Perou et al., 2000). Importantly, these gene expression patterns are associated with clinical prognosis (Sørlie et al., 2001).

Luminal A and B are characterized by the expression of estrogen and progesterone receptors (ER and PR), although Luminal B tumors show enhanced proliferative potential. HER-2 overexpressing tumors show HER-2 gene amplification (Slamon et al., 1989). Basal-like tumors express myoepithelial markers, such as vimentin and keratin-5 (K5) and are characterized by poor prognosis compared with the other subtypes. The basal subtypes include triple negative breast cancers (TNBC), which lack expression of ER, PR and HER-2 and it is considered the breast cancer type with the worst prognosis. Recently it has been proposed another kind of molecular classification that sort breast cancer into 10 different molecular subtypes (Curtis et al., 2012).

Group	ER	PR	HER2
Luminal A	+	+	-
Luminal B	+	+	-/+
HER2	-	-	+++
Basal/triple negative	-	-	-

Table 1.1 ER, PR and HER status in different breast cancer subtypes

3.2 Breast cancer treatment

Breast cancer treatment depends on the case but, in general, women with breast cancer are treated by a combination of surgery, radiotherapy, chemo or hormonal therapy. Patient biopsies are screened for ER, PR and HER2 expression as well as p53 and Ki67, a marker of cell proliferation. Classically, breast cancer patients can be stratified according to the stage of the disease (from 0 to 4) (Maughan et al., 2010). Stage 0 represents *in situ* lubular carcinoma, which is a microscopic proliferating lesion. Chemoprevention is applicable at this stage, while ductal carcinoma *in situ* tends to pregress further generating a malignant carcinoma. In this case, surgery and radiation therapy are indicated. Stage 1 is characterized by initial local lymph node metastasis (the so-called “sentinel lymph node”). In this case, breast cancer surgery followed by radiotherapy is often considered as first choice treatment, when the tumor size does not exceed 1 cm in diameter. Stage 2-3 (locally advanced) are more aggressive stages, and chemotherapy, hormone therapy in ER+ patients and anti-HER2 therapy with Trastuzumab (monoclonal antibody against HER2 receptor) is indicated in such cases. The fourth stage is the metastatic one, in which the patient is affected by long distant-metastases. In these cases, 5-year survival is around 23,3%, and generally radiation therapy followed by endocrine therapy combined with chemotherapy is applied (Maughan et al., 2010).

Trastuzumab *plus chemotherapy* is used only in case of HER2+ patients, (Knutson et al., 2016). Bisphosphonates associated with endocrine therapy, radiation and chemotherapy may ameliorate pain arising from bone metastasis. Triple negative breast cancer are treated with chemotherapy, normally anthracyclines as doxorubicin and taxanes as paclitaxel or docetaxel (Sharma, 2016).

During the last few years, the concept of precision medicine has emerged, based on the development of therapeutic strategies focused on the analysis of patient specific clinical features coupled with genomic-based diagnostics and targeted therapeutics (Schmidt et al., 2016). Genetic profiling platforms such as Mammaprint® (70 genes) or Oncotype DX® (20 genes) enable the molecular analysis of breast tumors, that helps to identify the most appropriate therapeutic approach for each patient.

3.3 Endocrine resistance in breast cancer and molecular mechanism associated

Resistance to current therapy still represents a major challenge to cancer patient management (Rondón-Lagos et al., 2016; Shibue and Weinberg, 2017) Resistance to endocrine therapy could results from genetic or epigenetic changes within the tumor that activate hormone-independent mitogenic pathways and various mechanisms have been proposed to explain the development of resistance to hormonal therapy (Riggins et al., 2007).

Resistance to tamoxifen has been classified as metabolic, intrinsic and acquired (Jordan and O'Malley, 2007)**.** Metabolic resistance is due to the presence of certain isoform of the enzyme CYP2D6 that does not convert tamoxifen to the active form N-desmethyltamoxifen with its subsequent transformation to the active hydroxyl metabolite endoxifen (Kiyotani et al., 2012). Genetic population studies have shown that approximately 10% of the population has this variant, so these patients should be considered for other antiestrogenic intervention (such as aromatase inhibitors).

ER expression is generally maintained in most tumors that develop resistance to hormone therapy, and it is important to point out that another cause of tamoxifen resistance includes mutation of ER as demonstrated by *in vitro* studies (Riggins et al., 2007). Nevertheless, this kind of resistance accounts only for 0,2-0,3% of breast tumors and ESR1 mutations have been reported in breast cancer metastasis. (Wang et al., 2016b).

The intrinsic resistance may be due to activation of growth factor receptors such as EGFR, HER2 or IGF-R1 and proteins that function downstream of these receptors, such as the Mitogen-Activated Protein (MAP) kinases (MAPKs), ERK1/2 and p38 (Massarweh et al., 2008). MAPKs comprise a family of ubiquitous proline-directed, protein-serine/threonine kinases, which participate in signal transduction pathways that control intracellular events including acute responses to hormones and major

developmental changes in organisms (Pearson et al., 2001). Normally MAPKs responds to external stimuli as the epidermal growth factor (EGF) or platelet derived growth factor (PDGF) that activate their membrane receptors (EGFR or PDGFR) which transduce their signals intracellularly through the sequential phosphorylation of downstream kinases including RAF, MEK and ERK1/2. The signals transduced by MAPKs are often associated with cell migration, proliferation and survival (Montagut and Settleman, 2009).

For example, using a model of acquired tamoxifen resistance based on MCF-7-tamoxifen resistant cells, increased mRNA and protein levels of c-erbB2 (HER2) have been observed compared to control cells, while no difference in expression was detected in c-erbB3 levels (Knowlden et al., 2003). In fact, overexpression of HER2 in MCF-7 cells is able to induce tamoxifen resistance (Shou et al., 2004). Similarly, in our lab we have observed that MCF-7 cells resistant to tamoxifen (MCF-7-TamR) show increased expression of HER-2 compared to control cells (unpublished observations).

HER2 overexpression it is accompanied by the expression of antiapoptotic proteins as Bcl-2 and Bcl-xl in tamoxifen resistant cells (Kumar et al., 1996).

In breast cancer, aberrant activity of MAPKs pathway has been reported, accompanied by uncontrolled cell proliferation and resistance to apoptosis (Giltnane and Balko, 2014). MAPK and other kinases activation in tamoxifen resistance as protein kinase A (PKA) and p21-activated protein kinase (Pak1), results in ER phosphorylation of the residues S104, S106, S118 and S167 (Lannigan, 2003). In particular, S118 phosphorylation has been associated with tamoxifen resistance (Chen et al., 2013).

MCF-7-TamR cells have also been shown to contain phosphorylated EGFR, and c-erbB2 and c-erbB3, indicating an increased activation of such receptors that positively associated with an increased activation of the downstream MAPK activity in terms of phosphorylated MAPK p42/p44 (Riggins et al., 2007).

Likewise, MCF-7-TamR cells can be more sensitive to MAPK and HER2 inhibition than parental tumor cells, suggesting that the inhibition of EGFR/HER2/MAPK may have therapeutical potential once tamoxifen resistance develops (Knowlden et al., 2003).

Indeed, breast cancer growth in mice has been shown to be significantly delayed by treatment with gefitinib, an EGFR/HER2 inhibitor (Massarweh et al., 2008). Interestingly, promoter methylation of the phosphatase DUSP4, (which in turn increases the RAS-ERK signaling in breast cancer) sensitized cells to MAPK inhibition, suggesting that patients with low level of DUSP4 may benefit from MAPK targeting (Balko et al., 2012). Despite these observations, MAPK inhibition is often associated with the appearance of resistance, most likely due to reprogramming of the pool of kinases present into the cells, called “kinome”, as an adaptive mechanism of resistance (Duncan et al., 2012). Therefore, MAPK inhibition may not represents an effective approach to treat breast cancer. In fact, clinical results using MAPK inhibitors by themselves did not appear encouraging, since Phase 1 clinical trials with MEK1/2 inhibitors in solid tumors didn’t appear efficient (Farley et al., 2013; Robert et al., 2013). In this context, it has been shown that MEK inhibition can be bypassed by the activation of other mechanisms of resistance, including BRAF elevation, IGF1R activation and PDGFRβ overexpression (Corcoran et al., 2011).

More recently, it has been found that the dual inhibition of EGR/HER2 with a compound called AZD8931 reduced growth of tamoxifen resistant breast cancer cell lines *in vitro*, while it was not fully capable of inducing tumor growth regression *in vivo*, suggesting that other pathways may be activated under such circumstances (Morrison et al., 2014). However, in combination with docetaxel, MAPK inhibition strongly reduced tumor growth in xenografts, suggesting that the potential application of MAPK inhibitors in breast cancer is through combinatorial therapies (Balko et al., 2012).

Phosphatidylinositol 3-kinase (PI3K)–Akt–mammalian target of rapamycin (mTOR) signaling pathway is also important in tamoxifen resistance, since overexpression of constitutively active Akt in breast cancer cell lines induces estrogen independence and tamoxifen resistance (Faridi et al., 2003) while Akt inhibition increases tamoxifen sensitivity (deGraffenried et al., 2004). A clinical study confirmed the efficacy combinatorial therapy of mTOR inhibition with an aromatase inhibitor (Baselga et al., 2012). Akt induces tamoxifen resistance through ER phosphorylation on S167, which confers ligand independent activation of the receptor (Campbell et al., 2001) and

activation of antiapoptotic proteins (Riggins et al., 2007). Akt downregulation in tamoxifen resistant cells has been achieved also through the use of histone deacethylase inhibitors (HDAC) (Thomas et al., 2013).

Furthermore, it has been shown that the combination of HDAC inhibitors such as valproic acid, suberoanylide hydrossamic acid (SAHA) or vorinostat, among others, reverts tamoxifen resistance in breast cancer cell lines (Raha et al., 2015). These compounds induce p21 expression, enhance reactive oxygen species (ROS) production and inhibit cell cycle progression (Xu et al., 2007). The combination of vorinostat and tamoxifen appeared able to revert tamoxifen resistance also in breast cancer patients, as shown by a recent clinical trial (Munster et al., 2011). These data look very encouraging, nevertheless, HDAC inhibitor resistance may develops through the up-regulation of antiapoptotic proteins (Bcl2/Bcl-xl), the increased expression of antioxidant/ROS scavenger proteins (thioredoxin), the expression of MDR-1 (ABCB1), as well as the activation of MAPK (Robey et al., 2011).

Another molecular pathway associated with endocrine resistance is the Wnt pathway. Recently our lab demonstrated that development of tamoxifen resistance is driven by Sox2-dependent activation of Wnt signaling in cancer stem cells (Piva et al., 2014). Indeed, another laboratory observed as well that Wnt signaling was increased in an *in vitro* model of acquired tamoxifen resistant cells (Loh et al., 2013). A more detailed description of the Wnt pathway will be provided later on in this introduction. Notch pathway has been associated as well with endocrine resistance, and in particular NOTCH4 protein *in vitro* in MCF-7 cells (Lombardo et al., 2014). Similarly, JAG1-NOTCH4 axis has been demonstrated to be relevant in tamoxifen resistance in patient derived xenografts (PDX) *in vivo* (Simões et al., 2015).

4. Stem cells in adult and in cancer tissues

4.1 Adult stem cells

It is well established that adult tissues contain adult stem cells implicated in tissue repair and regeneration. Adult stem cells were first described in the bone marrow

(Spangrude et al., 1988). Hematopoietic stem cells (HSCs) give rise to all kinds of cells present in the blood; in fact, these cells differentiate into progenitor cells that in subsequent passages of differentiation give rise to the various types of blood cells (Bryder et al., 2006). This discovery represented undoubtedly the basis for the identification of stem cells in other adult tissues, for example, in endothelial cells, skin, pancreas, gut and colon.

It has been shown that there is a bone marrow-derived subset of $CD34^+$ cells that differentiates into endothelial cells (Shi et al., 1998). Stem cells identified in the gut are characterized by the high expression of the membrane receptor Lgr5 (Barker et al., 2007).

These cells are responsible for the complete regeneration of intestinal epithelium turnover, that in humans happens quickly every 5-7 days (Barker, 2014). Adult stem cells have also been identified in the skin, which is another organ characterized by high cellular turnover. These cells are characterized by keratins α6 and β1 expression (Alonso and Fuchs, 2003). Hair follicles also contain stem cells, which are marked by the transcription factor Sox9 and by the ability to retain nuclear marker dyes as BrDU (BromoDeoxyUridine). In fact, these cells are also known as “label-retaining cells” (Nowak et al., 2008). Hepatic stem cells are characterized by EpCAM expression (Kordes and Häussinger, 2013).

Putative pancreatic stem cells existence is still under debate (Bonner-Weir and Sharma, 2002), and methods are available to study them and amplify/differentiate pancreatic stem cells (Tremblay et al., 2016). CD133 is considered a marker of these cells, showing stem/progenitor characteristics and are able to give rise to multilineage colonies *in vitro* (Jin et al., 2014). Adult breast stem cells have also been identified, and this will be discussed in a detailed manner in the following section.

4.2 Breast stem cells

The dramatic regenerative capacity of the breast epithelium to undergo many cycles of growth and involution, suggests that the breast contains mammary stem cells that retain the ability to self-renew and differentiate in order to generate the different kind of cells that compose the epithelial component of the mammary gland. In 1959, a report

already suggested the presence of stem cells in the mammary gland. In this pioneering work done by Deome and colleagues it was shown the reconstitution of an entire mammary gland by transplantation of portions of the mammary gland in cleared fat pat of receiving syngeneic mouse (Deome et al., 1959). Later on, it was demonstrated the potential to regenerate the mammary gland starting from a single cells (Kordon and Smith, 1998).

Cells isolated as $Lin^{-}CD29^{hi}CD24^{+}$ have been shown to be enriched for stem cells by transplantation, in fact, a single cell of that population was able to reconstitute a complete mammary gland *in vivo* (Shackleton et al., 2006). $CD49f^{high}CD24^{+}$ is another phenotype to identify mammary stem cells in mouse (Stingl et al., 2006). One year later, the phenotype $Lin^{-}CD29^{high}CD24^{+}CD61^{+}$ was identified as marker of mouse luminal progenitor cells for their ability to form colonies in matrigel and generate luminal colonies (Asselin-Labat et al., 2007a).

In addition, it has shown that during pregnancy (a period in which luminal differentiation is massive) the proportion of $CD61^{+}$ declines massively in mice. Interestingly, it was shown that the transcription factor GATA3 is important for luminal differentiation and that its silencing expands $CD61^{+}$ progenitor cells (Asselin-Labat et al., 2007a). Furthermore, very recently, Jane Visvader's group identified another molecular subtype within mouse basal mammary stem cells ($CD29^{high}/CD24^{+}$), which is characterized by high expression of the receptor Lgr5 and the transmembrane transporter Tspan8 ($Lgr5^{+}/Tspan8^{high}$) expression (Fu et al., 2017). These quiescent, slow-cycling cells were strongly able to generate outgrowth in mice in limiting-dilution assays than basal $Lgr5^{-}/Tspan8^{high}$, $Lgr5^{+}/Tspan8^{-}$ and $Lgr5^{-}/Tspan8^{-}$ cells. Same pattern was observed in their ability to form complex structures in three-dimensional culture on matrigel. Finally, $Lgr5^{+}/Tspan8^{high}$ cells were found located at the primordial tree of mammary glands embryo, and remained there also in adult mice, retaining their slow-dividing/quiescent characteristic (Fu et al., 2017). This study demonstrated the complex nature of mammary stem cells, showing that they present strong heterogeneity.

It is important to point out that all these experiments have been carried out through *ex-vivo* manipulation, separating these cells through FACS and then analyses their

phenotypes and ability to reconstitute a mammary gland in mice. So, it was important to find out a method to follow stem cells fate *in vivo* under physiological condition, and lineage tracing experiments have opened the possibility to follow the destiny of certain labelled cells throughout the entire animal lifespan, from embryological development through puberty, lactation and mammary gland involution (Visvader, 2009). The most widely used labeling system in mouse models involves the excision of a “floxed” stop-cassette upstream a fluorescent reporter gene (as GFP) by a CRE recombinase expressed under the control of a cell-type specific promoter (Kretzschmar and Watt, 2012).

Lineage tracing study from Cédric Blanpain laboratory showed the existence, into the mouse mammary gland, of distinct long-lived stem cells that give rise to luminal (Keratin8, K8) or myoepithelial (Keratin14, K14) cells. In particular, K14 progenitor are able to give rise to luminal and myoepitelial mammary gland cells during embryo development, but during adult life and puberty only to myoepithelial-restricted cells, while K8-expressing stem cells are responsible for luminal lineage expansion and maintenance throughout animal lifespan (Van Keymeulen et al., 2011).

Similarly, stem cells exists also in the human mammary gland. A combination of FACS studies of cell surface markers and the evaluation of colony formation determined the presence of cells with stem/progenitor characteristics. Cells with the phenotype $EpCAM^{+}CALLA^{\pm/+}EMA^{-/\pm}$ were bipotent progenitors able to generate mixed colonies of luminal and myoepithelial cells when seeded at low clonal density in two-dimensional and three-dimensional cultures (Stingl et al., 1998). Another study showed that in human breast epithelial cells it is possible to find luminal, myoepitelial and bipotent progenitor cells. Using CD49f (or integrin α6) and EpCAM, restricted luminal and bipotent progenitor cells were identified as α6 $integrin^{+/}EpCAM^{+}$, while myoepithelial-restricted progenitors were α6 $integrin^{+}/EpCAM^{-}$ (Stingl et al., 2001). Another group showed that cells with the phenotype $MUC^{-}EpCAM^{+}$ were able to self-renew and generate $MUC^{+}/EpCAM^{+}$ cells as well as to form complex branching structure in three dimensional collagen substrate (Gudjonsson et al., 2002).

The very low percentage of stem cells in the human mammary gland has pushed research into the study and the development of methods to enrich for cells with stem cells potential. *In vitro* enrichment of mammary stem cells has been introduced during the first decade of 2000. Human primary epithelial cells can be grown in suspension as floating colonies called mammospheres (Dontu et al., 2003). These structures contain mammary stem cells and retain the ability to grow in Matrigel, to give rise to colonies with myoepithelial and luminal markers (differentiation potential) as well as to form secondary and tertiary mammospheres upon subsequential disgregation and seeding as single cells (self-renewal potential).

In addition, studies in the hematopoietic and muscle systems have suggested that stem cells have the ability to efflux the dye Hoechst 33342, a phenotype known as the side population (SP) (Goodell et al., 1997). Based on that knowledge, the existence of undifferentiated SP in human and murine mammary epithelium was demonstrated *in vitro* and *in vivo* (Alvi et al., 2003), constituting the first report of a common marker for both human and mouse mammary stem cells in the mammary gland (Behbod and Vivanco, 2015).

Later studies have identified other phenotypes that identifiy stem and progenitor cells in the human mammary gland. $EpCAM^{+}CD49f^{+}$ ductal-derived cells were able to form complex branching structure in three dimensional cultures, forming terminal duct lobulat unit (TDLU)-like structures *in vitro* (Villadsen et al., 2007), even though at this stage was not shown their potential ability to reconstituite a mammary gland through transplantation studies in recipient mice.

Later studies shed light on this issue, showing that cells characterized by $EpCAM^{-}CD49f^{+}$ phenotype behaved as cells with stem cell properties, while $EpCAM^{+}CD49f^{+}$ cells were found to represent luminal progenitor cells. In fact, both cell populations are able to grow in matrigel and to form colonies, while only $EpCAM^{-}CD49f^{+}$ cells are able to give rise to an entire mammary gland when transplanted into cleared mouse fat-pads. $EpCAM^{+}CD49f^{+}$ cells express both luminal and myoepithelial markers and respond to lactogenic stimuli, while $EpCAM^{-}CD49f^{+}$ cells express mostly myoepithelial markers and in matrigel cultures form more ductal complex structures than $EpCAM^{+}CD49f^{+}$ cells.

CD49f^{+} cells can be serially transplanted in mice, as an indication of self-renewal *in vivo*, indicating “mammary repopulating capacity”, a feature of stem cells (Eirew et al., 2008).

Another marker of stem and progenitor cells in the mammary gland is represented by the expression of the aldehyde-dehydrogenase enzymes (ALDHs). ALDH enzymes (19 different isoforms exist in humans), convert aldehydes into the corresponding carboxylic acid, contributing to reduce the toxicity of aldehydic compounds (Tomita et al., 2016) and, importantly, ALDHs convert retinaldehyde into retinoic acid (Duester et al., 2003). The first association between stem/progenitor cells and the expression of ALDH enzyme reported that blood stem/progenitor cells were characterized by high ALDH activity, in contrast to terminally differentiated T-lymphocytes (Kastan et al., 1990).

Ginestier and collaborators showed that human mammary epithelial ALDH positive cells (ALDEFLUOR^{+}) isolated through FACS, had the ability to reconstitute an entire mammary gland in mice and to grow in suspension as mammospheres (Ginestier et al., 2007).

Later on, in 2010, Pece and collaborators showed the presence of label-retaining cells in human breast epithelial cells, which stained for the lipophilic dye PKH26 (Pece et al., 2010; Tosoni et al., 2012).

PKH26^{+} cells are relatively quiescent and present into primary luminal epithelial cells mammospheres culture and, furthermore, they are able to form complex structures in three-dimensional cultures in matrigel as well as being able to reconstitute a mammary gland when transplanted into humanized cleared mouse fat pad. This led to the conclusion that PKH26^{+} cells are stem cells.

4.3 Cancer stem cells

Breast tumors are heterogeneous, containing cancer cells, stromal and endothelial cells, in addition to cells with progenitor-like or stem cell properties (Stingl and Caldas, 2007). In many types of cancer, it has been widely accepted that some of the stem like cells may get mutated leading to the generation of cancer stem cells (CSCs) or tumor initiating cells (TICs) that are considered to be at the apex of the cellular hierarchy of many tumors (Reya et al., 2001). CSCs have been identified in different cancer types,

including brain (Vora et al., 2015) colon (Ricci-Vittiani et al., 2015), prostate (Collins et al., 2005), liver (Yang et al., 2008) and breast cancer, that will be discussed extensively later on in the next section.

CSCs share many characteristics of normal stem cells, including the ability to differentiate and self-renew. Besides, CSCs are characterized by tumor initiation capacity, chemoresistance to current therapies and radioresistance.

In addition, stem cells are characterized by survival in absence of adherence to a substrate, a characteristic known as “anoikis”. Under this condition, anoikis-resistant cells are able to form floating colonies called mammospheres (Dontu et al., 2003). These colonies are enriched for the $CD44^{+}CD24^{-/low}ESA^{+}$ phenotype (which will be further explained in the next pages), demonstrating that the *in vitro* propagation and expansion of breast CSCs lead to the expansion of this phenotype (Fillmore and Kuperwasser, 2008; Piva et al., 2014). Crucially, the mammospheres are not composed only by stem cells, but they contain cells showing various degree of differentiation and, in fact, very few of them are stem cells, as previously explained for the presence of few $PKH26^{+}$ cells (Pece et al., 2010).

Some pathways are associated with mammosphere formation and, in turn, cancer stem cells maintenance. In fact, MAPKs activation has been shown to promote stemness in breast cancer; conversely MAPK inhibitors suppress mammosphere generation in a basal breast cancer cell line (Balko et al., 2013). Another pathway associated with mammosphere formation is the NOTCH pathway and in particular NOTCH4 (Farnie et al., 2007). In fact, NOTCH inhibition has been shown to reduce mammosphere generation in a dose dependent manner, as well as an anti-NOTCH4 neutralizing antibody (Farnie et al, 2007). Wnt pathway inhibition also reduces mammosphere formation in tamoxifen resistant cells, reducing CSCc content (Piva et al., 2014). These sphere-forming cells have also been studied in the contest of CSCs in other tissues, including the prostate (Fan et al., 2012) and glioma (Garros-Regulez et al., 2016a) and are generally called “oncospheres” or “tumorspheres”. Finally, it has been shown that mammosphere cells derived from human primary breast pleural effusions are more tumorigenic in mice

(Grimshaw et al., 2008), further confirming the conception that mammosphere cultures are enriched for cells with tumorigenic potential.

Chemotherapy has been shown to increase the CSC content (Dean et al., 2005; Lewis and Wicha, 2009) and chemoresistance is possible due to the increased expression of a membrane transporter of the ABCG family (MDR1 or ABCG2) that extrudes cytotoxic drugs from the cells (Martin et al., 2014). The increased radioresistance of the CSCs compartment over the rest of the tumor bulk is mostly due to the increase DNA-repairing mechanisms (Krause et al., 2011). These characteristics make CSCs responsible for tumor maintenance and recurrence; in fact, in the current and widely accepted model, treatment with chemotherapy or radiotherapy leads to tumor shrinkage, but CSCs remain mostly unaffected. However, the CSC properties, differentiation and self-renewal, induce a *de-novo* tumor formation, a phenomenon called “recurrence”.

Therefore, it is important to define and discover new markers of CSCs, as well as the molecular pathways that maintain these cells, in order to learn more about CSCs as potential new therapeutic targets. In this context, both targeting signaling pathways such as Wnt, Sonic Hedgehog (Shh) or Notch, (Pannuti et al., 2010; Takahashi-Yanaga and Kahn, 2010) and differentiation therapy to induce CSC differentiation in order to make them more sensitive to current therapies (Hu and Fu, 2012) are possible approaches that are under study.

4.4 Breast cancer stem cells

The field of breast cancer stem cells (CSCs) has expanded tremendously since their identification. In 2003, Al-Hajj and colleagues showed that cells from human breast tumors with the phenotype $CD44^{+}CD24^{-/low}ESA^{+}$ have high tumorigenic potential in vivo (Al-Hajj et al., 2003). Intriguingly, the proportion of $CD44^{+}CD24^{-}$ cells was found to be increased in breast cancer patients after chemotherapy, and this increase correlated with worst outcome in breast cancer patients (Lee et al., 2011). Cells with this phenotype have also been identified as CSCs in other tumors, including pancreas (Li et al., 2007). High CD44 expression is associated with cancer stem cells features also in other kinds of cancer, including glioma (Anido et al., 2010), lung (Shi et al., 2014) and prostate (Liu et

al., 2011). In breast cancer, the $CD44^{+}CD24^{-/low}$ phenotype by itself already has an increased tumorigenic potential compared to the rest of the population, but the expression of epithelial-specific antigen (ESA) even increments such tumorigenicity (Al-Hajj et al., 2003). Studies from our lab have also shown the increased migration and invasion capacity of $CD44^{+}CD24^{-/low}$ ESA^{+} cells sorted from breast cancer cells compared to the rest of the cells (Piva et al., 2014).

Intriguingly, $CD44^{+}CD24^{-/low}$ ESA^{+} cells could also be isolated from breast cancer cell lines, and these cells were present at highest numbers in the basal-like breast cancer compared to ER^{+} cell lines (Fillmore and Kuperwasser, 2008). Besides, immunohistochemistry analysis revealed that triple negative breast cancer are characterized by high level of $CD44^{+}CD24^{-low}$ cells (Idowu et al., 2012).

Furthermore, It has been observed that radiotherapy increases the proportion of $CD44^{+}CD24^{-/low}$ ESA^{+} cells (Phillips et al., 2006) and our lab has shown that tamoxifen treatment also results in an expansion of the CSCs population (Piva et al., 2014). Furthermore, the stem cell niche is often located in areas with low oxygen availability and we and others have shown that hypoxia leads to the expansion of CSCs (Harrison et al., 2013; Iriondo et al., 2015). In particular, in our laboratory we observed that hypoxia induced stem cells expansion both in normal breast epithelial cells and in breast cancer cells. In cancer stem cells context, the proportion of $CD44^{+}CD24^{-/low}$ ESA^{+} was increased in ER- but not ER+ breast cancer cells, observation that was further confirmed analyzing primary tumor breast epithelial cells growing in normoxia or hypoxia (Iriondo et al., 2015)

In the previous section, it has been introduced $ALDEFLUOR^{+}$ cells as marker of progenitor/stem cells in the human mammary gland.

It is important to point out that these cells have also CSCs capacity; in fact, $ALDEFLUOR^{+}$ cells derived from primary tumor samples were more tumorigenic than $ALDEFLUOR^{-}$ cells (Ginestier et al., 2007). This implies that the high expression of ALDH enzymes is a common feature of both normal and breast CSCs. In breast cancer, it has been shown that the mayor ALDH isoform involved in the $ALDEFLUOR^{+}$ phenotype is ALDH1A3 (Marcato et al., 2011a), which has also been implicated in mesothelioma

(Canino et al., 2015) and non-small cell lung adenocarcinoma tumorigenicity (Shao et al., 2014).

STAT3 pathway appears to be activated in ALDEFLUOR$^+$ breast cancer cells (Lin et al., 2013) as well as Wnt signaling (Jang et al., 2015). ALDH1A3 has been found to play a tumorigenic role in glioma due to its association with invasion and reduced patient survival (Zhang et al., 2015), and also in breast cancer, where it has been associated with invasiveness and metastatic potential (Charafe-Jauffret et al., 2010). High ALDHs expression protects cells against alkylating agents of the oxazaphosphorine (OP) family, such as cyclophosphamyde (CP) and its derivatives, since these enzymes convert CP to no toxic compounds (Moreb et al., 1996).

These findings suggest that ALDEFLUOR$^+$ cells could represent a potential metabolic target for cancer treatment, which, in fact, has led to the development of new inhibitory compounds (Pors and Moreb, 2014). Nevertheless, natural compounds have shown strong activity against this CSCs population. In fact, curcumin and piperine extracted respectively from *Curcuma longa* and *Piper nigrum* have been shown to reduce ALDEFLUOR$^+$ cells (Kakarala et al., 2010) as well as suphorafane, derived from cruciferous vegetables (Li et al., 2010). Recently, it has been shown that the compound citral, a terpenoid present in the oil of several plants, inhibits ALDH1A3 expression and its related tumorigenicity in breast cancer cells (Thomas et al., 2016).

5. Sox proteins

Sox proteins are transcription factors that belong to the high mobility group (HMG) superfamily, sharing a common DNA-Binding Domain (DBD) (Kiefer, 2007). In general, proteins containing an HMG domain with 50% or higher amino acid similarity to the HMG are referred to as Sox proteins (*Sry*-related HMG box) (Jo et al., 2014). Sox proteins are animal-specific and can be identified based on a conserved motif within the HMG domain, RPMNAFMVW (Bowles et al., 2000; Kiefer, 2007). These transcription factors bind to the consensus DNA sequence (A/T)(A/T)CAA(A/T)G and they can function as transcriptional activators or repressors. Phylogenetic studies have led to Sox proteins classification are according to their similarities in the encoded protein sequences, leading to the Sox classification in different groups: A, B1, B2, C, D, E, F, G and H (Bowles et al., 2000; Guth

and Wegner, 2008). Within each group, Sox members show a high similarity that is close to 70%, while Sox proteins of different groups share very little sequence similarity apart from HMG (Guth and Wegner, 2008). In human and mouse, 20 Sox proteins have been identified (Guth and Wegner, 2008).

5.1 Sox2

Sox2 (SRY (sex determining region Y)-box 2) is a 34 kDa member of the of Sox transcription factors family. Sox2 is well known as one of the master regulators of the stem/pluripotency program in embryonic stem cells (ES). In particular, in mouse embryonic stem cells, the cytokine LIF (leukaemia inhibitory factor) induces Sox2 expression, contributing to the maintenance of pluripotency (Niwa et al., 2009). Sox2 functions together with the other two core stem cell factors OCT4 and NANOG (Niwa, 2007). In particular, Sox2 forms dimers with OCT4, which in turn can bind to palindromic sequences on the DNA (Tapia et al., 2015). Notably, it has been shown that the introduction of four factors Sox2, Klf4, c-Myc and Oct3/4 was sufficient to induce pluripotent stem cells in murine cells (Takahashi and Yamanaka, 2006) and from human fibroblasts (Takahashi et al., 2007), famously demonstrating successful reprogramming of differentiated human somatic cells into a pluripotent state. This observation launched a new research field (induced pluripotent stem cells or iPS) with considerable potential for the development of patient and disease-specific stem cells.

Sox2 appears to be very important for the development of the central nervous system; in fact, neural stem cells are Sox2 positive and its inhibition induces neural progenitor cells to start differentiation and enter cell cycle (Graham et al., 2003). Finally, Sox2 gene deletion causes abnormality in the central nervous system (Ferri et al., 2004). Sox2 has also been found implicated in tumorigenicity in glioma (Garros-Regulez et al., 2016b) and melanoma (Santini et al., 2014).

In the mammary gland, we showed that Sox2 (in addition to Nanog and Oct4) is more expressed in breast cancer tissue than in normal epithelial cells, suggesting that these embryonic stem cell factors are also markers of mammary stem cells (Simões et al., 2011). In breast cancer, we found that Sox2 is a positive regulator of the Wnt pathway and its expression associated with development of resistance to tamoxifen (Piva et al.,

2014), suggesting that it could be a biomarker of resistance to identify patients with a higher risk of failing to respond to hormone therapy.

5.2 Sox9

Sox9 is a member of the SoxE group of structurally-related Sox protein: Sox8, Sox9 and Sox10 (Jo et al., 2014). Structurally, Sox9 is composed by three alpha helices that are arranged in a twisted L-shape and a hydrophobic core to form the HMG domain, which binds to the DNA. Sox9 structure (Fig. 1.2) contains a dimerization domain between the aminoacids 64-102 (Jo et al., 2014). Sox9 is able to dimerize also with other Sox proteins, especially with proteins from the SoxE group (Huang et al., 2015b). The HMG domain, situated between the residues 103-181, contains nuclear importing and exporting sequences. In fact, Sox9 can be located both in the nucleus and in the cytoplasm as observed immunohistochemically in breast cancer tissues (Chakravarty et al., 2011a). Two transactivation domains have been mapped: one called K2 between aminoacids 229-303 and another called TA at the C-terminus, between the residues 402-509. Sox9 contains a proline, glutamine and alanine rich domain (PQA), whose function is unknown.

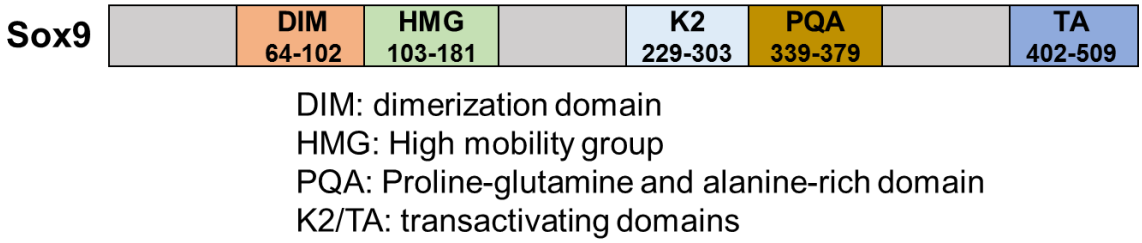

Fig 1.2. Sox9 domains

Sox9 can also be target of post-translational modifications that influences Sox9 function and localization. For example, Sox9 phosphorylation by Protein-kinase A (PKA) induces Sox9 binding to Col2A1 condrocyte-specific enhancer (Huang et al., 2000). Sox9 can also be modified by SUMOylation, since cotransfection of SUMO-1 with Sox9 repressed its transcriptional activity (Oh et al., 2007). Sox9 can also be ubiquitinated in chondrocytes by the protein E6-AP/UBE3A (Hattori et al., 2013). Finally, ubiquitination of Sox9 by the ubiquitin ligase FBW7 has been reported in medulloblastoma, leading to

Sox9 degradation by the proteasome. Mutation or reduced level of FBW7 leads to increased Sox9 level and then tumorigenicity in medulloblastoma (Suryo Rahmanto et al., 2016).

5.3 Sox9 maintains progenitor and stem cells

Sox9 has been extensively studied because of its action as inducer of cartilage and chondrocyte formation (Bi et al., 1999). Sox9 activates the expression of collagen gene Col2a1 (Bridgewater et al., 1998) and Sox9 mutations can lead to campomelic dysplasia in humans (Foster et al., 1994). Campomelic dysplasia is a severe disorder that affects development of the skeleton, reproductive system, and other parts of the body, often life-threatening in the newborn period. Sox9 has been characterized as an important regulator of progenitor and stem cells in different tissues. In the central nervous system (CNS), Sox9 appeared as a regulator of neural stem cells, inducing neurosphere formation; in addition, Sox9 expression was induced by the Sonic Hedgehog pathway (SHH) in neuroepithelial cells, together with Sox2, Sox8 and Sox10 (Scott et al., 2010). Sox9 is also relevant in the development of the neural crest (Cheung and Briscoe, 2003).

Sox9 has also been associated with pancreatic development, maintaining pluripotent progenitor cells (PDX1+ cells) in mouse pancreas (Seymour et al., 2007). Interestingly, differential Sox9 level could be able to identify different population of cells in the small intestine; in particular, cells with high Sox9 level correspond to non-dividing cells, corresponding to the stem cell population, while a decreasing gradient of Sox9 expression is associated with cells with enhanced progenitor proliferation (Ramalingam et al., 2012). In hepatocellular carcinoma Sox9 promotes stem cells self-renewal (Liu et al., 2016a). Interestingly, it has been suggested that Sox9-expressing cells are pivotal for renal tubular epithelial cells regeneration in mice (Kang et al, 2016).

In breast, Sox9 is able to cooperate with the EMT transcription factor SLUG to maintain stemness in the mouse mammary gland (Guo et al., 2012a). Coexpression of both transcription factors increased organoid formation *in vitro* and repopulation of the mouse mammary fat pad. In addition, they showed that stable Sox9 silencing in MDA-MB-231 breast cancer cells reduces tumorigenicity in mice. In addition, Sox9 KO mice

have presented defects in mammary gland development and side-branching (Malhotra et al., 2014).

Recently, an innovative method to culture human mammary epithelial cells in three-dimensions (3D), in a hydrogel composed by collagen, hyaluronan, laminin and other components of the ECM, has been reported to better mimic the environment in which mammary epithelial cells grow normally *in vivo*. With this method primary breast epithelial cells can form complex structures *in vitro* as ducts, lobules and TDLU-like structures (Sokol et al., 2016), representing another advance within the recent efforts to study the human mammary gland development and differentiation processes in a more physiological environment. Interestingly, in this study researchers found $Sox9^{+}$/$SLUG^{+}$ cells at the tip of the developing three-dimensional structures, corresponding to the TDLU-like structure.

Finally, it is important to mention the Sry-Sox9 role in sexual determination in mammals. The first Sox gene identified was *Sry* (sex-determining region Y) (Sinclair et al., 1990), also known as testis-determining factor (TDF). The mammalian embryo is a bipotential gonad, since it is able to differentiate both toward testis or ovary (Matzuk and Lamb, 2008). Male-specific cells are Sertoli cells, which populates testis cords. These cells will mature into structures that will support sperm maturation, called seminiferous tubules. Sry is necessary for testis development, as it starts a trascriptional cascade that lead to male-sex determination; in its absence, XY subjects develop female genitalia. On the other hand, its ectopic expression is sufficient to induce testis development in XX transgenic mice (Berta et al., 1990). Sry activates Sox9 expression, and together lead to male testis development (Matzuk and Lamb, 2008).

5.4 Sox9 in cancer development and progression

Sox9 has been extensively studied in the context of cancer development and progression of a wide variety of solid tumors. In prostate, it has been shown that Sox9 enhances tumorigenicity and invasion of prostate cancer cells (Wang et al., 2008a). Similar results were observed in bladder cancer (Ling et al., 2011), in which it has also been observed an increase in Sox9 expression in bladder tumor tissue compared to normal adjacent bladder cells. Sox9 expression also correlates with poor prognosis in

patients with hepatocellular carcinoma (Guo et al., 2012b). Recently it has been published that Sox9 enhances tumorigenicity in esophageal carcinoma (Hong et al., 2015) and medulloblastoma (Suryo Rahmanto et al., 2017). In addition, it has been published that Sox9 is a tumorigenic factor in hepatocellular carcinoma, in which Sox9 deletion impairs cell tumorigenicity and stemness (Leung et al., 2016), as well as invasion and migration of hepatocellular cancer cells (Liu et al., 2016b). Sox9 has been also associated with cell invasion in pancreatic carcinoma (Sun et al., 2013) and, to promote pancreatic cancer cell aggressiveness through the induction of hypoxia-induced genes (Camaj et al., 2014). Sox9 plays an important role in tumorigenicity in colorectal cancer too (Matheu et al., 2012). More recently, it has been shown that Sox9 induces S100P expression in colon cancer, which it is required for Sox9 induction of invasion and migration of colon cancer cells *in vitro* (Shen et al, 2014). On the other hand, Sox9 has also been shown to inhibit colon cancer cell growth and invasion *in vivo*, contradicting previous results (Prévostel et al., 2016).

In fact, Sox9 has been found to promote a pro-malignant phenotype in various types of cancer. For example, the role of Sox9 in melanoma is still quite debated. It has been described that Sox9 induction in melanoma cells reduces cell proliferation and sensitize cells to retinoic acid (Passeron et al., 2009), suggesting a positive effect of Sox9 upon melanoma patient outcome, but another group showed that Sox9 upregulation in melanoma induces tumorigenicity in mice and that Sox9 silencing impairs melanoma cells migration and invasion (Cheng et al., 2015). Nevertheless, both groups observed that Sox9 reduces melanoma cell proliferation, but Cheng and colleagues observed that even though the Sox9-overexpressing cells were less cell-cycling, but more invasive than controls and that Sox9 expression correlates with worst clinical outcome in melanoma patients. Interestingly, a recent publication showed that Sox9 induced p21 expression, reduced tumorigenicity in mice and slowed down G1/S-G2 transition progression in cervical cancer, claiming for a role of Sox9 as oncosuppressor in cervical cancer (Wang et al., 2015a). These results suggest that Sox9 may play a different role depending on the type of cancer, however, in general, Sox9 is recognized as a bad prognostic factor in the majority of cancers studied.

In breast cancer, it has been shown that Sox9 is expressed especially in ER- tumors compared to ER+ breast tumors. Interestingly, cytoplasmic Sox9 localization has been found to correlate with Ki67+ in immunohistochemistry staining of breast tumor samples and poor prognosis (Chakravarty et al., 2011a). Similar conclusion has been found in pancreatic cancer, in which cytoplasmic Sox9 expression was associated with mutant p53 expression, reduced overall survival and disease-free survival (Huang et al., 2015a). Sox9 stable silencing in the triple negative breast cancer cell line MDA-MB-231 reduced tumor growth, cell invasion and lung metastasis in mice (Guo et al., 2012a). Together, these findings support a tumorigenic role of Sox9 in breast cancer.

6. Wnt signaling

6.1 Wnt signaling: an overview

The Wnt (Wingless-type MMTV integration site family) signaling pathway has been associated with the maintenance of stem cells in a self-renewal state (Nusse, 2008). In humans and mouse, Wnts comprise a large family of 19 secreted proteins, 7 in *Drosophila* and 5 in *C. elegans* (Nusse, 2005). Wnt proteins are palmitoylated and characterized by glycosylation and several highly charged amino acids residues. Palmitoylation is required for the correct Wnt secretion, and requires the membrane bound O-acyl transferase (MBOAT) porcupine (PORCN) (Bartscherer and Boutros, 2008). This phenomenon converts Wnts into hydrophobic highly glycosylated proteins.

Classically, Wnt signaling is known to transduce signals in two ways: the canonical and non-canonical pathways. The canonical Wnt pathway it is associated with Frizzled-LRP signaling and its key signaling molecule is β-catenin. β-catenin, according to the classical model, is actively degraded by a molecular structure called “destruction complex” which is a multiprotein structure composed by Axin, glycogen synthase kinase-3 (GSK3), casein kinase 1 (CK1) and adenomatous polyposis coli (APC) and the E3-ubiquitin ligase β-TrCP (Bengoa-Vergniory and Kypta, 2015; Clevers and Nusse, 2012; Stamos and Weis, 2013). The complex segregates and GSK-3 phosphorylates β-catenin in the cytoplasm, which in turn is ubiquitinated by the E3-ubiquitin ligase TrCP and then

degraded by the proteasome. β-catenin releasing from the complex is a multistep process that is triggered by Wnt proteins binding to specific membrane receptors.

The first Wnt receptor identified was the seven transmembrane receptor Frizzled (FZ) (Bhanot et al., 1996). One Wnt can binds to multiple FZs and, conversely, single FZ can interact with multiple Wnts. These receptors contain an extracellular domain rich in cysteine residues called cysteine rich domain (CRD), that has been shown to bind to Wnt proteins with high affinity (Bhanot et al., 1996). FZ receptors are closely associated to the coreceptor LRP5/6 in vertebrates (Pinson et al., 2000). Wnt binding induces a ligand-induced conformational change that increases FZ binding to the protein Dishevelled (DVL) which in turn facilitates the interaction between LRP tail and the protein AXIN. This causes the destabilization of the "destruction complex" which in turn leads to the release of unphosphorylated β-catenin which translocates into the nucleus, where it binds to the Lef1/TCF transcription factor e and activates Wnt target genes (such as AXIN2, CD44 or cyclin D1) by displacing the co-repressors and recruiting co-activators to this complex (Clevers and Nusse, 2012). It is important to point out that a more recent version of the model has been proposed. In this model, the destruction complex is not disrupted by Wnt activation and that changes in the levels of free and transcriptionally active β-catenin result from relocation of the complex to the membrane, which disrupts β-catenin ubiquitination rather than the complex itself, leading to β-catenin accumulation (Li et al., 2012).

Other Wnt ligands have been discovered that can modulate Wnt activation, as secreted-frizzled related proteins (sFRPs) and Dickkops (DKK) (Kawano and Kypta, 2003). In particular, sFRP proteins (as sFRP1-5, WIF-1 and Cerberus) bind directly to secreted Wnt, preventing its receptor binding ability, while DKK proteins (DKK1-4) as DKK-1 binds to Wnt receptor LRP5/6 inducing its endocytosis, preventing the formation of the complex Wnt-FZ-LRP5/6 (Kawano and Kypta, 2003).

In addition to canonical Wnt pathway, there are the non-canonical ones, which comprises a series of molecular events that do not involve the activation of β-catenin. In particular, there are two non-canonical pathways: the planar cell polarity (PCP) pathway,

the calcium Ca^{2+}/WNT pathway and other β-catenin/TCF independent events (Bengoa-Vergniory and Kypta, 2015)

The PCP pathway involves Frizzled receptors but without the involvement of the co-receptors LRP5/6. FZD receptors activate a signaling cascade that involves the small GTPases RhoA and Rac1 and c-Jun N-terminal kinase (JNK), leading to changes in the cytoskeleton as well as ATF-2 activation (Bengoa-Vergniory and Kypta, 2015). PCP pathway is relevant in events as morphogenetic events in vertebrates as gastrulation, neural tube closure and stereocilia orientation in the inner ear (Gómez-Orte et al., 2013)

The Ca^{2+}/WNT pathway has been discovered thanks to the observation that some Wnts are able to increase intracellular Ca^{2+} levels (Komiya and Habas, 2008). Under this circumstance, Wnt binding to FZ leads to activation of phospholipase C (PLC), producing 1,2 diacylglycerol (DAG), which activates protein kinase C (PKC), and inositol 1,4,5-triphosphate (IP3), which activates calcium release from the endoplasmic reticulum (Gómez-Orte et al., 2013). In Xenopus embryogenesis, intracellular release of Ca^{2+} can be induced by Wnt5a and Wnt11 that are able to activate calcium-sensitive kinases such as PKC or CAMKII (Kühl et al., 2000).

Furthermore, non-canonical Wnt pathway involves different receptors as the tyrosine kinase-like orphan receptors ROR1 and ROR2. ROR1-2 mouse knock-out mimics Wnt5a silencing, indicating that ROR1-2 serve as Wnt5a receptor (Yoda et al., 2003). Recognized downstream effector or ROR2 are JUN and ATF-2. Other non-canonical Wnt receptors are the receptor-like tyrosine kinase (RYK), which is involved in axon guidance and neurodevelopmental processes (Clark et al., 2012) and Van Gogh-like (VANGL1/2), which mutations have been linked to neurodevelopmental defects in humans (Kibar et al., 2007).

Finally, it is important to mention that Wnt signaling it is a druggable pathway, and it is possible to either block or activate it. Previously, it has been mentioned that Wnt palmitoilation due to PORCN is pivotal for Wnt secretion; to this end, there are available drugs that block Wnt secretion through the PORCN inhibition (Polakis, 2012) . Some drugs used to achieve this effect are IWP-2 (Chen et al., 2009), C59 (Proffitt et al., 2013) and LGK-974 (Liu et al., 2013a).

Wnt inhibition can be achieved by blocking the interaction between FZ receptors and Wnts. The antibody OMP-18R5 reduces Wnt binding to the frizzled domain CRD (Gurney et al., 2012), while molecules as NSN668036 and 3289-8625 reduces FZ8 interaction with Wnts through the binding to the FZ CRD (Lee et al., 2015).

In addition, it has been shown that the antihelminth compound niclosamide reduces Dvl2 expression in colon cancer cells, showing no cytotoxicity in no tumorigenic control cells (Osada et al., 2011) and another report showed how niclosamide impairs LRP6 expression in prostate and breast cancer cells (Lu et al., 2011). Wnt signaling can be inhibited also by stabilization of the destruction complex. Pyrvinium binds to and activates casein kinase 1α (CK1α), which is part of the β-catenin destruction complex. Therefore, it contributes to the destruction of β-catenin, stopping further relays of the Wnt signal (Thorne et al., 2010). In addition, IWR-1/2, by tankyrase inhibition, stabilize Axin and in turn preserve the destruction complex structure and function (Chen et al., 2009).

Other inhibitors block β-catenin function, impairing Wnt activation downstream. As an instance, ICG-001 blocks the interaction between cyclic AMP binding protein CPB and β-catenin, which binding is fundamental for TCF-β-catenin interaction, reducing Wnt signaling (Grigson et al., 2015). Finally, another potent molecule which block downstream Wnt activation is the Dsv inhibitor J01-017a (Shan et al., 2012).Conversely, Wnt pathway can be activated by GSK3 inhibition by molecules as BIO (Sato et al., 2004) and CHIR99021 (An et al., 2010). It is important to point out that results obtained by Wnt activation through GSK3 inhibition have to be interpreted carefully, since GSK3 is involved in other functions besides its Wnt signaling involvement (Klevers and Nusse, 2012).

6.2 Wnt pathway in mammary gland development

Wnt signaling plays an important role in breast organogenesis. As mentioned previously, a special link has been found between Wnt pathway and progesterone. Wnt4 knock out mice developed ductal branching during pregnancy, suggesting that Wnt4 is not the only Wnt or factor involved in this process, and that other compensatory factors can be involved (Brisken et al., 2000). It has been shown that progesterone induces Wnt4

expression, which can influence surrounding cells in a paracrine manner (Fernandez-Valdivia and Lydon, 2012; Joshi et al., 2010).

Wnts maintain and expand mammary stem cells in mice, as Wnt1, Wnt2 and Wnt4, while the non-canonical Wnt5B acts as an inhibitor of this process (Kessenbrock et al., 2013). Other researchers observed that overexpressing a constitutive active β-catenin in mice (the downstream effector of canonical Wnt pathway) results in early mammary gland development and morphogenesis (Imbert et al., 2001). Overexpression of the Wnt inhibitor protein DKK1 (Semënov et al., 2001) in mice embryos leaded to the complete absence of the mammary gland placode, that is the first structure formed in the mammary gland during development in mice (Andl et al., 2002). In addition, a potential link between proteins associated to chromatin modification such as the methylation reader Pygo2 and Wnt activity in the maintenance of stem cells in the mammary gland has been reported (Gu et al., 2013). In addition, it has been shown that knock-out mice for LRP5 ($LRP5^{-/-}$) lack proper mammary gland morphogenesis and present fewer mammary gland end buds (Lindvall et al., 2006). Zerb laboratory showed that Wnt5A it is able to reduce mammary gland side branching *in vivo* and *in vitro* signaling through ROR2 and expands mammary stem cells through the receptor RYK (Kessenbrock et al., 2017). In summary, these results show the relevance of Wnt signaling in mammary gland development and morphogenesis.

6.3 Wnt in breast cancer development

A link between Wnt and breast cancer tumorigenesis is well established. Transgenic expression of Wnt1 or β-catenin induces mammary gland hyperplasia and adenocarcinoma in mice (Tsukamoto et al., 1988). Wnt seems not only relevant in the context of mammary gland tumorigenesis in mice, but also in human; in fact, β-catenin appears stabilized and actively expressed in human breast tumors, and its cytonuclear expression correlates with worst prognosis in breast cancer (Lin et al., 2000).

Various Wnt proteins have been found to be expressed in breast cancer cell lines (Suzuki et al., 2008), as well as most of the Frizzled receptors, (Benhaj et al., 2006). It

has been shown that Wnt signaling induces cell proliferation in breast cancer cells, and treatment with the Wnt inhibitor sFRP-1 (or reduced DVL expression) diminished cell proliferation in breast cancer cells (Schlange et al., 2007). Wnt inhibition (through over-expression of sFRP-1) reduced tumorigenicity of triple negative breast cancer cells MDA-MB-231 *in vivo*, by affecting tumor growth and invasion (Matsuda et al., 2009).

Wnt signaling is strongly activated in basal/triple negative breast cancer cell lines in which it is associated with metastasis (Dey et al., 2013) and another study published the same year indicated how Wnt10B was mostly associated with proliferation and metastasis in basal/triple negative breast cancers (Wend et al., 2013). Stable knock-out of the downstream canonical effector β-catenin reduced tumorigenicity *in vitro* and *in vivo* of basal/triple negative breast cancer cells (Xu et al., 2015).

Wnt pathway has been associated to chemoresistance. β-catenin stable silencing increased sensitivity to doxorubicin and cisplatin as well as reduced tumorigenicity *in vitro* and *in vivo* in HCC38 triple negative breast cancer cells (Xu et al., 2015). The increased chemoresistance due to β-catenin expression may be explained by the fact that has been shown that transcription factor Pygo2 can induce the multidrug resistant protein MDR-1 through β-catenin expression (Zhang et al., 2016).

Wnt is also associated with endocrine resistance. Adding recombinant Wnt1 to culture medium rescued tamoxifen sensitivity in MCF-7 and T47D breast cancer cells (Schlange et al., 2007) and canonical Wnt pathway in increased in MCF-7 tamoxifen resistant cells compared to control cells (Loh et al., 2013).

In addition, our laboratory observed a positive regulatory loop between Wnt and Sox2 in tamoxifen resistant breast cancer cells showing that both Sox2 silencing and Wnt inhibition restored tamoxifen sensitivity in MCF-7 tamoxifen resistant cells and in naturally endocrine-resistant BT474 cells (Piva et al., 2014). We also observed that *in vivo*, Sox2-overexpressing MCF-7 cells were more resistant to tamoxifen than control cells. Examination of patient tumours indicated that Sox2 levels are higher in patients after endocrine therapy failure, and also in the primary tumours of these patients, compared to

those of responders. All together, these data point to Wnt as a potential target for breast cancer treatment.

Chapter 2: Materials and methods

1. Cell Culture

1.1 Adherent cell culture

MCF-7-OH, MCF-7-TamR, T47D-OH, T47D-TamR, ZR-75-1, MDA-MB-231, BT549 (and their derivatives shC and shSox9 cells), 293FT and MDA-MB-468 cell lines were obtained from American Type Culture Collection (ATCC) and cultured in DMEM:F-12 medium with GlutaMAX supplemented with 8% FBS and 1% penicillin/streptomycin (Gibco) at 37° C in 5% CO_2. For treatment with 17-β-estradiol, cells were washed 3 times with PBS (Gibco) and hormone depleted for 72 hours in phenol-red free DMEM/F-12 medium supplemented with 8% charcoal-stripped FBS. MCF-7-TamR, T47D-TamR and ZR-75-1 TamR cells were developed in our laboratory after long-term exposure to tamoxifen (at least 3 months), till only tamoxifen resistant cells survived, that were maintained in culture in the presence of $5x10^{-7}$ M 4-OH-tamoxifen (Piva et al, 2014, Domenici et al., 2014). Control cell lines are MCF-7, T47D and ZR-75-1 cells growing in parallel in the presence of vehicle, ethanol. MCF10A cells were cultured in DMEM/F-12 medium with GlutaMAX supplemented with 5% horse serum, 20 µg/ml EGF (Invitrogen), 0,5 µg/ml Hydrocortisone (Sigma), 10 µg/ml Insuline (Sigma), 1% penicillin/streptomycin solution (Gibco) and cholera toxin 100 ng/ml (Sigma). All cell lines were routinely checked for mycoplasma contamination.

Stable shRNA clones form primary human breast epithelial cells (HBECs) were cultured with WIT-P-NC™ MEDIUM (Stemgent) supplemented with 1% penicillin/streptomycin. All the experiments done using primary cells have been performed untill approximately passage 4 in culture, when signs of reduced cell growth and senescence were detected.

1.2 Isolation of human breast epithelial cells (HBECs)

Normal breast tissues were obtained from women undergoing reduction mammoplasty with no previous history of breast cancer (Supplementary table 1). Tumor samples were obtained from core biopsies or from women who underwent therapeutic surgery. In all cases (normal and malignant). A consultant breast pathologist reviewed the samples. All patients provided written informed consent, and the procedures were

approved by the local Hospital Research Ethics Committee and by the 'Ethics Committee of Clinical Investigation of Euskadi'. The breast tissue was immediately processed as previously described (Clayton et al., 2004). Briefly, cut breast material was digested shaking overnight at 37ºC with collagenase (Type I, Sigma) to a final concentration of 0.25 to 0.35 mg/ml. Following enzyme digestion, the breast tissue was washed and the breast organoids (ductal and lobulo-alveolar fragments) separated from persisting unwanted collagenous material. The organoids were filtered, washed and disaggregated with 0.05% trypsin-EDTA (Gibco), and finally filtered through a 40 μm sieve (BD) to yield a predominantly single cell suspension. Tumor cells were isolated using the same procedure. Cell suspension was incubated in lysis buffer (155 mM NH_4Cl, 10 mM $KHCO_3$, 0.1 mM EDTA, pH 7.3) for 10 min to eliminate the erythrocytes and cells were counted using trypan blue (Sigma) to discriminate between alive and death cells.

1.3 Mammosphere (MS) culture

MCF-7-OH, MCF-7-TamR, MDA-MB-231, HBECs and BT549 cells were plated in six-well plates coated with poly-HEMA at 10.000 cells/ml in MS medium (DMEM/F-12 medium with GlutaMAX, supplemented with B27 (Gibco), 10 ng/ml EGF (Invitrogen), 2 ng/ml bFGF (Millipore). At day 5-7, MS were counted under the microscope. For secondary MS formation, primary MS were disaggregated using a solution of TRYPLE 1X (Gibco) and plated again in MS medium for another 5-7 days and then counted. MS formation efficiency (shown as fold change) was calculated by dividing the number of MS formed by the original number of single cells seeded. Ability of mammosphere formation was evaluated in MDA-MB-231 and MDA-MB-468 in the presence of MEK inhibitor U0126 at a final concentration of 10 μM. DMSO was used as vehicle diluted 1/1000 in cell culture medium.

1.4 Cell treatments with hormones or inhibitors

To test the effect of RAS/RAF/MEK/ERK (MAPK) inhibition upon Sox9 expression, MCF-7-TamR, T47D-TamR, MDA-MB-231 and MDA-MB-468 cells were plated in complete medium in 6- well plates (250.000 cells/well). The next day, cells were treated with the MEK inhibitor U0126 (Tocris Biosciences) at a final concentration of 10 or 20 μM,

dissolved in DMSO (Sigma). Cells were exposed to U0126 for 24 hours before harvesting for RNA or protein extraction. Cells treated with estrogen (10^{-8} M) were plated, washed with PBS and starved three days with complete medium supplemented with charcoal-stripped serum before estrogen treatment.

2. Development of stable shRNA cell lines/Sox9 overexpressing cells

2.1 shRNA stable expression in HBECs and breast cancer cell lines

A set of three pLKO.1 lentiviral shRNA vectors targeting Sox9 was purchased from Open Biosystems (source ID: TRCN0000020834, TRCN0000020835, TRCN0000020836). An empty vector and a shRNA against a random sequence, called shCNTR, was used as negative control. Lentiviruses were made by transfection of 293FT packaging cells with a 3-plasmid system.

293FT cells were grown in DMEM medium containing 8% FBS and 1% penicillin/streptomycin and transiently transfected with the shRNA vector along with PAX2 and VSV plasmids (which provide pivotal sequences required for virus assembling, packaging and production, provided by Dr. Carracedo). For 293T cell transfection, we used the calcium phosphate method.

Briefly, for a 10 cm^2 plate, 5 µg of lentiviral vector along with 2.5 µg PAX2 and 2,5 VSV plasmids were mixed in 500 µl of water, and then we added 50 µl of $CaCl_2$ 2,5 M. After that, we mixed this solution of DNA/Water/ $CaCl_2$ with 2X HBS (50 mM HEPES, 10 mM KCl, 1,5 mM Na_2HPO_4, 12 mM Glucose, 280 mM NaCl, ph 7,04) and waited 20 minutes before adding it to 293T cells. After overnight incubation, 293T medium was changed to fresh medium and, after 24 hours, we filtered viral supernatants with 0,45 µm filter (to avoid cross-contamination of the target cells with 293T virus-producing cells). We used this lentivirus-containing medium to transduce breast cancer cells with protamin sulphate (Sigma) at final concentration of 1 µg/ml. Protamin sulphate enhance virus binding and internalization into target cells. 293T cells were then feeded with fresh culture medium and incubated overnight for a second round of virus production and subsequent infection as before explained. Stably transduced cells were selected after culturing cells

for 2 days with 2 µg/ml of puromycin and afterwards kept in medium containing 0,5 µg/ml of puromycin. Stable Sox9 downregulation was assessed by western blot.

For stable Sox9 silencing in human breast epithelial cells, the same protocol mentioned before was employed, with the difference that 293T cells were transfected in Optimem medium (Gibco) in order to generate a virus supernatant without serum.

2.2 Establishment of Sox9 overexpressing cells

Sox9 overexpression in MCF10A cells was performed with the same protocol described for shRNA, but now using a plenti6.2-GFP and plenti6.2-Sox9 (kindly provided by Vincent J Hearing, NCI). For ALDEFLUOR analysis, a control cell line stably transfected with an empty vector (pLenti6.2-CMV-DEST) only carrying blasticidin resistance and no GFP gene was used to avoid green fluorescence that could interfere with the ALDEFLUOR assay. Stable cell lines were selected by using blasticidin hydrocloryde (Sigma), at a final concentration of 20 µg/ml. Experiments with MCF10A cells were performed for 10-15 passages after blasticidin selection.

3. Functional assays

3.1 Clonogenic assays

MCF-7-OH, MCF-7-TamR, T47D-OH, T47D-TamR, MDA-MB-231, BT549, were seeded at 500 cells/well in 6-well plates in DMEM/F12 (Gibco), 8% FBS (Sigma) 1% Pen/Strep (Gibco) and medium changed every three days. After 7-10 days, once visible colonies were formed, the medium was removed and cells were washed with PBS 1X. Colonies were fixed and stained with a 0.2% crystal violet -20% methanol solution and counted under the microscope.

3.2 Soft agar colony formation assays

In order to evaluate the ability of the cells with modulated level of Sox9 to grow in three-dimension in an anchorage-independent a two-layer soft agar colony formation assay was employed. Briefly, 10000 cells/well in 6-well plate were cultured in triplicate in complete medium with 0.35% low-melting agar (Pronadisa) over a bottom layer of complete medium with 0.7% regular agar (Pronadisa) for a period of 7-10 days (MCF-7,

MCF-7-TamR, T47D, T47D-TamR) or 3 weeks (MDA-MB-231) untill visible colonies were formed. Number of colonies formed was evaluated counting colonies in 9 independent fields in each well and representing the values as fold change of colony number formed respect to the control.

3.3 Cell proliferation assay

To check tamoxifen effect on cell proliferation on plastic surfaces, 1,000 MCF-7-TamR shCNTR and shSox9 cells were plated in triplicate in 96-well plate in complete medium. The day after, cells were treated with increasing concentration of tamoxifen ranging from 10^{-11} M to 10^{-6} M. Cell proliferation was evaluated after 4 days, removing the medium, washing with PBS and stain the cells with crystal violet (0.1% in 20% methanol). After removing crystal violet excess, the remaining crystals were dissolved with 10% Acetic acid (Sigma) and the relative 595 nm absorbance was measured in a spectrophotometer. The results are shown as fold change in proliferation compared to vehicle-treated cells (Ethanol) set as 1.

HBECs and MCF10A cells proliferation was evaluated similarly, plating 500 cells/well in triplicate in 96- well plate in supplemented WIT medium ad let grow for 6 days, changing the medium after 3 days.

3.4 MCF10A Aciny formation in Matrigel

HBECs and MCF10A (1000/well) were seeded in 96-well plate in triplicate, on the top of a layer of Matrigel (BD). HBECs were grown in in WIT-P-NC™ MEDIUM (Stemgent) supplemented with 1% penicillin/streptomicin and cholera toxin (Sigma), while MCF10A were grown in DMEM:F12 supplemented with 2% horse serum, 1% penicillin/streptomycin and 5 ng/ml EGF (Invitrogen). Colonies were grown for 8-10 days at 37° C in 5% CO_2 until acinar growth were reached; then colonies were counted under light microscope. Culture medium was replaced every 3 days. For immunofluorescent staining of MCF10A-GFP and MCF10A-Sox9 colonies, cell were grown 20 days to ensure lumen formation.

3.5 Colony differentiation assay on collagen

HBECs (1000/well) were seeded on glasses coverslips in a 12-well plates previously coated with Collagen (Sigma) and cultured with WIT-P-NC™ MEDIUM (Stemgent) supplemented with 1% penicillin/streptomicin. Culture medium was replaced every 3 days. Cells were cultured under this condition until colony formation was reached, then washed with PBS 1X and fixed in paraformaldeyde 4%. Subsequently, colonies were stained according to our immunofluorescence staining procedure (as following reported) with specific antibody for luminal (K18) or myoepithelial (K14) keratins and then counted with fluorescence microscope (Zeiss).

3.6 Invasion assay

In vitro invasion and migration assays were performed in a 24-well BD FalconTM HTS Multiwell Insert System containing an 8 µm pore size PET (PolyEthyleneTerepthalate) membrane. For invasion assays, the top of the upper wells was coated with 5 µg of Matrigel basement membrane matrix (BD) diluted in 50 µl of DMEM:F12 medium and allowed to air-dry overnight. The following day, matrigel was re-hydrated with medium for 2-3 h, and 20,000 MDA-MB-231 cells, previously starved in serum-free medium for 24 h, were added to the upper chamber. The lower chambers were filled with DMEM:F12 medium supplemented with 20% serum as chemoattractant. After 6 hours of incubation at 37°C in 5% CO_2, cells on the upper surface of the membrane were removed mechanically by cotton swab wiping, and invading cells on the lower side of the membrane were fixed and stained with crystal violet solution. At least nine different fields from each well were counted in triplicate to determine the number of invading cells.

4. Protein analysis

4.1 Western blot

Cells medium was removed and cells were washed with PBS and then lysed. Cell lysates were prepared directly with homemade Laemmli buffer (50 mM Tris pH 6,8, 1,25% SDS, 15%glycerol). All extracts were heated at 95ºC for 15 minutes for a complete lysis and denaturation and Lowry protein assay (BioRad) was used for the quantification of

protein extracts in a spectrophotometer. For nuclear and cytosolic protein fractionation, cells were washed with cold PBS and harvested with a buffer that maintain cell nuclei intact and lyse only the cytoplasmic membranes (composed by 10 mM HEPES, 1.5 mM MgCl2, 10 mM KCl, 0.5 mM DTT (Invitrogen) and protease and phosphatase inhibitors mix (Roche)). Extracts were kept on ice for 10´ and centrifuged at 5500 RPM for 5´.

Supernatants were stored as cytosolic fraction and the remaining were resuspended with an "high salt" buffer (composed by 20 mM HEPES, 1.5 mM $MgCl_2$, 25% glycerol, 420 mM NaCl, 0.2 mM EDTA, 0.5 mM DTT and protease and phosphatase inhibitors mix(Roche)) 20´ on ice. Lysates were centrifuged at 12000 RPM 10´ and cleared supernatant kept as nuclear extract. Cytosolic and nuclear extracts were stored at -80 ºC. Protein concentration was determined by spectrometry. After adjusting protein concentrations of all samples, β-mercaptoethanol (Applichem, 5% final concentration) and bromophenol blue (Sigma) were added. The resolving or running gels were prepared at a different concentration of acrylamide (BioRad). In most cases, 10% acrylamide resolving gels were used. After polymerisation was complete, a 4% acrylamide stacking gel was poured on the surface of the running gel.

A plastic comb was inserted into the stacking gel and then carefully removed after gel polymerization. Aliquots of the cell lysates were incubated at 95º C for 5 minutes and then loaded in the gel. The electrophoresis tank was filled with running buffer (1X, Running Buffer Omnipur® TG-SDS, Calbiochem, 9015-4L) and the samples were run fixing a constant voltage (below 15 mA during the stacking gel, up to 30 mA during the resolving gel). To visualize protein molecular weight ranges during electrophoresis, a marker (Prestained Protein Marker, BioLabs), containing colored proteins in the range of 7-175 kDa, was loaded on each gel. After running, the stacking gel was cut away and the transfer was set up in a semy-dry transfer apparatus (Trans-Blot SD Semi-Dry Transfer Cell, BioRad). At this stage, it was mounted in the following order on the transfer apparatus: three pieces of 3 MM paper (pre-wet in the transfer buffer (TRIS-SDS-glycine, containing 20% Ethanol), a piece of nitrocellulose (Protran BA 85, 0.45 µm, Whatman), the running gel, and other three pieces of pre-wet 3 MM paper.

After transfer procedure, membranes were washed twice with TBST and once with TBS. Prior to incubation with the antibody, all membranes were incubated in blocking solution (TBST 3% BSA or 5% milk) for 1 hour at room temperature. The blots were then incubated overnight at 4º C with the primary antibodies diluted in TBST 3% BSA. After incubation, the membranes were washed three times for 10´ at room temperature with TBST buffer and once with TBS buffer. To visualise the antigen/antibody interaction the membranes were then incubated for 45´ at room temperature with specific secondary antibodies conjugated with HorseRadish Peroxidase (HRP) diluted in TBS 1% milk. Finally, the membranes were washed three times with TBST and once with TBS, as described before. All incubations and washes were carried out with gentle agitation on a shaker. To detect the peroxidase label of secondary antibodies, membranes were incubated with a chemiluminescent substrate. Depending on the amount of the target protein and/or the efficiency of the antibody, two different substrates were used: the ECL TM (Amersham) and the SuperSignal West Femto (Pierce). The working solution for all substrates was prepared by combining the Luminol Enhancer and the Stable Peroxidase Buffer following manufacturer's instructions. The membranes were incubated with the appropriate working solution at different time-point, placed in an X-ray film cassette and covered with plastic wrap (primary and secondary antibodies are listed in table 2.1 and 2.2).

Finally, the proteins were visualized by exposing the membranes to X-ray films (HyperfilmTM ECL, Amersham or Konica Minolta films), which were developed using the AGFA Curix 60 Film Processor, or by acquiring digital images with the Molecular Imager ChemiDoc XRS System (BioRad). GAPDH, β-tubulin or β-actin were used as loading control. If necessary, the membranes were reprobed. To this purpose, the immunoassay was restarted from the blocking step.

Antibody	Isotype	Dilution	Clone/Cat.No.	Diluent
Sox9	Rabbit IgG1	1:2000	Millipore, AB-5535	3% BSA in TBST
Sox2	Goat IgG	1:500	Santacruz, sc-17320	3% BSA in TBST
ERα	Mouse IgG1	1:1000	6F11/Novocastra, NCL-L-ER	3%BSA in TBST
GAPDH	Mouse IgG1	1:50000	Sigma, G8795	3% BSA in TBST
β-ACTIN	Mouse IgG1	1:50000	AC-15/A5441	3% BSA in TBST
ERK	Rabbit IgG1	1:2000	Cell Signaling, #9102	3% BSA in TBST
Phospho-ERK	Rabbit IgG1	1:2000	Cell Signaling, #4377	3% BSA in TBST
β-tubulin	Mouse IgG	1:50000	Sigma	3% BSA in TBST
Lamin B1	Rabbit IgG	1:1000	Proteintech, 12987-1-AP	3% BSA in TBST

Table 2.1 List of primary antibodies used

Antibody/Conjugation	Host	Dilution	Company/Cat.No.
Anti-Mouse IgG (H+L)/HRP	Goat	1:3000	Biorad/170-6516
Anti-Rabbit IgG (H+L)/HRP	Donkey	1:10000	Jackson/711-035-152
Anti-Goat IgG (H+L)/HRP	Donkey	1:20000	Jackson/705-035-147

Table 2.2 List of secondary antibodies used

4.2 Immunofluorescence

Generally, approximately 100.000 primary cells were FACS sorted and then cytospun for 5´ at 800 RPM on poly-lysine coated slides. Cell lines were grown directly on glass slides. Cells were fixed with 4% paraformaldehyde (Sigma), permeabilized with PBS 0.3% Triton-X-100 and blocked with 8% FBS in PBT (PBS containing 0.05% Tween-20). Cells were then incubated overnight at 4º C with one of the following primary antibodies: rabbit anti-Sox9 (Millipore, AB5535) and mouse anti-ERα (6F11, Novocastra, NCL-L-ERα); and then with anti-rabbit alexa 568 (Molecular Probes, A10042) or anti-mouse alexa 647 (Molecular Probes, A31571) secondary antibodies. Finally, slides were mounted in Vectashield with DAPI (Vector) and visualized on the Leica confocal

microscope. MCF10A acini were stained according to Joan Brugge Lab indication (http://brugge.med.harvard.edu/protocols).

Briefly, MCF10A-GFP and Sox9 acini growing on matrigel have been fixed 10´ with paraformaldehye 4% (PFA, Santacruz) then permeabilized with pre-chilled 0.5% Triton X-100 in PBS for 10´at 4º C. Then, acini were rinsed with a PBS-Glycine 100 mM solution 3 times, (10´ each wash) to remove PFA and then permeabilyzed with IF blocking solution buffer (composed by 0,2% Triton-X-100, BSA 1% and Tween 0,05%) for 1 hour at RT. Subsequently, acini were incubated overnight with a mouse anti-human CD49f antibody directly conjugated with the fluorocrome APC. The following day, acini were washed 3 times with IF buffer (20´ each) and then incubated with 1 µg/ml of DAPI (Sigma) for 15´ at RT. After 5' wash in PBS, acini were incubated with Phalloidin-TRITC 15' at RT and then washed again with PBS. Slides were mounted using Vectashield (Vector) and photos were taken with a Leica confocal microscope.

4.3 Immunohistological analysis

Immunohistological staining on formalin-fixed, paraffin-embedded breast carcinomas was performed using the Leica Bond-III stainer. Following a preheating step for antigen retrieval (Bond epitope retrieval solution I, 20´, 100ºC), sections were washed (Bond wash solution) and incubated with anti-Sox9 antibody (1:100, Stemcell Technologies, cat. N. 01438) for 20´ at room temperature. Peroxidase was blocked for 10 min, followed by HRP and DAB with hematoxyline for contrast. Negative controls included omission of the primary antibody and IgG-matched control antibody. Two pathologists reviewed the samples blindly and graded the nuclear staining for Sox9 depending on its intensity and the percentage of positive neoplastic cells according to the Allred score. This method has been used also by other researchers (Harvey et al., 1999).

4.4 ALDEFLUOR assay and fluorescent activated cell sorting (FACS)

To measure cells with ALDH activity, the ALDEFLUOR assay was carried out according to manufacturer's (Stemcell Technologies) guidelines. Briefly, dissociated single cells were suspended in ALDEFLUOR assay buffer containing an ALDH substrate, bodipyaminoacetaldehyde (BAAA) at 1.5 mM, and incubated for 45 min at 37ºC. To

distinguish between ALDH-positive and -negative cells, a fraction of cells was incubated under identical conditions in the presence of a 2-fold molar excess of the ALDH inhibitor, diethylaminobenzaldehyde (DEAB). Negative cells were gated on the DEAB treated-cells and positive cells appeared in the no-DEAB teated cells, only in presence of ALDEFLUOR substate, BAA. In some experiments, the ALDEFLUOR assay was followed by staining with CD49f antibody conjugated with allophycocyanin (APC, eBioscience, 17-0495, diluted 1:100) and EpCAM conjugated to FITC (Stemcell technologies, 60147I, diluted 2:100). When antibodies staining for FACS was performed without ALDEFLUOR assay, cells were stained in PBS containing 3% BSA (Sigma) in which antibodies were diluted.

After 30' incubation on ice, cells were washed two times to remove the excess of unconjugated antibody and resuspended in FACS flow buffer (HEPES 25 mM, EDTA 5 mM, BSA 1% in PBS).

All incubations with antibodies, which were diluted in ALDEFLUOR assay buffer, were carried out on ice for 30 minutes and followed by two washes with ALDEFLUOR assay buffer.

For CD44/CD24/EpCAM analysis, cells were detached with TRyPLE 1X (Gibco) and stained with CD44 (BD, diluted 2:100) antibody conjugated with APC and CD24 conjugated with PE (BD, diluted 2:100). The viability dye 7-aminoactinomycin D (7AAD, BD) was added for dead cell exclusion. Cells were analysed or sorted using a FACSAria (BD) flow cytometer and analysed using the FACSDiva software.

5. mRNA analysis

5.1 RNA extraction, reverse-transcription (synthesis of first strand of cDNA) and Real-Time Polymerase Chain Reaction (PCR).

RNA was isolated using the GE healthcare Minispin Kit (GE Healthcare) or RNA Micro (Purelink) from Invitrogen, according to manufacturer instructions. Genomic DNA degradation was performed directly in column-retaining RNAs using DNAse included in the commercial Kit used. This is a very important step, since contaminations by genomic DNA may change profoundly the result. 1µg of DNAse-treated RNA was converted in the corresponding cDNA. 1 µM oligo(dT) (Ambion), 5X reaction buffer (Final 1X, Invitrogen),

5mM DTT (Invitrogen), 250 µM dNTPs (Biotools), 48 units RNAse OUT (Invitrogen) and 240 units of M-MLV reverse transcriptase (Invitrogen) were added to a total volume of 20 µl and the mixture was incubated at 25 ºC for 10´, followed by 50´ at 37 ºC. Finally, reaction is inactivated by 15´ samples incubation at 70 ºC. The resulting cDNAs were stored at -20 ºC. When RNA amount was very low, (for example from sorted population, a SuperScript® VILO ™ cDNA synthesis Kit (Invitrogen) was used instead, according to manufacturer instructions.

Real-time PCR was performed on a 7300 Real-Time PCR System (Applied Biosystems) or ViiA7 PCR System (Thermo Fisher). Briefly, real-time PCR was performed using the iTaq™ SYBR® Green Supermix with ROX (BioRad). cDNA was amplified using the following conditions: 95º C for 5´ , 40 cycles of amplification (95º C for 15´´, 61ºC for 1´) and dissociation stage. 36B4 was used as a reference transcript for normalization. The results are presented as fold change calculated with 2-ΔΔct method. Primer (Invitrogen) sequences can be found in the following table 2.3.

5.2 RNAseq analysis and Gene set enrichment analysis (GSEA)

RNA extraction from MCF7-TamR and MDA-MB-231 shCNTR and shSox9 cells was performed with the miRNeasy Mini Kit (Catalog no. 217004 QUIAGEN) according to manufacturer protocol. RNAseq analysis and GSEA analysis was performed at the Genomic Platform at CICbioGUNE.

GENE	FWD 5'-3'	REV 5'-3'
Sox9	AGACCTTTGGGCTGCCTTAT	TAGCCTCCCTCACTCCAAGA
Sox2	GCACATGAACGGCTGGAGCAACG	TGCTGCGAGTAGGACATGCTGTAGG
PS2	TCGGGGGTCGCCTTTGGAGCAG	GAGGGCGTGACACCAGGAAAACCA
ALDH1A3	TCTCGACAAAGCCCTGAAGT	TATTCGGCCAAAGCGTATTC
ALDH1A1	TGTTAGCTGATGCCGACTTG	TTCTTAGCCCGCTCAACACT
FZD4	GACAACTTTCACACCGCTCA	TCTTCTCTGTGCACATTGGC
AXIN2	AAGTGCAAACTTTCGCCAAC	ACAGGATCGCTCCTCTTGAA
BMI-1	TTGTCTTTTCCGCCCGCTTC	AGTACCCTCCACAAAGCACAC
36B4	GTGTTCGACAATGGCAGCAT	GACACCCTCCAGGAAGCGA
ERα	CCACCAACCAGTGCACCATT	GGTCTTTTCGTATCCCACCTTTC
PgR	CGCGCTCTACCCTGCACTC	TGAATCCGGCCTCAGGTAGTT
AREG	TGGAAGCAGTAACATGCAAATGTC	GGCTGCTAATGCAATTTTTGATAA
GATA3	CTGCTTCATGGATCCCTACC	GATGGACGTCTTGGAGAAGG
ELF5	AGTCTGCACTGACATTTTCTCATC	CAGAAGTCCTAGGGGCAGTC
FOXA1	CATTGCCATCGTGTGCTTGT	CCCGTCTGGCTATACTAACACCAT
FOXO3A	CAAGGATAAGGGCGACAGCA	GGACCCGCATGAATCGACTA
c-KIT	GGCACGGTTGAATGTAAGGC	CAGGGTGTGGGGATGGATTT
α-SMA	TATCCCCGGGACTAAGACGG	CTTACAGAGCCCAGAGCCATT
SNAI1	UUGUCCUCCUCGCUCUCCUUCUUCA	TGAGTGGGTCTGGAGGTGG
SNAI2/SLUG	GCCAAACTACAGCGAACTGG	AGTGATGGGGCTGTATGCTC
ZEB-1	AAGAATTCACAGTGGAGAGAAGCCA	CGTTTCTTGCAGTTTGGGCATT
Vimentin	GCTTCAGAGAGAGGAAGCCG	AAGGTCAAGACGTGCCAGAG

Table 2.3. Primers list used.

6. siRNA and DNA transfections

6.1 Small interfering RNA transfection (siRNA transfections)

Small interfering RNA oligonucleotides (siRNAs) were transfected in MCF-7-TamR and ZR75-1 cells using Lipofectamine 2000 (Invitrogen) according to the manufacturer's

protocol. In MDA-MB-231 and BT549 cells, RNAiMAX (Invitrogen) has been used instead, according to manufacturer instructions. siRNA oligos (40 nM) were used to transfect siRNA and after 48 hours RNA, protein, or cells were harvested and analysed. Sox9 silencing was confirmed by western blot or qRT-PCR. siRNA sequences used in this study are listed below:

siCNTR (siMISSION from Sigma, Cat. Number: SIC001),

SiSox9 (1): UGAAGAAGGAGAGCGAGGAGGACAA

SiSox9 (2): UUGUCCUCCUCGCUCUCCUUCUUCA

SiSox2: 5' CCUGUGGUUACCUCUUCCUCCCACU 3'

6.2 WnT transcriptional assay (TOP/FOP assay)

To evaluate the WnT/β-catenin transcriptional activity in MDA-MB-231 and BT549 cells with modulated Sox9 level, we employed a WnT/β-catenin TOP/FOP assay. Briefly, 40000 cells were seeded in triplicate in 24-well plate, and the following day the cells were transfected using Lipofectamine LTX/Plus (Invitrogen), according to manufacturer instructions. Dr. R. Kypta kindly provided 8XTOPflash and 8XFOPflash plasmids and a vector expressing beta-galactosidase was used as control for the efficiency of transfection. A β-catenin plasmid was used to activate transcriptionally the FOP/TOP plasmid.

24 hours post-transfection, cells were harvested and assayed for luciferase and beta-galactosidase activities using, respectively, the Luciferase Assay Kit (Promega) and the Tropix Galacto-Light-Plus Assay (Applied Biosystems). Results are shown as TOP/FOP transcriptional activity in MDA-MB-231 or BT549 shSox9 cells versus shCNTR cells, which value has been set as 1.

7. DNA-protein interaction

7.1 CHromatin ImmunoPrecipitation (CHIP)

In order to evaluate DNA-protein interaction, we used CHromatin ImmunoPrecipitation (CHIP), carried out following a commercial kit from Cell Signaling (SimpleChIP® Enzymatic IP Kit (Magnetic beads, cat. Num. 9003).

Briefly, at least 10^7 cells were cross-linked with 1% formaldehyde and reaction was quenched by 1M glycine. Cells were lysed by using buffers provided, called A and B. Subsequently, nucleic acids were digested by the addition of Micrococcal nuclease for 20´ at 37 Cº in an orbital shaker. Reaction was quenched by the addition of EDTA. Micrococcal nuclease digestion was followed by sonication to shear chromatin. Resulting chromatin was stored at -80º for subsequent chromatin immunoprecipitation and a small sample of the chromatin was used to analyse the effectiveness of chromatin digestion (in a 1% agarose gel) and determination of chromatin concentration obtained. A proper chromatin digestion give rise to genomic DNA fragments between 100-1000 nucleotides.

Each ChIP reaction was carried out by using 10 ug of chromatin incubating overnight (with rotation) with control rabbit IgG, Sox9 (AB5535, Millipore) or Sox2 (AB5603, Millipore) antibodies, both used at 2 ug/ChIP. For this last step, chromatin was subjected to RNAse and Proteinase K treatment (to eliminate RNA and protein from the sample preparation) and then DNA was purified through columns provided by the Kit.

Before immunoprecipitation, 2% of the diluted chromatin have been removed and stored at -20 Cº for subsequent DNA purification and used as “chromatin input”. The next day, 30 µl of protein G-magnetic beads were added to the chromatin–antibody solution and incubated with rotation for 2 hours at 4º C. Washes and elution of antibody-bound chromatin were performed following manufacturer’s instructions, using a magnetic beads separator. Chromatin elution from the antibody/protein G magnetic beads was obtained in ChIP elution buffer, incubating protein G/antibody/chromatin complex at 65 Cº for 30´ and protein-DNA crosslink reversal was performed treating with Proteinase K 2 hours at 65 Cº. Bounded DNA from antibodies and in the 2% input chromatin was purified by using column (Cell Signalling Kit-provided) and then stored at -20 Cº. Quantitative real time

PCR (qRT-PCR) was carried in triplicate by using a Viia7 PCR system (Thermo Fisher) with SybrGreen reagents, combining for each reaction: 6 µl of water, 1 µL of 5 µM FWD primer, 1µl of 5 µM REV primer and 10 µl SybrGreen reagents and 2 µl of eluted DNA. Primers used for amplification are listed below (Table 2.4)..

Promoter binding site	FWD 5'-3'	REV 5'-3'
Site A Sox9 in ALDH1A3 promoter	**CGATTAGCAGCAAAGGTCTCATGT**	**ACACCGCCTTCCATCCCAGA**
Site B Sox9 in ALDH1A3 promoter	**GGAGCAGAGTTCTAAGCTCAA**	**GAAATTATGTCACTGCCAGG**
Sox9 on Sox2 promoter	**GTAAGAGAGGAGAGCGGAAGAG**	**CGGCTGTCCAACTCGTATTTCT**
Sox2 on Sox9 promoter	**CCAGAGTGGAGCGTTTTGTC**	**TGTCTGGGGGAGAGTTTGCTA**
Sox2 on Cyclin D1 promoter	**TGCCGGGCTTTGATCTTT**	**CGGTCGTTGAGGAGGTTGG**

Table 2.4. primers used in ChIP analysis.

8. Statistical analysis

Data from at least three independent experiments were expressed as means SD. Each data point of real-time PCR, mammosphere formation, colony formation, luciferase activity assays and proliferation was run at least in triplicates and independent experiments were performed at least three times. Student's t-test or Anova were used to determine statistically significant differences and $p<0.05$ was considered to be statistically significant unless otherwise specified.

Chapter 3: Results

1. Sox9 expression in the human breast

We sought to determine whether Sox9 was expressed differentially among different cell sub-populations luminal, progenitor cells, stromal or stem/myoepithelial cells. We employed Fluorescence-Activated–Cell-Sorting (FACS) in order to separate different breast cell populations derived from mammary gland tissue obtained by reduction mammoplasty.

Cells were sorted according to commonly used membrane markers (Lim et al., 2009) to differentiate between mature luminal ($CD49f^{-}EpCAM^{+}$), luminal progenitor ($CD49f^{+}EpCAM^{+}$), myoepithelial/stem ($CD49f^{+}EpCAM^{-}$) and negative/stromal cells ($CD49f^{-}EpCAM^{-}$) (Fig. 3.1.1).

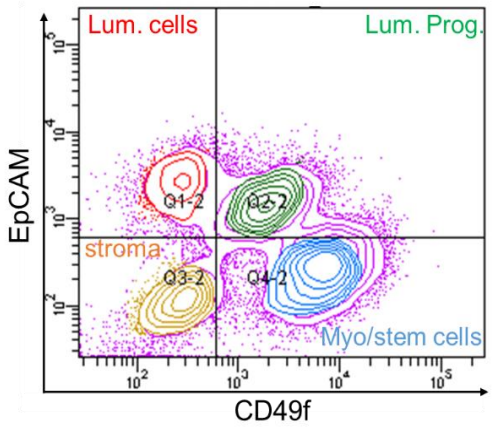

Fig 3.1.1. Representative FACS distribution of mature luminal cells ($CD49f^{-}EpCAM^{+}$), luminal progenitor cells ($CD49f^{+}/EpCAM^{+}$), myoepithelial/stem cells ($CD49f^{+}EpCAM^{-}$) and negative/stromal cells ($CD49f^{-}EpCAM^{-}$) in the human breast.

We performed cell sorting in human glandular mammary epithelial cells deriving from 3 different patients (Fig. 3.1.2). The luminal progenitor cells, characterized by the expression of both CD49f and EpCAM ($CD49f^{+}EpCAM^{+}$), expressed the highest level of Sox9, compared to the other cell populations. Stromal cells barely expressed Sox9, similarly to the mixed stem/myoepithelial cells. Modest levels of Sox9 expression were detected in luminal differentiated cells.

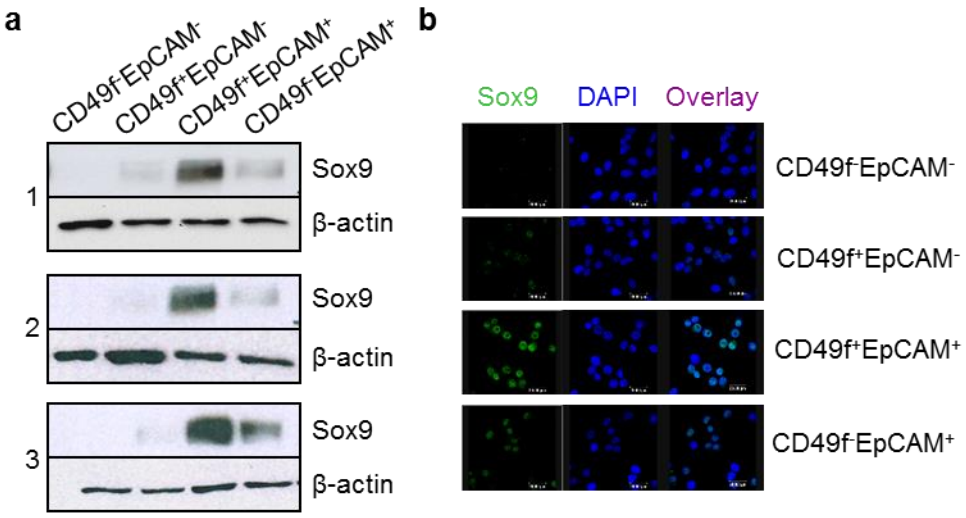

Fig. 3.1.2 Sox9 expression in sorted breast epithelial cell populations. **(a)** Sox9 protein levels in $CD49f^{-}EpCAM^{-}$, $CD49f^{+}EpCAM^{-}$, CD49f+$EpCAM^{+}$ and $CD49f^{-}EpCAM^{+}$ cell populations from three different primary human breast epithelial cell samples were assessed by western blot. **(b)** Immunofluorescence analysis of Sox9 expression in $CD49f^{-}EpCAM^{-}$, $CD49f^{+}EpCAM^{-}$, $CD49f^{+}EpCAM^{+}$ and $CD49f^{-}EpCAM^{+}$ cell populations sorted from primary human breast epithelial cells.

Almost 80% of the $ALDEFLUOR^{+}$ population were luminal progenitor cells ($CD49^{+}EPCAM^{+}$), while most of the mixed stem/myoepithelial cell population was found in the $ALDEFLUOR^{-}$ population in the various human breasts analyzed, suggesting that $ALDEFLUOR^{+}$ and $CD49f^{+}EpCAM^{+}$ cells mostly identify the same cell population (Fig. 3.1.3).

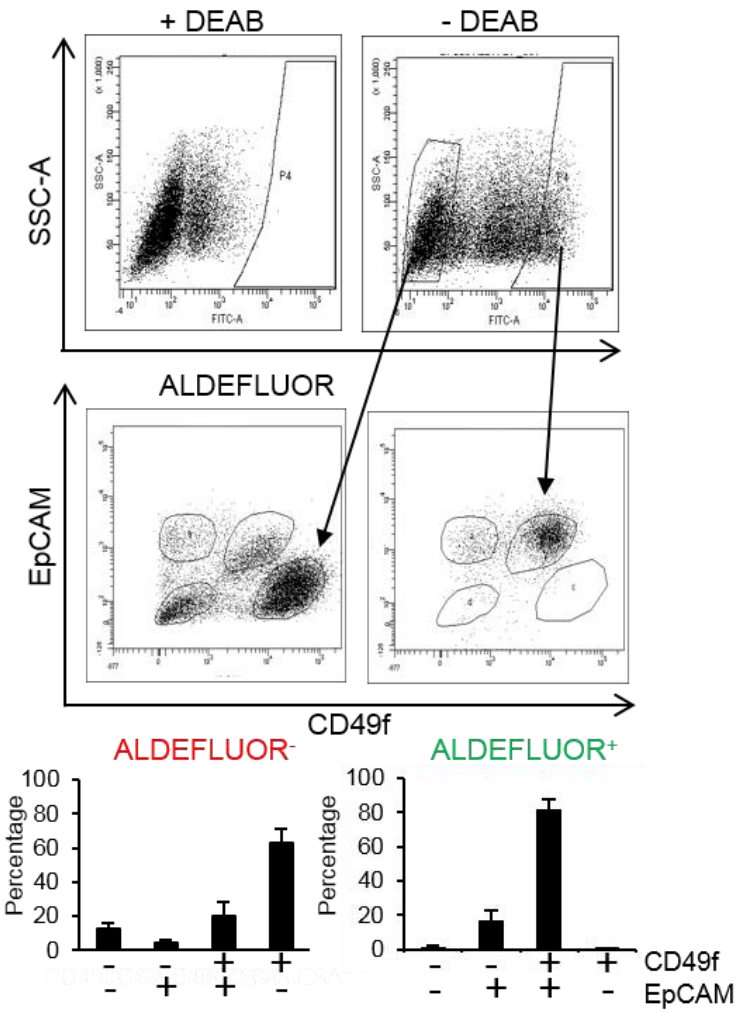

Fig. 3.1.3 ALDEFLUOR$^+$ cells distribution in the human mammary gland. Representative FACS plots show that ALDEFLUOR$^+$ cells in the human breast are mostly CD49f$^+$EpCAM$^+$ luminal progenitor cells. Error bars represent standard deviation (SD). SSC-A: side scatter.

Analysis of Sox9 levels in ALDEFLUOR$^-$ and ALDEFLUOR$^+$ cells sorted form human mammary epithelial cells showed the increased expression of Sox9 in ALDEFLUOR$^+$ cells compared with negative cells (Fig. 3.1.4)

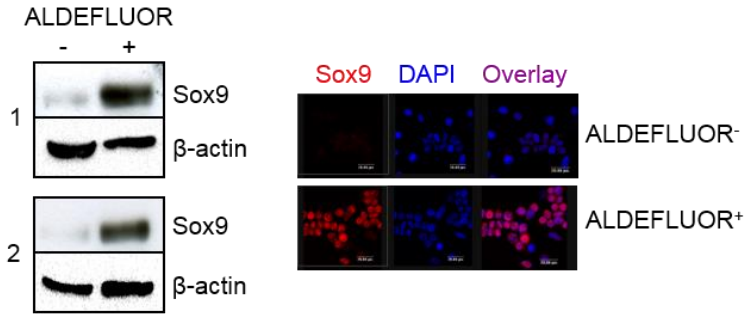

Fig 3.1.4. Sox9 expression in ALDEFLUOR$^-$ and ALDEFLUOR$^+$ cells sorted form human breast epithelial cells. Sox9 levels in ALDEFLUOR$^-$ (-) and ALDEFLUOR$^+$ (+) cells sorted from two different samples (1 and 2). An Immunofluorescence analysis of Sox9 expression in ALDEFLUOR$^+$ and ALDEFLUOR$^-$ cells sorted from human breast epithelial cells.

These results suggest that Sox9 marks luminal progenitor cells in the human breast, and it is mainly expressed in ALDEFLUOR$^+$ and CD49f$^+$EpCAM$^+$ cells.

Conclusions:

Sox9 is expressed in the human mammary gland, especially in luminal progenitor cells (CD49f$^+$EpCAM$^+$ALDEFLUOR$^+$); in addition, these two populations are mostly overlapping. These observations suggest that Sox9 is a marker of luminal progenitor cells in the human breast.

2. Effect of Sox9 level modulation in human breast epithelial cells (HBECs)

We sought to determine the effect of Sox9 modulation in human breast epithelial cells. Since primary cells are hard to transfect, we employed a shRNA lentiviral-based approach to silence Sox9, which levels were successfully reduced in these lentiviral-transduced primary cells (Fig. 3.2.1).

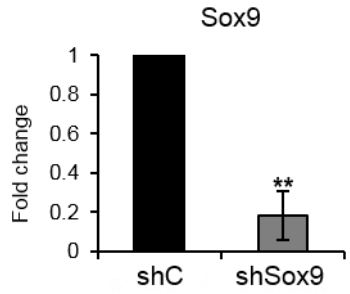

Fig. 3.2.1 Sox9 mRNA expression in human primary breast epithelial cells stably transduced with shcontrol (shc) and shSox9 lentivirus (n=5). ** =p<0.001.

Analysis of the ALDEFLUOR$^+$ population in shSox9 and shCNTR HBECs from 3 independent human primary epithelial cell preparations, showed a clear decline in ALDEFLUOR$^+$ in shSox9 cells compared to control cells (Fig. 3.2.2).

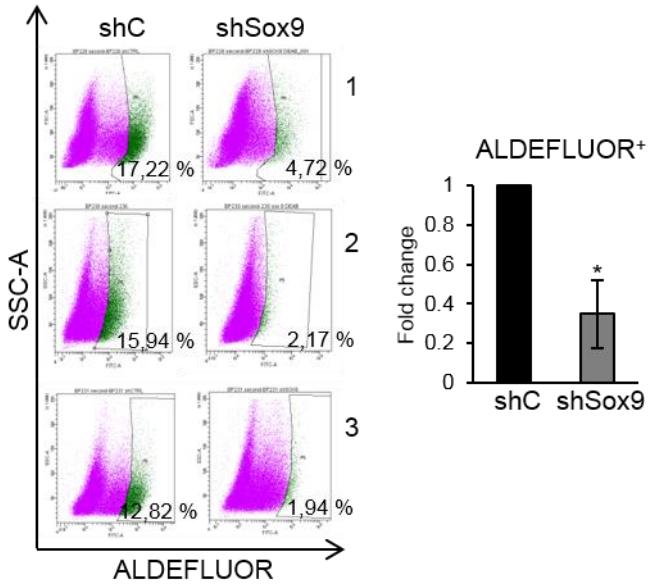

Fig. 3.2.2 Representative FACS plots and graph showing ALDEFLUOR$^+$ cells (in green) in shcontrol (shC) and shSox9 human breast epithelial cells obtained from 3 different tissue donors.

On the other hand, Sox9 overexpression in human non-tumorigenic epithelial MCF10A cells led to a slight but significant increase in ALDEFLUOR+ cells (Fig 3.2.3).

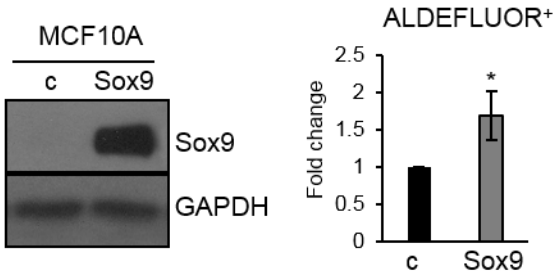

Fig. 3.2.3 ALDEFLUOR+ cells in MCF10A Sox9 overexpressing cells. Immunoblot of Sox9 in MCF10A cells stably transduced with pLenti-6.2-GFP (c) and pLenti-6.2-Sox9 (Sox9). * p<0.05 by t-test.

This results claims that Sox9 marks and maintains ALDEFLUOR+ luminal progenitor cells in human breast. In addition, the effect of Sox9 silencing on HBECs proliferation onplastic surface and in three-dimentions (3D)was evaluated (Lim et al., 2009). Interestingly, Sox9 silencing in HBECs significantly reduced proliferation both on adherent conditions and in matrigel, while Sox9 overexpression modestly, but significantly, increased colony formation in MCF10A cells in Matrigel, without affecting cell proliferation (Fig. 3.2.4).

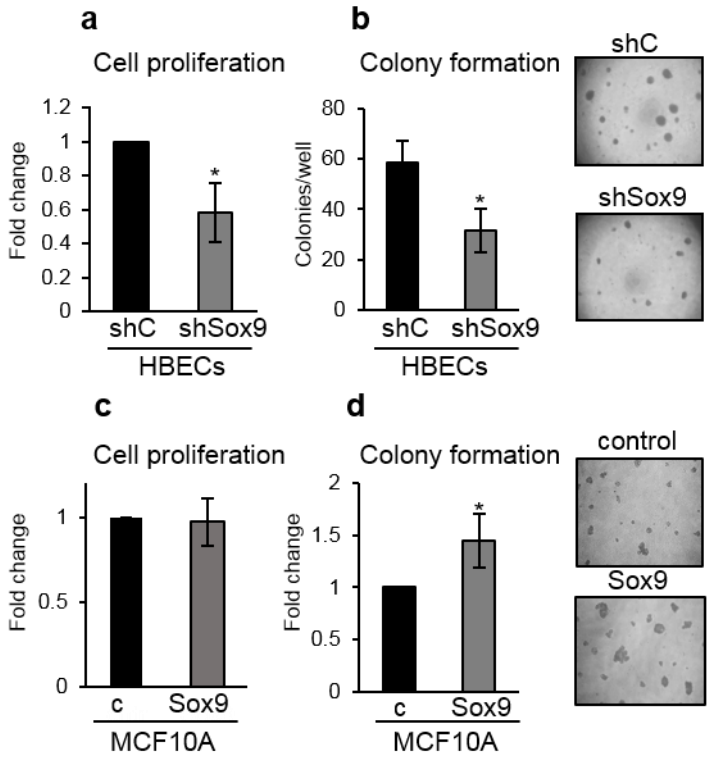

Fig. 3.2.4. Sox9 modulation alters HBECs proliferation and colony formation. Effect of Sox9 silencing on cell proliferation **(a)** and colony formation **(b)** of HBECs. MCF10A cell

proliferation in control cells (overexpressing GFP) or with increased Sox9 levels **(c)** and in matrigel **(d).** Representative photos are shown**.** * p<0.05**.**

In addition, we also evaluated the effect of Sox9 modulation on stem/progenitor cell self-renewal capacity by analyzing primary and secondary mammosphere formation. In cells derived from 4 different primary samples, Sox9 stable silencing reduced primary and secondary sphere formation compared to control cells (Fig. 3.2.5a). Conversely, Sox9 overexpression in MCF10A cells increased primary and secondary mammosphere formation (Fig. 3.2.5b) suggesting that Sox9 maintains the stem cell content and positively influences stem cell self-renewal of normal breast epithelial cells.

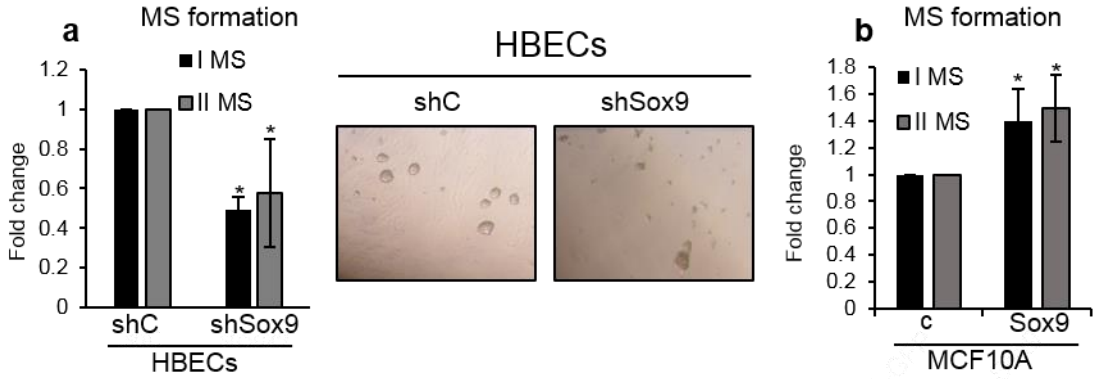

Fig. 3.2.5 Sox9 modulation alters mammosphere formation. **(a)** Primary (I MS) and secondary (II MS) mammosphere formation in HBECs shC (sh Control) and shSox9. **(b)** I MS and II MS formation in MCF10A control and MCF10A-Sox9. * p<0.05.

Finally, the levels of expression of relevant genes involved in mammary gland stem cell biology was analyzed using 5 different sets of breast epithelial cells stably silenced for Sox9 (shC as control). Sox9 down-regulation did not significantly affect the luminal cell differentiation marker GATA3 (Asselin-Labat et al., 2007b) (at least at mRNA level), while ELF5 (Choi et al., 2009) was reduced in shSox9 cells compared to control cells.

The stem/luminal progenitor markers ALDH1A3 (Eirew et al., 2012), c-KIT (Regan et al., 2012), and stem markers FOXO3A (Miyamoto et al., 2007) and SNAI2/SLUG (Guo et al., 2012a) were reduced compared to control cells (Fig. 3.2.6). In particular, ALDH1A3 mRNA reduction among the 5 different breast epithelial cell preparations analyzed is consistent with the observation that Sox9 down-regulation reduces the amount of ALDEFLUOR^{+} cells. ALDH1A1 level was not affected by Sox9 modulation.

FOXA1, important for estrogen signaling (Hurtado et al., 2011) and PR, a marker of ER activity (ref), were reduced by Sox9 silencing (Fig. 3.2.6).

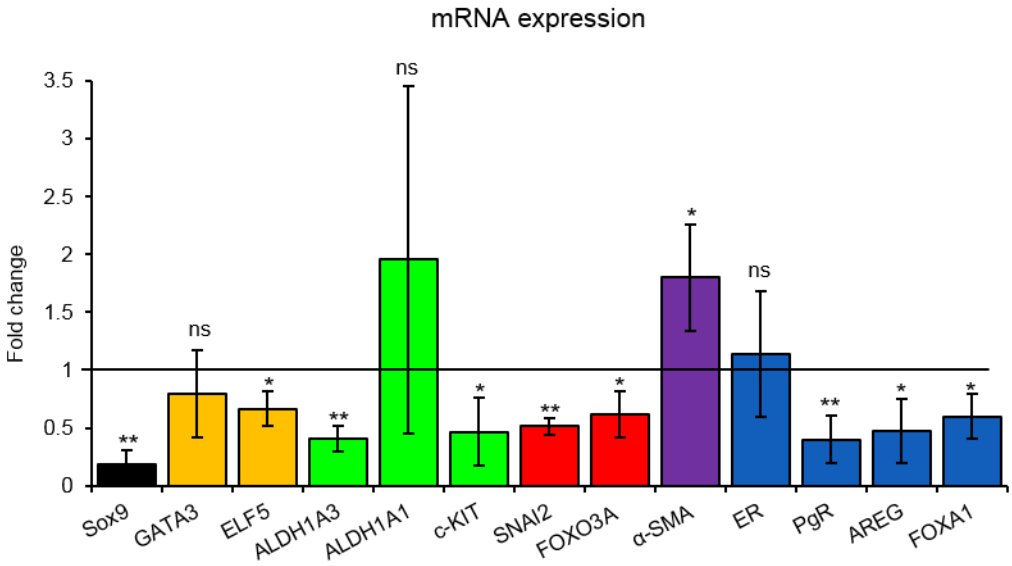

Fig. 3.2.6 Transcript levels of different genes in shSox9 primary human breast epithelial cells compared to shcontrol cells (n=4/5). Error bars represent standard deviation (SD). *p<0.05, **p<0,001). (Two-tail t-test).

In order to determine whether Sox9 expression levels influence the differentiation potential of the progenitor cells, the number of multilineage colonies generated by shcontrol and shSox9 epithelial cells was tested by culture on collagen. The percentage of cells with bilineage differentiation potential (mixed colonies, $K18^{+}K14^{+}$) was unaffected (Fig. 3.2.7). In contrast, silencing of Sox9 clearly reduced the number of luminal colonies ($K18^{+}$) formed, while the percentage of myoepithelial colonies ($K14^{+}$) was increased (Fig. 3.2.7). These results support the hypothesis that Sox9 regulates lineage specification by human luminal progenitors.

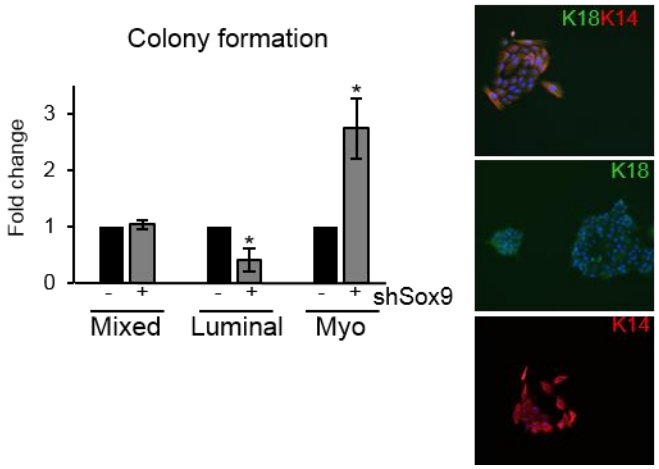

Fig. 3.2.7 Luminal (K18+), myoepithelial (K14+) and mixed (K18+/K14+) colonies formed on collagen-coated wells from human primary breast epithelial cells shcontrol (-) and shSox9 (+). Results are shown as fold change in number of colonies compared to shcontrol cells (n=3). Representative colony images are shown. *p<0.05

Some of the patient characteristics from which samples breast epithelial cells were isolated are summarized in the following table (Table 3.1):

Breast preparation number	Age	Day of menstrual cycle	Number of children	Number of Breast-fed Children	Contraceptive Pill Intake
Sample 1	24	21	0	N/A	No
Sample 2	29	24	3	0	No
Sample 3	42	22	1	1	No
Sample 4	15	N/A	0	0	No
Sample 5	19	N/A	0	0	No

Table 3.1 Clinical data of patients participating in this study. Samples were obtained from women undergoing reduction mammoplasty with no previous history of breast cancer. N/A – Not Applicable.

Conclusions:

These results indicate that Sox9 could be either successfully silenced in HBECs, or overexpressed in MCF10A mammary epithelial cells by using respectively shRNA or Sox9 cDNA carried by lentiviral vectors. Sox9 silencing in HBECs led to a reduction in the

ALDEFLUOR$^+$ cell population, cell proliferation and mammosphere formation, while Sox9 overexpression in MCF10A cells increased growth in Matrigel and ALDEFLUOR$^+$ cells. Finally, Sox9 silencing reduced luminal epithelial cell differentiation on collagen. Collectively, these results suggest a role for Sox9 in human mammary stem/progenitor cell maintenance and luminal differentiation (Fig. 3.2.7).

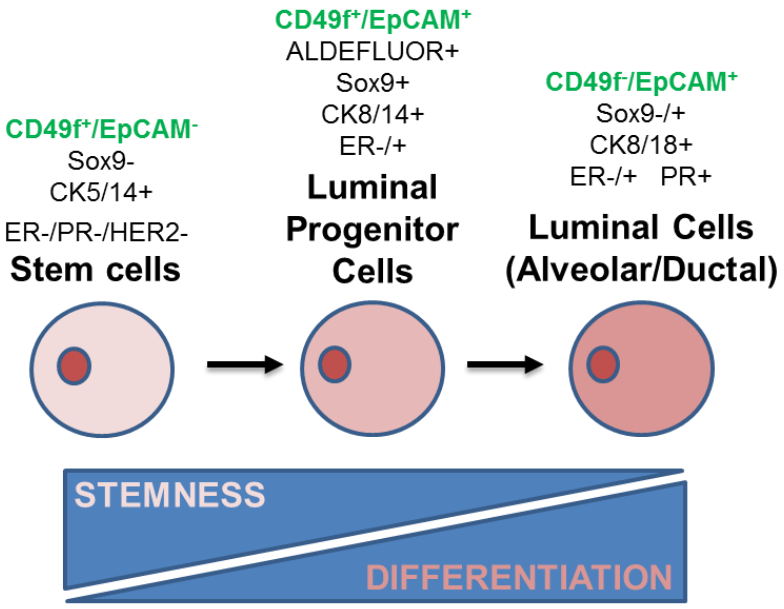

Fig. 3.2.7 Luminal cells differentiation hierarchy in the human breast.

3. Sox9 expression in breast tumors

It has been reported that Sox9 is involved in tumorigenicity in different tissues, so we investigated whether Sox9 was more expressed in breast tumor cells compared to normal breast tissue.

We attempted to answer this question by using primary breast samples received from the local hospital of Galdakao (Galdakao, Bilbao, Spain) or from a clinic located in Bilbao (PreteImagen). Increased Sox9 expression was observed in tumor tissue compared to the normal counterpart both at mRNA (Fig. 3.3.1a) and protein level (Figure 3.3.1b).

In general, Sox9 was more expressed in samples coming from ER- patients (n=5) than ER+ positive patients (n=6), which confirms the observation made by Chakavarty and collaborators (Chakravarty et al., 2011a). In two cases (10 and 11) we checked also Sox9 expression in peritumoral tissue but compared to normal, peritumoral and tumoral tissues, only tumor tissues showed Sox9 expression (Fig. 3.3.1b). A table of patient's characteristics is shown in Table 3.2 and Table 3.3.

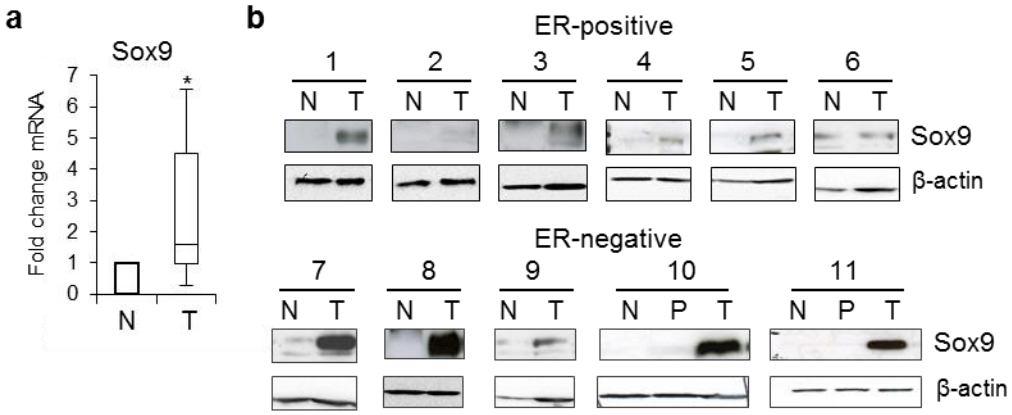

Fig. 3.3.1 Sox9 expression in normal and tumor breast tissues. **(a)** Sox9 mRNA expression levels in human breast tumour (T) samples compared to their normal (N) counterparts (n=13). **(b)** Immunoblot of Sox9 and β-actin (loading control) in a set of ER-positive and ER-negative breast tumours (T) compared to the corresponding normal (N) and peritumoral (P) tissue. *p<0.05.

Number	1	2	3	4	5	6	7	8	9	10	11	12	13
Age	78	49	68	45	59	76	72	76	59	51	34	41	80
ER	+	+	+	+	+	-	-	-	-	+	+	+	-
PR	+	+	+	+	+	-	-	-	-	-	+	-	-
HER2	+++	-	-	+++	-	+++	+++	+++	+++	+++	++	+++	-
Ki67	7%	20%	5%	25%	50%	20%	30%	90%	10%	20%	60%	60%	?

Table 3.2: Characteristics of the tumor samples in figure 3.3.1a ?: not known

Number	1	2	3	4	5	6	7	8	9	10	11
Age	73	49	?	52	47	46	79	?	38	79	72
ER	+	+	+	+	+	+	-	-	-	-	-
PR	+	+	+	+	+	+	-	-	-	-	-
HER2	+	-	-	-	-	?	-	-	-	-	-
Grade	2	3	3	2	2	2	2	?	?	3	3
Ki67	10%	25%	?	50%	15%	?	7%	?	30%	60%	80%

Table 3.3 Characteristics of the tumor samples in figure 3.3.1b ?: not known.

Interestingly, human breast cancer cell lines recapitulate this observation, since ER+ cell lines, such as MCF-7, T47D and ZR-75-1 expressed lower Sox9 levels than the triple negative breast cancer cell lines MDA-MB-231 and MDA-MB-468, both at mRNA (Fig. 3.3.2a) and protein level (Fig. 3.3.2b).

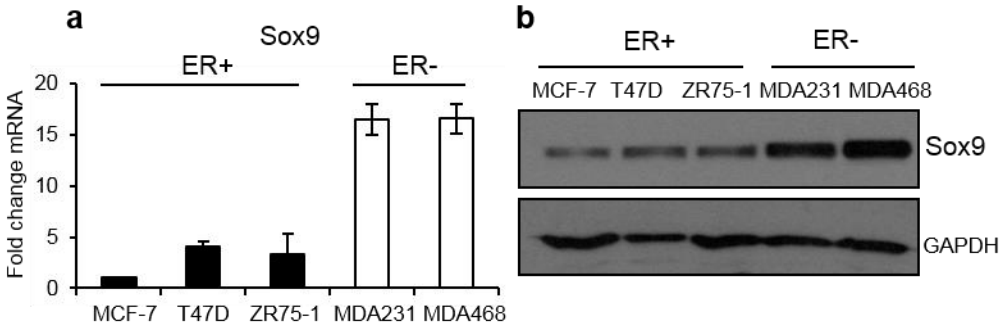

Fig. 3.3.2 Sox9 expression in ER- and ER+ breast cancer cell lines. Sox9 mRNA **(a)** and protein **(b)** expression levels in ER-positive (MCF7, T47D, and ZR75-1) and ER-negative (MDA-MB-231 and MDAMB-468) breast cancer cells.

This observation was further supported by interrogating publicly available breast tumor datasets for Sox9 levels. For example, in a study by the group of Massagué (Minn et al., 2005) GEO2R code: GSE2603), Sox9 was significantly more expressed in ER- samples (n=42) than in ER+ tumors (n=57) (Fig. 3.3.3a).

Furthermore, we also checked the **GOBO** database (**G**lobal expression-based **O**utcome for **B**reast cancer **O**nline, (http://co.bmc.lu.se/gobo, (Ringnér et al., 2011), and confirmed increased Sox9 expression in ER- tumors using a large patient cohort (ER+= 1225, ER-=395) (Fig. 3.3.3b). In the GOBO database we analyzed as well the expression of Sox9 in different breast cancer cell lines grouped by breast cancer subtype. The highest

Sox9 expression was found in the basal A and TNBC subtypes, while the lowest expression was foiund in hormone-responsive cells (fig. 3.3.3c).

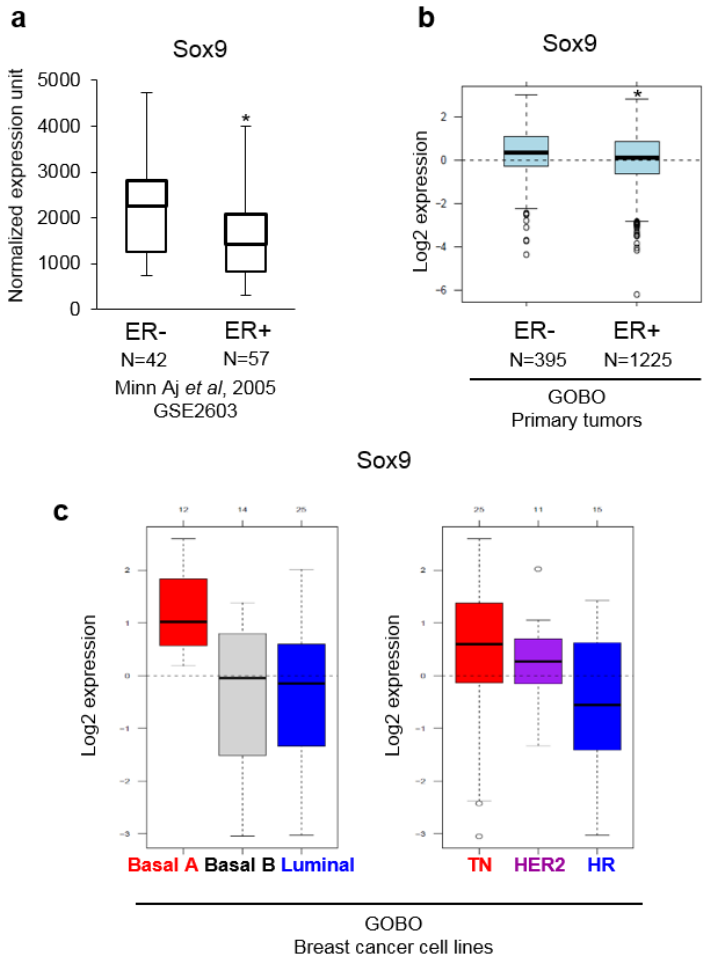

Fig. 3.3.3 ***In silico*** **analysis of Sox9 expression in ER- and ER+ breast tumors and breast cancer cell lines**. **(a)** Sox9 expression in ER-negative and ER-positive tumours in a public GEO2R dataset (GSE2603). Sox9 mRNA expression in ER-negative and ER-positive tumours (**b)** and in breast cancer cell lines (**c**) in the GOBO database. *p<0.05.

Examination of the public database Kaplan-Meyer plotter (http://kmplot.com/analysis/) showed that high Sox9 expression in patients with basal breast cancer correlated with significantly reduced recurrence-free survival (RFS) compared with patients with low Sox9 expression (Fig. 3.3.4).

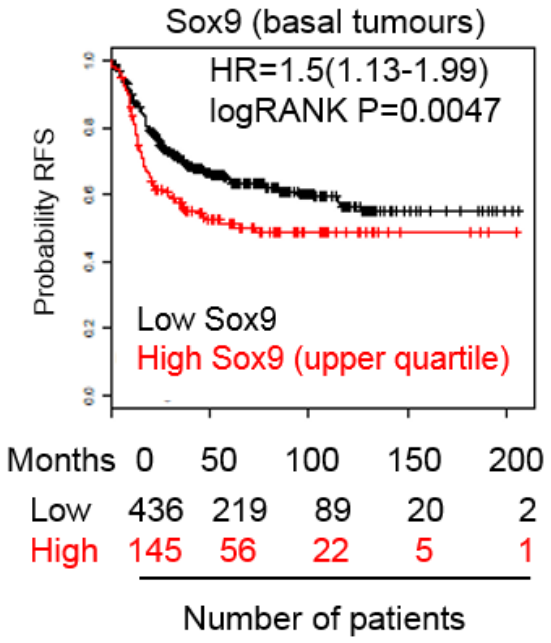

Fig. 3.3.4 RFS in patients with breast cancer separated according to Sox9 expression in the upper quartile and the rest of the population (KM plotter). Patients with high (red) and low (black) expression are indicated. Hazard ratio (HR) and *p*-value (log rank p) is depicted for the survival analysis. RFS: relapse free survival.

Conclusions:

All together, these results show that Sox9 is induced during breast tumorigenesis and it is more expressed in ER- and basal tumors than in ER- tumors and, accordingly, its expression negatively correlates with survival in basal breast cancers.

4. Sox9 is regulated by estrogen

ER expression in breast cancer is correlated with increased survival and response to tamoxifen treatment (Cleator et al., 2009; Sørlie et al., 2001). Estrogen signaling induces a stem cell differentiation in the breast stem cell compartment (Domenici et al. 2014; Simões et al., 2011) so, we sought to determine whether Sox9 could be regulated by estrogen. MCF-7 cells treated with estrogen showed strong downregulation of Sox9 mRNA in a time-dependent manner (Fig 3.4.1a). PS2 (also known as TFF1), a well-known ER target gene used as a positive control, was increased in parallel, (Fig 3.4.1a). This reduction was also observed at the protein level in different ER-positive breast cancer cell lines, T47D and ZR-75-1 (Fig 3.4.1b). This observation was further confirmed by using

another pharmacological approach. Treatment of MCF-7 cells with the ER antagonist ICI 182,720 (Fulvestrant®), which induces ER proteasomal degradation, resulted in a significant recovery of Sox9 expression, both at the mRNA and protein level (Fig 3.4.1c).

In addition, such observation was further confirmed with available *in silico* data. (Al Saleh et al., 2011a). Microarray analysis of transiently reduced ER levels by siRNA in MCF-7 cells (GSE27743,) showed that siERα cells expressed more Sox9 compared to control (siC) cells, mimicking the effect observed by pharmacological disruption of ERα using Fulvestrant treatment in MCF-7 cells (Fig. 3.4.1d).

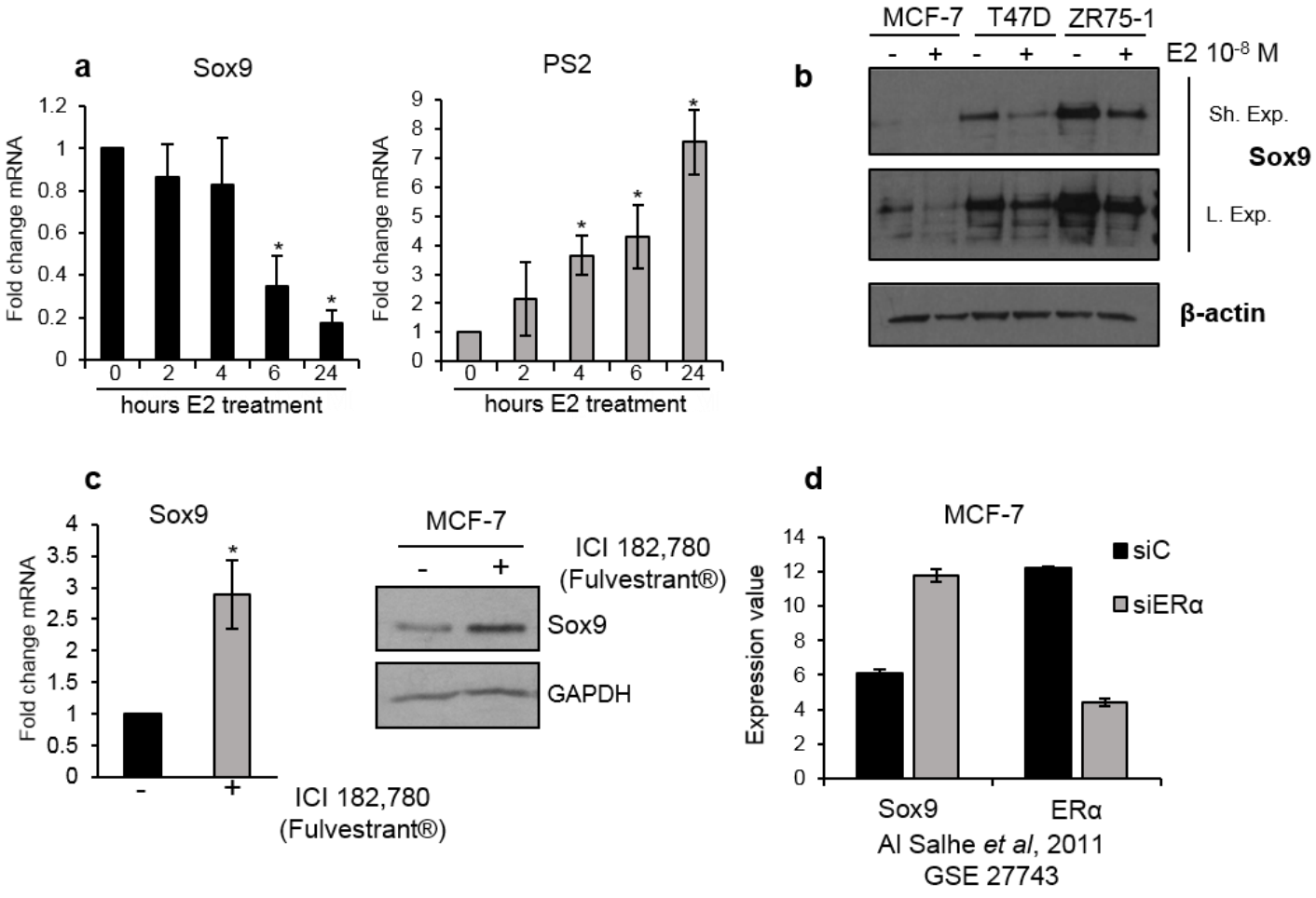

Fig. 3.4.1 Estrogen suppresses Sox9 expression. **(a)** Transcript levels of Sox9 and pS2 expression in MCF7 cells after 10-8 M estrogen (E2) treatment. **(b)** Immunoblots of Sox9 in MCF7, T47D and ZR75-1 cells treated for 2days with 10^{-8} M estrogen. β-actin was used as loading control.. **(c)** Sox9 mRNA (left) and protein (right) expression levels after 10-7 M ICI 182,780 treatment in MCF7 cells (n=3). **(d)** Sox9 and ER expression in MCF7 cells transiently silenced for ERα in a public database (GSE27743). siC: scramble siRNA, siERα: siRNA against ERα.. (E2: estrogen, Sh exp: short exposure, L. exp.: long exposure). * $p<0.05$.

Finally, we wished to examine Sox9 and ER cellular localization. Using three different breast cancer cells, it was observed that cells with high Sox9 levels expressed low ER and vice-versa, further supporting the observation that estrogen signaling has a negative effect on Sox9 expression (Fig. 3.4.2).

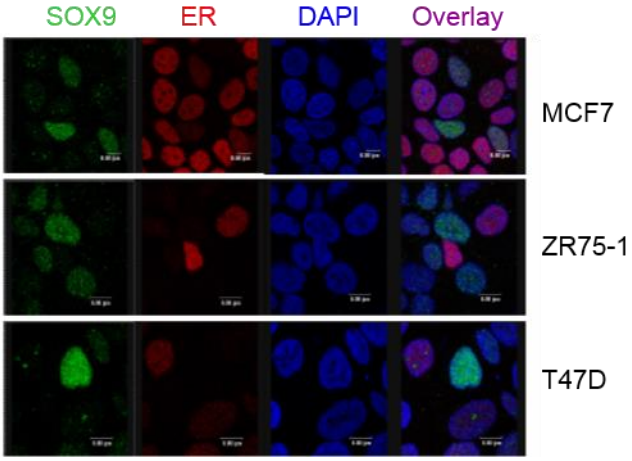

Fig. 3.4.2 Inverse correlation between Sox9 and ER in breast cancer cells. Immunofluorescence analysis of Sox9 and ERexpression in MCF7, ZR75-1 and T47D breast cancer cells.

ER expression in the human mammary gland is limited to the luminal epithelial compartment ($CD49f^{-}EpCAM^{+}$), while the luminal progenitor ($CD49f^{+}EpCAM^{+}$) and myoepithelial/stem cells ($CD49f^{+}EpCAM^{-}$) are ER-. Indeed, ER and PR (marker of ER activity) expression levels were highest in luminal cells, while they were found to be low in the luminal progenitor and the myoepithelial/stem cell compartments (n=3, Fig. 3.4.3)

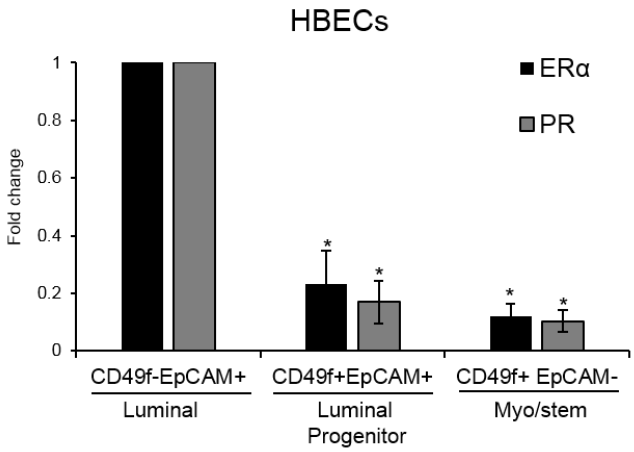

Fig 3.4.3. **ER and PR expression in sorted breast epithelial cells derived from human mammary gland organoids**: luminal cells ($CD49f^{-}/EpCAM^{+}$), luminal progenitor cells ($CD49f^{+}/EpCAM^{+}$) and myo/stem cells ($CD49f^{+}/EpCAM^{-}$). *p<0.05.

Conclusions:

Estrogen represses Sox9 expression both at mRNA and protein level and a lack of association between Sox9 and ER expression was observed both in normal and cancer cells. These results may partly explain why ER^- breast cancer cells express higher Sox9 level than $ERα^+$ cells.

5. Sox9 expression is enhanced in tamoxifen-resistant cells

Our group showed that Sox2 expression was enhanced in tamoxifen resistant cells compared to control cells, both in *in vitro* cell models and in patient-derived breast tissue samples. Furthermore, modulation of Sox2 expression levels affects tamoxifen sensitivity in breast cancer cells (Piva et al., 2014).

In the microarray published in this study, we observed that Sox2 overexpression in MCF-7 cells induced Sox9 expression, and this led us to think that Sox9 could be more expressed in tamoxifen resistant cells compared to control cells. Firstly, we confirmed Sox9 overexpression in MCF-7-Sox2 cells both at mRNA and protein level (Fig. 3.5.1a and 3.5.1b). Then, we checked Sox9 expression in control and tamoxifen resistant breast cancer cell lines developed in our lab (MCF-7, T47D and ZR-75-1 cells). Tamoxifen resistant cells expressed higher levels of Sox9 than the tamoxifen sensitive counterparts, both at mRNA and protein levels (Fig. 3.5.1c and 3.5.1d).

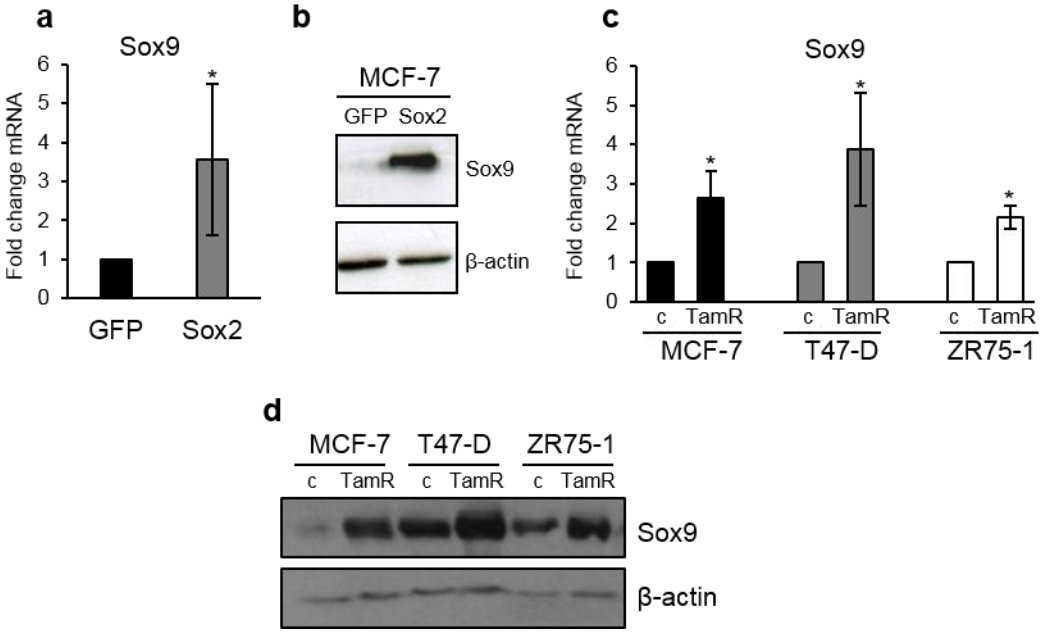

Fig 3.5.1 Sox9 expression in MCF7-Sox2 cells and in tamoxifen resistant cells (a). Sox9 mRNA expression in MCF-7 GFP and Sox2 cells**. (b).** western blot showing Sox9 expression in MCF-7 GFP and Sox2 cells. **(c)** Sox9 mRNA levels in MCF-7, T47D and ZR75-1 parental and tamoxifen resistant (TamR) cells. **(d)** Immunoblot analysis of Sox9 and β-actin (loading control) expression in MCF-7, T47D and ZR75-1 and parental and tamoxifen resistant (TamR) cells.

This observation suggests that development of tamoxifen resistance leads to increased Sox9 expression, suggesting a potential role of Sox9 as biomarker in the detection of endocrine resistance in breast cancer. Sox9 is known to be a transcription factor that can be found both in the nucleus and in the cytoplasm of the cells, since it contains nuclear importing and exporting sequences (Malki et al., 2005). In 2011, Chackravarty and collaborators (Chakravarty et al., 2011a), described that cytoplasmic Sox9 is often found in intraductal invasive carcinomas (IDC) and that cytoplasmic Sox9 staining correlated with Ki67 staining and increased cell proliferation. Since MCF-7-TamR cells are characterized by increased tumorigenicity and invasive potential (Piva et al, 2014), we sought to determine whether these cells expressed more cytoplasmic Sox9 than parental cells. Indeed, western blot analysis of nuclear and cytoplasmic fractions of MCF-7 and MCF-7-TamR cells, revealed an increased cytoplasmic staining in tamoxifen resistant cells. (Fig. 3.5.2a).

To determine whether the same changes in localisation were observed in breast tumours, a cohort of breast cancer patients that included responders (n=20) and non-

responders (primary n=18 and recurrent tumours n=23) to tamoxifen treatment was analyzed. Tumor cells showed a wide heterogeneity in terms of Sox9 localization, even within the same tumor sample, nevertheless, tumor samples from patients that did not respond to tamoxifen treatment and their recurrent tumors clearly showed increased cytoplasmic Sox9 staining (50% and 45%, respectively) when compared to tumors from responder (20%) patients (Fig. 3.5.2b). In addition, non-responders presented a higher percentage of samples with Sox9 distributed similarly among cytosol and nucleus (38.8%) than responders (10%). Conversely, the percentage of samples with higher nuclear than cytoplasmic staining was 70% in responding patients, but only 10% in non-responders. In addition, Allred scores distribution in nuclear and cytosolic staining showed a similar pattern, with increased cytoplasmic Sox9 scores in no responders and recurrent breast cancer tissue (Fig. 3.5.2c). These findings suggest that presence of cytosolic Sox9 is associated to a higher risk of recurrence, although analysis of a larger cohort would be necessary to confirm this observation. Immunohistochemical images of Cytoplasmic, cytoplasmic and nuclear and nuclear Sox9 staining are showed in figure 3.5.2d.

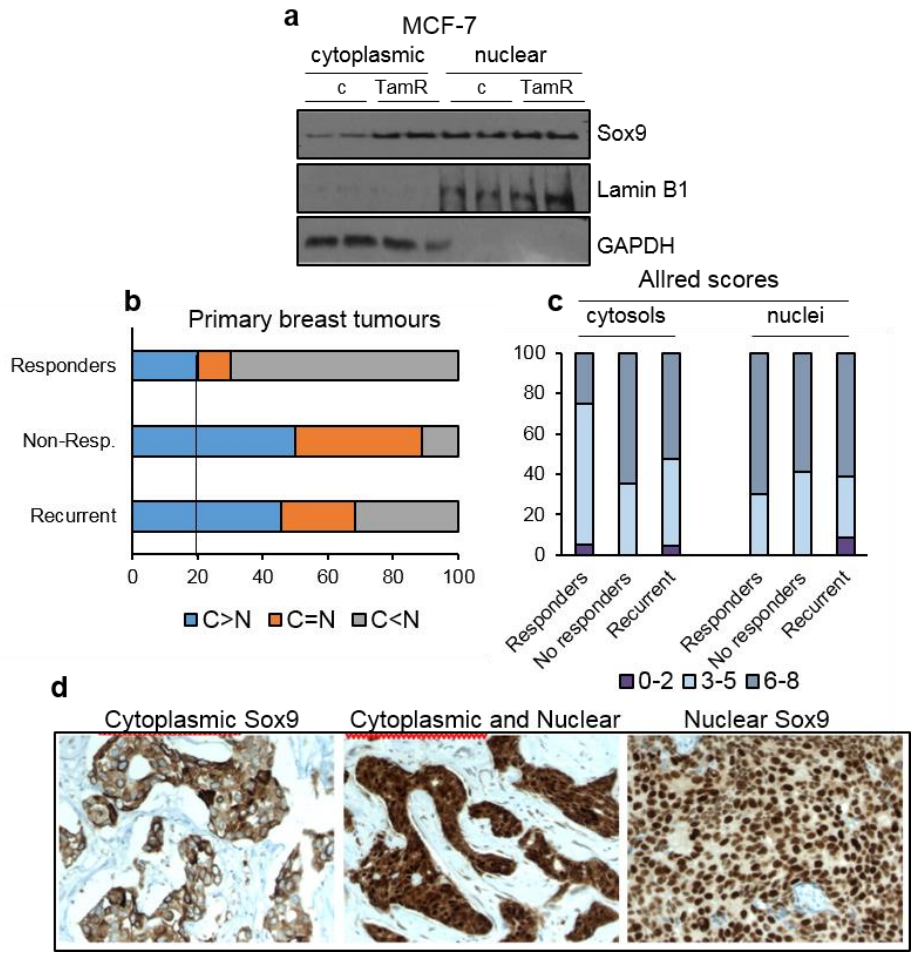

Fig. 3.5.2 Figure 5. Sox9 is highly expressed in tamoxifen resistant cells. (a) Immunoblot analysis of Sox9 expression in cytosolic and nuclear subfractions of MCF7 and MCF7TamR cells. Lamin B1 was used as nuclear marker and GAPDH as cytosolic loading control. **(b)** Percentage of breast tumours with higher cytosolic than nuclear (C>N), similar (N=C) and more nuclear than cytosolic (C<N). **(c)** Sox9 expression levels analysed by immunohistochemistry in breast tumour samples with low (0-2), medium (3-5) and high (6-8) Allred staining levels in nuclear and cytosolic cell compartments obtained from patients responding to tamoxifen (Responders, n=20), resistant to tamoxifen (Non responders, n=18) and recurrent after treatment failure (Recurrent, n=23). **(d)** Representative image of cytoplasmic, nuclearcytoplasmic and nuclear Sox9 expression in primary breast tumour

Despite the fact that cytosolic Sox9 has been previously reported its functional relevance is not understood. Sox9 phosphorylation has been associated with its localization (Malki et al., 2005) and we found that treatment of MCF-7-TAmR cells with the MAPK inhibitor U0126 induced accumulation of cytosolic Sox9 (Fig 3.5.3), suggesting that Sox9 phosphorylation by MAPK induces its nuclear translocation. We are currently carrying out more experiments in the lab to understand better these findings.

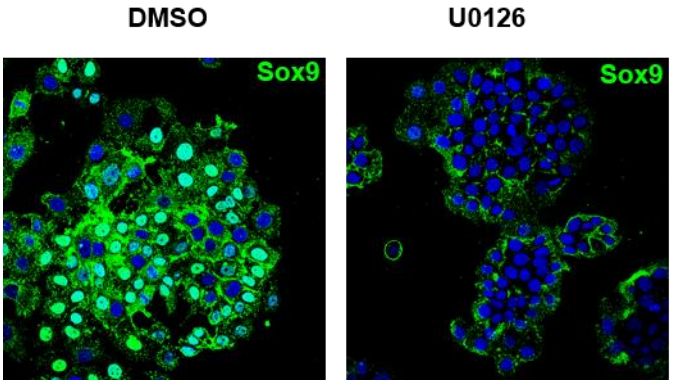

Fig. 3.5.3 MAPK inhibitor U0126 induces cytosolic Sox9 accumulation. MCF-7-TamR cells treated with DMSO or MAPK inhibitor U0126 (6 hours exposure) were analyzed by immunofluorescence (blue, DAPI; green, Sox9 expression).

Since we found increased Sox9 levels in tamoxifen resistant cells, we wished to examine the potential effect of Sox9 on tamoxifen sensitivity. Stable Sox9 silencing in MCF-7-TamR cells restored tamoxifen sensitivity both in soft-agar colony formation assays (n=4)(Fig. 3.5.4a) and in 2D clonogenic assays (n=5) (Fig. 3.5.4b). Contrarily, when we performed proliferation assays on plastic surface (n=4) (Fig. 3.5.4c), we observed no differences, suggesting that Sox9 may be relevant for the response to tamoxifen *in vitro* only when cells grow under diluted conditions, in clonogenic density or in anchorage-independent manner.

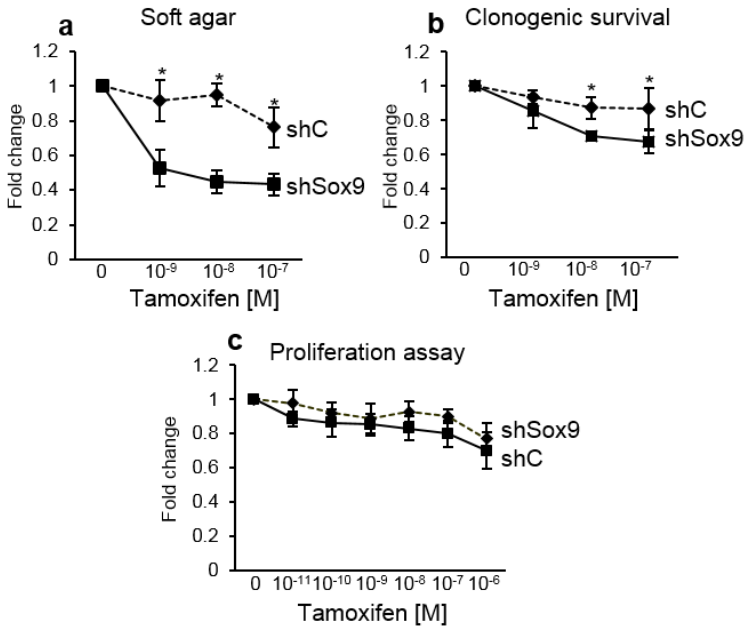

Fig. 3.5.4 Sox9 silencing and tamoxifen resistance. Soft agar colony formation assay **(a)**, 2D clonogenic assay **(b)** and cell proliferation assay **(c)** with MCF-7-TamR shcontrol (dashed lines) and shSox9 (continuous line) cells with increasing concentrations (10^{-9}-10^{-7} M) of tamoxifen. * $p<0.05$.

Conclusions:

Sox2 induces Sox9 expression in breast cancer cells and this process of development of tamoxifen resistance leads to increased Sox9 expression. Sox9 is found both in the cytosol and nuclei of primary breast cancer cells, and a proportion of cells in endocrine resistant/recurrent tumors showed increased cytosolic over nuclear staining, as observed in MCF-7-TamR cells.

These preliminary results could be validated with a large cohort of tumors, aiming to define the presence of cytosolic Sox9 as a potential marker of tamoxifen resistance in clinical patient assessment. Sox9 silencing appears to sensitize tamoxifen resistant cells to tamoxifen, at least when cells grow under anchorage-independent/clonogenic conditions. All together, these data suggest that Sox9 expression and localization may be relevant during development of endocrine resistance in breast cancer patients.

6. Sox9 and breast cancer stem cells

To investigate the possible association of Sox9 with the different cancer stem cell phenotypes that have been described extensively we analyzed mammosphere formation

ability (Dontu et al., 2003), aldheyde-dehydrogenase activity (ALDEFLUOR$^+$) (Ginestier et al., 2007) and the CD44$^+$CD24$^{-/low}$EpCAM$^+$ phenotype (Al-Hajj et al., 2003).

First of all, we wanted to confirm the observation that Sox9 expression was high in the ALDEFLUOR$^+$ subpopulation in cancer cells, as observed in normal breast tissue, and to this end we used MCF-7-TamR cells, which have increased ALDEFLUOR$^+$ activity compared to parental cells (Piva et al, 2014). Similarly to HBECs, ALDEFLUOR$^+$ cells isolated from tamoxifen resistant cells showed higher Sox9 expression than negative cells (Fig. 3.6.1a).

In addition, cell cultures of primary breast tumors (growing as mammospheres to enrich for stem cells) showed increased Sox9 mRNA expression in ALDEFLUOR$^+$ compared to ALDEFLUOR$^-$ cells sorted from the same patient (Fig. 3.6.1b and 3.6.1c). ALDH1A3 isoform was chosen as positive control of cell sorting, since it has been shown to be the most expressed isoform in ALDEFLUOR$^+$ cells in primary human breast cells (Marcato et al., 2011b) and a general increase of ALDH1A3 expression was observed in ALDEFLUOR$^+$ cells, as we showed previously in the lab (Iriondo et al., 2015). Patient's characteristics are shown in Table 3.4.

In a study including 8 different breast cancer patients RNA was extracted from ALDEFLUOR$^-$ and ALDEFLUOR+ cell populations and subjected to microarray analysis (Liu et al., 2014), GEO2R accession number: GSE52327). Analysis of the expression of Sox9 and ALDH1A3 in this publicly available dataset showed a tendency for increased Sox9 expression in ALDEFLUOR+ cells compared to ALDEFLUOR$^-$ cells from the same patient (Fig. 3.6.1d).

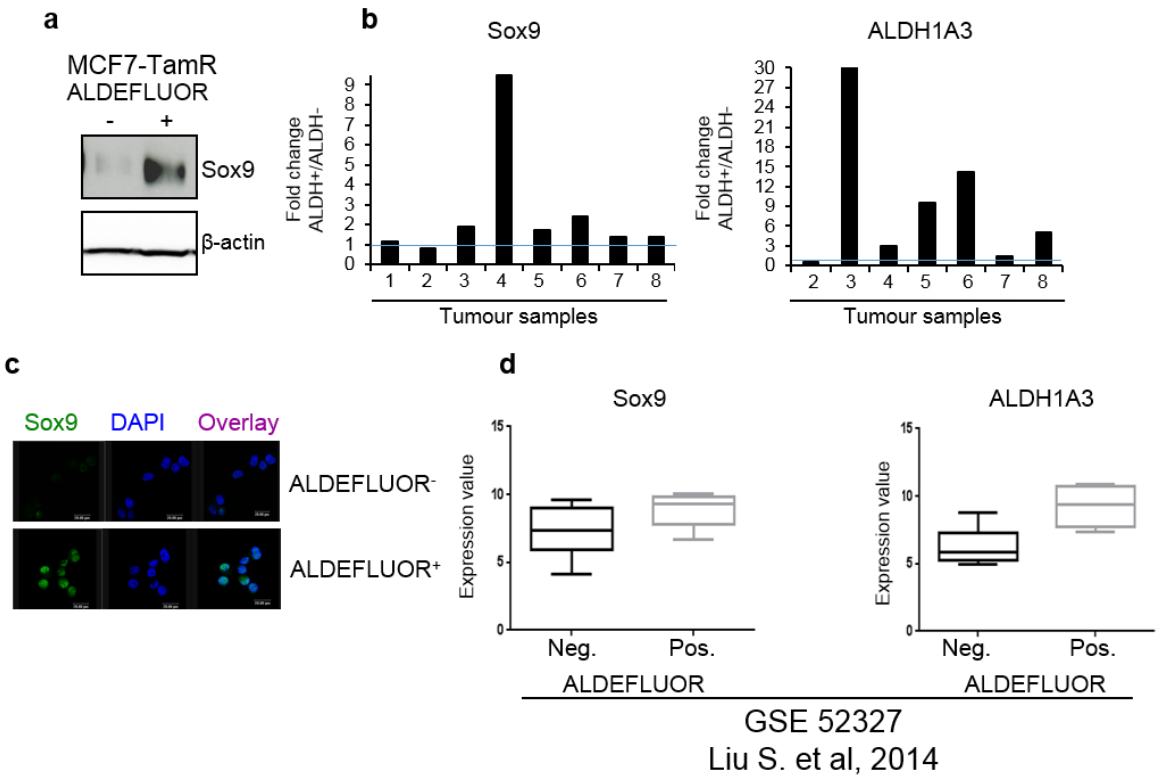

Fig. 3.6.1 Sox9 marks ALDEFLUOR⁺ cells. (a) Immunoblot of Sox9 in ALDEFLUOR- and ALDEFLUOR+cells sorted from MCF7TamR cells **(b)** Transcript levels of Sox9 in ALDEFLUOR- and ALDEFLUOR+ cells sorted from 8 different human primary breast tumours grown in suspension as mammospheres. Note: ALDH1A3 data on tumor sample 1 is not available. **(c)** Representative immunofluorescence of ALDEFLUOR⁻ and ALDEFLUOR⁺ cells sorted from a primary breast tumor **(d)** Sox9 and ALDH1A3 mRNA expression levels in ALDEFLUOR- and ALDEFLUOR+ cells analysed in a public GEO2R dataset containing 8 different primary breast tumour specimens (GSE52327).

Number	1	2	3	4	5	6	7	8
Age	77	79	50	59	46	64	71	42
ER	-	-	+	+	+	+	-	-
PR	-	-	+	+	+	+	-	-
HER2	0	++	-	-	-	-	++	-
GRADE	3	3	2	2	2	3	3	3
Ki67	10%	60%	43%	5%	3%	5%	30%	50%

Table 3.4. Characteristics of the tumor samples used in Fig. 3.6.1b

Given the importance of ALDEFLUOR$^+$ cells in breast cancer tumorigenicity, we proceed to modulate Sox9 levels in breast cancer cells to determine whether Sox9 regulates this population.

Initial experiments in MCF-7-TamR and ZR-75-1 cells, using 2 siRNA sequences against Sox9 showed a strong reduction of the ALDEFLUOR$^+$ population compared to siCNTR transfected cells (ZR-75-1; n=6, * $P< 0.05$, red bars and MCF-7-TamR cells; n=3, * $P<0.05$, black bars). Western blots confirmed Sox9 silencing (Fig. 3.6.2a). Similarly, lentiviral-transduced cells showed reduced ALDH activity in shSox9 cells in both tamoxifen resistant cell types (MCF-7-TamR and T47D-TamR cells) (Fig 3.6.2b and 3.6.2c). Sox9 downregulation by shRNA was assessed by western blot analysis (Fig. 3.6.2d).

Given the correlation between Sox9 expression and ALDH activity, we sought to determine whether Sox9 silencing might affect the expression of ALDH1A3, the main isoform described to be responsible for ALDH activity (Marcato et al., 2011b). Indeed, stable Sox9 silencing reduced significantly ALDH1A3 mRNA expression in MCF-7-TamR and T47D-TamR cells, while Sox9 up-regulation in MCF10A cells enhanced ALDH1A3 expression (Fig. 3.6.2e).

Furthermore, the reduction in the percentage of ALDEFLUOR$^+$ cells was observed also with another two different shRNA sequences in MCF-7-TamR cells (Fig 3.6.3).

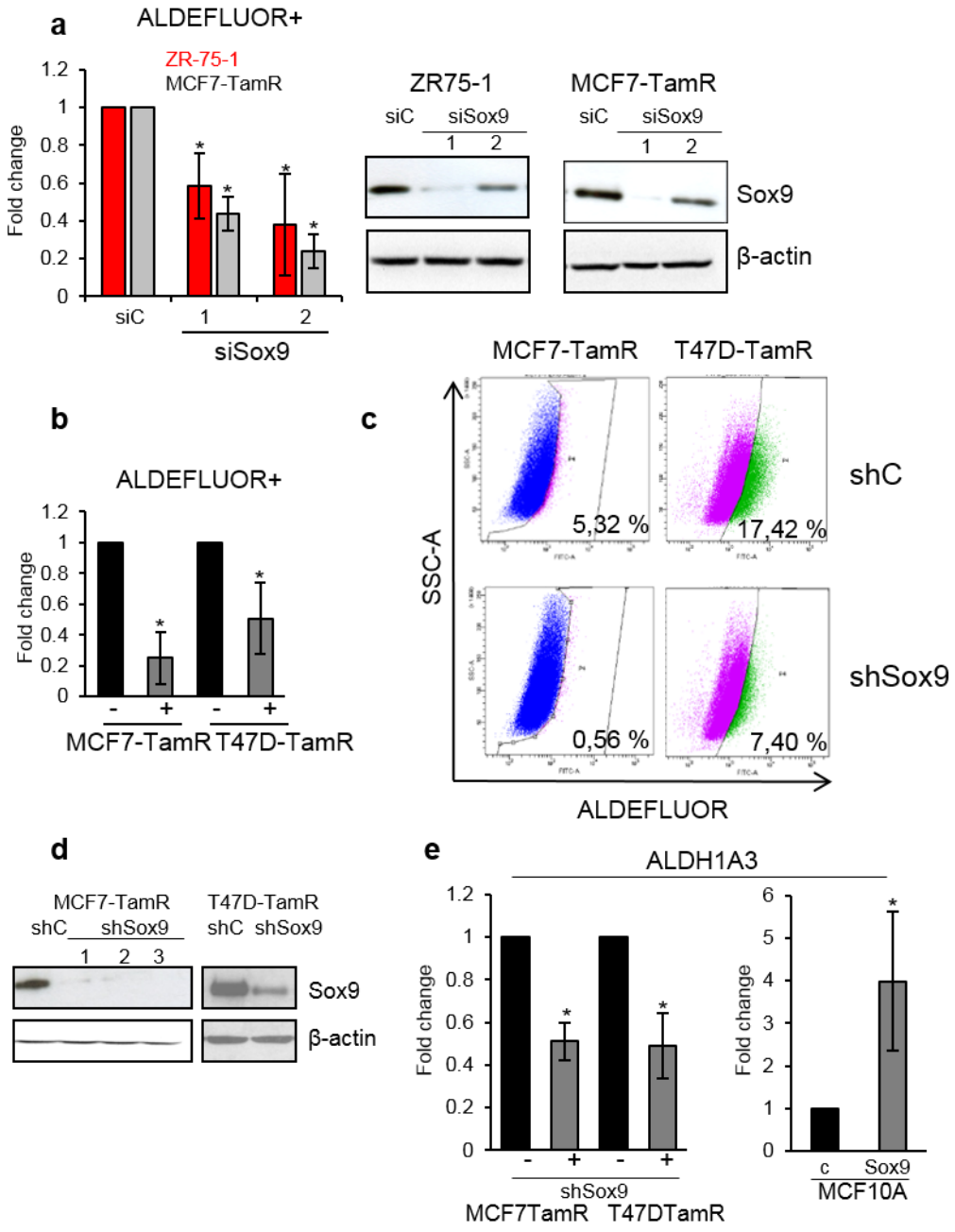

Fig. 3.6.2. **Sox9 modulation alters ALDEFLUOR+ cell content in breast cancer cells. (a)** ALDEFLUOR+ cells in ZR-75-1 (red bars) and MCF-7-TamR (black bars) cells with endogenous Sox9 silenced with control (sic) or specific siRNA sequences against Sox9 (siSox9). A representative immunoblot of Sox9 is shown and β-actin was used as loading control. **(b)** Fold change of ALDEFLUOR$^+$ cells in MCF-7-TamR and T47D-TamR shcontrol (-) and shSox9 (+) cells, (n=4). **(c)** Representative FACS plot of MCF-7-TamR and T47D-TamR shC and shSox9. **(d)** Western blot showing Sox9 down-regulation in shSox9 cells. **(e)** ALDH1A3 mRNA expression in shC (shControl) MCF-7-TamR and T47D-TamR cells and in MCF10A-GFP and MCF10A-Sox9. * p<0.05.

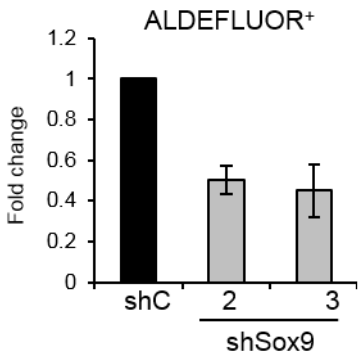

Fig. 3.6.3 ALDEFLUOR+ cells in MCF-7-TamR cells, shC (shControl) and two additional shSox9 sequences (2 and 3, n=3).

These results show that modulation of Sox9 expression levels is positively associated with ALDH1A3 levels and, consequently, ALDEFLUOR+ cell content.

In fact, ALDH1A3 expression and, consequently, ALDEFLUOR activity positively correlates as published by our lab (Iriondo et al, 2015).

So, we speculated that Sox9 might target ALDH1A3 promoter directly, inducing ALDH1A3 transcription. Analysis of ENSEMBL ALDH1A3 promoter sequences showed two potential Sox9 binding sites around 845 and 1828 base pairs before the ALDH1A3 transcription starting site (TSS).

Primers where then designed to amplify these genomic sequences. Chromatin immunoprecipitation (ChIP) analysis revealed that Sox9 binding was significantly enhanced over the Immunoglobulin G (IgG) control (Fig. 3.6.4). This result suggests that Sox9 transcriptionally regulates ALDH1A3 gene expression.

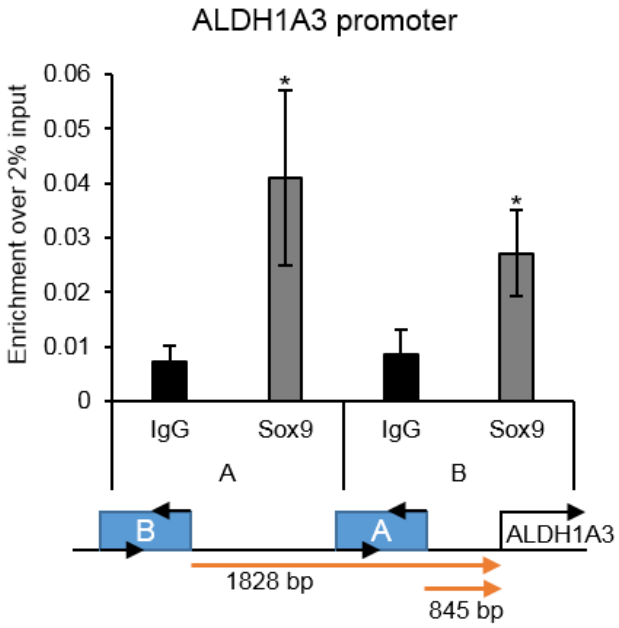

Fig. 3.6.4 IgG and Sox9 chromatin binding enrichment in ALDH1A3 promoter in MCF-7-TamR cells (n=4) *p<0.05.

In addition, we checked ALDEFLUOR$^+$ cell content in TNBCs MDA-MB-231 and BT549 control (shCNTR) and shSox9 cells, and we found no differences (Fig. 3.6.5)

We wanted to confirm this data with another TNBC cell line as MDA-MB-468, notably very rich in ALDEFLUOR$^+$ cells (Marcato et al., 2011a), but stable Sox9 silencing in these cells was not successfully obtained (data not shown).

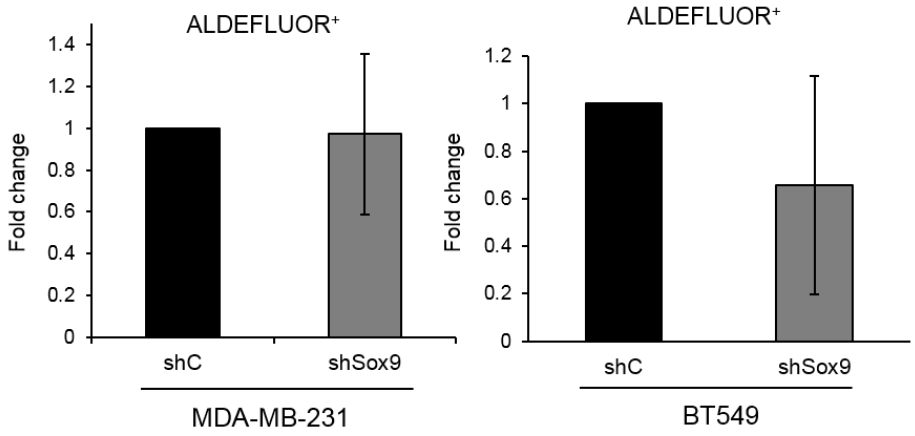

Fig. 3.6.5 ALDEFLUOR+ cells in TNBCs MDA-MB-231 and BT549 shC and shSox9.

The mammosphere (MS) formation assay represents a common *in vitro* method to evaluate the stem and progenitor cell content within a cell population (Dontu et al., 2003),

so we decided to investigate the effect of Sox9 levels on MS formation ability in breast cancer cell lines. We speculated that, since Sox9 appeared associated with stem/progenitor ALDEFLUOR$^+$ cells, its expression should increase when cells are cultured in suspension as MS (enriched for stem cells) compared to cells growing in adherent conditions in the presence of serum (differentiating conditions). According to our hypothesis, we observed that Sox9 expression was enhanced in different breast cancer cell lines growing as MS, compared to cells growing in adherent conditions (Fig 3.6.6a, 3.6.6b and 3.6.6c), as observed with Sox2 levels, indicating that Sox9 expression is induced in conditions that lead to an un-differentiated state.

Primary and secondary MS formation was significantly reduced upon Sox9 down-regulation in MCF-7-TAmR cells (Fig 3.6.6d). The capacity of the cells to form secondary MS is associated with their “self-renewal” capacity and a reduction in number of spheres is interpreted as a reduction of the stemness and an induction of the differentiation of the cells present in the spheres due to the reduction of Sox9 levels. Sphere formation in the triple negative breast cancer cell lines MDA-MB-231 and BT549 showed similar results (Fig. 3.6.6e). On the other hand, Sox9 overexpression in MCF10A cells increased both primary and secondary MS (Fig. 3.6.6f). Collectively, these results suggest that Sox9 is important for MS formation in different breast cancer cell types.

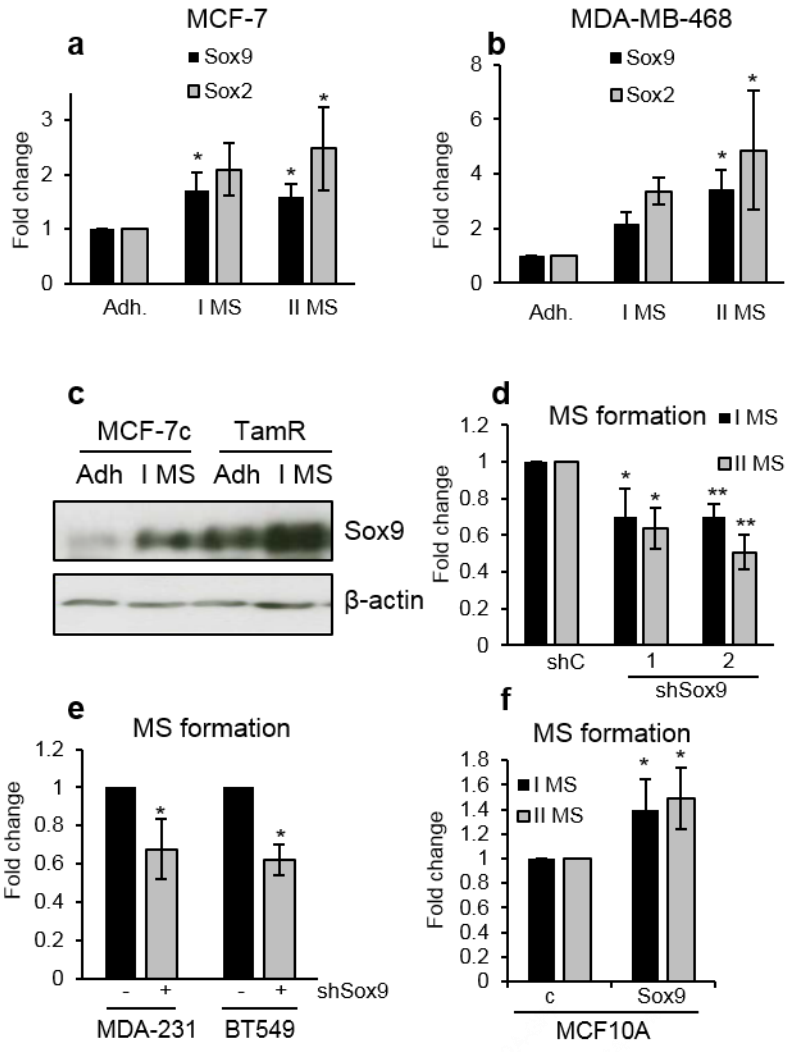

Fig. 3.6.6 Sox9 expression in MS cultures and MS formation ability in cells with modulated Sox9 levels. Sox9 and Sox2 mRNA expression in MCF-7 **(a)** and MDA-MB-468 **(b)** grown in adherent condition (adh.), primary mammospheres (I MS) and secondary MS (II MS). **(c)** Sox9 protein expression in MCF-7c and MCF-7-TamR cultivated in adherent condition and as primary MS. **(d)** Relative I MS and II MS formation in MCF-7-TamR cells. **(e)** MS formation in MDA-231 and BT549 cells shCNTR (-) and shSox9 (+) cells. **(f)** I and II MS formation in MCF10A control cells and MCF10A-Sox9 cells expression. * $p<0.05$, ** $p<0.01$.

We have previously shown that overexpression of the stem cell genes Sox2, OCT4 and NANOG enhanced MS formation, ALDEFLUOR$^+$ cells, cell invasion and migration, as well as induction of CD44$^+$/CD24$^{-/low}$/ESA$^+$ breast cancer stem cell content (Simöes et al., 2011). We already showed that Sox9 levels were increased in MCF-7-Sox2 cells compared to control cells MCF-7-GFP (Fig. 3.5.1a and 3.5.1b). Determination of Sox9 levels in MCF-7 stable cell lines overexpressing NANOG and OCT4 showed, similarly to

Sox2 overexpressing cells, that NANOG or OCT4 overexpression was sufficient to induce Sox9 levels in MCF-7, both at mRNA (Fig 3.6.7a) and protein level and (3.6.7b).

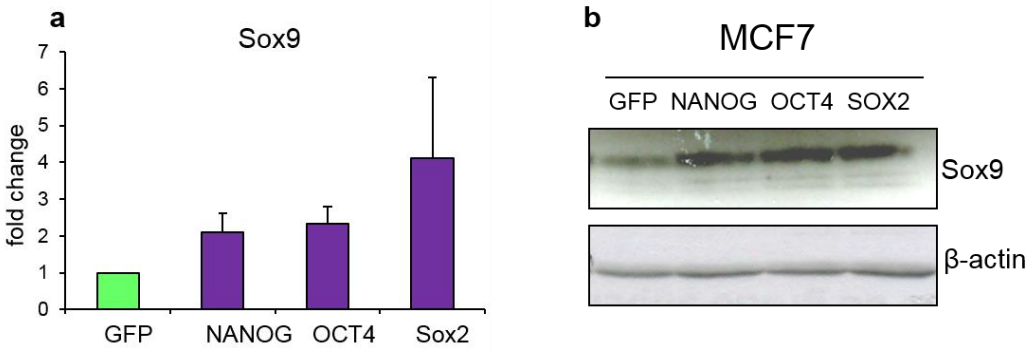

Fig. 3.6.7 Sox9 expression in MCF-7 cells overexpressing GFP, NANOG, OCT4 and Sox2. At mRNA (A) and protein (b). β-actin was used as loading control.

Next, we sought to determine whether Sox9 was involved in the maintenance of cancer stem cells characterized by the phenotype $CD44^{+}CD24^{-/low}EpCAM^{+}$. This phenotype is particularly relevant in the basal/triple negative tumors (Idowu et al., 2012). We determined the percentage of this population in the triple negative breast cancer cell lines MDA-MB-231 and BT549, stably silenced for Sox9 and found that, compared to control cells, there were no significant differences in the percentage of $CD44^{+}CD24^{-/low}ESA^{+}$ cells in MDA-MB-231 cells, and an increase in BT549 cells when Sox9 was silenced (Fig. 3.6.8).

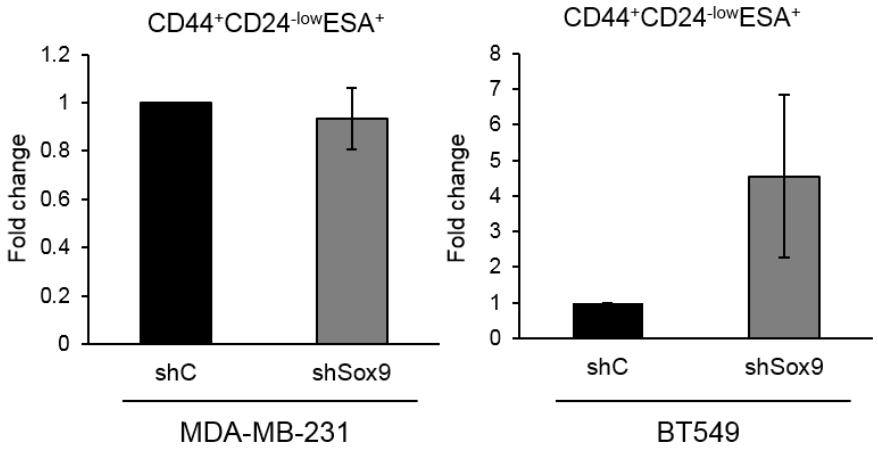

Fig. 3.6.8 $CD44^{+}CD24^{-/low}ESA^{+}$ cells content represented as fold change between shC (set as 1) and shSox9 MDA-MB-231 and BT549 cells.

PKH26^{+} cells represent stem and label-retaining cells, characterized by their slow dividing ability. Sox9 was more expressed in PKH26^{+} compared to PKH26^{-} cells (Fig. 3.6.8) (Pece et al., 2010b), further confirming the observation that Sox9 is expressed in mammary stem/progenitor cells, both in normal and breast cancer cells. Additionally, RNA sequencing of control and shSox9 MDA-MB-231 cells and Gene Set Enrichment Analysis (GSEA) showed a significant increase of transcript expression (83/140) in shcontrol versus shSox9 in a dataset called “Mammary_Stem_Cell_UP” (Fig. 3.6.9). This GSEA dataset (Pece et al., 2010b) describes a set of differentially expressed genes between PKH26^{-} and PKH26^{+} labeled cells from primary breast epithelial cells cultured as mammospheres.

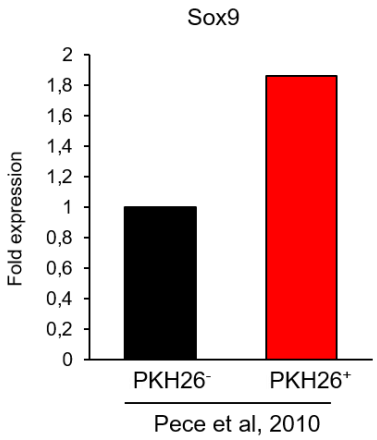

Fig. 3.6.8 Sox9 expression in PKH26- and PKH26+ cells separated from HBECs (Pece et al, 2010).

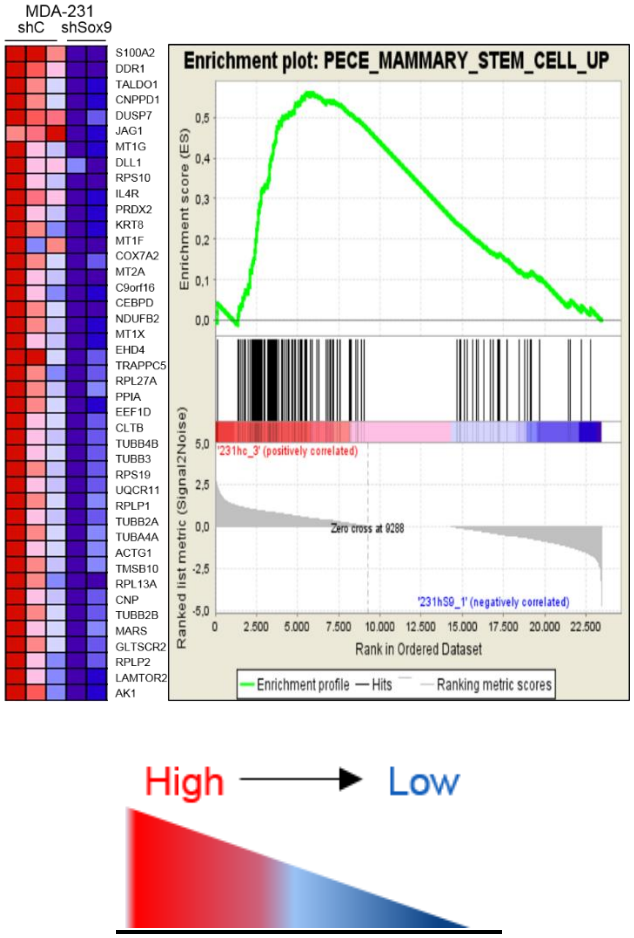

Fig. 3.6.9 GSEA dataset "PECE_MAMMARY_STEM_CELL_UP" in shCNTR and shSox9 MDA-MB-231 cells. On the left corner, the top of the list of differentially expressed genes is shown.

Conclusions:

These results demonstrate that Sox9 is more expressed in ALDEFLUOR^{+} cells compared to ALDEFLUOR^{-} cells, both in luminal breast cancer cells and in primary tumors, and Sox9 expression reduction impairs ALDEFLUOR+ cell population in luminal breast cancer cells, whether this seems not to be the case in TNBCs. In addition, Sox9 is highly expressed in mammospheres, suggesting that Sox9 plays a role in stemness maintenance.

CD44^{+}CD24^{-low}EpCAM^{+} staining in TNBCs MDA-MB-231 and BT549 revealed cell-type specific effect.

7. Effect of Sox9 on breast cancer cell tumorigenicity

Sox9 has been shown to be related to tumorigenesis in different types of tumors, such as bladder, colon and lung cancer (Ling et al., 2011; Matheu et al., 2012; Shen et al., 2015; Wang et al., 2015b), and also in MDA-MB-. 231 breast cancer cells (Guo et al., 2012a).To determine if this was the case also for tamoxifen resistant breast cancer cells, several *in vitro* assays were used. In MCF-7-TamR, T47D-TamR, MDA-MB-231 and BT549 cells, stable Sox9 silencing impaired the ability of these cells to generate colonies when seeded at clonogenic density on plastic (Fig. 3.7.1a). Furthermore, Sox9 silencing in MCF-7-TamR, T47D-TamR and MDA-MB-231 cells strongly reduced the ability of these cells to grow in anchorage-independent conditions (Fig 3.7.1b). Unfortunately, we failed to see BT459 growth in anchorage-independent conditions for unknown reasons. MDA-MB-231 cells are highly invasive metastatic cells *in vivo* and *in vitro*, so we evaluated cell invasion through matrigel-coated transwells of shcontrol and shSox9 MDA-MB-231 cells. Cells with reduced Sox9 levels displayed decreased ability to invade through Matrigel (Fig. 3.7.1c). In addition, the regular cell morphology was altered in MDA-MB-231 cells stably silenced for Sox9 (Fig. 3.7.1d), from a regular splindle-like morphology to a more cobblestone-like shape. A similar morphological alteration was observed in BT549 cells (Fig 3.7.1d). Sox9 downregulation was checked by western blot analysis (Fig. 3.7.1e and 3.6.2e).

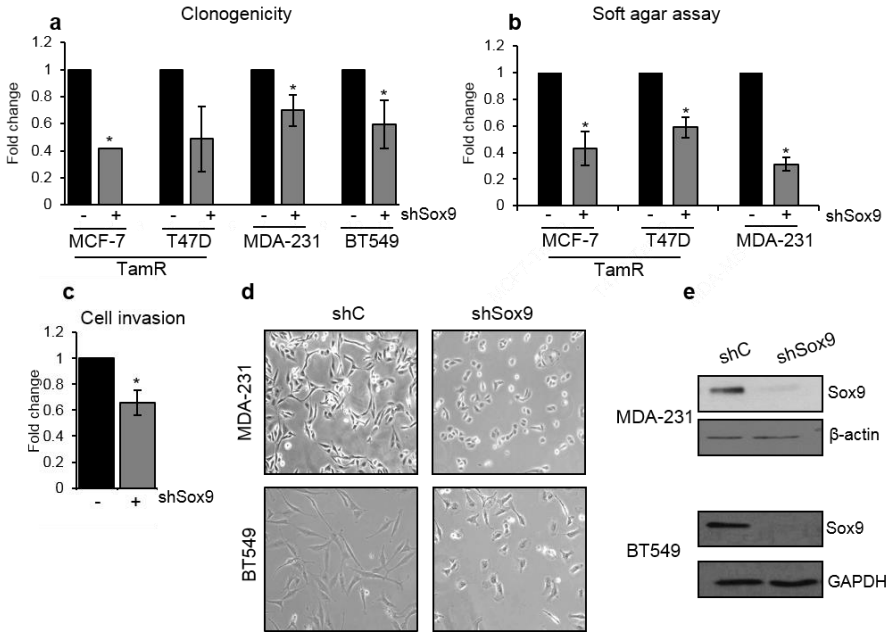

Fig. 3.7.1 Sox9 stable silencing reduces clonogenicity and growth in anchorage independent condition in different breast cancer cell lines as well as invasion in MDA-MB-231 cells. Sox9 stable silencing alters morphology in triple negative breast cancer cells. **(a)** Clonogenicity assay using MCF-7TamR, T47DTamR, MDA-MB-231 and BT549 shcontrol (-) and shSox9 (+) cells (n=3). **(b)** Soft agar colony formation assay in MDA-MB-231 shcontrol and shSox9 cells (n=2). **(c)** Cell invasion assay of MDA-MB-231 shcontrol and shSox9 cells. **(d)** Representative image of shcontrol (shC) and shSox9 MDA-MB-231 and BT549 cells. **(e)** Representative western blot showing Sox9 expression in shCNTR (shC) and shSox9 in MDA-231 and BT549 cells. β-actin and GAPDH were used as loading control * $p<0.05$.

Finally, we were trying to explain the reduced cell invasion ability of MDA-MB-231 shSox9 cells analyzing whether Sox9 silencing could be able to induce an “epithelial state” in triple negative breast cancer cells, altering the expression of epithelial-to-mesenchymal-transition (EMT), well studied and known process that converts cells more invasive and motile. EMT is generally characterized by the loss of cell adhesion protein E-cadherin and the increased expression of transcription factors as ZEB-1, SNAI1, SNAI2 or TWIST (Felipe Lima et al., 2016). In this case, we analyzed a very metastatic and aggressive cell line (MDA-MB-231) and another TNBCs, BT549, so we were expecting to observe a reduction of such markers involved with EMT. We were analyzing by qRT-PCR the expression of these markers, but no relevant differences were detected between control and shSox9 cells (Fig. 3.7.2).

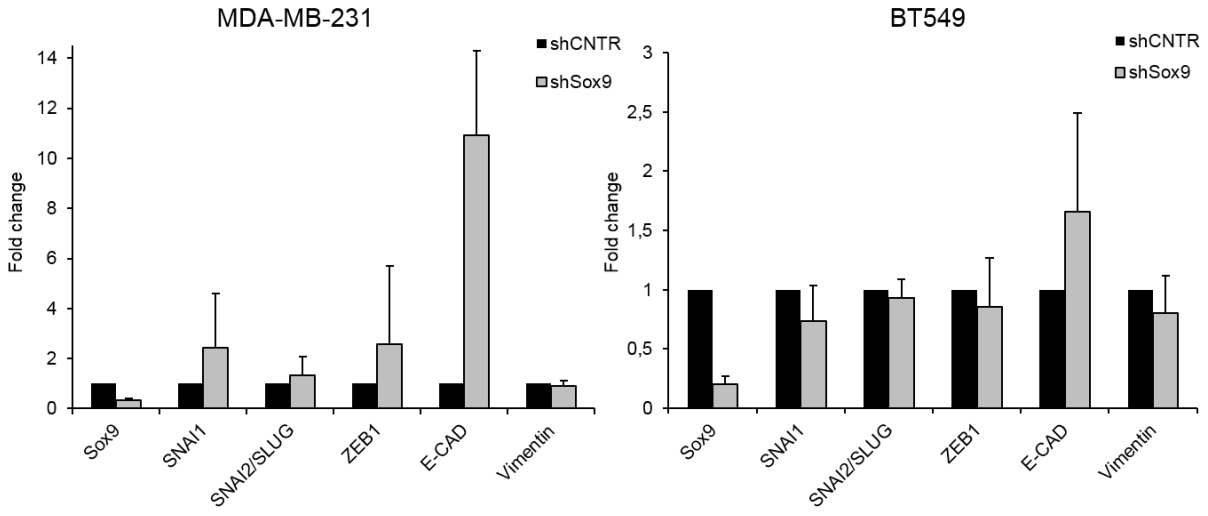

Fig. 3.7.2 Sox9 and epithelial-to-mesenchymal transition (EMT). mRNA expression of genes involved in epithelial-to-mesenchymal transition in MDA-MB-231 and BT549 cells (shCNTR, black bar, shSox9, grey bar)

We also cultured MCF10A control cells and Sox9 overexpressing cells in Matrigel to determine the effect of Sox9 overexpression in invasion. three-dimensional (3D) cell culture in Matrigel is an useful tool to study the potential oncogenic role of candidate genes *in vitro* (Debnath et al., 2003). MCF10A cells are able to grow in Matrigel in polarized structures called “acini”. Initially, MCF10A cells proliferate in Matrigel forming spherical structures and, around 7-10 days after seeding, the cells in the middle of the structure start to dye due to apoptosis, leading to the formation of a central hollow lumen. Oncogenes such as cyclin D1 or ErbB2, if overexpressed in MCF10A cells, lead to a disorganization of such 3D structures, with cells that continue to grow into the cavity as a sign of hyper-proliferation and induction of a “protumorigenic” status, and generally such structures tend to be more disorganized, irregular and with a reduced spherical shape (Debnath et al., 2003). As shown, MCF10A-Sox9 cells formed slightly more colonies in matrigel than control cells (Fig. 3.2.4d) (MCF10A cells stably lentivirus-transduced with an empty plasmid) and the colonies originated from Sox9 overexpressing cells were bigger and more irregular compared to control cells (Fig. 3.7.3). In addition, confocal microscopy analysis revealed that MCF10A-Sox9 colonies tend to loose cell polarity and show increased luminal filling and irregular morphology than control cells. Finally, Sox9 colonies appeared more disorganized than control cells, indicating that Sox9 promotes

lumen disruption and cell proliferation, suggesting a potential tumorigenic role in these cells (Fig. 3.7.3).

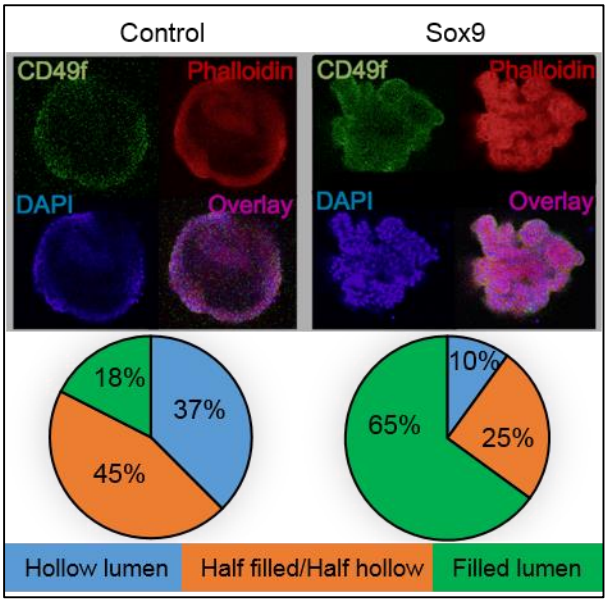

Fig. 3.7.3 Sox9 overexpression in MCF10A cells induces an irregular morphology and filled lumen compared to control cells. Representative confocal images of MCF10A control cells stably transfected with a control plasmid and MCF10A-Sox9 cells stained with CD49f (green), Phalloidin (red) and DAPI (blue). Below, a pie-graphs showed the percentage of colonies of each group showing, hollow lumens, half-filled/half-hollow lumens and filled lumens

Conclusions:

Collectively, the observations of reduced cell clonogenicity, growth in anchorage independent conditions and invasion through Matrigel suggest that Sox9 contributes to tumorigenicity in tamoxifen resistant cells and triple negative breast cancer cells. Sox9 overexpression in MCF10A cells alters lumen polarity and confers a pro-tumorigenic phenotype.

8. Sox9 is important for Wnt activity in breast cancer cells

The previous findings have shown that Sox9 maintains the ALDEFLUOR^{+} population, supports mammosphere formation and promotes *in vitro* tumorigenicity of breast cancer cells. In order to analyze the molecular mechanisms by which Sox9 affects stem cell maintenance we conducted RNA-Seq analysis of MCF-7-TamR shC and shSox9, as well as of MDA-MB-231 shC and shSox9 cells. shSox9 cells Both MCF-7-TamR and MDA-MB-231 cells showed a reduced activation of The expression of Wnt

target gene AXIN2 and the receptors FZD4 and FZD7, as well as that of other components of Wnt signaling such as Kremen2 and TCF7L1/Tcf-3 and several Wnt proteins, including WNT9A, WNT5B, WNT7B, and WNT6. We validated some of these genes by qRT-PCR (Fig 3.8.1 a and b; Fig.3.8.2a, 3.8.2b, 3.8.2c and 3.8.2d) and found that they were down-regulated upon Sox9 silencing.

In addition, the effects of Wnt signaling were confirmed using a transcriptional assay to evaluate the level of activation of canonical Wnt in the cells, called TOP/FOP assay, in which cells are transfected with a luciferase reporter under the control of a β-catenin responsive plasmid (TOP)or a control plasmid, called FOP, containing a mutated β-catenin binding site. Cells were transfected with the reporters and with or without a β-catenin expression vector and found that Sox9 absence significantly impaired transcriptional activation by β-catenin, suggesting that Sox9 contributes to Wnt activation in breast cancer cells (Fig 3.8.2f).

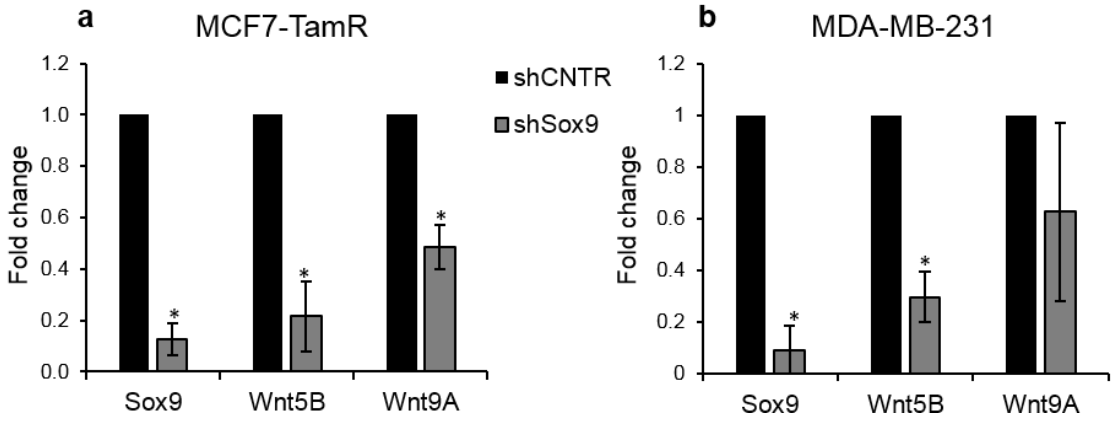

Fig 3.8.1. Expression of Sox9, Wnt5B and Wnt9A in MCF-7-TamR (a) and MDA-MB-231 cells (b) stably silenced for Sox9. * $p<0.05$.

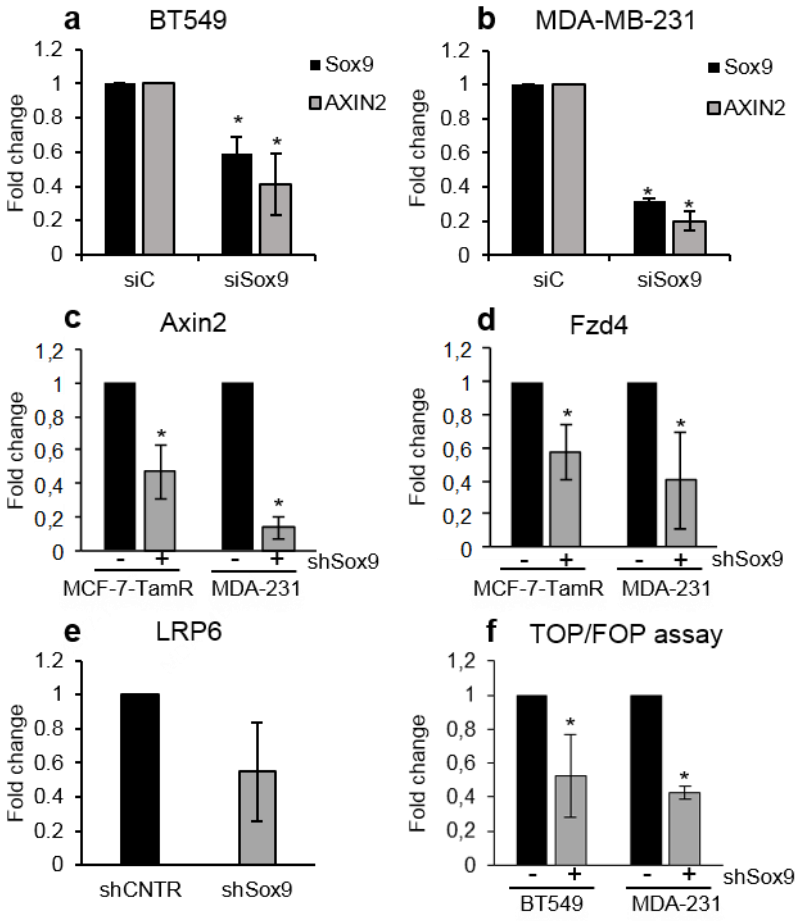

Fig. 3.8.2 Wnt signaling in breast cancer cells with modulated Sox9 level. Sox9 and AXIN2 mRNA expression in BT549 **(a)** and MDA-MB-231 cells **(b)** transfected with siCNTR (siC) and siSox9. AXIN2 **(c)** and Fzd4 **(d)** mRNA level in MCF-7-TamR and MDA-MB-231 shCNTR cells (black bar) and shSox9 (grey bars) **(e)** LRP6 mRNA level in MCF-7-TamR shCNTR and shSox9 cells. **(f)** TOP/FOP assay in BT549 and MDA-MB-231 cells. * $p<0.05$.

Conclusions:

Our results show that Sox9 is a positive regulator of Wnt signaling since its inhibition reduces the expression of various components of Wnt signaling as well as Wnt transcriptional activity in breast cancer cells.

9. Sox9 and Sox2 regulation of Wnt signaling

Previously, our lab showed that Sox2 is a positive regulator of Wnt activity in tamoxifen resistant breast cancer cells (Piva et al., 2014) and here it has been shown that Sox2 over-expression increases Sox9 levels in MCF-7 cells.

In addition, we observed that Sox2 and Sox9 often colocalize in MCF-7-TamR cells using confocal fluorescence analysis (Fig. 3.9.1). However, since the expression of Sox9 is more frequent in these cells, there were plenty of cells negative for Sox2 that expressed Sox9. A higher degree of colocalization of both Sox factors was observed in sorted ALDEFLUOR+ cells than in the general population (Fig. 3.9.2). Nevertheless, still it was possible to find cells with exclusive Sox2 or Sox9 staining.

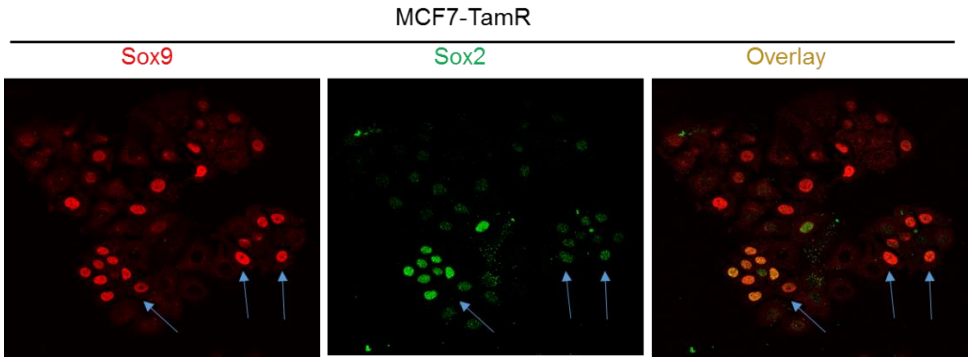

Fig. 3.9.1 Sox2/Sox9 expression in MCF-7-TamR cells by Immunofluorescence. Arows indicate events of colocalisation withinh the cells.

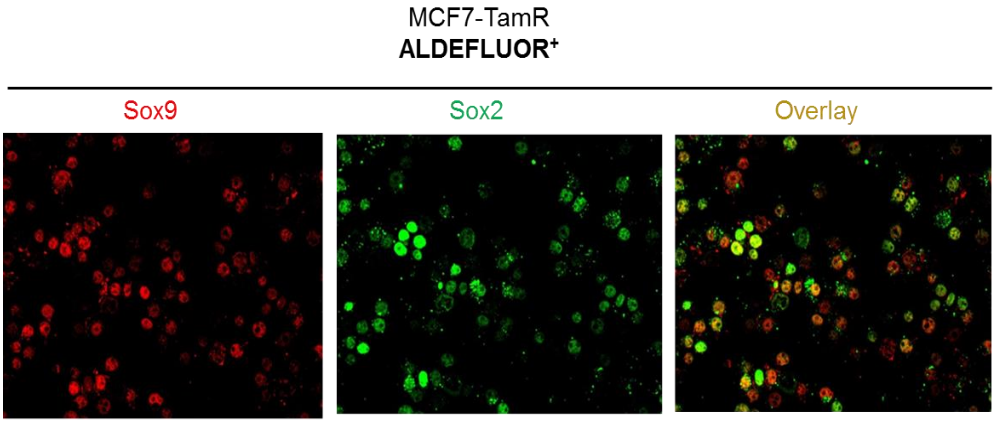

Fig. 3.9.2 Sox2/Sox9 expression in ALDEFLUOR+ cells sorted from MCF-7-TamR cells

This finding led us to hypothesize that Sox2 and Sox9 could regulate each other. MCF7-TAMR cells with stable Sox9 silencing only showed modest reduction of Sox2 levels, however, it is possible that long-term Sox9 silencing may induce some compensatory mechanism that contribute to recover Sox2 levels. Intriguingly, transient Sox9 silencing by siRNA in MCF-7-TamR, BT549 and MDA-MB-231 cells resulted in reduced Sox2 mRNA expression (Fig. 3.9.3), suggesting that a positive loop may exist, since Sox2 overexpression leads to enhanced Sox9 expression (3.5.1a and 3.5.1b).

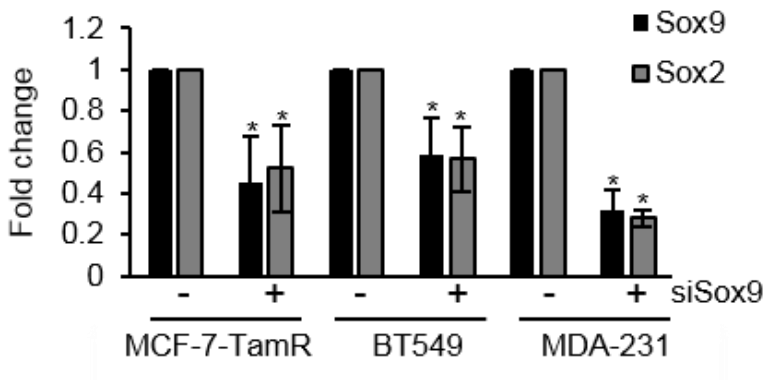

Fig 3.9.3 Sox2/Sox9 mRNA level in breast cancer cells transfected with siC (-) and siSox9(+)

These findings suggested that the relationship between these two transcription factors could be mediated by direct binding to their promoters. Analysis of the promoter sequences close to the transcription starting sites (TSS) showed that the Sox2 promoter contains a Sox9 binding sequence (AGAACAATGA) at 852 base pairs from the Sox2 TSS, while the Sox9 promoter displays a potential Sox2 binding site (CATTTGTT) at 1261 base pairs from the Sox9 TSS. We further checked the amplicon around these areas in an open-access database for matrix models describing DNA-binding preferences for transcription factors (http://jaspar.genereg.net/) and confirmed the potential for binding by Sox9 and Sox2, respectively.

PCR primers were designed for these regions and specificity confirmed using PRIMER BLAST (https://www.ncbi.nlm.nih.gov/tools/primer-blast/). ALDH1A3 promoter (the site A, as in Fig. 3.6.4) was used as positive control for Sox9 binding and a fragment of the cyclin D1 (CCND1) promoter, one of the well-known Sox2 direct target gene (Li et al., 2017), for Sox2 binding. Chromatin immunoprecipitation on MCF-7-Sox2 cells showed that Sox9 and Sox2 bind reciprocally on their respective promoters (Fig.3.9.4).

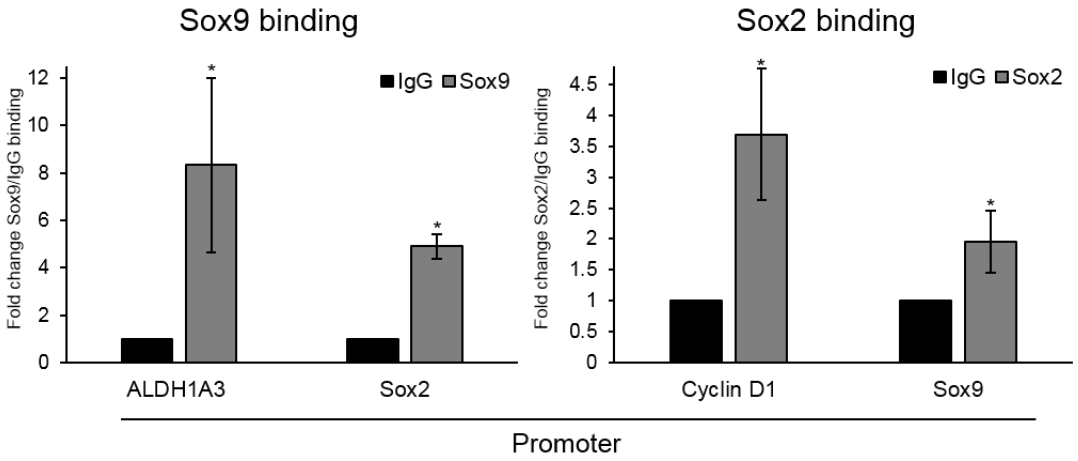

Fig. 3.9.4 Sox9 binding upon ALDH1A3 and Sox2 promoter and Sox2 binding upon Cyclin D1 and Sox9 promoter in MCF-7 overexpressing Sox2 (MCF-7-Sox2).

To determine whether Sox2 requires Sox9 expression in order to activate Wnt signaling or whether they act independently we transiently silenced Sox2 in MDA-MB-231 shControl and shSox9 cells by using a specific siRNA. Stable Sox9 silencing resulted in decreased AXIN2 levels in these cells (around 60%). Transient Sox2 silencing was sufficient to reduce Sox9 and AXIN2 to levels comparable to those reached in the shSox9 cells. Additionally, transient Sox2 silencing in cells already stably silenced for Sox9 did not further decrease Sox9 or AXIN2 levels, suggesting that Sox2 requires Sox9 in order to affect AXIN2 levels (Fig. 3.9.5).

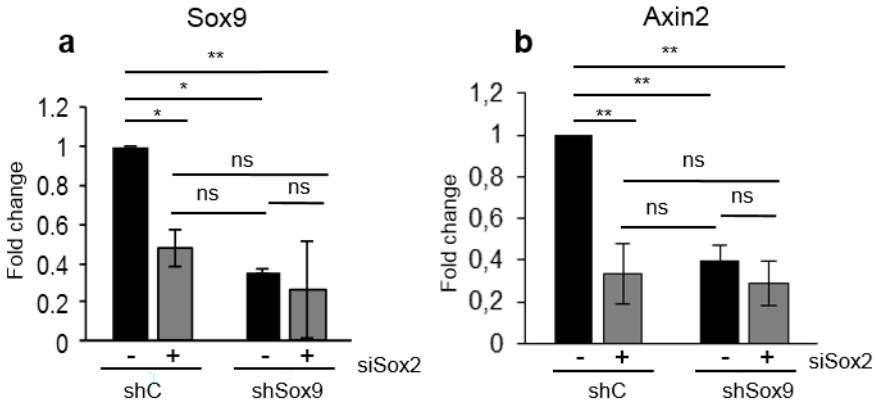

Fig 3.9.5. Sox9 (a) and Axin2 (b) mRNA levels in shC and shSox9 MDA-MB-231 cells transiently silenced for Sox2 (+) or siControl (-). * p<0.05, ** p<0.01.

Furthermore, analysis of the effect of Sox2 silencing on endogenous Wnt signaling in shControl and shSox9 MDA-MB-231 cells showed a 20% reduction in the TOP/FOP ratio due to Sox2 silencing, which was not further reduced in shSox9 cells (Fig. 3.9.6). All

together, these findings confirm that Sox2 regulates Wnt signaling through Sox9, although it does not exclude the possibility that Sox2 may play additional roles, independently of Sox9. In addition, they suggest that a positive Sox2-Sox9 loop exists that leads to enhanced Wnt signaling in breast cancer cells.

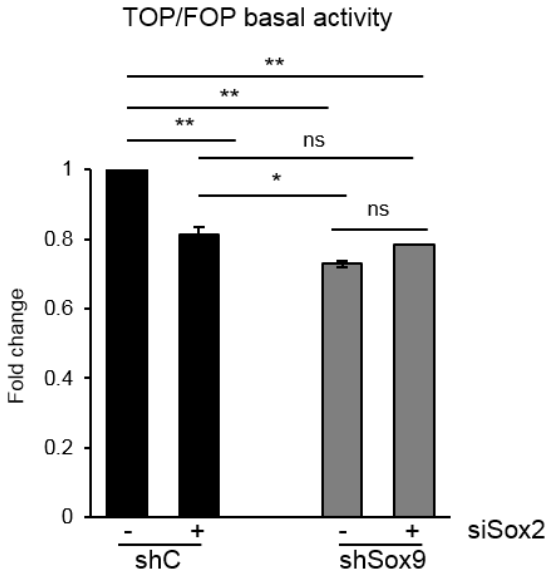

Fig. 3.9.6 TOP/FOP ratio in shC and ShSox9 MDA-MB-231 cells transfected with siControl (-) and siSox2 (+). * p<0.05, ** p<0.01

10. Wnt secretion inhibition reduces ALDEFLUOR+ cell population in breast cancer cells

As previously shown, Sox9 is a critical regulator of ALDEFLUOR progenitor/stem cell population in breast cancer cells and a positive regulator of Wnt signaling. To assess whether Wnt signaling may regulate the ALDEFLUOR$^+$ cell population, tamoxifen resistant cells, MCF-7-TamR and T47D-TamR, were treated with the Wnt secretion inhibitor IWP-2 that inhibit porcupine activity and in turn Wnt proteins palmitoylation (Bengoa-Vergniory and Kypta, 2015) and the canonical pathway inhibitor IWR-1 (which stabilizes β-catenin destruction complex and then blocks canonical Wnt pathway) (Huang et al., 2009). FACS analysis showed that treatment with Wnt inhibitors reduced the percentage of ALDEFLUOR$^+$ cells, suggesting that Wnt signaling is a positive regulator of this stem/progenitor cell population in breast cancer cells (Fig. 3.10).

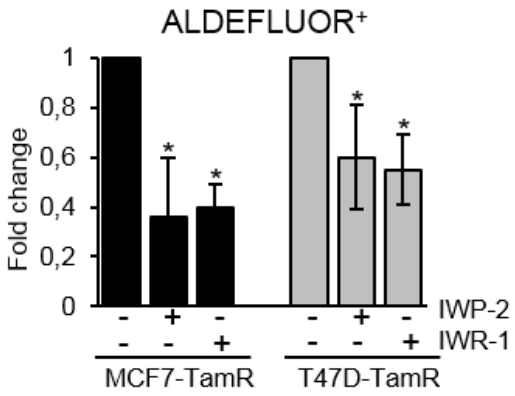

Fig 3.10 ALDEFLUOR+ content in tamoxifen resistant cells treated with Wnt inhibitors. ALDEFLUOR+ cells in MCF-7-TamR and T47D-TamR cells treated 48 hours with the Wnt secretion inhibitor IWP-2 and the canonical Wnt inhibitor IWR-1. DMSO has been used as drug vehicle control. * $p<0.05$.

Conclusion:

Both, Wnt secretion impairment and canonical Wnt signaling inhibition reduces the percentage of ALDEFLUOR+ cells in breast cancer cells, similar to Sox9 silencing in breast cancer cells. As previously suggested by own lab and others, Wnt inhibitors may represent a potential therapeutic approach against breast cancer stem cells (Piva et al., 2014).

11. ERK pathway regulates Sox9 expression in breast cancer cells

We sought to explore potential pathways implicated in Sox9 regulation in breast cancer cells. As previously shown, Sox9 appears to be mostly expressed in triple negative breast cancer cell lines and the same was observed in primary breast tumors. ERK pathway has been shown to be more active in basal/triple negative breast tumors and therefore, it could represent an attractive target in this breast cancer molecular subtype (Giltnane and Balko, 2014). Interestingly, MEK/ERK activation has been shown to increase Sox9 expression in several tissues, including mesenchymal stem cells (Wang et al., 2016a) and chondrocytes (Murakami et al., 2000) and bladder cancer cells (Ling et al., 2011b). To determine whether MEK/ERK signaling was affecting Sox9 expression in breast cancer cells, U0126, a selective inhibitor of MAPK kinase MEK1 and MEK2 that prevents the activation of the MAP kinases p42 and p44, was used to treat the triple negative breast cancer cell lines MDA-MB-468 and MDA-MB-231.

U0126 reduced Sox9 mRNA levels in both cell types (Fig. 3.11.1a), as well as at protein level, correlating with inhibition of MAPK phosphorylation (Fig 3.11.1b), suggesting that the ERK pathway exerts a positive effect on Sox9 expression in triple negative breast cancer cells. Tamoxifen resistant cells behaved similarly to TNBCs, although T47D-TamR cells appeared to be more sensitive than MCF-7-TamR. In fact, Sox9 down-regulation was detected in MCF-7-TamR cells only when treated with 20 μM of MEK inhibitor, while T47DTamR cells showed reduced Sox9 levels already at 10μM after 24 hours of treatment. Sox2 expression was not affected by U0126 treatment in tamoxifen resistant cells (Fig. 3.11.2).

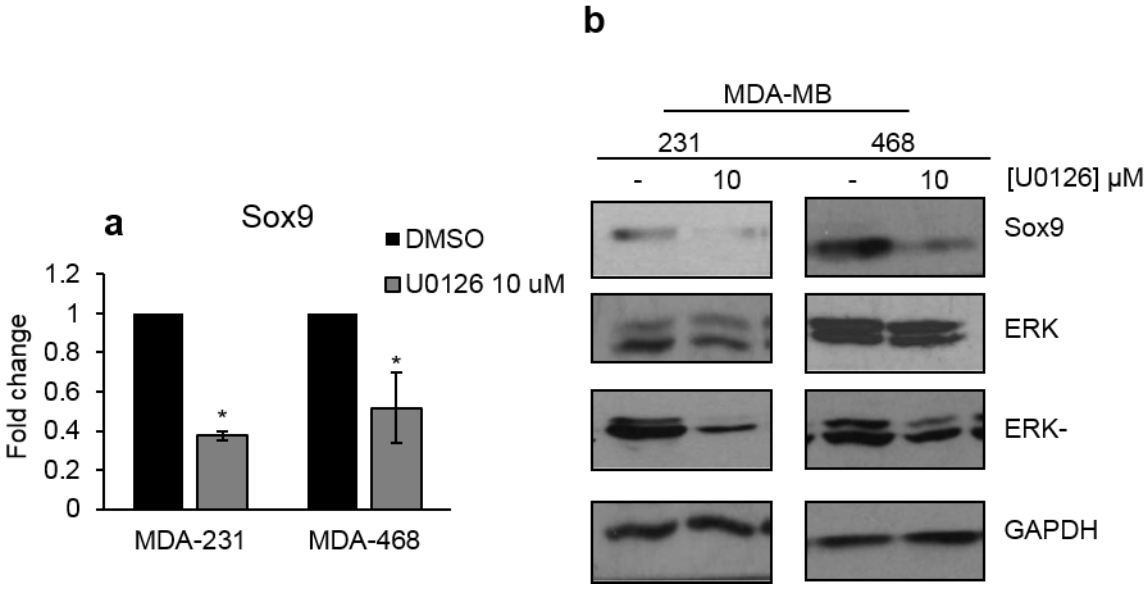

Fig. 3.11.1 Sox9 expression in triple negative breast cancer cells treated with MEK inhibitor U0126. **(a)** Sox9 mRNA expression in MDA-MB-231 and MDA-MB-468 cells treated 24 hours with the MEK inhibitor U0126. **(b)** Sox9 protein expression in MDA-MB-231 and MDA-MB-468 cells treated 24 hours with the MEK inhibitor U0126. Membrane were blotted also with phosphorylated ERK (ERK-P) to ensure inhibitor worked properly. GAPDH has been used as loading control. * $p<0.05$.

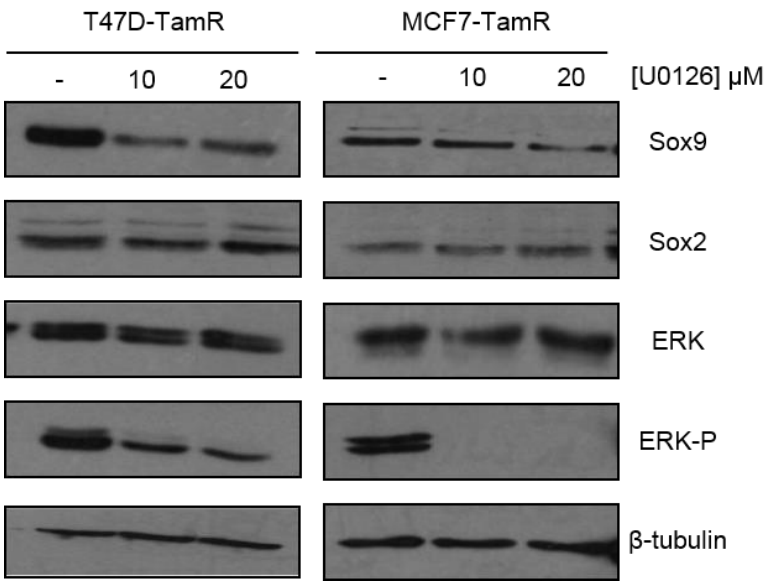

Fig. 3.11.2 Sox9, Sox2, ERK, ERK-P, β-tubulin in tamoxifen resistant cells tretated with MEK inhibitor U0126

Next, we wished to determine whether Sox9 was required by the ERK pathway to control breast cancer cell growth and stemness. Cells with reduced Sox9 levels were more refractory to the U0126-dependent inhibitory effects on colony formation (Fig. 3.11.3a), implicating Sox9 activation by the ERK pathway in tumorigenicity, as suggested in other systems. It has been reported that MEK inhibition reduces mammosphere formation and stemness in basal-like breast cancer cells (Balko et al., 2013), which we confirmed treating two triple negative breast cancer cell lines with U0126 (Fig. 3.11.3b). On the basis of these observations, we hypothesized that signaling through MAPK activation could be mediated by Sox9. Accordingly, we observed that reduction of mammosphere formation by MEK inhibition was impaired in MDA-MB-231 cells with reduced endogenous Sox9 levels (Fig. 3.11.4c). These findings provide support for the relevant regulation of Sox9 by MAPK in breast cancer and its role in tumorigenesis and stemness.

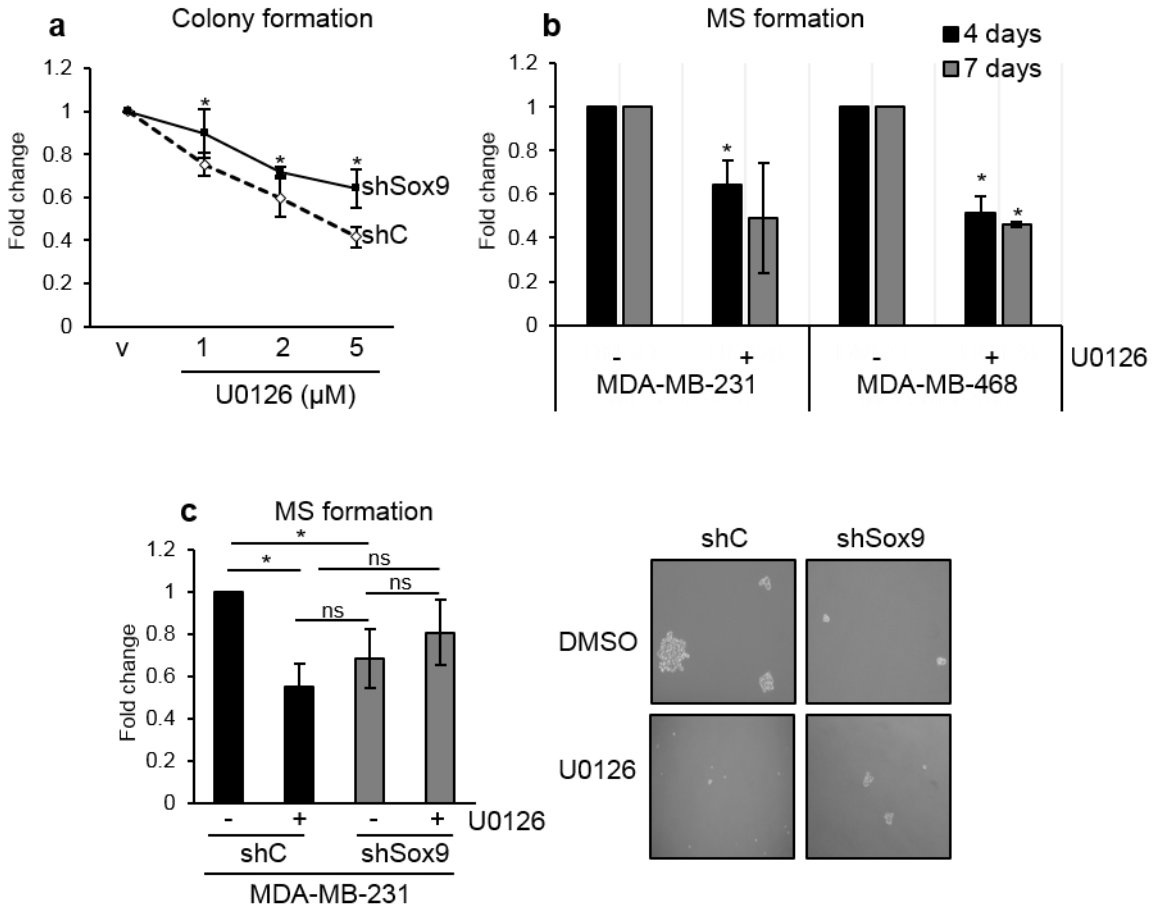

Fig. 3.11.3 Clonogenicity and mammosphere formation in MDA-MB-231 treated with MEK inhibitor U0126. **(a)** Fold change of the number of colonies formed by shcontrol and shSox9 MDA-MB-231 cells exposed to increasing concentration of U0126. The results are shown as fold change in colony formation compared to DMSO treated cells (v). **(b)** Mammosphere formation in MDA-MB-231 and MDA-MB-468 cells in the absence or presence of 10 μM MEK inhibitor U0126. Mammospheres were counted at day 4 and 7 post plating. **(c)** Mammosphere formation assayusing shcontrol (shc) and shSox9 MDA-MB-231 treated with DMSO or 10 μM U0126; representative images are shown. shC: shCNTR, ns: no significant, v: U0126 vehicle, (DMSO), * $p<0.05$.

Conclusion:

These results show that the ERK pathway induces Sox9 expression in breast cancer cells leading to increased cell clonogenicity and mammosphere formation.

Chapter 4: Discussion

1. Sox9 marks and maintains luminal progenitor cells in the human mammary gland

The existence of cellular hierarchy in the mammary gland is a well-accepted concept and many in vitro analysis, transplantation and lineage tracing studies have demonstrated the existence of mammary stem/progenitor cells in the mouse and human mammary gland (Visvader and Stingl, 2014).

Our results show that the transcription factor Sox9 marks luminal progenitor cells, that are characterized by high expression of the integrin alpha 6 (CD49f) and epithelial specific antigen (EpCAM), ($CD49f^{+}EpCAM^{+}$), and also by increased ALDH activity and mammosphere-forming efficiency. Our results fit observations in other tissue contexts. Sox9 has been associated with progenitor cells in exocrine pancreas (Seymour et al., 2007), gut and liver (Furuyama et al., 2011), kidney (Kang et al., 2016), retinal cells (Poché et al., 2008), and prostate. Our results show that most $CD49f^{+}EpCAM^{+}$ are found in the $ALDEFLUOR^{+}$ cell population, which has been observed also by another group (Eirew et al., 2012).

The relevance of Sox9 in the maintenance of a “mammary stem cell status” was claimed for the first time by Robert Weinberg laboratory in 2012 (Guo et al., 2012) They showed that Sox9 cooperates with the transcription factor SLUG (SNAI2) in order to determine stemness in mice. Using a conditional Sox9 knockout mouse model, it has been shown that Sox9 depletion impairs mammary gland development, and reduces the number of luminal progenitor and luminal cells (Malhotra et al., 2014). Another report showed that Sox9 depletion reduces mammary gland branching in mice (Wang et al, 2013).

We observed that Sox9 reduction is sufficient to reduce the pool of $ALDEFLUOR^{+}$ cells in HBECs as well as the growth in extracellular matrix (matrigel). Growth in matrigel is considered an hallmark of stem/progenitor cells in the mammary gland (Lim et al., 2009) and the reduced growth we observed in shSox9 HBECs compared to control cells highlights the relevance of Sox9 in the maintenance of progenitor cells in HBECs.

Differentiation studies show that the number of luminal differentiated colonies, expressing cytokeratin 18 (CK18), was reduced, suggesting that the number of luminal

progenitor cells has been affected, confirming what was observed in the context of the mouse mammary gland (Malhotra et al., 2014). In this report, when researchers looked at the aspect of the mouse mammary gland knockdown for Sox9, major changes were observed in mouse from 3 to 5 weeks, with reduced ductal outgrowth and side branching. Unfortunately, in this mouse model, the mammary gland lost Cre expression after week 5, which explains why they did not observe any effect of Sox9 deletion during pregnancy and lactation (Malhotra et al., 2014).

Another report showed that Sox9 overexpression induced mammary gland side-branching (Wang et al., 2013). Very recently it has been shown, using lineage tracing, that Sox9+ progenitor cells give rise to ERα- cells in the mouse mammary gland, and that there is strong Sox9 expression in alveoli. In addition, in this study, CD133+ (Prominin1) marks progenitor cells able to give rise to ERα+ cells (Wang et al., 2017). Malhotra and colleagues also obtained similar results with lineage tracing some years before, showing that luminal cells and in particular CD61+ luminal progenitor cells were Sox9+ (Malhotra et al., 2014). We found similar results in the human mammary gland, in which Sox9 marks luminal progenitor cells, and Sox9 depletion, among other things, reduces the amount of differentiated luminal colonies. In addition, ALDEFLUOR^{+} cells are ERα- as shown by us and others (Li et al., 2013; Simões et al., 2015), confirming our observation of lack of co-localization between Sox9 and ER.

Conversely, the growth in Matrigel and the number of ALDEFLUOR^{+} cells was increased by Sox9 overexpression in the non-tumorigenic MCF10A mammary epithelial cells. We did not check the effect on differentiation on these cells since they already express myoepithelial markers. Sox9 silencing reduces primary and secondary mammosphere formation in primary breast epithelial cells, while Sox9 upregulation in MCF10A cells induces both, supporting further the relevance of Sox9 in progenitor cell maintenance. Similar results were observed in prostate mouse cells, in which Sox9 deletion reduces prostatosphere formation (Huang et al., 2012).

Analysis of various markers contributed to support Sox9 role in progenitor cells. Sox9 silencing in human breast epithelial cells reduces the expression of the luminal progenitor marker c-KIT (Regan et al., 2012), the stemness factor FOXO3A (Miyamoto et

al., 2007), which has also been shown to be important for ER expression and activity (Guo and Sonenshein., 2004). Sox9 silencing reduces the expression of the transcription factor SNAI2/SLUG, which cooperates with Sox9 to maintain mammary gland stemness in mice (Guo et al., 2012).

The luminal differentiation transcription factor GATA3 (Asselin-Labat et al., 2007b) was not affected, even if a reduction trend was observed. Interestingly, ELF5 expression was reduced in breast epithelial cells by Sox9 silencing and Sox9 overexpression has been shown to lead to ELF5 overexpression in mouse organoids (Guo et al., 2012), which supports our observation. ELF5 has been extensively studied and its main role in breast development is alveologenic development and differentiation. In fact, ELF5 is highly expressed in luminal progenitor cells upon progesterone stimulation in mice, and it drives luminal branching and alveologenic differentiation (Lee et al., 2013). We have not analyzed this in a detailed manner, but it is possible that Sox9 could be involved, at least at a certain stage, in alveologenesis, since Sox9 depletion reduces the pool of luminal progenitor cells and luminal colonies in a differentiation assay. It would be interesting to perform an alveologenic differentiation assay *in vitro* with cells expressing different levels of Sox9 treated with an alveologenic stimulus such as prolactin to check this hypothesis. Lineage tracing experiments have shown that mice alveoli express high Sox9 levels during pregnancy, but they do not demonstrate, whether alveologenesis is impaired for example by Sox9 deletion (Wang et al., 2017). Interestingly, ALDH1A3, c-KIT and ELF5 are highly expressed in mouse mammary gland and human breast luminal progenitor cells, serving as common markers (Lim et al., 2010). Sox9 down-regulation reduces these markers in luminal progenitor cells, suggesting a direct or indirect positive regulation by Sox9.

Notably, it was not observed a reduction of ALDH1A1 transcript in shSox9 cells compared to control cells, but still ALDEFLUOR^{+} cells content after Sox9 silencing was detected. This observation suggests that the ALDH isoform that it is contributing to the ALDEFLUOR phenotype is the ALDH1A3, which has been shown to be the most abundant isoform expressed in the human mammary gland (Eirew et al., 2012) and it is consistently reduced by Sox9 silencing.

Finally, we speculate that during human mammary gland development, Sox9 maintains luminal progenitor cells ($CD49f^+EpCAM^+$ or $ALDEFLUOR^+$ cells) and during differentiation, Sox9 drives luminal differentiation in which ER and PR are expressed in terminally-differentiated luminal cells. in this context, estrogen signaling may contribute to the reduced Sox9 expression observed in differentiated luminal cells. The relationship between Sox9 and estrogen signaling will be further discussed next.

2. Sox9 in breast cancer and endocrine resistance

2.1 Sox9 is expressed in breast cancer and is regulated by estrogen

Sox9 expression is enhanced in breast tumors compared to normal breast tissue, confirming observations by another laboratory (Chakravarty et al., 2011a). This finding suggests that Sox9 increase in breast cancer is an event associated with the development of tumorigenesis. Elevation of Sox9 expression has also been observed in other tumorigenic contexts, such as colon cancer (Matheu et al., 2012) and lung cancer (Wang et al., 2015b).

Our data using breast cancer cell lines, primary breast tumors and in-silico analysis confirm the observation that Sox9 is more highly expressed in ER- breast cancers than in ER+ tumors.

This led us to speculate about the existence of a relationship between ER signaling and Sox9 expression in breast cancer cells. Several findings supported this hypothesis: we found an inverse gradient of expression of Sox9 and ER, estrogen treatment reduces Sox9 expression,*in silico* analysis shows that ER silencing induces Sox9 expression in MCF-7 cells (Al Saleh et al., 2011b) and we previously demonstrated that estrogen reduces the stem cell pool both in normal and cancer cells (Simões et al., 2011).Finally, very recently, lineage tracing experiments have shown that Sox9 and ER+/PR+ cells are also mutually exclusive in the mouse mammary gland (Wang et al., 2017).

Together, these findings may explain, in part, the observation that basal/triple negative breast tumors express higher Sox9 levels than ERα+ tumors and confirm previous reports showing that aggressive breast tumors contain more cancer stem cells

than differentiated tumors (Pece et al., 2010) and our own data about the role of Sox2 on development of resistance to tamoxifen and cancer stem cell enrichment.

The negative regulation of Sox9 expression by estrogen has not only been observed in cancer. During sex determination of the red-eared slider turtle *Trachemys scripta,* estrogen signaling suppresses Sox9 expression, driving male-to-female sex reversal (Barske and Capel, 2010). This is quite relevant from an ecological point of view, since it can be a potential explanation of male-to-female sex reversal (is that a problem? Need to explain, not clear point) in turtles due to estrogens (Crews et al., 1991). In marsupials, it has been shown that estrogen prevents Sox9 translocation to the nucleus of differentiating ovaries, thus blocking male differentiation, even though in this context Sox9 levels appear unaffected by estrogen treatment (Pask et al., 2010). Finally, an inverse association between Sox9 and ERαβ expression has also been described in mice granulosa cells (Dupont et al., 2003).

The fairly rapid hormonal downregulation of Sox9 expression led us to speculate that ER may bind directly to the Sox9 promoter in order to repress its expression. In fact, analysis of ER ChIP (Chromatin ImmunoPrecipitation) data available online, shows two publications in which the presence of ER binding sites in the human Sox9 promoter is revealed (Bourdeau et al., 2004; Jin et al., 2005). In particular, Bourdeau and collaborators showed a list of promoters containing ERE sequences, and this list includes Sox9, with an ERE at -2700/-2650 base pairs from the transcription star site. We designed specific ChIP primers to amplify this region and there are ongoing experiments in the lab to define whether ERα binds directly to this promoter sequences.

All together, these data suggest the negative regulation of Sox9 by estrogen in different cell contexts. Nevertheless, it is important to point out that in strongly ER positive breast cancer cells Sox9 was barely expressed, and yet estrogen treatment reduces Sox9 expression. This may be explained by the fact that both ER expression reduces directly in the same cells Sox9 expression or ER-induced paracrine factors may reduce Sox9 expression.

3. Sox9 is induced in tamoxifen resistant cells exhibiting a preferential cytosolic localization

A study from our lab demonstrated that Sox2 elevation drives tamoxifen resistant in breast cancer (Piva et al., 2014., Domenici et al., 2014) and genetic profiling showed that MCF-7 cells overexpressing Sox2 display elevated Sox9 levels. Therefore, we wished to determine whether Sox9 expression is also associated to the development of endocrine resistance in breast cancer. Increased Sox9 expression in three different models of tamoxifen resistant cell lines was observed. The reduction in estrogen activity and increase in Sox2 levels may contribute, among other signals, to enhance Sox9 expression in tamoxifen resistant cells. Similar result was observed when Sox2 was overexpressed in U87 glioma cells (Garros-Regulez et al., 2016b). Other researchers observed that Sox2 and Sox9 were both highly expressed in a ductal carcinoma cell line (MCF10A-DCIS) compared to control cells (MCF10A) even though they didn't show that the two Sox factors are related (Li et al., 2014a). These data support the observation that Sox9 expression is induced by Sox2.

Importantly, the relevance of Sox2 in tamoxifen resistance was confirmed by the finding that Sox2 was clearly overexpressed in tumors that have developed resistance to tamoxifen therapy (Piva et al., 2014). This same cohort (n=53) of patients, including responder and resistant tumors, was employed to determine Sox9 expression.

We observed Sox9 immunostaining reflected wide heterogeneity within tumors, including expression levels as well as localization. In particular, cytoplasmic localization was more consistent in recurrent than in sensitive tumors. The same pattern was detected in tamoxifen resistant MCF-7 cells.

Sox9 has been described both in the nucleus and cytoplasm of cells. In fact, Sox9 high mobility group (HMG) domain contains a nuclear exporting sequence (NES) that allows Sox9 nuclear import into during mammalian testis differentiation. Cytoplasmic Sox9 has also been found in the cytoplasm of invasive ductal carcinoma (IDC) cells, which are highly tumorigenic and it has been associated with Ki67 staining, reflecting high proliferative status (Chakravarty et al., 2011b).

More recently, Sox9 cytoplasmic expression has been correlated with p53 mutations and reduced survival in pancreatic cancer patients, although this association has not been analyzed further (Huang et al., 2015a).

Interestingly, another Sox gene, Sox11, was detected in the cytoplasm of mantle lymphoma cells, which correlates with shorter overall survival than nuclear Sox11 (Wang et al., 2008b).

The role of Sox9 in the cytoplasm is not presently understood, but some studies have demonstrated that the differential Sox9 localization is due to post-transductional modifications. As an example, protein-kinase A (PKA) inhibition causes Sox9 cytoplasmic-to-nuclear shift in human pluripotent embryonal carcinoma NT2/D1 cells (Malki et al., 2005). In addition, in chondrocytes, it has been shown that TGFβ signaling activates Rho-kinase (ROCK), which in turn induces Sox9 phosphorylation at Serine 181 (Haudenschild et al., 2010) and its translocation to the nucleus. In addition, Sox9 can also be acetylated in chondrocytes leading to reduced nuclear entry (Bar Oz et al., 2016).

In conclusion, even if there are known stimuli that induce changes in Sox9 localization, to our knowledge, the functions of Sox9 in the cytoplasm are not known. An approach to answer this question could be to generate mutant cell lines through Cas9-CRISPR system with specific mutations in the Sox9 NLS and NES sites (or plasmids carrying mutant Sox9 protein) in order to analyze the resulting functional alterations. Our observation that MAPK inhibition induces Sox9 accumulation in the cytoplasm may suggest that Sox9 could be phosphorylated by MAPK to induce Sox9 nuclear localization as observed in other systems, but this requires further studies which are currently ongoing in the laboratory.

Sox9 inhibition in tamoxifen resistant breast cancer cells, through shRNA, reduces cell clonogenicity and growth in anchorage-independent conditions, suggesting that Sox9 has a pro-tumorigenic role in these cells. Furthermore, Sox9 depletion sensitized cells to tamoxifen treatment, but only under clonogenic conditions. This observation suggests that Sox9 gain importance in tamoxifen resistance only when cells are growing in a clonogenic and isolated manner but when cells grow closer to each other, other factors may help and supply the Sox9 absence in terms of growth and survival under tamoxifen treatment.

4. Sox9, breast cancer stem cells and tumorigenicity

Breast Cancer Stem Cells (BCSCs) represent an important target for breast cancer therapy, since these cells are considered to be responsible for cancer relapse, metastasis, chemotherapy and endocrine resistance (Piva et al., 2014; Simões and Vivanco, 2011). According to this, there is an increasing interest in developing pharmacological strategies to selectively target BCSCs. Cells with high ALDH activity display tumorigenicity in breast (Ginestier et al., 2007), pancreatic (Kim et al., 2011), and gastric (Wu et al., 2016). Very interestingly, immunological approaches have been proposed, by the utilization of “cancer stem cell primed” dendritic cells (DCs) (Hu et al., 2016; Lu et al., 2015). Lu and collaborators showed that ALDEFLUOR^{+} primed DCs can reduce tumor growth in mice models of melanoma and squamous cell carcinoma and metastasis formation in the melanoma model. Both approaches appear promising and hopefully further future studies will prove their effectiveness in cancer patients. In addition to the pharmacological and immunological approaches to target cancer stem cells it is interesting also to identify pathways and transcription factors/genes involved in the maintenance of these tumorigenic cells population, for a better understanding of the basic cell biology that stands behind their growth and maintenance in different kinds of tumors.

Here we show that in primary breast epithelial cells and in luminal breast cancer cells Sox9 is associated with progenitor/stem cells, regulating ALDH activity, sphere formation and luminal differentiation. Sox9 induces sphere formation also in colon cancer cells (Carrasco-Garcia et al., 2016), glioma cells (Garros-Regulez et al., 2016b) and basal cell carcinoma (Larsimont et al., 2015), suggesting a common effect of Sox9 in the maintenance of cancer stem cells in different tissues. We observed that after Sox9 silencing, the percentage of ALDEFLUOR^{+} cells declined in all the luminal cancer cells analyzed (MCF-7-TamR, T47D-TamR, and ZR-75-1) but not in TNBCs (MDA-MB-231 and slightly reduced in BT549). Sox9 then appears to be relevant in ALDEFLUOR^{+} cells maintenance in luminal cells but not in basal cells, even though this observation should be confirmed analyzing a large cohort of primary breast cancer samples.

Sox9 depletion in MDA-MB-231 cells did not affect CD44^{+}CD24$^{-/low}$ cancer initiating cells, while a slight increase was detected in Sox9-silenced BT549 cells compared to

control cells, revealing a Sox9 cell line specific effect. This observation suggests that Sox9 has a cell line specific effect on this population, making difficult to drawn any conclusion at this stage. This can be potentially explained by the fact that ALDEFLUOR^{+} and CD44^{+}CD24$^{-/low}$ show very little genetic overlap in human breast tumors (Ginestier et al., 2007).

Sox9 depletion reduces breast cancer cell clonogenicity and invasion *in vitro*. Additionally, we have also participated in an *in vivo* study that reveals a STAT-PML-Sox9 axis that induces tumorigenicity and stemness in triple negative breast cancer cells (Martin-Martin et al, 2016). This article is showed at the end of the thesis in the annexes section.

Analysis of EMT markers including ZEB1, SNAI1 and SNAI2 in triple negative breast cancer cells stably silenced for Sox9 showed no difference in the mRNA expression of these genes, except for a slight increase in E-cadherin expression. This is in agreement with the report in Weinberg laboratory which show that SLUG cooperate with Sox9 to maintain mammary stem cells in mice, but no changes in E-cadherin and Vimentin expression were detected when Sox9 was overexpressed in mouse luminal mammary epithelial cells (Guo et al., 2012a). Nevertheless, in other context it was shown Sox9 involvement with EMT phenotype, as in thyroid cancer cells (Huang and Guo, 2017) and in hepatocarcinoma, in which Sox9^{+} cells were responsive to TGFβ-induced EMT (Kawai et al., 2016), indicating that Sox9-EMT relationship is tissue-dependent.

To our knowledge, this is the first report that directly links Sox9 expression to ALDH activity. Previously, it has been shown that miR-140 directly targets and reduces the expression of both Sox9 and ALDH1 (Li et al., 2014a), suggesting a differentiating role for this miRNA in basal breast carcinoma. We found that Sox9 silencing reduces ALDH1A3 expression both in normal breast and in cancer cells. In addition, a small cohort of primary breast tumor cells show increased Sox9 and ALDH1A3 levels in ALDEFLUOR^{+} cells. We also showed previously that ALDEFLUOR^{+} cells are enriched in ALDH1A3 mRNA level in normoxic and hypoxic conditions (Iriondo et al, 2015).

We focused on ALDH1A3 since it is the ALDH isoform that appears to be relevant in the maintenance of ALDEFLUOR^{+} in breast cancer cells (Marcato et al, 2011). In fact,

it was shown that only ALDH1A3 silencing was able to reduce significantly ALDEFLUOR+ cell content, while ALDH1A2 or ALDH1A1 did not.

Genetic profiling of NT2/D1 cells stably expressing Sox9 revealed the upregulation of ALDH1A3 (Ludbrook et al., 2016), supporting our observation of increased ALDH1A3 levels in MCF10A cells stably transduced with Sox9. ALDH1 was shown to be responsible for the activity observed in stem cells, with no specification of the isoform involved (Ginestier et al, 2007). However, a later study demonstrated that both ALDH1A3 and ALDH1A1 may affect stemness in breast epithelial cells (Honeth et al., 2014). Previous data from our lab show that ALDH1A1 is not expressed in MCF-7, T47D or MCF-7-TamR cells (data not shown), discarding the possibility that ALDH1A1 is regulated by Sox9 in our experimental models.

Furthermore, Sox9 modulation regulates ALDH activity, and this happens through direct Sox9 binding to the ALDH1A3 promoter, while the expression levels of ALDH1A1 are not affected by Sox9 silencing.

Recently, it has been shown that ALDEFLUOR^{+} cells sorted from human articular chondrocytes contains higher expression of Sox9, along with different ALDH isoforms compared to ALDEFLUOR^{-} cells (Unguryte et al., 2016), suggesting that Sox9 may be a marker of ALDEFLUOR^{+} cells not only in the human breast, but also in other tissues. In contrast, in these cells the expression of the stem cell genes Sox2, OCT4 and NANOG was not altered in ALDEFLUOR^{+} cells, while we observed that Sox2 is highly expressed in such cells (Piva et al, 2014) and that Sox2, OCT4 or NANOG overexpression is sufficient to increase the ALDEFLUOR^{+} population in breast cancer cells (Simöes et al, 2011). Overexpression of core stem cell genes OCT4 and NANOG in MCF-7 cells led to increased Sox9 expression. This could be due to a direct transcriptional effect of these genes on the Sox9 promoter, but this possibility remains to be tested. Sox2 overexpression in MCF-7 cells increases Sox9 too, but this will be discussed further later on. In conclusion, ours and other published results suggest a role for Sox9 in the maintenance of cancer stem cells and tumorigenicity, partly through the regulation of ALDH1A3 expression.

Based on these findings, Sox9 may be considered an interesting target in a variety of different breast cancer subtypes, from endocrine resistant to triple negative breast cancer. However, one of the main problems is represented by the fact that transcription factors (TFs) (as Sox2 and Sox9) are pharmacologically difficult to target. However, recent research improvements have been achieved (Hagenbuchner and Ausserlechner, 2016). Different strategies are currently employed to target TFs activity and function. These are represented by: 1) inhibition of protein/protein interaction since many TFs act as homo-heterodimers and depend on co-factors for appropriate function, 2) blocking TFs-DBD interaction and 3) targeting chromatin remodeling/epigenetic reader proteins which are pivotal for DNA access of TFs. Examples of successful TFs targeting are represented by p53 stabilization by drugs that inhibit the E3 ubiquitin ligase MDM2 (which ubiquitinates and thereby marks for degradation p53) (Issaeva et al., 2004; Secchiero et al., 2011) and blocking protein-protein and protein-DNA STAT3 binding (Fletcher et al., 2008). Another example is represented by hypoxia inducing factors 1α and 2α (HIF-1α and HIF-2α) which activate hypoxia-responsive genes (Iriondo et al., 2015). Acriflavine blocks both TFs (Lee et al., 2009).

Recently, an interesting paper has shown that small molecules can block transcription factor activity through interference with their “interactome”. In particular, the small molecule Sm4 blocks Sox18 interactome, blocking angiogenesis in Zebrafish and tumor vascularization and metastasis in a mouse model of breast cancer (Overman et al., 2017).

5. Sox9 maintains Wnt activity in breast cancer cells

A study from our laboratory showed that tamoxifen resistant cells have increased Wnt signaling, which contributes to maintain endocrine treatment resistance (Piva et al., 2014). Wnt1 rescues breast cancer cells from growth arrest induced by tamoxifen (Schlange et al., 2007). Increased expression of Wnt target genes as DKK1, c-myc has been observed in breast cancer tamoxifen resistant cells *in vitro* (Loh et al., 2013). Wnt activity has also been largely studied in the context of TNBCs in which appears upregulated (Matsuda et al., 2009) and correlates with worst outcome (Geyer et al., 2011). In addition, stable β-catenin silencing in HCC38 TNBCs reduces ALDEFLUOR^{+}

cells, cell invasion, tumor growth *in vitro* and *in vivo* and sensitivity to doxorubicin and cisplatin, suggesting that the canonical Wnt pathway is involved in triple negative breast cancer tumorigenicity (Xu et al., 2015). This effect is in agreement with the reduction of ALDEFLUOR$^+$ cells in breast cancer cells treated with Wnt inhibitors. Furthermore, clinical data reveals that nuclear β-catenin localization, which indicate Wnt activation in breast cancer cells, correlates with worst outcome in breast cancer patients, regardless of the breast cancer subtypes analized (Li et al., 2014b).

Collectively, these findings strongly support the role of Wnt signaling in tamoxifen resistance. A number of small molecules targeting the Wnt pathway are currently in pre-clinical development and, therefore, it may be an interesting target in tamoxifen resistant and basal/triple negative breast cancers.

Sox9 downregulation reduces expression of the Wnt target genes Axin2 and FZD4 and inhibits β-catenin-dependent transcriptional activation. It has been shown that FZD4 associates with tumorigenicity and stemness in glioblastoma (Jin et al., 2011), as well as Sox9 (Wang et al., 2012), which suggests that Sox9 activate FZD4 not only in breast cancer cells but potentially also in glioma cells. Similarly, it has been shown that Sox9 silencing reduces LRP6 and Tcf4 transcription (Wang et al., 2013). In addition, we report here that stable Sox9 silencing reduces significantly Wnt5B mRNA levels. Recently, it has been shown that Wnt5B positively correlates with growth, invasion and survival of TNBCs and, in addition, high Wnt5B expression is associated with reduced survival (Yang et al., 2014) and it has been observed in brain metastasis (Klemm et al., 2011). These findings support Sox9-mediated b-catenin activation as one of the molecular mechanisms underlying aberrant Wnt signaling in breast cancer. Moreover, Sox9 activates Wnt pathway also in prostate cancer (Ma et al., 2016) and during gastric cancer progression (Santos et al., 2016). Intriguingly, the association between Sox9 and Wnt pathway seems to be bi-directional. Indeed, it has been observed that Wnt signaling drives Sox9 phosphorylation at the serine residues 64 and 181, which results in Sox9 SUMOylation and transcriptional activation to induce neural crest cells delamination (Liu et al., 2013b). In addition, a positive loop between TCF4 and Sox9 may exist, since it has been observed that deletion of TCF4 suppress Sox9 expression in mouse colon epithelium (Blache et

al., 2004), although it is important to point out that these effects can also be tissue-dependent.

Previously we have shown that development of resistance to tamoxifen is driven by Sox2-dependent activation of Wnt signaling in CSCs. Our findings demonstrate that Sox2 induces Sox9 expression and this suggests a model in which Sox9 activity may be required for the described effects of Sox2 on Wnt signaling. In addition, Sox9 silencing reduces Sox2 and Wnt activity, suggesting that a positive loop between Sox2 and So9 may exists in breast cancer cells.

Interestingly, Sox2 over-expression has been shown to induce Sox9 overexpression in U87 glioma cells and vice-versa, Sox9 overexpression enhanced Sox2 levels (Garros-Regulez et al., 2016b). In particular, Sox2 silencing caused reduced cell proliferation and oncosphere formation from glioblastoma cells (analogue to mammospheres), effects that were rescued by Sox9 overexpression, suggesting that Sox9 acts downstream of Sox2 in order to maintain cell growth and stemness in glioma cells.

Collectively, these data indicate a positive and bidirectional connection between Sox9 and Wnt pathway in different cellular contexts. Nevertheless, further studies are required to assess the potential clinical application of Wnt inhibition as therapy for different breast cancer subtypes.

6. MAPK pathway induces Sox9 expression

During chondrogenic differentiation, the mitogen-activated protein kinase pathway (MAPK) has been reported to induce Sox9 expression upon activation by fibroblast growth factor (FGF) signaling (Murakami et al., 2000). In bladder cancer, epidermal growth factor (EGF) induces MAPK activity that induces Sox9 expression, which is prevented by the MEK inhibitor U0126, the tyrosine kinase inhibitor Erlotinib and the p38 MAPK inhibitor PD169316 (Ling et al., 2011b). Similar results were obtained in urogenital epithelium, in which the MAPK inhibitor CI-1040 abrogates Sox9 expression, while FGF induces it, as well as stable transfection of mutated and constitutively active RasV and MEK protein (Huang et al., 2012). In addition, RAS activation has been associated with

increased Sox9 expression in liver progenitor cells, even though it has not described how this happens (Song et al., 2016).

MEK/ERK inhibition strongly reduces Sox9 expression both at mRNA and protein level, suggesting that MAPK pathway positively activates Sox9 expression, both in TNBC and in tamoxifen resistant cells. MAPK pathway has been extensively studied and reported to be important for breast cancer tumorigenesis (Adeyinka et al., 2002) as well as stem cell maintenance (Balko et al., 2013). In addition, recently it has been reported that high MAPK signaling it is associated with ER negativity, poor outcome, reduced recurrence-free and survival in patients and poor response to hormone therapy (Miller et al., 2015).

Clinical studies are addressing the possibility that MAPK inhibitors may be useful as treatment alone or in combination with standard chemotherapy in breast cancer (Giltnane and Balko, 2014), while MAPK inhibitors as Dabrafenib or Cobimetinib are routinely used in the treatment of melanoma patients (Wellbrock and Arozarena, 2016). Here we show that silencing Sox9 expression through shRNA in MDA-MB-231 cells increases their resistance to MEK inhibition. These observations suggest that MAPK pathway induces Sox9 expression in order to maintain cell clonogenicity and stemness and therefore, it can be speculated that high Sox9 expression in breast cancer tumors could predict the response to MAPK inhibitor as breast cancer treatment, but this requires further and more detailed studies.

7. CONCLUSIVE REMARKS

To summarize, the scientific work presented in this doctoral thesis shows that:

- Sox9 represents a luminal progenitor marker in the human mammary gland
- Luminal progenitor cells in the human mammary gland are mostly ALDEFLUOR$^+$
- Sox9 maintains ALDEFLUOR$^+$ cells and mammosphere formation both in the normal mammary gland and luminal breast cancer cells

- Sox9 expression is suppressed by estrogen and strongly expressed in ER^- and tamoxifen resistant breast tumors. Sox9 cytosolic localization is common in endocrine resistant tumors.
- Sox9/Sox2 regulate each other through direct promoter binding
- Sox9 regulates Wnt activity in breast cancer cells and cancer stem cell content along with Sox2 expression. Wnt pathway is a relevant stem cells-associated pathway that could be interesting to explore further to find other combinatorial and therapeutical strategy to fight endocrine resistant breast cancer and cancer stem cells;
- MAPK pathway activates Sox9 expression in breast cancer cells in order to induce clonogenicity and stemness, suggesting a stratification in the use of MAPK inhibitors in the treatment of breast cancer when Sox9 is highly expressed;

Chapter 5: Bibliography

Adeyinka, A., Nui, Y., Cherlet, T., Snell, L., Watson, P.H., and Murphy, L.C. (2002). Activated mitogen-activated protein kinase expression during human breast tumorigenesis and breast cancer progression. Clin. Cancer Res. Off. J. Am. Assoc. Cancer Res. *8*, 1747–1753.

Akarolo-Anthony, S.N., Ogundiran, T.O., and Adebamowo, C.A. (2010). Emerging breast cancer epidemic: evidence from Africa. Breast Cancer Res. BCR *12 Suppl 4*, S8.

Al Saleh, S., Al Mulla, F., and Luqmani, Y.A. (2011a). Estrogen receptor silencing induces epithelial to mesenchymal transition in human breast cancer cells. PloS One *6*, e20610.

Al Saleh, S., Al Mulla, F., and Luqmani, Y.A. (2011b). Estrogen receptor silencing induces epithelial to mesenchymal transition in human breast cancer cells. PloS One *6*, e20610.

Al-Hajj, M., Wicha, M.S., Benito-Hernandez, A., Morrison, S.J., and Clarke, M.F. (2003). Prospective identification of tumorigenic breast cancer cells. Proc. Natl. Acad. Sci. U. S. A. *100*, 3983–3988.

Alonso, L., and Fuchs, E. (2003). Stem cells of the skin epithelium. Proc. Natl. Acad. Sci. U. S. A. *100 Suppl 1*, 11830–11835.

Alvi, A.J., Clayton, H., Joshi, C., Enver, T., Ashworth, A., Vivanco, M. d M., Dale, T.C., and Smalley, M.J. (2003). Functional and molecular characterisation of mammary side population cells. Breast Cancer Res. BCR *5*, R1-8.

An, W.F., Germain, A.R., Bishop, J.A., Nag, P.P., Metkar, S., Ketterman, J., Walk, M., Weiwer, M., Liu, X., Patnaik, D., et al. (2010). Discovery of Potent and Highly Selective Inhibitors of GSK3b. In Probe Reports from the NIH Molecular Libraries Program, (Bethesda (MD): National Center for Biotechnology Information (US)),

Andl, T., Reddy, S.T., Gaddapara, T., and Millar, S.E. (2002). WNT signals are required for the initiation of hair follicle development. Dev. Cell *2*, 643–653.

Anido, J., Sáez-Borderías, A., Gonzàlez-Juncà, A., Rodón, L., Folch, G., Carmona, M.A., Prieto-Sánchez, R.M., Barba, I., Martínez-Sáez, E., Prudkin, L., et al. (2010). TGF-β Receptor Inhibitors Target the CD44(high)/Id1(high) Glioma-Initiating Cell Population in Human Glioblastoma. Cancer Cell *18*, 655–668.

Antal, M.C., Krust, A., Chambon, P., and Mark, M. (2008). Sterility and absence of histopathological defects in nonreproductive organs of a mouse ERβ-null mutant. Proc. Natl. Acad. Sci. *105*, 2433–2438.

Asselin-Labat, M.-L., Sutherland, K.D., Barker, H., Thomas, R., Shackleton, M., Forrest, N.C., Hartley, L., Robb, L., Grosveld, F.G., van der Wees, J., et al. (2007a). Gata-3 is an essential regulator of mammary-gland morphogenesis and luminal-cell differentiation. Nat. Cell Biol. *9*, 201–209.

Asselin-Labat, M.-L., Sutherland, K.D., Barker, H., Thomas, R., Shackleton, M., Forrest, N.C., Hartley, L., Robb, L., Grosveld, F.G., van der Wees, J., et al. (2007b). Gata-3 is an essential regulator of mammary-gland morphogenesis and luminal-cell differentiation. Nat. Cell Biol. *9*, 201–209.

Asselin-Labat, M.-L., Vaillant, F., Sheridan, J.M., Pal, B., Wu, D., Simpson, E.R., Yasuda, H., Smyth, G.K., Martin, T.J., Lindeman, G.J., et al. (2010). Control of mammary stem cell function by steroid hormone signalling. Nature *465*, 798–802.

Balko, J.M., Cook, R.S., Vaught, D.B., Kuba, M.G., Miller, T.W., Bhola, N.E., Sanders, M.E., Granja-Ingram, N.M., Smith, J.J., Meszoely, I.M., et al. (2012). Profiling of residual breast cancers after neoadjuvant chemotherapy identifies DUSP4 deficiency as a mechanism of drug resistance. Nat. Med. *18*, 1052–1059.

Balko, J.M., Schwarz, L.J., Bhola, N.E., Kurupi, R., Owens, P., Miller, T.W., Gómez, H., Cook, R.S., and Arteaga, C.L. (2013). Activation of MAPK pathways due to DUSP4 loss promotes cancer stem cell-like phenotypes in basal-like breast cancer. Cancer Res. *73*, 6346–6358.

Bar Oz, M., Kumar, A., Elayyan, J., Reich, E., Binyamin, M., Kandel, L., Liebergall, M., Steinmeyer, J., Lefebvre, V., and Dvir-Ginzberg, M. (2016). Acetylation reduces SOX9 nuclear entry and ACAN gene transactivation in human chondrocytes. Aging Cell *15*, 499–508.

Barker, N. (2014). Adult intestinal stem cells: critical drivers of epithelial homeostasis and regeneration. Nat. Rev. Mol. Cell Biol. *15*, 19–33.

Barker, N., van Es, J.H., Kuipers, J., Kujala, P., van den Born, M., Cozijnsen, M., Haegebarth, A., Korving, J., Begthel, H., Peters, P.J., et al. (2007). Identification of stem cells in small intestine and colon by marker gene Lgr5. Nature *449*, 1003–1007.

Barske, L.A., and Capel, B. (2010). Estrogen represses SOX9 during sex determination in the red-eared slider turtle Trachemys scripta. Dev. Biol. *341*, 305–314.

Bartscherer, K., and Boutros, M. (2008). Regulation of Wnt protein secretion and its role in gradient formation. EMBO Rep. *9*, 977–982.

Baselga, J., Campone, M., Piccart, M., Burris, H.A., Rugo, H.S., Sahmoud, T., Noguchi, S., Gnant, M., Pritchard, K.I., Lebrun, F., et al. (2012). Everolimus in postmenopausal hormone-receptor-positive advanced breast cancer. N. Engl. J. Med. *366*, 520–529.

Behbod, F., and Vivanco, M.D.M. (2015). Side population. Methods Mol. Biol. Clifton NJ *1293*, 73–81.

Bengoa-Vergniory, N., and Kypta, R.M. (2015). Canonical and noncanonical Wnt signaling in neural stem/progenitor cells. Cell. Mol. Life Sci. CMLS *72*, 4157–4172.

Benhaj, K., Akcali, K.C., and Ozturk, M. (2006). Redundant expression of canonical Wnt ligands in human breast cancer cell lines. Oncol. Rep. *15*, 701–707.

Berta, P., Hawkins, J.R., Sinclair, A.H., Taylor, A., Griffiths, B.L., Goodfellow, P.N., and Fellous, M. (1990). Genetic evidence equating SRY and the testis-determining factor. Nature *348*, 448–450.

Bhanot, P., Brink, M., Samos, C.H., Hsieh, J.C., Wang, Y., Macke, J.P., Andrew, D., Nathans, J., and Nusse, R. (1996). A new member of the frizzled family from Drosophila functions as a Wingless receptor. Nature *382*, 225–230.

Bi, W., Deng, J.M., Zhang, Z., Behringer, R.R., and de Crombrugghe, B. (1999). Sox9 is required for cartilage formation. Nat. Genet. *22*, 85–89.

Blache, P., van de Wetering, M., Duluc, I., Domon, C., Berta, P., Freund, J.-N., Clevers, H., and Jay, P. (2004). SOX9 is an intestine crypt transcription factor, is regulated by the Wnt pathway, and represses the CDX2 and MUC2 genes. J. Cell Biol. *166*, 37–47.

Bocchinfuso, W.P., Lindzey, J.K., Hewitt, S.C., Clark, J.A., Myers, P.H., Cooper, R., and Korach, K.S. (2000). Induction of mammary gland development in estrogen receptor-alpha knockout mice. Endocrinology *141*, 2982–2994.

Bonner-Weir, S., and Sharma, A. (2002). Pancreatic stem cells. J. Pathol. *197*, 519–526.

Bourdeau, V., Deschênes, J., Métivier, R., Nagai, Y., Nguyen, D., Bretschneider, N., Gannon, F., White, J.H., and Mader, S. (2004). Genome-wide identification of high-affinity estrogen response elements in human and mouse. Mol. Endocrinol. Baltim. Md *18*, 1411–1427.

Bowles, J., Schepers, G., and Koopman, P. (2000). Phylogeny of the SOX family of developmental transcription factors based on sequence and structural indicators. Dev. Biol. *227*, 239–255.

Bridgewater, L.C., Lefebvre, V., and Crombrugghe, B. de (1998). Chondrocyte-specific Enhancer Elements in the Col11a2Gene Resemble the Col2a1 Tissue-specific Enhancer. J. Biol. Chem. *273*, 14998–15006.

Brisken, C., and O'Malley, B. (2010). Hormone action in the mammary gland. Cold Spring Harb. Perspect. Biol. *2*, a003178.

Brisken, C., Heineman, A., Chavarria, T., Elenbaas, B., Tan, J., Dey, S.K., McMahon, J.A., McMahon, A.P., and Weinberg, R.A. (2000). Essential function of Wnt-4 in mammary gland development downstream of progesterone signaling. Genes Dev. *14*, 650–654.

Bryder, D., Rossi, D.J., and Weissman, I.L. (2006). Hematopoietic stem cells: the paradigmatic tissue-specific stem cell. Am. J. Pathol. *169*, 338–346.

Camaj, P., Jäckel, C., Krebs, S., De Toni, E.N., Blum, H., Jauch, K.-W., Nelson, P.J., and Bruns, C.J. (2014). Hypoxia-independent gene expression mediated by SOX9 promotes aggressive pancreatic tumor biology. Mol. Cancer Res. MCR *12*, 421–432.

Campbell, R.A., Bhat-Nakshatri, P., Patel, N.M., Constantinidou, D., Ali, S., and Nakshatri, H. (2001). Phosphatidylinositol 3-Kinase/AKT-mediated Activation of Estrogen Receptor α A NEW MODEL FOR ANTI-ESTROGEN RESISTANCE. J. Biol. Chem. *276*, 9817–9824.

Canino, C., Luo, Y., Marcato, P., Blandino, G., Pass, H.I., and Cioce, M. (2015). A STAT3-NFkB/DDIT3/CEBPβ axis modulates ALDH1A3 expression in chemoresistant cell subpopulations. Oncotarget *6*, 12637–12653.

Carrasco-Garcia, E., Lopez, L., Aldaz, P., Arevalo, S., Aldaregia, J., Egaña, L., Bujanda, L., Cheung, M., Sampron, N., Garcia, I., et al. (2016). SOX9-regulated cell plasticity in colorectal metastasis is attenuated by rapamycin. Sci. Rep. *6*, 32350.

Carroll, J.S., Liu, X.S., Brodsky, A.S., Li, W., Meyer, C.A., Szary, A.J., Eeckhoute, J., Shao, W., Hestermann, E.V., Geistlinger, T.R., et al. (2005). Chromosome-wide mapping of estrogen receptor binding reveals long-range regulation requiring the forkhead protein FoxA1. Cell *122*, 33–43.

Chakravarty, G., Moroz, K., Makridakis, N.M., Lloyd, S.A., Galvez, S.E., Canavello, P.R., Lacey, M.R., Agrawal, K., and Mondal, D. (2011a). Prognostic significance of cytoplasmic SOX9 in invasive ductal carcinoma and metastatic breast cancer. Exp. Biol. Med. Maywood NJ *236*, 145–155.

Chakravarty, G., Rider, B., and Mondal, D. (2011b). Cytoplasmic compartmentalization of SOX9 abrogates the growth arrest response of breast cancer cells that can be rescued by trichostatin A treatment. Cancer Biol. Ther. *11*, 71–83.

Charafe-Jauffret, E., Ginestier, C., Iovino F, F., Tarpin, C., Diebel, M., Esterni, B., Houvenaeghel, G., Extra, J.-M., Bertucci, F., Jacquemier, J., et al. (2010). ALDH1-positive cancer stem cells mediate metastasis and poor clinical outcome in inflammatory breast cancer. Clin. Cancer Res. Off. J. Am. Assoc. Cancer Res. *16*, 45–55.

Chen, B., Dodge, M.E., Tang, W., Lu, J., Ma, Z., Fan, C.-W., Wei, S., Hao, W., Kilgore, J., Williams, N.S., et al. (2009). Small molecule-mediated disruption of Wnt-dependent signaling in tissue regeneration and cancer. Nat. Chem. Biol. *5*, 100–107.

Chen, M., Cui, Y.-K., Huang, W.-H., Man, K., and Zhang, G.-J. (2013). Phosphorylation of estrogen receptor α at serine 118 is correlated with breast cancer resistance to tamoxifen. Oncol. Lett. *6*, 118–124.

Cheng, P.F., Shakhova, O., Widmer, D.S., Eichhoff, O.M., Zingg, D., Frommel, S.C., Belloni, B., Raaijmakers, M.I., Goldinger, S.M., Santoro, R., et al. (2015). Methylation-dependent SOX9 expression mediates invasion in human melanoma cells and is a negative prognostic factor in advanced melanoma. Genome Biol. *16*.

Cheung, M., and Briscoe, J. (2003). Neural crest development is regulated by the transcription factor Sox9. Dev. Camb. Engl. *130*, 5681–5693.

Choi, Y.S., Chakrabarti, R., Escamilla-Hernandez, R., and Sinha, S. (2009). Elf5 conditional knockout mice reveal its role as a master regulator in mammary alveolar development: failure of Stat5 activation and functional differentiation in the absence of Elf5. Dev. Biol. *329*, 227–241.

Ciarloni, L., Mallepell, S., and Brisken, C. (2007). Amphiregulin is an essential mediator of estrogen receptor alpha function in mammary gland development. Proc. Natl. Acad. Sci. U. S. A. *104*, 5455–5460.

Clark, C.E.J., Nourse, C.C., and Cooper, H.M. (2012). The tangled web of non-canonical Wnt signalling in neural migration. Neurosignals *20*, 202–220.

Clayton, H., Titley, I., and Vivanco, M. dM (2004). Growth and differentiation of progenitor/stem cells derived from the human mammary gland. Exp. Cell Res. *297*, 444–460.

Cleator, S.J., Ahamed, E., Coombes, R.C., and Palmieri, C. (2009). A 2009 update on the treatment of patients with hormone receptor-positive breast cancer. Clin. Breast Cancer *9 Suppl 1*, S6–S17.

Clevers, H., and Nusse, R. (2012). Wnt/β-catenin signaling and disease. Cell *149*, 1192–1205.
Collins, A.T., Berry, P.A., Hyde, C., Stower, M.J., and Maitland, N.J. (2005). Prospective identification of tumorigenic prostate cancer stem cells. Cancer Res. *65*, 10946–10951.

Corcoran, R.B., Settleman, J., and Engelman, J.A. (2011). Potential Therapeutic Strategies to Overcome Acquired Resistance to BRAF or MEK Inhibitors in BRAF Mutant Cancers. Oncotarget *2*, 336–346.
Crews, D., Bull, J.J., and Wibbels, T. (1991). Estrogen and sex reversal in turtles: a dose-dependent phenomenon. Gen. Comp. Endocrinol. *81*, 357–364.

Crowley, W.R. (2015). Neuroendocrine regulation of lactation and milk production. Compr. Physiol. *5*, 255–291.

Curtis, C., Shah, S.P., Chin, S.-F., Turashvili, G., Rueda, O.M., Dunning, M.J., Speed, D., Lynch, A.G., Samarajiwa, S., Yuan, Y., et al. (2012). The genomic and transcriptomic architecture of 2,000 breast tumours reveals novel subgroups. Nature *486*, 346–352.

Cuzick, J. (2008). Assessing risk for breast cancer. Breast Cancer Res. BCR *10 Suppl 4*, S13.
Dean, M., Fojo, T., and Bates, S. (2005). Tumour stem cells and drug resistance. Nat. Rev. Cancer *5*, 275–284.

Debnath, J., Muthuswamy, S.K., and Brugge, J.S. (2003). Morphogenesis and oncogenesis of MCF-10A mammary epithelial acini grown in three-dimensional basement membrane cultures. Methods San Diego Calif *30*, 256–268.

deGraffenried, L.A., Friedrichs, W.E., Russell, D.H., Donzis, E.J., Middleton, A.K., Silva, J.M., Roth, R.A., and Hidalgo, M. (2004). Inhibition of mTOR activity restores tamoxifen response in breast cancer cells with aberrant Akt Activity. Clin. Cancer Res. Off. J. Am. Assoc. Cancer Res. *10*, 8059–8067.

Deome, K.B., Faulkin, L.J., Bern, H.A., and Blair, P.B. (1959). Development of mammary tumors from hyperplastic alveolar nodules transplanted into gland-free mammary fat pads of female C3H mice. Cancer Res. *19*, 515–520.

Dey, N., Barwick, B.G., Moreno, C.S., Ordanic-Kodani, M., Chen, Z., Oprea-Ilies, G., Tang, W., Catzavelos, C., Kerstann, K.F., Sledge, G.W., et al. (2013). Wnt signaling in triple negative breast cancer is associated with metastasis. BMC Cancer *13*, 537.

Domenici G., Rábano M., Piva M., Iriondo O., Zabalza I., López-Rúiz JA, Vivanco MdM. (2014) Respuesta hormonal de las células madre de mama y resistencia a tamoxifeno. Rev Senol Patol Mam 27(4) 149-157.

Dontu, G., Abdallah, W.M., Foley, J.M., Jackson, K.W., Clarke, M.F., Kawamura, M.J., and Wicha, M.S. (2003). In vitro propagation and transcriptional profiling of human mammary stem/progenitor cells. Genes Dev. *17*, 1253–1270.

Druege, P.M., Klein-Hitpass, L., Green, S., Stack, G., Chambon, P., and Ryffel, G.U. (1986). Introduction of estrogen-responsiveness into mammalian cell lines. Nucleic Acids Res. *14*, 9329–9337.

Duester, G., Mic, F.A., and Molotkov, A. (2003). Cytosolic retinoid dehydrogenases govern ubiquitous metabolism of retinol to retinaldehyde followed by tissue-specific metabolism to retinoic acid. Chem. Biol. Interact. *143–144*, 201–210.

Duncan, J.S., Whittle, M.C., Nakamura, K., Abell, A.N., Midland, A.A., Zawistowski, J.S., Johnson, N.L., Granger, D.A., Jordan, N.V., Darr, D.B., et al. (2012). Dynamic Reprogramming of the Kinome In Response to Targeted MEK Inhibition In Triple Negative Breast Cancer. Cell *149*, 307–321.

Dupont, S., Dennefeld, C., Krust, A., Chambon, P., and Mark, M. (2003). Expression of Sox9 in granulosa cells lacking the estrogen receptors, ERalpha and ERbeta. Dev. Dyn. Off. Publ. Am. Assoc. Anat. *226*, 103–106.

Eirew, P., Stingl, J., Raouf, A., Turashvili, G., Aparicio, S., Emerman, J.T., and Eaves, C.J. (2008). A method for quantifying normal human mammary epithelial stem cells with in vivo regenerative ability. Nat. Med. *14*, 1384–1389.

Eirew, P., Kannan, N., Knapp, D.J.H.F., Vaillant, F., Emerman, J.T., Lindeman, G.J., Visvader, J.E., and Eaves, C.J. (2012). Aldehyde dehydrogenase activity is a biomarker of primitive normal human mammary luminal cells. Stem Cells Dayt. Ohio *30*, 344–348.

Engel, C., and Fischer, C. (2015). Breast cancer risks and risk prediction models. Breast Care Basel Switz. *10*, 7–12.

Fan, X., Liu, S., Su, F., Pan, Q., and Lin, T. (2012). Effective enrichment of prostate cancer stem cells from spheres in a suspension culture system. Urol. Oncol. *30*, 314–318.

Faridi, J., Wang, L., Endemann, G., and Roth, R.A. (2003). Expression of constitutively active Akt-3 in MCF-7 breast cancer cells reverses the estrogen and tamoxifen responsivity of these cells in vivo. Clin. Cancer Res. Off. J. Am. Assoc. Cancer Res. *9*, 2933–2939.

Farley, J., Brady, W.E., Vathipadiekal, V., Lankes, H.A., Coleman, R., Morgan, M.A., Mannel, R., Yamada, S.D., Mutch, D., Rodgers, W.H., et al. (2013). A Phase Ii Trial Of Selumetinib (Azd6244) In Women With Recurrent Low-Grade Serous Carcinoma Of The Ovary Or Peritoneum: A Gynecologic Oncology Group Trial. Lancet Oncol. *14*, 134–140.

Farnie, G., Clarke, R.B., Spence, K., Pinnock, N., Brennan, K., Anderson, N.G., and Bundred, N.J. (2007). Novel cell culture technique for primary ductal carcinoma in situ: role of Notch and epidermal growth factor receptor signaling pathways. J. Natl. Cancer Inst. *99*, 616–627.

Felipe Lima, J., Nofech-Mozes, S., Bayani, J., and Bartlett, J.M.S. (2016). EMT in Breast Carcinoma-A Review. J. Clin. Med. *5*.

Ferlay, J., Shin, H.-R., Bray, F., Forman, D., Mathers, C., and Parkin, D.M. (2010). Estimates of worldwide burden of cancer in 2008: GLOBOCAN 2008. Int. J. Cancer *127*, 2893–2917.
Fernandez-Valdivia, R., and Lydon, J.P. (2012). From the ranks of mammary progesterone mediators, RANKL takes the spotlight. Mol. Cell. Endocrinol. *357*, 91–100.

Ferri, A.L.M., Cavallaro, M., Braida, D., Di Cristofano, A., Canta, A., Vezzani, A., Ottolenghi, S., Pandolfi, P.P., Sala, M., DeBiasi, S., et al. (2004). Sox2 deficiency causes neurodegeneration and impaired neurogenesis in the adult mouse brain. Dev. Camb. Engl. *131*, 3805–3819.

Fillmore, C.M., and Kuperwasser, C. (2008). Human breast cancer cell lines contain stem-like cells that self-renew, give rise to phenotypically diverse progeny and survive chemotherapy. Breast Cancer Res. BCR *10*, R25.

Fletcher, S., Turkson, J., and Gunning, P.T. (2008). Molecular approaches towards the inhibition of the signal transducer and activator of transcription 3 (Stat3) protein. ChemMedChem *3*, 1159–1168.
Foster, J.W., Dominguez-Steglich, M.A., Guioli, S., Kwok, C., Weller, P.A., Stevanović, M., Weissenbach, J., Mansour, S., Young, I.D., and Goodfellow, P.N. (1994). Campomelic dysplasia and autosomal sex reversal caused by mutations in an SRY-related gene. Nature *372*, 525–530.

Fu, N.Y., Rios, A.C., Pal, B., Law, C.W., Jamieson, P., Liu, R., Vaillant, F., Jackling, F., Liu, K.H., Smyth, G.K., et al. (2017). Identification of quiescent and spatially restricted mammary stem cells that are hormone responsive. Nat. Cell Biol. *19*, 164–176.

Furuyama, K., Kawaguchi, Y., Akiyama, H., Horiguchi, M., Kodama, S., Kuhara, T., Hosokawa, S., Elbahrawy, A., Soeda, T., Koizumi, M., et al. (2011). Continuous cell supply from a Sox9-expressing progenitor zone in adult liver, exocrine pancreas and intestine. Nat. Genet. *43*, 34–41.

Garros-Regulez, L., Aldaz, P., Arrizabalaga, O., Moncho-Amor, V., Carrasco-Garcia, E., Manterola, L., Moreno-Cugnon, L., Barrena, C., Villanua, J., Ruiz, I., et al. (2016a). mTOR inhibition decreases SOX2-SOX9 mediated glioma stem cell activity and temozolomide resistance. Expert Opin. Ther. Targets *20*, 393–405.

Gaudet, M.M., Carter, B.D., Brinton, L.A., Falk, R.T., Gram, I.T., Luo, J., Milne, R.L., Nyante, S.J., Weiderpass, E., Beane Freeman, L.E., et al. (2016). Pooled analysis of active cigarette smoking and invasive breast cancer risk in 14 cohort studies. Int. J. Epidemiol.

Geyer, F.C., Lacroix-Triki, M., Savage, K., Arnedos, M., Lambros, M.B., MacKay, A., Natrajan, R., and Reis-Filho, J.S. (2011). β-Catenin pathway activation in breast cancer is associated with triple-negative phenotype but not with CTNNB1 mutation. Mod. Pathol. Off. J. U. S. Can. Acad. Pathol. Inc *24*, 209–231.

Giltnane, J.M., and Balko, J.M. (2014). Rationale for targeting the Ras/MAPK pathway in triple-negative breast cancer. Discov. Med. *17*, 275–283.

Ginestier, C., Hur, M.H., Charafe-Jauffret, E., Monville, F., Dutcher, J., Brown, M., Jacquemier, J., Viens, P., Kleer, C.G., Liu, S., et al. (2007). ALDH1 is a marker of normal and malignant human mammary stem cells and a predictor of poor clinical outcome. Cell Stem Cell *1*, 555–567.

Giordano, S.H., Cohen, D.S., Buzdar, A.U., Perkins, G., and Hortobagyi, G.N. (2004). Breast carcinoma in men: a population-based study. Cancer *101*, 51–57.
Gómez-Orte, E., Sáenz-Narciso, B., Moreno, S., and Cabello, J. (2013). Multiple functions of the noncanonical Wnt pathway. Trends Genet. TIG *29*, 545–553.

Goodell, M.A., Rosenzweig, M., Kim, H., Marks, D.F., DeMaria, M., Paradis, G., Grupp, S.A., Sieff, C.A., Mulligan, R.C., and Johnson, R.P. (1997). Dye efflux studies suggest that hematopoietic stem cells expressing low or undetectable levels of CD34 antigen exist in multiple species. Nat. Med. *3*, 1337–1345.

Goodsell, D.S. (2002). The molecular perspective: tamoxifen and the estrogen receptor. The Oncologist *7*, 163–164.

Graham, J.D., Mote, P.A., Salagame, U., van Dijk, J.H., Balleine, R.L., Huschtscha, L.I., Reddel, R.R., and Clarke, C.L. (2009). DNA replication licensing and progenitor numbers are increased by progesterone in normal human breast. Endocrinology *150*, 3318–3326.

Graham, V., Khudyakov, J., Ellis, P., and Pevny, L. (2003). SOX2 functions to maintain neural progenitor identity. Neuron *39*, 749–765.

Green, S., Walter, P., Kumar, V., Krust, A., Bornert, J.M., Argos, P., and Chambon, P. (1986). Human oestrogen receptor cDNA: sequence, expression and homology to v-erb-A. Nature *320*, 134–139.

Grigson, E.R., Ozerova, M., Pisklakova, A., Liu, H., Sullivan, D.M., and Nefedova, Y. (2015). Canonical Wnt pathway inhibitor ICG-001 induces cytotoxicity of multiple myeloma cells in Wnt-independent manner. PloS One *10*, e0117693.

Grimshaw, M.J., Cooper, L., Papazisis, K., Coleman, J.A., Bohnenkamp, H.R., Chiapero-Stanke, L., Taylor-Papadimitriou, J., and Burchell, J.M. (2008). Mammosphere culture of metastatic breast cancer cells enriches for tumorigenic breast cancer cells. Breast Cancer Res. BCR *10*, R52.

Gu, B., Watanabe, K., Sun, P., Fallahi, M., and Dai, X. (2013). Chromatin effector Pygo2 mediates Wnt-notch crosstalk to suppress luminal/alveolar potential of mammary stem and basal cells. Cell Stem Cell *13*, 48–61.

Gudjonsson, T., Villadsen, R., Nielsen, H.L., Rønnov-Jessen, L., Bissell, M.J., and Petersen, O.W. (2002). Isolation, immortalization, and characterization of a human breast epithelial cell line with stem cell properties. Genes Dev. *16*, 693–706.

Guo, S., and Sonenshein, G.E. (2004). Forkhead box transcription factor FOXO3a regulates estrogen receptor alpha expression and is repressed by the Her-2/neu/phosphatidylinositol 3-kinase/Akt signaling pathway. Mol. Cell. Biol. *24*, 8681–8690.

Guo, W., Keckesova, Z., Donaher, J.L., Shibue, T., Tischler, V., Reinhardt, F., Itzkovitz, S., Noske, A., Zürrer-Härdi, U., Bell, G., et al. (2012a). Slug and Sox9 cooperatively determine the mammary stem cell state. Cell *148*, 1015–1028.

Guo, X., Xiong, L., Sun, T., Peng, R., Zou, L., Zhu, H., Zhang, J., Li, H., and Zhao, J. (2012b). Expression features of SOX9 associate with tumor progression and poor prognosis of hepatocellular carcinoma. Diagn. Pathol. *7*, 44.

Gurney, A., Axelrod, F., Bond, C.J., Cain, J., Chartier, C., Donigan, L., Fischer, M., Chaudhari, A., Ji, M., Kapoun, A.M., et al. (2012). Wnt pathway inhibition via the targeting of Frizzled receptors results in decreased growth and tumorigenicity of human tumors. Proc. Natl. Acad. Sci. *109*, 11717–11722.

Guth, S.I.E., and Wegner, M. (2008). Having it both ways: Sox protein function between conservation and innovation. Cell. Mol. Life Sci. CMLS *65*, 3000–3018.

Hagenbuchner, J., and Ausserlechner, M.J. (2016). Targeting transcription factors by small compounds--Current strategies and future implications. Biochem. Pharmacol. *107*, 1–13.

Harrison, H., Rogerson, L., Gregson, H.J., Brennan, K.R., Clarke, R.B., and Landberg, G. (2013). Contrasting hypoxic effects on breast cancer stem cell hierarchy is dependent on ER-α status. Cancer Res. *73*, 1420–1433.

Harvey, J.M., Clark, G.M., Osborne, C.K., and Allred, D.C. (1999). Estrogen receptor status by immunohistochemistry is superior to the ligand-binding assay for predicting response to adjuvant endocrine therapy in breast cancer. J. Clin. Oncol. Off. J. Am. Soc. Clin. Oncol. *17*, 1474–1481.

Hattori, T., Kishino, T., Stephen, S., Eberspaecher, H., Maki, S., Takigawa, M., de Crombrugghe, B., and Yasuda, H. (2013). E6-AP/UBE3A protein acts as a ubiquitin ligase toward SOX9 protein. J. Biol. Chem. *288*, 35138–35148.

Haudenschild, D.R., Chen, J., Pang, N., Lotz, M.K., and D'Lima, D.D. (2010). Rho kinase-dependent activation of SOX9 in chondrocytes. Arthritis Rheum. *62*, 191–200.

Honeth, G., Lombardi, S., Ginestier, C., Hur, M., Marlow, R., Buchupalli, B., Shinomiya, I., Gazinska, P., Bombelli, S., Ramalingam, V., et al. (2014). Aldehyde dehydrogenase and estrogen receptor define a hierarchy of cellular differentiation in the normal human mammary epithelium. Breast Cancer Res. BCR *16*, R52.

Hong, Y., Chen, W., Du, X., Ning, H., Chen, H., Shi, R., Lin, S., Xu, R., Zhu, J., Wu, S., et al. (2015). Upregulation of sex-determining region Y-box 9 (SOX9) promotes cell proliferation and tumorigenicity in esophageal squamous cell carcinoma. Oncotarget *6*, 31241–31254.

Howard, B.A., and Gusterson, B.A. (2000). Human breast development. J. Mammary Gland Biol. Neoplasia *5*, 119–137.

Howell, A., Anderson, A.S., Clarke, R.B., Duffy, S.W., Evans, D.G., Garcia-Closas, M., Gescher, A.J., Key, T.J., Saxton, J.M., and Harvie, M.N. (2014). Risk determination and prevention of breast cancer. Breast Cancer Res. BCR *16*, 446.

Hu, Y., and Fu, L. (2012). Targeting cancer stem cells: a new therapy to cure cancer patients. Am. J. Cancer Res. *2*, 340–356.

Hu, Y., Lu, L., Xia, Y., Chen, X., Chang, A.E., Hollingsworth, R.E., Hurt, E., Owen, J., Moyer, J.S., Prince, M.E.P., et al. (2016). Therapeutic Efficacy of Cancer Stem Cell Vaccines in the Adjuvant Setting. Cancer Res. *76*, 4661–4672.

Huang, J., and Guo, L. (2017). Knockdown of SOX9 Inhibits the Proliferation, Invasion, and EMT in Thyroid Cancer Cells. Oncol. Res. *25*, 167–176.

Huang, L., Holtzinger, A., Jagan, I., BeGora, M., Lohse, I., Ngai, N., Nostro, C., Wang, R., Muthuswamy, L.B., Crawford, H.C., et al. (2015a). Ductal pancreatic cancer modeling and drug screening using human pluripotent stem cell- and patient-derived tumor organoids. Nat. Med. *21*, 1364–1371.

Huang, S.-M.A., Mishina, Y.M., Liu, S., Cheung, A., Stegmeier, F., Michaud, G.A., Charlat, O., Wiellette, E., Zhang, Y., Wiessner, S., et al. (2009). Tankyrase inhibition stabilizes axin and antagonizes Wnt signalling. Nature *461*, 614–620.

Huang, W., Zhou, X., Lefebvre, V., and de Crombrugghe, B. (2000). Phosphorylation of SOX9 by cyclic AMP-dependent protein kinase A enhances SOX9's ability to transactivate a Col2a1 chondrocyte-specific enhancer. Mol. Cell. Biol. *20*, 4149–4158.

Huang, Y.-H., Jankowski, A., Cheah, K.S.E., Prabhakar, S., and Jauch, R. (2015b). SOXE transcription factors form selective dimers on non-compact DNA motifs through multifaceted interactions between dimerization and high-mobility group domains. Sci. Rep. *5*, 10398.
Huang, Z., Hurley, P.J., Simons, B.W., Marchionni, L., Berman, D.M., Ross, A.E., and Schaeffer, E.M. (2012). Sox9 is required for prostate development and prostate cancer initiation. Oncotarget *3*, 651–663.

Hurtado, A., Holmes, K.A., Ross-Innes, C.S., Schmidt, D., and Carroll, J.S. (2011). FOXA1 is a key determinant of estrogen receptor function and endocrine response. Nat. Genet. *43*, 27–33.

Idowu, M.O., Kmieciak, M., Dumur, C., Burton, R.S., Grimes, M.M., Powers, C.N., and Manjili, M.H. (2012). CD44(+)/CD24(-/low) cancer stem/progenitor cells are more abundant in triple-negative invasive breast carcinoma phenotype and are associated with poor outcome. Hum. Pathol. *43*, 364–373.

Imbert, A., Eelkema, R., Jordan, S., Feiner, H., and Cowin, P. (2001). Delta N89 beta-catenin induces precocious development, differentiation, and neoplasia in mammary gland. J. Cell Biol. *153*, 555–568.

Inman, J.L., Robertson, C., Mott, J.D., and Bissell, M.J. (2015). Mammary gland development: cell fate specification, stem cells and the microenvironment. Dev. Camb. Engl. *142*, 1028–1042.

Iriondo, O., Rábano, M., Domenici, G., Carlevaris, O., López-Ruiz, J.A., Zabalza, I., Berra, E., and Vivanco, M. dM (2015). Distinct breast cancer stem/progenitor cell populations require either HIF1α or loss of PHD3 to expand under hypoxic conditions. Oncotarget *6*, 31721–31739.

Issaeva, N., Bozko, P., Enge, M., Protopopova, M., Verhoef, L.G.G.C., Masucci, M., Pramanik, A., and Selivanova, G. (2004). Small molecule RITA binds to p53, blocks p53-HDM-2 interaction and activates p53 function in tumors. Nat. Med. *10*, 1321–1328.

Jacobsen, B.M., and Horwitz, K.B. (2012). Progesterone Receptors, their Isoforms and Progesterone Regulated Transcription. Mol. Cell. Endocrinol. *357*, 18–29.

Jakowlew, S.B., Breathnach, R., Jeltsch, J.M., Masiakowski, P., and Chambon, P. (1984). Sequence of the pS2 mRNA induced by estrogen in the human breast cancer cell line MCF-7. Nucleic Acids Res. *12*, 2861–2878.

Jang, G.-B., Kim, J.-Y., Cho, S.-D., Park, K.-S., Jung, J.-Y., Lee, H.-Y., Hong, I.-S., and Nam, J.-S. (2015). Blockade of Wnt/β-catenin signaling suppresses breast cancer metastasis by inhibiting CSC-like phenotype. Sci. Rep. *5*, 12465.

Jin, L., Feng, T., Zerda, R., Chen, C.-C., Riggs, A.D., and Ku, H.T. (2014). In vitro multilineage differentiation and self-renewal of single pancreatic colony-forming cells from adult C57BL/6 mice. Stem Cells Dev. *23*, 899–909.

Jin, V.X., Sun, H., Pohar, T.T., Liyanarachchi, S., Palaniswamy, S.K., Huang, T.H.-M., and Davuluri, R.V. (2005). ERTargetDB: an integral information resource of transcription regulation of estrogen receptor target genes. J. Mol. Endocrinol. *35*, 225–230.

Jin X[1], Jeon HY, Joo KM, Kim JK, Jin J, Kim SH, Kang BG, Beck S, Lee SJ, Kim JK, Park AK, Park WY, Choi YJ, Nam DH, Kim H (2011). Frizzled 4 regulates stemness and invasiveness of migrating glioma cells established by serial intracranial transplantation. Cancer Res. 7(8):3066-75.

Jo, A., Denduluri, S., Zhang, B., Wang, Z., Yin, L., Yan, Z., Kang, R., Shi, L.L., Mok, J., Lee, M.J., et al. (2014). The versatile functions of Sox9 in development, stem cells, and human diseases. Genes Dis. *1*, 149–161.

Jordan, V.C., and O'Malley, B.W. (2007). Selective estrogen-receptor modulators and antihormonal resistance in breast cancer. J. Clin. Oncol. Off. J. Am. Soc. Clin. Oncol. *25*, 5815–5824.

Joshi, P.A., Jackson, H.W., Beristain, A.G., Di Grappa, M.A., Mote, P.A., Clarke, C.L., Stingl, J., Waterhouse, P.D., and Khokha, R. (2010). Progesterone induces adult mammary stem cell expansion. Nature *465*, 803–807.

Kakarala, M., Brenner, D.E., Korkaya, H., Cheng, C., Tazi, K., Ginestier, C., Liu, S., Dontu, G., and Wicha, M.S. (2010). Targeting breast stem cells with the cancer preventive compounds curcumin and piperine. Breast Cancer Res. Treat. *122*, 777–785.

Kang, H.M., Huang, S., Reidy, K., Han, S.H., Chinga, F., and Susztak, K. (2016). Sox9-Positive Progenitor Cells Play a Key Role in Renal Tubule Epithelial Regeneration in Mice. Cell Rep. *14*, 861–871.

Kastan, M.B., Schlaffer, E., Russo, J.E., Colvin, O.M., Civin, C.I., and Hilton, J. (1990). Direct demonstration of elevated aldehyde dehydrogenase in human hematopoietic progenitor cells. Blood *75*, 1947–1950.

Kastner, P., Krust, A., Turcotte, B., Stropp, U., Tora, L., Gronemeyer, H., and Chambon, P. (1990). Two distinct estrogen-regulated promoters generate transcripts encoding the two functionally different human progesterone receptor forms A and B. EMBO J. *9*, 1603–1614.

Kawai, T., Yasuchika, K., Ishii, T., Miyauchi, Y., Kojima, H., Yamaoka, R., Katayama, H., Yoshitoshi, E.Y., Ogiso, S., Kita, S., et al. (2016). SOX9 is a novel cancer stem cell marker surrogated by osteopontin in human hepatocellular carcinoma. Sci. Rep. *6*.

Kawano, Y., and Kypta, R. (2003). Secreted antagonists of the Wnt signalling pathway. J. Cell Sci. *116*, 2627–2634.

Kessenbrock, K., Dijkgraaf, G.J.P., Lawson, D.A., Littlepage, L.E., Shahi, P., Pieper, U., and Werb, Z. (2013). A role for matrix metalloproteinases in regulating mammary stem cell function via the Wnt signaling pathway. Cell Stem Cell *13*, 300–313.

Kessenbrock, K., Smith, P., Steenbeek, S.C., Pervolarakis, N., Kumar, R., Minami, Y., Goga, A., Hinck, L., and Werb, Z. (2017). Diverse regulation of mammary epithelial growth and branching morphogenesis through noncanonical Wnt signaling. Proc. Natl. Acad. Sci. U. S. A. *114*, 3121–3126.

Kibar, Z., Torban, E., McDearmid, J.R., Reynolds, A., Berghout, J., Mathieu, M., Kirillova, I., De Marco, P., Merello, E., Hayes, J.M., et al. (2007). Mutations in VANGL1 associated with neural-tube defects. N. Engl. J. Med. *356*, 1432–1437.

Kiefer, J.C. (2007). Back to basics: Sox genes. Dev. Dyn. Off. Publ. Am. Assoc. Anat. *236*, 2356–2366.

Kim, M.P., Fleming, J.B., Wang, H., Abbruzzese, J.L., Choi, W., Kopetz, S., McConkey, D.J., Evans, D.B., and Gallick, G.E. (2011). ALDH activity selectively defines an enhanced tumor-initiating cell population relative to CD133 expression in human pancreatic adenocarcinoma. PloS One *6*, e20636.

Kispert, S., and McHowat, J. (2017). Recent insights into cigarette smoking as a lifestyle risk factor for breast cancer. Breast Cancer Dove Med. Press *9*, 127–132.

Kiyotani, K., Mushiroda, T., Nakamura, Y., and Zembutsu, H. (2012). Pharmacogenomics of tamoxifen: roles of drug metabolizing enzymes and transporters. Drug Metab. Pharmacokinet. *27*, 122–131.

Klemm, F., Bleckmann, A., Siam, L., Chuang, H.N., Rietkötter, E., Behme, D., Schulz, M., Schaffrinski, M., Schindler, S., Trümper, L., et al. (2011). β-catenin-independent WNT signaling in basal-like breast cancer and brain metastasis. Carcinogenesis *32*, 434–442.

Knowlden, J.M., Hutcheson, I.R., Jones, H.E., Madden, T., Gee, J.M.W., Harper, M.E., Barrow, D., Wakeling, A.E., and Nicholson, R.I. (2003). Elevated levels of epidermal growth factor receptor/c-erbB2 heterodimers mediate an autocrine growth regulatory pathway in tamoxifen-resistant MCF-7 cells. Endocrinology *144*, 1032–1044.

Knutson, K.L., Clynes, R., Shreeder, B., Yeramian, P., Kemp, K., Ballman, K., Tenner, K.S., Erskine, C.L., Norton, N., Northfelt, D.W., et al. (2016). Improved survival of HER2+ breast cancer patients treated with trastuzumab and chemotherapy is associated with host antibody immunity against the HER2 intracellular domain. Cancer Res.

Komiya, Y., and Habas, R. (2008). Wnt signal transduction pathways. Organogenesis *4*, 68–75.

Kordes, C., and Häussinger, D. (2013). Hepatic stem cell niches. J. Clin. Invest. *123*, 1874–1880.

Kordon, E.C., and Smith, G.H. (1998). An entire functional mammary gland may comprise the progeny from a single cell. Dev. Camb. Engl. *125*, 1921–1930.

Kratochwil, K., and Schwartz, P. (1976). Tissue interaction in androgen response of embryonic mammary rudiment of mouse: identification of target tissue for testosterone. Proc. Natl. Acad. Sci. U. S. A. *73*, 4041–4044.

Krause, M., Yaromina, A., Eicheler, W., Koch, U., and Baumann, M. (2011). Cancer stem cells: targets and potential biomarkers for radiotherapy. Clin. Cancer Res. Off. J. Am. Assoc. Cancer Res. *17*, 7224–7229.

Kretzschmar, K., and Watt, F.M. (2012). Lineage tracing. Cell *148*, 33–45.

Kühl, M., Sheldahl, L.C., Malbon, C.C., and Moon, R.T. (2000). Ca(2+)/calmodulin-dependent protein kinase II is stimulated by Wnt and Frizzled homologs and promotes ventral cell fates in Xenopus. J. Biol. Chem. *275*, 12701–12711.

Kuiper, G.G., Enmark, E., Pelto-Huikko, M., Nilsson, S., and Gustafsson, J.A. (1996). Cloning of a novel receptor expressed in rat prostate and ovary. Proc. Natl. Acad. Sci. U. S. A. *93*, 5925–5930.

Kuiper, G.G., Carlsson, B., Grandien, K., Enmark, E., Häggblad, J., Nilsson, S., and Gustafsson, J.A. (1997). Comparison of the ligand binding specificity and transcript tissue distribution of estrogen receptors alpha and beta. Endocrinology *138*, 863–870.

Kumar, R., Mandal, M., Lipton, A., Harvey, H., and Thompson, C.B. (1996). Overexpression of HER2 modulates bcl-2, bcl-XL, and tamoxifen-induced apoptosis in human MCF-7 breast cancer cells. Clin. Cancer Res. Off. J. Am. Assoc. Cancer Res. *2*, 1215–1219.

Kumar, V., Green, S., Stack, G., Berry, M., Jin, J.R., and Chambon, P. (1987). Functional domains of the human estrogen receptor. Cell *51*, 941–951.

Labrie, F. (2015). All sex steroids are made intracellularly in peripheral tissues by the mechanisms of intracrinology after menopause. J. Steroid Biochem. Mol. Biol. *145*, 133–138.

Lannigan, D.A. (2003). Estrogen receptor phosphorylation. Steroids *68*, 1–9.

Larsimont, J.-C., Youssef, K.K., Sánchez-Danés, A., Sukumaran, V., Defrance, M., Delatte, B., Liagre, M., Baatsen, P., Marine, J.-C., Lippens, S., et al. (2015). Sox9 Controls Self-Renewal of Oncogene Targeted Cells and Links Tumor Initiation and Invasion. Cell Stem Cell *17*, 60–73.

Lee, H.E., Kim, J.H., Kim, Y.J., Choi, S.Y., Kim, S.-W., Kang, E., Chung, I.Y., Kim, I.A., Kim, E.J., Choi, Y., et al. (2011). An increase in cancer stem cell population after primary systemic therapy is a poor prognostic factor in breast cancer. Br. J. Cancer *104*, 1730–1738.

Lee, H.J., Gallego-Ortega, D., Ledger, A., Schramek, D., Joshi, P., Szwarc, M.M., Cho, C., Lydon, J.P., Khokha, R., Penninger, J.M., et al. (2013). Progesterone drives mammary secretory differentiation via RankL-mediated induction of Elf5 in luminal progenitor cells. Dev. Camb. Engl. *140*, 1397–1401.

Lee, H.-J., Bao, J., Miller, A., Zhang, C., Wu, J., Baday, Y.C., Guibao, C., Li, L., Wu, D., and Zheng, J.J. (2015). Structure-based Discovery of Novel Small Molecule Wnt Signaling Inhibitors by Targeting the Cysteine-rich Domain of Frizzled. J. Biol. Chem. *290*, 30596–30606.

Lee, K., Zhang, H., Qian, D.Z., Rey, S., Liu, J.O., and Semenza, G.L. (2009). Acriflavine inhibits HIF-1 dimerization, tumor growth, and vascularization. Proc. Natl. Acad. Sci. U. S. A. *106*, 17910–17915.

Lees, J.A., Fawell, S.E., and Parker, M.G. (1989). Identification of two transactivation domains in the mouse oestrogen receptor. Nucleic Acids Res. *17*, 5477–5488.

Leung, C.O.-N., Mak, W.-N., Kai, A.K.-L., Chan, K.-S., Lee, T.K.-W., Ng, I.O.-L., and Lo, R.C.-L. (2016). Sox9 confers stemness properties in hepatocellular carcinoma through Frizzled-7 mediated Wnt/β-catenin signaling. Oncotarget.

Lewis, M.T., and Wicha, M.S. (2009). Tumor-initiating cells and treatment resistance: how goes the war? J. Mammary Gland Biol. Neoplasia *14*, 1–2.

Li, C., Heidt, D.G., Dalerba, P., Burant, C.F., Zhang, L., Adsay, V., Wicha, M., Clarke, M.F., and Simeone, D.M. (2007). Identification of pancreatic cancer stem cells. Cancer Res. *67*, 1030–1037.

Li, C., He, B., Huang, C., Yang, H., Cao, L., Huang, J., and Hu, C. (2017). Sex-Determining Region Y-box 2 Promotes Growth of Lung Squamous Cell Carcinoma and Directly Targets Cyclin D1. DNA Cell Biol.

Li, H., Ma, F., Wang, H., Lin, C., Fan, Y., Zhang, X., Qian, H., and Xu, B. (2013). Stem cell marker aldehyde dehydrogenase 1 (ALDH1)-expressing cells are enriched in triple-negative breast cancer. Int. J. Biol. Markers *28*, e357-364.

Li, Q., Yao, Y., Eades, G., Liu, Z., Zhang, Y., and Zhou, Q. (2014a). Downregulation of miR-140 promotes cancer stem cell formation in basal-like early stage breast cancer. Oncogene *33*, 2589–2600.

Li, S., Li, S., Sun, Y., and Li, L. (2014b). The expression of β-catenin in different subtypes of breast cancer and its clinical significance. Tumour Biol. J. Int. Soc. Oncodevelopmental Biol. Med. *35*, 7693–7698.

Li, V.S.W., Ng, S.S., Boersema, P.J., Low, T.Y., Karthaus, W.R., Gerlach, J.P., Mohammed, S., Heck, A.J.R., Maurice, M.M., Mahmoudi, T., et al. (2012). Wnt signaling through inhibition of β-catenin degradation in an intact Axin1 complex. Cell *149*, 1245–1256.

Li, Y., Zhang, T., Korkaya, H., Liu, S., Lee, H.-F., Newman, B., Yu, Y., Clouthier, S.G., Schwartz, S.J., Wicha, M.S., et al. (2010). Sulforaphane, a dietary component of broccoli/broccoli sprouts, inhibits breast cancer stem cells. Clin. Cancer Res. Off. J. Am. Assoc. Cancer Res. *16*, 2580–2590.

Lim, E., Vaillant, F., Wu, D., Forrest, N.C., Pal, B., Hart, A.H., Asselin-Labat, M.-L., Gyorki, D.E., Ward, T., Partanen, A., et al. (2009). Aberrant luminal progenitors as the candidate target population for basal tumor development in BRCA1 mutation carriers. Nat. Med. *15*, 907–913.

Lim, E., Wu, D., Pal, B., Bouras, T., Asselin-Labat, M.-L., Vaillant, F., Yagita, H., Lindeman, G.J., Smyth, G.K., and Visvader, J.E. (2010). Transcriptome analyses of mouse and human mammary cell subpopulations reveal multiple conserved genes and pathways. Breast Cancer Res. BCR *12*, R21.

Lin, L., Hutzen, B., Lee, H.-F., Peng, Z., Wang, W., Zhao, C., Lin, H.-J., Sun, D., Li, P.-K., Li, C., et al. (2013). Evaluation of STAT3 signaling in ALDH+ and ALDH+/CD44+/CD24- subpopulations of breast cancer cells. PloS One *8*, e82821.

Lin, S.Y., Xia, W., Wang, J.C., Kwong, K.Y., Spohn, B., Wen, Y., Pestell, R.G., and Hung, M.C. (2000). Beta-catenin, a novel prognostic marker for breast cancer: its roles in cyclin D1 expression and cancer progression. Proc. Natl. Acad. Sci. U. S. A. *97*, 4262–4266.

Lindvall, C., Evans, N.C., Zylstra, C.R., Li, Y., Alexander, C.M., and Williams, B.O. (2006). The Wnt signaling receptor Lrp5 is required for mammary ductal stem cell activity and Wnt1-induced tumorigenesis. J. Biol. Chem. *281*, 35081–35087.

Ling, S., Chang, X., Schultz, L., Lee, T.K., Chaux, A., Marchionni, L., Netto, G.J., Sidransky, D., and Berman, D.M. (2011). An EGFR-ERK-SOX9 signaling cascade links urothelial development and regeneration to cancer. Cancer Res. *71*, 3812–3821.

Liu, C., Kelnar, K., Liu, B., Chen, X., Calhoun-Davis, T., Li, H., Patrawala, L., Yan, H., Jeter, C., Honorio, S., et al. (2011). The microRNA miR-34a inhibits prostate cancer stem cells and metastasis by directly repressing CD44. Nat. Med. *17*, 211–215.

Liu, C., Liu, L., Chen, X., Cheng, J., Zhang, H., Shen, J., Shan, J., Xu, Y., Yang, Z., Lai, M., et al. (2016a). Sox9 Regulates Self-Renewal and Tumorigenicity by Promoting Symmetrical Cell Division of Cancer Stem Cells in Hepatocellular Carcinoma. Hepatol. Baltim. Md.

Liu, J., Pan, S., Hsieh, M.H., Ng, N., Sun, F., Wang, T., Kasibhatla, S., Schuller, A.G., Li, A.G., Cheng, D., et al. (2013a). Targeting Wnt-driven cancer through the inhibition of Porcupine by LGK974. Proc. Natl. Acad. Sci. U. S. A. *110*, 20224–20229.

Liu, J.A.J., Wu, M.-H., Yan, C.H., Chau, B.K.H., So, H., Ng, A., Chan, A., Cheah, K.S.E., Briscoe, J., and Cheung, M. (2013b). Phosphorylation of Sox9 is required for neural crest delamination and is regulated downstream of BMP and canonical Wnt signaling. Proc. Natl. Acad. Sci. U. S. A. *110*, 2882–2887.

Liu, S., Cong, Y., Wang, D., Sun, Y., Deng, L., Liu, Y., Martin-Trevino, R., Shang, L., McDermott, S.P., Landis, M.D., et al. (2014). Breast cancer stem cells transition between epithelial and mesenchymal states reflective of their normal counterparts. Stem Cell Rep. *2*, 78–91.

Liu, Y., Zhang, W., Liu, K., Liu, S., Ji, B., and Wang, Y. (2016b). miR-138 suppresses cell proliferation and invasion by inhibiting SOX9 in hepatocellular carcinoma. Am. J. Transl. Res. *8*, 2159–2168.

Loh, Y.N., Hedditch, E.L., Baker, L.A., Jary, E., Ward, R.L., and Ford, C.E. (2013). The Wnt signalling pathway is upregulated in an in vitro model of acquired tamoxifen resistant breast cancer. BMC Cancer *13*, 174.

Lombardo, Y., Faronato, M., Filipovic, A., Vircillo, V., Magnani, L., and Coombes, R.C. (2014). Nicastrin and Notch4 drive endocrine therapy resistance and epithelial to mesenchymal transition in MCF7 breast cancer cells. Breast Cancer Res. BCR *16*, R62.

Lu, L., Tao, H., Chang, A.E., Hu, Y., Shu, G., Chen, Q., Egenti, M., Owen, J., Moyer, J.S., Prince, M.E., et al. (2015). Cancer stem cell vaccine inhibits metastases of primary tumors and induces humoral immune responses against cancer stem cells. Oncoimmunology *4*, e990767.

Lu, W., Lin, C., Roberts, M.J., Waud, W.R., Piazza, G.A., and Li, Y. (2011). Niclosamide suppresses cancer cell growth by inducing Wnt co-receptor LRP6 degradation and inhibiting the Wnt/β-catenin pathway. PloS One *6*, e29290.

Ludbrook, L., Alankarage, D., Bagheri-Fam, S., and Harley, V. (2016). Dataset of differentially expressed genes from SOX9 over-expressing NT2/D1 cells. Data Brief *9*, 194–198.

Ma, F., Ye, H., He, H.H., Gerrin, S.J., Chen, S., Tanenbaum, B.A., Cai, C., Sowalsky, A.G., He, L., Wang, H., et al. (2016). SOX9 drives WNT pathway activation in prostate cancer. J. Clin. Invest. *126*, 1745–1758.

Malhotra, G.K., Zhao, X., Edwards, E., Kopp, J.L., Naramura, M., Sander, M., Band, H., and Band, V. (2014). The role of Sox9 in mouse mammary gland development and maintenance of mammary stem and luminal progenitor cells. BMC Dev. Biol. *14*, 47.

Malki, S., Nef, S., Notarnicola, C., Thevenet, L., Gasca, S., Méjean, C., Berta, P., Poulat, F., and Boizet-Bonhoure, B. (2005). Prostaglandin D2 induces nuclear import of the sex-determining factor SOX9 via its cAMP-PKA phosphorylation. EMBO J. *24*, 1798–1809.

Manrique Tejedor, J., Figuerol Calderó, M.I., and Cuéllar De Frutos, A. (2015). [BREASTFEEDING AS A METHOD OF BREAST CANCER PREVENTION]. Rev. Enferm. Barc. Spain *38*, 32–38.

Marcato, P., Dean, C.A., Pan, D., Araslanova, R., Gillis, M., Joshi, M., Helyer, L., Pan, L., Leidal, A., Gujar, S., et al. (2011a). Aldehyde dehydrogenase activity of breast cancer stem cells is primarily due to isoform ALDH1A3 and its expression is predictive of metastasis. Stem Cells Dayt. Ohio *29*, 32–45.

Marcato, P., Dean, C.A., Pan, D., Araslanova, R., Gillis, M., Joshi, M., Helyer, L., Pan, L., Leidal, A., Gujar, S., et al. (2011b). Aldehyde dehydrogenase activity of breast cancer stem cells is primarily due to isoform ALDH1A3 and its expression is predictive of metastasis. Stem Cells Dayt. Ohio *29*, 32–45.

Martin, H.L., Smith, L., and Tomlinson, D.C. (2014). Multidrug-resistant breast cancer: current perspectives. Breast Cancer Dove Med. Press *6*, 1–13.

Massarweh, S., Osborne, C.K., Creighton, C.J., Qin, L., Tsimelzon, A., Huang, S., Weiss, H., Rimawi, M., and Schiff, R. (2008). Tamoxifen resistance in breast tumors is driven by growth factor receptor signaling with repression of classic estrogen receptor genomic function. Cancer Res. *68*, 826–833.

Matheu, A., Collado, M., Wise, C., Manterola, L., Cekaite, L., Tye, A.J., Canamero, M., Bujanda, L., Schedl, A., Cheah, K.S.E., et al. (2012). Oncogenicity of the developmental transcription factor Sox9. Cancer Res. *72*, 1301–1315.

Matsuda, Y., Schlange, T., Oakeley, E.J., Boulay, A., and Hynes, N.E. (2009). WNT signaling enhances breast cancer cell motility and blockade of the WNT pathway by sFRP1 suppresses MDA-MB-231 xenograft growth. Breast Cancer Res. BCR *11*, R32.

Matzuk, M.M., and Lamb, D.J. (2008). The biology of infertility: research advances and clinical challenges. Nat. Med. *14*, 1197–1213.

Maughan, K.L., Lutterbie, M.A., and Ham, P.S. (2010). Treatment of breast cancer. Am. Fam. Physician *81*, 1339–1346.

Miller, P.C., Clarke, J., Koru-Sengul, T., Brinkman, J., and El-Ashry, D. (2015). A novel MAPK-microRNA signature is predictive of hormone-therapy resistance and poor outcome in ER-positive breast cancer. Clin. Cancer Res. Off. J. Am. Assoc. Cancer Res. *21*, 373–385.

Minn, A.J., Gupta, G.P., Siegel, P.M., Bos, P.D., Shu, W., Giri, D.D., Viale, A., Olshen, A.B., Gerald, W.L., and Massagué, J. (2005). Genes that mediate breast cancer metastasis to lung. Nature *436*, 518–524.

Miyamoto, K., Araki, K.Y., Naka, K., Arai, F., Takubo, K., Yamazaki, S., Matsuoka, S., Miyamoto, T., Ito, K., Ohmura, M., et al. (2007). Foxo3a is essential for maintenance of the hematopoietic stem cell pool. Cell Stem Cell *1*, 101–112.

Montagut, C., and Settleman, J. (2009). Targeting the RAF-MEK-ERK pathway in cancer therapy. Cancer Lett. *283*, 125–134.

Moreb, J., Schweder, M., Suresh, A., and Zucali, J.R. (1996). Overexpression of the human aldehyde dehydrogenase class I results in increased resistance to 4-hydroperoxycyclophosphamide. Cancer Gene Ther. *3*, 24–30.

Morrison, G., Fu, X., Shea, M., Nanda, S., Giuliano, M., Wang, T., Klinowska, T., Osborne, C.K., Rimawi, M.F., and Schiff, R. (2014). Therapeutic potential of the dual EGFR/HER2 inhibitor AZD8931 in circumventing endocrine resistance. Breast Cancer Res. Treat. *144*, 263–272.

Mulac-Jericevic, B., Mullinax, R.A., DeMayo, F.J., Lydon, J.P., and Conneely, O.M. (2000). Subgroup of reproductive functions of progesterone mediated by progesterone receptor-B isoform. Science *289*, 1751–1754.

Munster, P.N., Thurn, K.T., Thomas, S., Raha, P., Lacevic, M., Miller, A., Melisko, M., Ismail-Khan, R., Rugo, H., Moasser, M., et al. (2011). A phase II study of the histone deacetylase inhibitor vorinostat combined with tamoxifen for the treatment of patients with hormone therapy-resistant breast cancer. Br. J. Cancer *104*, 1828–1835.

Murakami, S., Kan, M., McKeehan, W.L., and de Crombrugghe, B. (2000). Up-regulation of the chondrogenic Sox9 gene by fibroblast growth factors is mediated by the mitogen-activated protein kinase pathway. Proc. Natl. Acad. Sci. U. S. A. *97*, 1113–1118.

Narod, S.A. (2006). Modifiers of risk of hereditary breast cancer. Oncogene *25*, 5832–5836.

Nilsson, S., and Gustafsson, J.-Å. (2011). Estrogen receptors: therapies targeted to receptor subtypes. Clin. Pharmacol. Ther. *89*, 44–55.

Niwa, H. (2007). How is pluripotency determined and maintained? Development *134*, 635–646.

Niwa, H., Ogawa, K., Shimosato, D., and Adachi, K. (2009). A parallel circuit of LIF signalling pathways maintains pluripotency of mouse ES cells. Nature *460*, 118–122.

Nowak, J.A., Polak, L., Pasolli, H.A., and Fuchs, E. (2008). Hair Follicle Stem Cells are Specified and Function in Early Skin Morphogenesis. Cell Stem Cell *3*, 33–43.

Nusse, R. (2005). Wnt signaling in disease and in development. Cell Res. *15*, 28–32.

Nusse, R. (2008). Wnt signaling and stem cell control. Cell Res. *18*, 523–527.

Obr, A.E., and Edwards, D.P. (2012). The biology of progesterone receptor in the normal mammary gland and in breast cancer. Mol. Cell. Endocrinol. *357*, 4–17.

Oh, H.J., Kido, T., and Lau, Y.-F.C. (2007). PIAS1 interacts with and represses SOX9 transactivation activity. Mol. Reprod. Dev. *74*, 1446–1455.

Osada, T., Chen, M., Yang, X.Y., Spasojevic, I., Vandeusen, J.B., Hsu, D., Clary, B.M., Clay, T.M., Chen, W., Morse, M.A., et al. (2011). Antihelminth compound niclosamide downregulates Wnt signaling and elicits antitumor responses in tumors with activating APC mutations. Cancer Res. *71*, 4172–4182.

Overman, J., Fontaine, F., Moustaqil, M., Mittal, D., Sierecki, E., Sacilotto, N., Zuegg, J., Robertson, A.A., Holmes, K., Salim, A.A., et al. (2017). Pharmacological targeting of the transcription factor SOX18 delays breast cancer in mice. ELife *6*.

Pannuti, A., Foreman, K., Rizzo, P., Osipo, C., Golde, T., Osborne, B., and Miele, L. (2010). Targeting Notch to target cancer stem cells. Clin. Cancer Res. Off. J. Am. Assoc. Cancer Res. *16*, 3141–3152.

Parkin, D.M., Boyd, L., and Walker, L.C. (2011). 16. The fraction of cancer attributable to lifestyle and environmental factors in the UK in 2010. Br. J. Cancer *105 Suppl 2*, S77-81.

Parmar, H., and Cunha, G.R. (2004). Epithelial-stromal interactions in the mouse and human mammary gland in vivo. Endocr. Relat. Cancer *11*, 437–458.

Pask, A.J., Calatayud, N.E., Shaw, G., Wood, W.M., and Renfree, M.B. (2010). Oestrogen blocks the nuclear entry of SOX9 in the developing gonad of a marsupial mammal. BMC Biol. *8*, 113.

Passeron, T., Valencia, J.C., Namiki, T., Vieira, W.D., Passeron, H., Miyamura, Y., and Hearing, V.J. (2009). Upregulation of SOX9 inhibits the growth of human and mouse melanomas and restores their sensitivity to retinoic acid. J. Clin. Invest. *119*, 954–963.

Pearson, G., Robinson, F., Beers Gibson, T., Xu, B.E., Karandikar, M., Berman, K., and Cobb, M.H. (2001). Mitogen-activated protein (MAP) kinase pathways: regulation and physiological functions. Endocr. Rev. *22*, 153–183.

Pece, S., Tosoni, D., Confalonieri, S., Mazzarol, G., Vecchi, M., Ronzoni, S., Bernard, L., Viale, G., Pelicci, P.G., and Di Fiore, P.P. (2010). Biological and molecular heterogeneity of breast cancers correlates with their cancer stem cell content. Cell *140*, 62–73.

Perou, C.M., Sørlie, T., Eisen, M.B., van de Rijn, M., Jeffrey, S.S., Rees, C.A., Pollack, J.R., Ross, D.T., Johnsen, H., Akslen, L.A., et al. (2000). Molecular portraits of human breast tumours. Nature *406*, 747–752.

Peterson, E.A., Jenkins, E.C., Lofgren, K.A., Chandiramani, N., Liu, H., Aranda, E., Barnett, M., and Kenny, P.A. (2015). Amphiregulin Is a Critical Downstream Effector of Estrogen Signaling in ERα-Positive Breast Cancer. Cancer Res. *75*, 4830–4838.

Phillips, T.M., McBride, W.H., and Pajonk, F. (2006). The response of CD24(-/low)/CD44+ breast cancer-initiating cells to radiation. J. Natl. Cancer Inst. *98*, 1777–1785.

Pinson, K.I., Brennan, J., Monkley, S., Avery, B.J., and Skarnes, W.C. (2000). An LDL-receptor-related protein mediates Wnt signalling in mice. Nature *407*, 535–538.

Piva, M., Domenici, G., Iriondo, O., Rábano, M., Simões, B.M., Comaills, V., Barredo, I., López-Ruiz, J.A., Zabalza, I., Kypta, R., et al. (2014). Sox2 promotes tamoxifen resistance in breast cancer cells. EMBO Mol. Med. *6*, 66–79.

Poché, R.A., Furuta, Y., Chaboissier, M.-C., Schedl, A., and Behringer, R.R. (2008). Sox9 is expressed in mouse multipotent retinal progenitor cells and functions in Müller glial cell development. J. Comp. Neurol. *510*, 237–250.

Polakis, P. (2012). Drugging Wnt signalling in cancer. EMBO J. *31*, 2737–2746.

Pors, K., and Moreb, J.S. (2014). Aldehyde dehydrogenases in cancer: an opportunity for biomarker and drug development? Drug Discov. Today *19*, 1953–1963.

Prévostel, C., Rammah-Bouazza, C., Trauchessec, H., Canterel-Thouennon, L., Busson, M., Ychou, M., Blache, P., Prévostel, C., Rammah-Bouazza, C., Trauchessec, H., et al. (2016). SOX9 is an atypical intestinal tumor suppressor controlling the oncogenic Wnt/ß-catenin signaling. Oncotarget *5*.

Proffitt, K.D., Madan, B., Ke, Z., Pendharkar, V., Ding, L., Lee, M.A., Hannoush, R.N., and Virshup, D.M. (2013). Pharmacological inhibition of the Wnt acyltransferase PORCN prevents growth of WNT-driven mammary cancer. Cancer Res. *73*, 502–507.

Protani, M., Coory, M., and Martin, J.H. (2010). Effect of obesity on survival of women with breast cancer: systematic review and meta-analysis. Breast Cancer Res. Treat. *123*, 627–635.

Raha, P., Thomas, S., Thurn, K.T., Park, J., and Munster, P.N. (2015). Combined histone deacetylase inhibition and tamoxifen induces apoptosis in tamoxifen-resistant breast cancer models, by reversing Bcl-2 overexpression. Breast Cancer Res. BCR *17*, 26.

Ramalingam, S., Daughtridge, G.W., Johnston, M.J., Gracz, A.D., and Magness, S.T. (2012). Distinct levels of Sox9 expression mark colon epithelial stem cells that form colonoids in culture. Am. J. Physiol. Gastrointest. Liver Physiol. *302*, G10-20.

Regan, J.L., Kendrick, H., Magnay, F.-A., Vafaizadeh, V., Groner, B., and Smalley, M.J. (2012). c-Kit is required for growth and survival of the cells of origin of Brca1-mutation-associated breast cancer. Oncogene *31*, 869–883.

Reya, T., Morrison, S.J., Clarke, M.F., and Weissman, I.L. (2001). Stem cells, cancer, and cancer stem cells. Nature *414*, 105–111.

Ricci-Vitiani, L., Lombardi, D.G., Pilozzi, E., Biffoni, M., Todaro, M., Peschle, C., and De Maria, R. (2007). Identification and expansion of human colon-cancer-initiating cells. Nature *445*, 111–115.

Riggins, R.B., Schrecengost, R.S., Guerrero, M.S., and Bouton, A.H. (2007). Pathways to tamoxifen resistance. Cancer Lett. *256*, 1–24.

Ringnér, M., Fredlund, E., Häkkinen, J., Borg, Å., and Staaf, J. (2011). GOBO: gene expression-based outcome for breast cancer online. PloS One *6*, e17911.

Robert, C., Dummer, R., Gutzmer, R., Lorigan, P., Kim, K.B., Nyakas, M., Arance, A., Liszkay, G., Schadendorf, D., Cantarini, M., et al. (2013). Selumetinib plus dacarbazine versus placebo plus dacarbazine as first-line treatment for BRAF-mutant metastatic melanoma: a phase 2 double-blind randomised study. Lancet Oncol. *14*, 733–740.

Robey, R.W., Chakraborty, A.R., Basseville, A., Luchenko, V., Bahr, J., Zhan, Z., and Bates, S.E. (2011). Histone deacetylase inhibitors: emerging mechanisms of resistance. Mol. Pharm. *8*, 2021–2031.

Rondón-Lagos, M., Villegas, V.E., Rangel, N., Sánchez, M.C., and Zaphiropoulos, P.G. (2016). Tamoxifen Resistance: Emerging Molecular Targets. Int. J. Mol. Sci. *17*.

Santini, R., Pietrobono, S., Pandolfi, S., Montagnani, V., D'Amico, M., Penachioni, J.Y., Vinci, M.C., Borgognoni, L., and Stecca, B. (2014). SOX2 regulates self-renewal and tumorigenicity of human melanoma-initiating cells. Oncogene *33*, 4697–4708.

Santos, J.C., Carrasco-Garcia, E., García-Puga, M., Aldaz, P., Montes, M., Fernandez-Reyes, M., de Oliveira, C.C., Lawrie, C.H., Arauzo-Bravo, M.J., Ribeiro, M., et al. (2016). SOX9 elevation acts with canonical WNT signaling to drive gastric cancer progression. Cancer Res.

Sato, N., Meijer, L., Skaltsounis, L., Greengard, P., and Brivanlou, A.H. (2004). Maintenance of pluripotency in human and mouse embryonic stem cells through activation of Wnt signaling by a pharmacological GSK-3-specific inhibitor. Nat. Med. *10*, 55–63.

Schlange, T., Matsuda, Y., Lienhard, S., Huber, A., and Hynes, N.E. (2007). Autocrine WNT signaling contributes to breast cancer cell proliferation via the canonical WNT pathway and EGFR transactivation. Breast Cancer Res. BCR *9*, R63.

Schmidt, K.T., Chau, C.H., Price, D.K., and Figg, W.D. (2016). Precision Oncology Medicine: The Clinical Relevance of Patient Specific Biomarkers Used to Optimize Cancer Treatment. J. Clin. Pharmacol.

Scott, C.E., Wynn, S.L., Sesay, A., Cruz, C., Cheung, M., Gomez Gaviro, M.-V., Booth, S., Gao, B., Cheah, K.S.E., Lovell-Badge, R., et al. (2010). SOX9 induces and maintains neural stem cells. Nat. Neurosci. *13*, 1181–1189.

Secchiero, P., Bosco, R., Celeghini, C., and Zauli, G. (2011). Recent advances in the therapeutic perspectives of Nutlin-3. Curr. Pharm. Des. *17*, 569–577.

Semënov, M.V., Tamai, K., Brott, B.K., Kühl, M., Sokol, S., and He, X. (2001). Head inducer Dickkopf-1 is a ligand for Wnt coreceptor LRP6. Curr. Biol. CB *11*, 951–961.

Seymour, P.A., Freude, K.K., Tran, M.N., Mayes, E.E., Jensen, J., Kist, R., Scherer, G., and Sander, M. (2007). SOX9 is required for maintenance of the pancreatic progenitor cell pool. Proc. Natl. Acad. Sci. U. S. A. *104*, 1865–1870.

Shackleton, M., Vaillant, F., Simpson, K.J., Stingl, J., Smyth, G.K., Asselin-Labat, M.-L., Wu, L., Lindeman, G.J., and Visvader, J.E. (2006). Generation of a functional mammary gland from a single stem cell. Nature *439*, 84–88.

Shan, J., Zhang, X., Bao, J., Cassell, R., and Zheng, J.J. (2012). Synthesis of potent dishevelled PDZ domain inhibitors guided by virtual screening and NMR studies. Chem. Biol. Drug Des. *79*, 376–383.

Shao, C., Sullivan, J.P., Girard, L., Augustyn, A., Yenerall, P., Rodriguez-Canales, J., Liu, H., Behrens, C., Shay, J.W., Wistuba, I.I., et al. (2014). Essential role of aldehyde dehydrogenase 1A3 for the maintenance of non-small cell lung cancer stem cells is associated with the STAT3 pathway. Clin. Cancer Res. Off. J. Am. Assoc. Cancer Res. *20*, 4154–4166.

Sharma, P. (2016). Biology and Management of Patients With Triple-Negative Breast Cancer. The Oncologist *21*, 1050–1062.

Shen, Z., Deng, H., Fang, Y., Zhu, X., Ye, G.-T., Yan, L., Liu, H., and Li, G. (2015). Identification of the interplay between SOX9 and S100P in the metastasis and invasion of colon carcinoma. Oncotarget *6*, 20672–20684.

Shi, Q., Rafii, S., Wu, M.H., Wijelath, E.S., Yu, C., Ishida, A., Fujita, Y., Kothari, S., Mohle, R., Sauvage, L.R., et al. (1998). Evidence for circulating bone marrow-derived endothelial cells. Blood *92*, 362–367.

Shi, Y., Liu, C., Liu, X., Tang, D.G., and Wang, J. (2014). The microRNA miR-34a inhibits non-small cell lung cancer (NSCLC) growth and the CD44hi stem-like NSCLC cells. PloS One *9*, e90022.

Shibue, T., and Weinberg, R.A. (2017). EMT, CSCs, and drug resistance: the mechanistic link and clinical implications. Nat. Rev. Clin. Oncol.

Shou, J., Massarweh, S., Osborne, C.K., Wakeling, A.E., Ali, S., Weiss, H., and Schiff, R. (2004). Mechanisms of tamoxifen resistance: increased estrogen receptor-HER2/neu cross-talk in ER/HER2-positive breast cancer. J. Natl. Cancer Inst. *96*, 926–935.

Simões, B.M., and Vivanco, M.D. (2011). Cancer stem cells in the human mammary gland and regulation of their differentiation by estrogen. Future Oncol. Lond. Engl. *7*, 995–1006.
Simões, B.M., Piva, M., Iriondo, O., Comaills, V., López-Ruiz, J.A., Zabalza, I., Mieza, J.A., Acinas, O., and Vivanco, M.D.M. (2011). Effects of estrogen on the proportion of stem cells in the breast. Breast Cancer Res. Treat. *129*, 23–35.

Simões, B.M., O'Brien, C.S., Eyre, R., Silva, A., Yu, L., Sarmiento-Castro, A., Alférez, D.G., Spence, K., Santiago-Gómez, A., Chemi, F., et al. (2015). Anti-estrogen Resistance in Human Breast Tumors Is Driven by JAG1-NOTCH4-Dependent Cancer Stem Cell Activity. Cell Rep. *12*, 1968–1977.

Sinclair, A.H., Berta, P., Palmer, M.S., Hawkins, J.R., Griffiths, B.L., Smith, M.J., Foster, J.W., Frischauf, A.M., Lovell-Badge, R., and Goodfellow, P.N. (1990). A gene from the human sex-determining region encodes a protein with homology to a conserved DNA-binding motif. Nature *346*, 240–244.

Slamon, D.J., Godolphin, W., Jones, L.A., Holt, J.A., Wong, S.G., Keith, D.E., Levin, W.J., Stuart, S.G., Udove, J., and Ullrich, A. (1989). Studies of the HER-2/neu proto-oncogene in human breast and ovarian cancer. Science *244*, 707–712.

Soerjomataram, I., de Vries, E., Engholm, G., Paludan-Müller, G., Brønnum-Hansen, H., Storm, H.H., and Barendregt, J.J. (2010). Impact of a smoking and alcohol intervention programme on lung and breast cancer incidence in Denmark: An example of dynamic modelling with Prevent. Eur. J. Cancer Oxf. Engl. 1990 *46*, 2617–2624.

Sokol, E.S., Miller, D.H., Breggia, A., Spencer, K.C., Arendt, L.M., and Gupta, P.B. (2016). Growth of human breast tissues from patient cells in 3D hydrogel scaffolds. Breast Cancer Res. BCR *18*, 19.

Song, C.-Q., Li, Y., Mou, H., Moore, J., Park, A., Pomyen, Y., Hough, S., Kennedy, Z., Fischer, A., Yin, H., et al. (2016). Genome-wide CRISPR Screen Identifies Regulators of MAPK as Suppressors of Liver Tumors in Mice. Gastroenterology.

Sørlie, T., Perou, C.M., Tibshirani, R., Aas, T., Geisler, S., Johnsen, H., Hastie, T., Eisen, M.B., van de Rijn, M., Jeffrey, S.S., et al. (2001). Gene expression patterns of breast carcinomas distinguish tumor subclasses with clinical implications. Proc. Natl. Acad. Sci. U. S. A. *98*, 10869–10874.

Soyal, S., Ismail, P.M., Li, J., Mulac-Jericevic, B., Conneely, O.M., and Lydon, J.P. (2002). Progesterone receptors - animal models and cell signaling in breast cancer: Progesterone's role in mammary gland development and tumorigenesis as disclosed by experimental mouse genetics. Breast Cancer Res. *4*, 191–196.

Spangrude, G.J., Heimfeld, S., and Weissman, I.L. (1988). Purification and characterization of mouse hematopoietic stem cells. Science *241*, 58–62.

Speirs, V., Skliris, G.P., Burdall, S.E., and Carder, P.J. (2002). Distinct expression patterns of ER alpha and ER beta in normal human mammary gland. J. Clin. Pathol. *55*, 371–374.

Stamos, J.L., and Weis, W.I. (2013). The β-catenin destruction complex. Cold Spring Harb. Perspect. Biol. *5*, a007898.

Stevenson, J.C., Hodis, H.N., Pickar, J.H., and Lobo, R.A. (2011). HRT and breast cancer risk: a realistic perspective. Climacteric J. Int. Menopause Soc. *14*, 633–636.

Stingl, J. (2011). Estrogen and progesterone in normal mammary gland development and in cancer. Horm. Cancer *2*, 85–90.

Stingl, J., and Caldas, C. (2007). Molecular heterogeneity of breast carcinomas and the cancer stem cell hypothesis. Nat. Rev. Cancer *7*, 791–799.
Stingl, J., Eaves, C.J., Kuusk, U., and Emerman, J.T. (1998). Phenotypic and functional characterization in vitro of a multipotent epithelial cell present in the normal adult human breast. Differ. Res. Biol. Divers. *63*, 201–213.

Stingl, J., Eaves, C.J., Zandieh, I., and Emerman, J.T. (2001). Characterization of bipotent mammary epithelial progenitor cells in normal adult human breast tissue. Breast Cancer Res. Treat. *67*, 93–109.

Stingl, J., Eirew, P., Ricketson, I., Shackleton, M., Vaillant, F., Choi, D., Li, H.I., and Eaves, C.J. (2006). Purification and unique properties of mammary epithelial stem cells. Nature *439*, 993–997.

Sun, L., Mathews, L.A., Cabarcas, S.M., Zhang, X., Yang, A., Zhang, Y., Young, M.R., Klarmann, K.D., Keller, J.R., and Farrar, W.L. (2013). Epigenetic regulation of SOX9 by the NF-κB signaling pathway in pancreatic cancer stem cells. Stem Cells Dayt. Ohio *31*, 1454–1466.

Suryo Rahmanto, A., Savov, V., Brunner, A., Bolin, S., Weishaupt, H., Malyukova, A., Rosén, G., Čančer, M., Hutter, S., Sundström, A., et al. (2016). FBW7 suppression leads to SOX9 stabilization and increased malignancy in medulloblastoma. EMBO J.

Suryo Rahmanto, A., Swartling, F.J., and Sangfelt, O. (2017). Targeting SOX9 for degradation to inhibit chemoresistance, metastatic spread, and recurrence. Mol. Cell. Oncol. *4*, e1252871.

Suzuki, H., Toyota, M., Caraway, H., Gabrielson, E., Ohmura, T., Fujikane, T., Nishikawa, N., Sogabe, Y., Nojima, M., Sonoda, T., et al. (2008). Frequent epigenetic inactivation of Wnt antagonist genes in breast cancer. Br. J. Cancer *98*, 1147–1156.

Takahashi, K., and Yamanaka, S. (2006). Induction of pluripotent stem cells from mouse embryonic and adult fibroblast cultures by defined factors. Cell *126*, 663–676.

Takahashi, K., Tanabe, K., Ohnuki, M., Narita, M., Ichisaka, T., Tomoda, K., and Yamanaka, S. (2007). Induction of pluripotent stem cells from adult human fibroblasts by defined factors. Cell *131*, 861–872.

Takahashi-Yanaga, F., and Kahn, M. (2010). Targeting Wnt signaling: can we safely eradicate cancer stem cells? Clin. Cancer Res. Off. J. Am. Assoc. Cancer Res. *16*, 3153–3162.

Tapia, N., MacCarthy, C., Esch, D., Gabriele Marthaler, A., Tiemann, U., Araúzo-Bravo, M.J., Jauch, R., Cojocaru, V., and Schöler, H.R. (2015). Dissecting the role of distinct OCT4-SOX2 heterodimer configurations in pluripotency. Sci. Rep. *5*.

Thomas, M.L., de Antueno, R., Coyle, K.M., Sultan, M., Cruickshank, B.M., Giacomantonio, M.A., Giacomantonio, C.A., Duncan, R., and Marcato, P. (2016). Citral reduces breast tumor growth by inhibiting the cancer stem cell marker ALDH1A3. Mol. Oncol. *10*, 1485–1496.

Thomas, S., Thurn, K.T., Raha, P., Chen, S., and Munster, P.N. (2013). Efficacy of histone deacetylase and estrogen receptor inhibition in breast cancer cells due to concerted down regulation of Akt. PloS One *8*, e68973.

Thorne, C.A., Hanson, A.J., Schneider, J., Tahinci, E., Orton, D., Cselenyi, C.S., Jernigan, K.K., Meyers, K.C., Hang, B.I., Waterson, A.G., et al. (2010). Small-molecule inhibition of Wnt signaling through activation of casein kinase 1α. Nat. Chem. Biol. *6*, 829–836.

Tomita, H., Tanaka, K., Tanaka, T., and Hara, A. (2016). Aldehyde dehydrogenase 1A1 in stem cells and cancer. Oncotarget.

Tosoni, D., Di Fiore, P.P., and Pece, S. (2012). Functional purification of human and mouse mammary stem cells. Methods Mol. Biol. Clifton NJ *916*, 59–79.
Tremblay, J.R., LeBon, J.M., Luo, A., Quijano, J.C., Wedeken, L., Jou, K., Riggs, A.D., Tirrell, D.A., and Ku, H.T. (2016). In Vitro Colony Assays for Characterizing Tri-potent Progenitor Cells Isolated from the Adult Murine Pancreas. J. Vis. Exp. JoVE.

Tsukamoto, A.S., Grosschedl, R., Guzman, R.C., Parslow, T., and Varmus, H.E. (1988). Expression of the int-1 gene in transgenic mice is associated with mammary gland hyperplasia and adenocarcinomas in male and female mice. Cell *55*, 619–625.

Unguryte, A., Bernotiene, E., Bagdonas, E., Garberyte, S., Porvaneckas, N., and Jorgensen, C. (2016). Human articular chondrocytes with higher aldehyde dehydrogenase activity have stronger expression of COL2A1 and SOX9. Osteoarthr. Cartil. OARS Osteoarthr. Res. Soc. *24*, 873–882.

Van Keymeulen, A., Rocha, A.S., Ousset, M., Beck, B., Bouvencourt, G., Rock, J., Sharma, N., Dekoninck, S., and Blanpain, C. (2011). Distinct stem cells contribute to mammary gland development and maintenance. Nature *479*, 189–193.

Villadsen, R., Fridriksdottir, A.J., Rønnov-Jessen, L., Gudjonsson, T., Rank, F., LaBarge, M.A., Bissell, M.J., and Petersen, O.W. (2007). Evidence for a stem cell hierarchy in the adult human breast. J. Cell Biol. *177*, 87–101.

Visvader, J.E. (2009). Keeping abreast of the mammary epithelial hierarchy and breast tumorigenesis. Genes Dev. *23*, 2563–2577.

Visvader, J.E., and Stingl, J. (2014). Mammary stem cells and the differentiation hierarchy: current status and perspectives. Genes Dev. *28*, 1143–1158.

Vora, P., Venugopal, C., McFarlane, N., and Singh, S.K. (2015). Culture and Isolation of Brain Tumor Initiating Cells. Curr. Protoc. Stem Cell Biol. *34*, 3.3.1-13.

Wang, C., Zhang, T., Liu, W., Meng, H., Song, Y., and Wang, W. (2016a). Sox9-induced chondrogenesis in mesenchymal stem cells was mediated by ERK5 signal pathway. Cell. Mol. Biol. Noisy--Gd. Fr. *62*, 1–7.

Wang, C., Christin, J.R., Oktay, M.H., and Guo, W. (2017). Lineage-Biased Stem Cells Maintain Estrogen-Receptor-Positive and -Negative Mouse Mammary Luminal Lineages. Cell Rep. *18*, 2825–2835.

Wang, H., Leav, I., Ibaragi, S., Wegner, M., Hu, G., Lu, M.L., Balk, S.P., and Yuan, X. (2008a). SOX9 is expressed in human fetal prostate epithelium and enhances prostate cancer invasion. Cancer Res. *68*, 1625–1630.

Wang, H., He, L., Ma, F., Regan, M.M., Balk, S.P., Richardson, A.L., and Yuan, X. (2013). SOX9 regulates low density lipoprotein receptor-related protein 6 (LRP6) and T-cell factor 4 (TCF4) expression and Wnt/β-catenin activation in breast cancer. J. Biol. Chem. *288*, 6478–6487.

Wang, H.-Y., Lian, P., and Zheng, P.-S. (2015a). SOX9, a potential tumor suppressor in cervical cancer, transactivates p21WAF1/CIP1 and suppresses cervical tumor growth. Oncotarget *6*, 20711–20722.

Wang, P., Bahreini, A., Gyanchandani, R., Lucas, P.C., Hartmaier, R.J., Watters, R.J., Jonnalagadda, A.R., Trejo Bittar, H.E., Berg, A., Hamilton, R.L., et al. (2016b). Sensitive Detection of Mono- and Polyclonal ESR1 Mutations in Primary Tumors, Metastatic Lesions, and Cell-Free DNA of Breast Cancer Patients. Clin. Cancer Res. Off. J. Am. Assoc. Cancer Res. *22*, 1130–1137.

Wang, X., Asplund, A.C., Porwit, A., Flygare, J., Smith, C.I.E., Christensson, B., and Sander, B. (2008b). The subcellular Sox11 distribution pattern identifies subsets of mantle cell lymphoma: correlation to overall survival. Br. J. Haematol. *143*, 248–252.
Wang, X., Ju, Y., Zhou, M.I., Liu, X., and Zhou, C. (2015b). Upregulation of SOX9 promotes cell proliferation, migration and invasion in lung adenocarcinoma. Oncol. Lett. *10*, 990–994.

Watson, C.J., and Kreuzaler, P.A. (2011). Remodeling mechanisms of the mammary gland during involution. Int. J. Dev. Biol. *55*, 757–762.

Wellbrock, C., and Arozarena, I. (2016). The Complexity of the ERK/MAP-Kinase Pathway and the Treatment of Melanoma Skin Cancer. Front. Cell Dev. Biol. *4*, 33.

Wend, P., Runke, S., Wend, K., Anchondo, B., Yesayan, M., Jardon, M., Hardie, N., Loddenkemper, C., Ulasov, I., Lesniak, M.S., et al. (2013). WNT10B/β-catenin signalling induces HMGA2 and proliferation in metastatic triple-negative breast cancer. EMBO Mol. Med. *5*, 264–279.

Wu, D., Mou, Y.-P., Chen, K., Cai, J.-Q., Zhou, Y.-C., Pan, Y., Xu, X.-W., Zhou, W., Gao, J.-Q., Chen, D.-W., et al. (2016). Aldehyde dehydrogenase 3A1 is robustly upregulated in gastric cancer stem-like cells and associated with tumorigenesis. Int. J. Oncol. *49*, 611–622.

Xu, J., Prosperi, J.R., Choudhury, N., Olopade, O.I., and Goss, K.H. (2015). β-Catenin is required for the tumorigenic behavior of triple-negative breast cancer cells. PloS One *10*, e0117097.

Xu, W.S., Parmigiani, R.B., and Marks, P.A. (2007). Histone deacetylase inhibitors: molecular mechanisms of action. Oncogene *26*, 5541–5552.

Xue, F., Willett, W.C., Rosner, B.A., Hankinson, S.E., and Michels, K.B. (2011). Cigarette smoking and the incidence of breast cancer. Arch. Intern. Med. *171*, 125–133.

Yang, L., Perez, A.A., Fujie, S., Warden, C., Li, J., Wang, Y., Yung, B., Chen, Y.-R., Liu, X., Zhang, H., et al. (2014). Wnt modulates MCL1 to control cell survival in triple negative breast cancer. BMC Cancer *14*, 124.

Yang, Z.F., Ho, D.W., Ng, M.N., Lau, C.K., Yu, W.C., Ngai, P., Chu, P.W.K., Lam, C.T., Poon, R.T.P., and Fan, S.T. (2008). Significance of CD90+ cancer stem cells in human liver cancer. Cancer Cell *13*, 153–166.

Yoda, A., Oishi, I., and Minami, Y. (2003). Expression and function of the Ror-family receptor tyrosine kinases during development: lessons from genetic analyses of nematodes, mice, and humans. J. Recept. Signal Transduct. Res. *23*, 1–15.

Zhang, W., Liu, Y., Hu, H., Huang, H., Bao, Z., Yang, P., Wang, Y., You, G., Yan, W., Jiang, T., et al. (2015). ALDH1A3: A Marker of Mesenchymal Phenotype in Gliomas Associated with Cell Invasion. PloS One *10*, e0142856.

Zhang, Z.-M., Wu, J.-F., Luo, Q.-C., Liu, Q.-F., Wu, Q.-W., Ye, G.-D., She, H.-Q., and Li, B.-A. (2016). Pygo2 activates MDR1 expression and mediates chemoresistance in breast cancer via the Wnt/β-catenin pathway. Oncogene.

Chapter 6. ANNEXES

Research Article

TRANSPARENT PROCESS OPEN ACCESS

EMBO Molecular Medicine

Sox2 promotes tamoxifen resistance in breast cancer cells

Marco Piva[1], Giacomo Domenici[1], Oihana Iriondo[1], Miriam Rábano[1], Bruno M Simões[1], Valentine Comaills[1], Inmaculada Barredo[2], Jose A López-Ruiz[3], Ignacio Zabalza[2], Robert Kypta[1,4] & Maria d M Vivanco[1,*]

Abstract

Development of resistance to therapy continues to be a serious clinical problem in breast cancer management. Cancer stem/progenitor cells have been shown to play roles in resistance to chemo- and radiotherapy. Here, we examined their role in the development of resistance to the oestrogen receptor antagonist tamoxifen. Tamoxifen-resistant cells were enriched for stem/progenitors and expressed high levels of the stem cell marker Sox2. Silencing of the *SOX2* gene reduced the size of the stem/progenitor cell population and restored sensitivity to tamoxifen. Conversely, ectopic expression of Sox2 reduced tamoxifen sensitivity *in vitro* and *in vivo*. Gene expression profiling revealed activation of the Wnt signalling pathway in Sox2-expressing cells, and inhibition of Wnt signalling sensitized resistant cells to tamoxifen. Examination of patient tumours indicated that Sox2 levels are higher in patients after endocrine therapy failure, and also in the primary tumours of these patients, compared to those of responders. Together, these results suggest that development of tamoxifen resistance is driven by Sox2-dependent activation of Wnt signalling in cancer stem/progenitor cells.

Keywords breast cancer; Sox2; stem cells; tamoxifen resistance; wnt signalling

Subject Categories Cancer; Stem Cells

DOI 10.1002/emmm.201303411 | Received 20 August 2013 | Revised 20 September 2013 | Accepted 24 September 2013 | Published online 31 October 2013

Introduction

Breast cancer is the most common female cancer and approximately 70–75% of cases express oestrogen receptor alpha (ERα). Tamoxifen, an oestrogen antagonist in the breast, has been the standard endocrine therapy for women with ERα-positive breast cancer for many years and remains so for premenopausal and a substantial number of postmenopausal patients (Jordan & O'Malley, 2007). In many cases, however, resistance to endocrine therapy develops, although ERα expression is maintained in most tumours that acquire resistance (Ali & Coombes, 2002).

The potential mechanisms underlying this resistance to endocrine therapy involve ER-coregulatory proteins and cross-talk between the ER pathway and other growth-factor signalling networks (Osborne *et al,* 2005). A growing body of evidence is accumulating supporting the hypothesis that cancer stem cells, or tumour-initiating cells, drive and maintain many types of human malignancies (Diehn *et al,* 2009). The cancer stem cell hypothesis has shed new light on the development of resistance to therapy, proposing that there exists a pool of malignant cells with stem/progenitor cell properties and increased capacity to resist common chemotherapeutic treatments, compared to their more differentiated non-tumourigenic counterparts, and therefore responsible for tumour recurrence after treatment (Reya *et al,* 2001). Breast cells with the phenotype $CD44^+CD24^{-/low}lineage^-$ isolated from metastatic pleural effusions by fluorescence activated cell sorting (FACS) are highly enriched for tumour-initiating cells (Al-Hajj *et al,* 2003). Importantly, the $CD44^+CD24^{-/low}$ cell population increases in size after chemotherapy and is associated with enhanced ability to form mammospheres, suggesting that these cells are more resistant to treatment (Li *et al,* 2008). In addition, normal and cancer breast epithelial cells with increased aldehyde dehydrogenase activity (ALDH) show stem/progenitor cell properties*in vitro* and *in vivo* and are associated with poor clinical outcome (Ginestier *et al,* 2007). Finally, poorly differentiated breast tumours contain a higher proportion of cancer stem cells than well-differentiated cancers (Pece *et al,* 2010).

Previously, we observed that oestrogen reduces the pool of breast stem cells while tamoxifen has the opposite effect (Simoes *et al,* 2011). The relevance of the increase in the proportion of cancer stem cells upon tamoxifen treatment is intriguing in the context of the development of tamoxifen resistance in breast cancer patients. Furthermore, normal and cancer stem cells share phenotypes that may reflect the activity of common signalling pathways, such as high expression of *NANOG*, *OCT4* and *SOX2*, which is reduced by oestrogen (Simoes *et al,* 2011). In breast tumours, an

1 Cell Biology and Stem Cells Unit, CIC bioGUNE, Bilbao, Spain
2 Department of Pathology, Galdakao-Usansolo Hospital, Galdakao, Spain
3 Servicio de Radiodiagno´stico Preteimagen, Bilbao, Spain
4 Department of Surgery and Cancer, Imperial College London, London, UK
*Corresponding author: Tel: +34 944061322; Fax: +34 944061301; E-mail: mdmvivanco@cicbiogune.es

embryonic stem cell (ES)-like signature characterized by activation of targets of Nanog, Oct4 and Sox2 is associated with high-grade ER-negative tumours and with aggressive tumour behaviour (Ben-Porath *et al,* 2008), supporting the possibility that ES genes contribute to the stem cell-like phenotype found in many tumours.

Here, we present evidence that Sox2, a transcription factor that is key in maintaining pluripotent properties of stem cells, is a crucial player in the development of resistance to tamoxifen in ER-positive breast cancer cells. Sox2 overexpression increases the proportion of breast cancer stem/progenitor cells by activating the Wnt signalling pathway, thereby rendering the cells insensitive to the growth inhibitory effects of tamoxifen. These findings, together with the observation that Sox2 levels are elevated in the primary tumours of patients that do not respond to endocrine therapy, suggest that Sox2 could represent a prognostic factor for development of resistance to tamoxifen and that Wnt signalling may be an attractive therapeutic target in these patients.

Results

Increased tumourigenicity during the development of tamoxifen resistance compromises ER transcriptional activity

The development of tamoxifen resistance in breast cancer cells was used as a model for the acquisition of resistance to oestrogen antagonists that occurs in breast cancer patients. The oestrogen sensitive MCF-7 breast cancer cell line was cultured in the presence of tamoxifen or, in parallel, with the carrier ethanol. Initially, cell growth rates were very much reduced in the presence of tamoxifen, but eventually cells adapted to the new environment leading to two new sub-lines: MCF-7TamR (resistant to tamoxifen treatment) and control MCF-7c cells. The control MCF-7c cells are indistinguishable from the parental MCF-7 cells with respect to their proliferation capacity in normal growth medium, which is also similar to the MCF-7TamR cells (Fig 1A). As expected, control cell proliferation was reduced by tamoxifen, while MCF-7TamR cells grew at a similar rate, independently of the presence of tamoxifen (Fig 1B). Subcutaneous transplantation of MCF-7TamR cells to athymic mice led to larger and faster growing tumours compared to the parental MCF-7 cells, indicating their increased tumourigenic potential (Fig 1C). Immunoblot analysis revealed that MCF-7TamR cells remain ERα positive (ERα will be referred to as ER), like parental MCF-7 cells (Fig 1D). Despite constant levels of ER expression, ER transcriptional activity was lower in MCF-7TamR cells than in control cells in the context of a consensus oestrogen response element (Fig 1E). In addition, expression of the progesterone receptor (PR), a well-known ER target gene, was strongly reduced in MCF-7TamR cells (Fig 1F). These results indicate that MCF-7TamR cells are more tumourigenic than parental MCF-7 cells and, although they

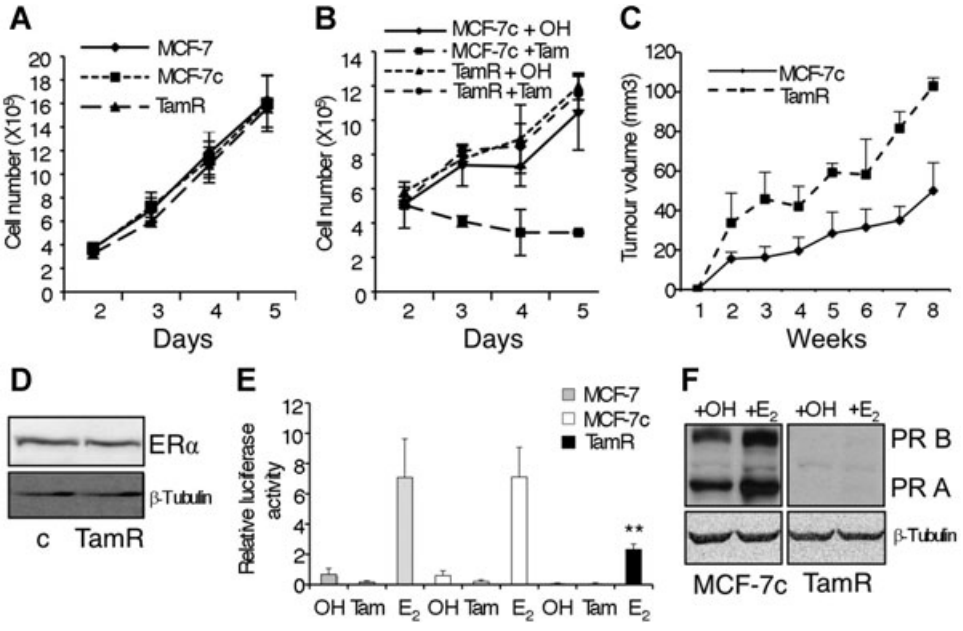

Figure 1. Characterization of MCF-7TamR cells.

A Proliferation assay of MCF-7 (wt), MCF-7c (control) and MCF-7TamR (tamoxifen resistant) cells (n = 3).

B Proliferation assay of MCF-7c and MCF-7TamR cells treated with ethanol (OH) or 5 9 10^{-7} M tamoxifen (Tam) (n = 3).

C Tumour growth curve of MCF-7c and MCF-7TamR cells implanted s.c. in athymic mice in the presence of an exogenous slow release, oestrogen implant (n = 5 mice/group).

D Western blot analysis of ERα expression in MCF-7c (c) and MCF-7TamR cells.

E MCF-7 (grey bars), MCF-7c (white bars) and MCF-7TamR (black bars) cells were transfected with a reporter plasmid containing three copies of a consensus ERE driving a luciferase reporter in the presence of the carrier ethanol (OH) or 5 9 10^{-7} M tamoxifen (Tam) or 10^{-8} M oestrogen (E_2). In all transfections, β-galactosidase activity was used to control for transfection efficiency (n = 5) $^{**}p$ = 0.007 by t-test.

F Progesterone receptor expression in control (MCF-7c) and resistant (TamR) cells by Western blot analysis.

express comparable levels of ER, its transcriptional activity is reduced in MCF-7TamR cells.

Tamoxifen resistant cells express high levels of SOX2

We have recently shown that the embryonic stem cell markers *NANOG*, *OCT4* and *SOX2* are expressed in normal breast stem cells and at higher levels in breast tumour cells and that their expression is reduced during cell differentiation (Simoes *et al,* 2011). Therefore, we wished to determine whether the expression of *NANOG*, *OCT4* and *SOX2* is differentially modulated during development of tamoxifen resistance. Real-time PCR analysis showed that the level of expression of *SOX2* was 30-fold higher in MCF-7TamR cells than in control cells. In comparison, the expression levels of *NANOG* and *OCT4* were not strongly affected (Fig 2A). In agreement with the PCR data, the levels of Sox2 protein were also clearly elevated in MCF-7TamR cells, although they were lower than Sox2 levels in undifferentiated human embryonal carcinoma stem cells (NTera2/D1 cell line) (Fig 2B). Finally, immunofluorescence analysis showed that Sox2 was strongly expressed in 20–30% of the MCF-7TamR cells (Fig 2C). These results indicate that Sox2 expression levels are higher in a subpopulation of tamoxifen resistant cells than in parental breast cancer cells.

Development of tamoxifen resistance in breast cancer cells increases the proportion of stem/progenitor cells

To monitor whether the self-renewal capacity of the breast stem/progenitor cell population was affected by the development of tamoxifen resistance, the efficiency of mammosphere formation was examined. We observed that MCF-7TamR cells formed a significantly higher number of primary and secondary mammospheres than the control cells, indicating increased self-renewal capacity (Fig 3A). Quantitative PCR analysis showed that *SOX2* expression is higher in primary and secondary mammospheres than in cells grown in adherent differentiating cultures (Fig 3B), mirroring the numbers of spheres formed. Furthermore, MCF-7TamR cells expressed higher levels of *SOX2* than control cells, both in adherent and suspension conditions (Fig 3B). In contrast, although the expression of *NANOG* and *OCT4* was higher in mammospheres than in adherent cultures, as previously shown (Simoes *et al,* 2011), there were no significant differences between their levels of expression in MCF-7TamR and control cells (supplementary Fig 1A). These findings suggest that Sox2 is relevant to the development of resistance to tamoxifen.

In breast carcinomas, a cell population with the phenotype $CD44^+CD24^{-/low}$ has been shown to be enriched for tumourigenic stem/progenitor cells (Al-Hajj *et al,* 2003). FACS analysis showed a significant increase in the proportion of $CD44^+CD24^{-/low}$ cells in secondary mammospheres when compared to cells grown in adherent cultures, both in control and MCF-7TamR cells, although this increase was significantly stronger in tamoxifen resistant cells than in MCF-7c cells (Fig 3C and supplementary Fig 1B and D). In addition, we determined the percentage of EMA^+CALLA^+ cells, since sorting for this cell population has been shown to enrich for normal (Clayton *et al*, 2004) and cancer (Simoes *et al,* 2011) breast stem/progenitor cells. Indeed, the proportion of EMA^+CALLA^+ cells was higher in mammospheres than in adherent cultures and

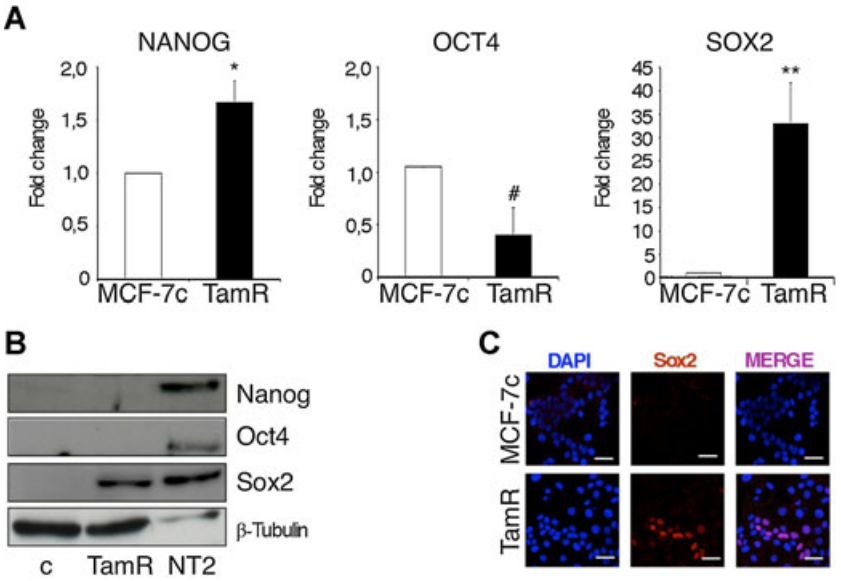

Figure 2. MCF-7TamR cells express high levels of SOX2.

A Transcript levels of NANOG, OCT4 and SOX2 in adherent MCF-7c and MCF-7TamR (TamR) cells were quantified by real-time PCR and presented as fold induction with MCF-7c value set as 1 (n = 5) *p = 0.03, $^{\#}p$ = 0.023, **p = 0.004 by t-test.

B Immunoblots of Nanog, Oct4, Sox2 and β-tubulin (loading control) in MCF-7c and MCF-7TamR cells. NTera2/D1 (NT2) cells were used as positive control for the expression of the stem cell markers.

C Immunofluorescence analysis of Sox2 expression in MCF7c and MCF-7TamR cells. Scale bar = 40 μm.

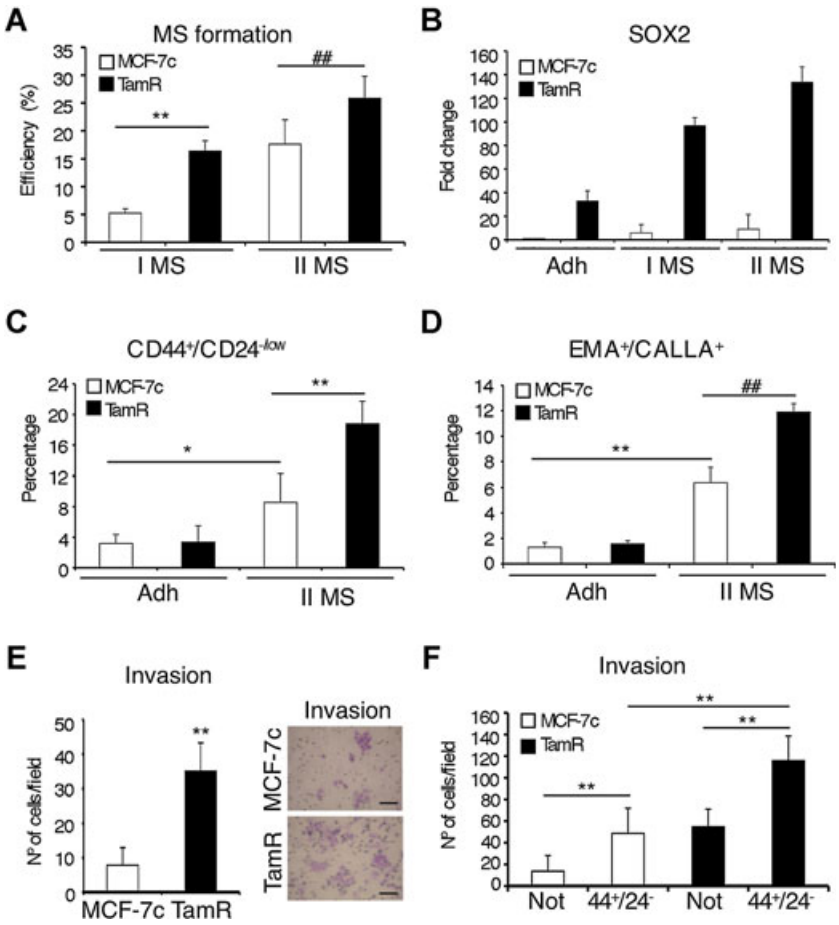

Figure 3. MCF-7TamR cells contain a higher proportion of stem cells than parental cells.

A Primary (I MS) and secondary (II MS) mammosphere efficiency formation from MCF-7c and MCF-7TamR cells represented as the percentage of mammospheres formed (n = 5) $^{**}p$ = 0.003, $^{\#\#}p$ = 0.008 by t-test.

B SOX2 mRNA expression levels in MCF-7c and MCF-7TamR cells grown in adherent (Adh) or mammosphere (I MS and II MS) cultures were quantified by real-time PCR (n = 3).

C, D Flow cytometry analysis of (C) $CD44^+/CD24^{-/low}$ (n = 5, $^*p$ = 0.028 $^{**}p$ = 0.0045 by t-test) and (D) $EMA^+/CALLA^+$ (n = 3, $^{**}p$ = 0.0021, $^{\#\#}p$ = 0.0028 by t-test) stem cell populations in MCF-7c and MCF-7TamR cells cultured as adherent cells (Adh) or as secondary mammospheres (II MS), represented as the percentage of cells with the indicated phenotype within the total population.

E Matrigel invasion assay was performed using adherent MCF-7c and MCF-7TamR cells. The photographs on the right show a representative field (n = 3) $^{**}p$ = 0.001 by t-test. Scale bar = 100 μm.

F Matrigel invasion assay was performed using secondary mammospheres from MCF-7c and MCF-7TamR cells FACS-sorted to isolate $CD44^+CD24^{-/low}$ (44^+24^-) stem cells and the remaining cell population lacking $CD44^+z24^{-/low}$ cells (Not) (n = 3) $^{**}p < 0.001$ by t-test.

was highest in MCF-7TamR cells (Fig 3D and supplementary Fig 1C). These results suggest that MCF-7TamR cells contain a higher percentage of stem/progenitor cells than parental breast cancer cells.

Previous studies have shown an association between the $CD44^+CD24^{-/low}$ phenotype and invasion (Sheridan *et al,* 2006). Consistent with this, MCF-7TamR cells exhibited an increased invasion capacity through Matrigel, compared with control cells (Fig 3E). Isolated stem cells with the phenotype $CD44^+CD24^{-/low}$ displayed a significant increase in their capacity to migrate in Transwell assays (supplementary Fig 1E), and particularly to invade through Matrigel (Fig 3F), compared to cells of the reverse phenotype. Furthermore, this increase was more evident in stem cells isolated from MCF-7TamR than more differentiated cells (Fig 3F). These results show that tamoxifen resistant cells possess higher invasion capacity than parental breast cancer cells and that this phenotype correlates with the proportion of $CD44^+CD24^{-/low}$ cells.

Inverse correlation of ER and Sox2 protein levels in tamoxifen resistant breast cancer cells

Breast stem/progenitor cells lack or express low levels of ER (Clayton *et al,* 2004; Liu *et al,* 2008). To examine the relationship between ER and Sox2 expression, immunofluorescence analysis was

performed. As shown previously, Sox2 expression was difficult to detect in control MCF-7c cells, whereas it was expressed in around 20–30% of MCF-7TamR cells (Fig 2C and 4A). Although MCF-7 cells express ER, they do so at quite variable levels and cells with the highest levels of ER expression did not express Sox2, while cells with the highest levels of Sox2 displayed the lowest levels of ER (Fig 4A). When 300 cells from random fields from three independent experiments were counted, approximately 30% of MCF-7TamR cells were found to express Sox2, and of those Sox2-positive cells, 70% expressed low levels of ER and 30% expressed a high level of ER (Fig 4B). Representative plots obtained using ImageJ 3D colour inspector analysis further demonstrate the segregation between ER and Sox2 expressing cells (Fig 4B). Similar results were obtained using the ER-positive breast cancer cell lines T-47D and ZR-75-1 (supplementary Fig 2A and B).

To enrich for stem/progenitor cells, we cultured MCF-7TamR cells as mammospheres. Western blot analysis showed that ER expression was reduced in mammosphere cultures (Fig 4C). Moreover, Sox2-positive cells generally did not express ER in mammospheres, as shown by immunofluorescence (Fig 4D and supplementary Fig 2C). Furthermore, FACS sorted $CD44^+CD24^{-/low}$ cells expressed barely detectable levels of ER, both when isolated from control and MCF-7TamR cultures (Fig 4E). As expected, Sox2 was detected at the highest levels in the $CD44^+CD24^{-/low}$ cells isolated from MCF-7TamR mammospheres and was consistently absent from the population lacking this phenotype (Fig 4E). These results indicate that the most undifferentiated stem cell-like Sox2-positive cells do not express ER. These findings support the association between the $CD44^+CD24^{-/low}$ phenotype of breast cancer tamoxifen-resistant cells and Sox2 expression and suggest that cells expressing high levels of Sox2 will be more resistant to tamoxifen.

Alteration of SOX2 expression levels affects stem cell content and tamoxifen sensitivity

To determine the relevance of Sox2 expression to the stem cell phenotype, we reduced endogenous *SOX2* levels in MCF-7TamR cells using siRNA. Transfection of two different siRNA sequences directed against Sox2 resulted in a strong reduction of Sox2 expression, as detected by immunofluorescence, while a control sequence did not have any effect (supplementary Fig 3A). Downregulation of Sox2 expression led to a significant inhibition of mammosphere formation by MCF-7TamR cells (Fig 5A), and a significant reduction in the percentage of cells with the phenotype $CD44^+CD24^{-/low}$ (Fig 5B and supplementary Fig 3C). Furthermore, MCF-7TamR cells contained a significantly higher population of ALDEFLUOR-positive cells, this is with high ALDH activity (Ginestier *et al,* 2007), than control cells (supplementary Fig 3B) and these cells expressed higher ALDH1A3 and Sox2 levels than the ALDEFLUOR-negative subpopulation (supplementary Fig 3E). Therefore, the ALDEFLUOR-positive subpopulation was also specifically reduced by Sox2 siRNA, while it was not affected by a control siRNA (Fig 5C and supplementary Fig 3D).

We have previously shown that stable overexpression of Sox2 in MCF-7 cells increases the frequency of stem cells and their capacity for invasion, properties associated with tumourigenesis and poor prognosis (Simoes *et al,* 2011). Importantly, breast cancer cells overexpressing Sox2 showed an enhanced resistance to the antiproliferative effects of tamoxifen treatment *in vitro* (Fig 5D) and *in vivo* (Fig 5E). In contrast, overexpression of Nanog or Oct4 did not affect sensitivity to tamoxifen (supplementary Fig 3F). On the other hand, stable downregulation of Sox2 expression (supplementary Fig 3G) in MCF-7TamR cells rendered them more sensitive to tamoxifen (Fig 5F). This reduction in cell viability under tamoxifen treatment was due to increased apoptosis rather than cell cycle arrest (supplementary Fig 4A and B, respectively). Finally, we wished to evaluate whether Sox2 levels are relevant to tamoxifen sensitivity in other tamoxifen resistance models. Reduction of endogenous Sox2 expression levels in tamoxifen resistant BT-474 cells (supplementary Fig 3H) was sufficient to increase their sensitivity to tamoxifen (Fig 5G). In addition, we developed breast cancer T47D cells resistant to tamoxifen (T47DTamR) by exposing them to tamoxifen for a period of over 8 months. Development of resistance to tamoxifen led to elevated endogenous Sox2 levels and decreased PR expression (supplementary Fig 4C), as observed in MCF-7TamR cells. Furthermore, Sox2 downregulation by specific siSox2 sequence in T47DTamR cells significantly reduced their resistance to tamoxifen (supplementary Fig 4D). Collectively, these results demonstrate that Sox2 plays a key role in the maintenance of the increased stem cell population associated with the development of tamoxifen resistance.

Elevated SOX2 expression levels correlate with poor prognosis and development of recurrence in breast cancer patients

The above findings raised the possibility that Sox2 expression may be altered during development of tamoxifen resistance in patients. To test this hypothesis, we examined a series of ER-positive breast tumour samples from 55 patients that had received tamoxifen therapy and a minimum of 6-year follow-up was available (supplementary Table S1). The cohort included patients for whom the endocrine therapy was successful (responders) and the tumour had not returned over a period of 8 years (n = 33 patients) and in which Sox2 was weakly expressed in a low percentage of cells (Allred score $\leq$2) (Fig 6A). In contrast, in non-responder patients all primary tumours stained positive for Sox2 (22 patients); furthermore, there was a significant increase in Sox2 expression in the recurrent lesions (26 samples, since four of them recurred twice), compared with the matched primary tumours. Representative photographs of tumour samples with negative (Fig 6C), moderate (Fig 6D) and strong (Fig 6E) Sox2 staining are shown. Interestingly, elevated Sox2 levels significantly correlated with decreased PR expression and increased histological grade during development of tamoxifen resistance (Fig 6B and supplementary Table S1).

In addition, in order to determine whether the expression of Sox2 has prognostic potential in breast cancer patients treated with tamoxifen, we analysed publicly available patient data sets (GSE9893, GSE12093 and GSE1379) where ER-positive patients (n = 154, 132 and 54, respectively) had been treated with tamoxifen therapy and a minimum of 5-year follow-up data are available. High Sox2 levels significantly correlated with poor overall survival and disease free survival (Fig 6F and G, and supplementary Fig 5). Taken together, these findings suggest that Sox2 expression in primary ER-positive tumours may be a clinical prognostic biomarker for tamoxifen resistance.

Increased expression of Sox2 leads to activation of Wnt signalling

To unravel the mechanism of action of Sox2 in adherent and mammosphere cultures of breast cancer cells, we performed global gene

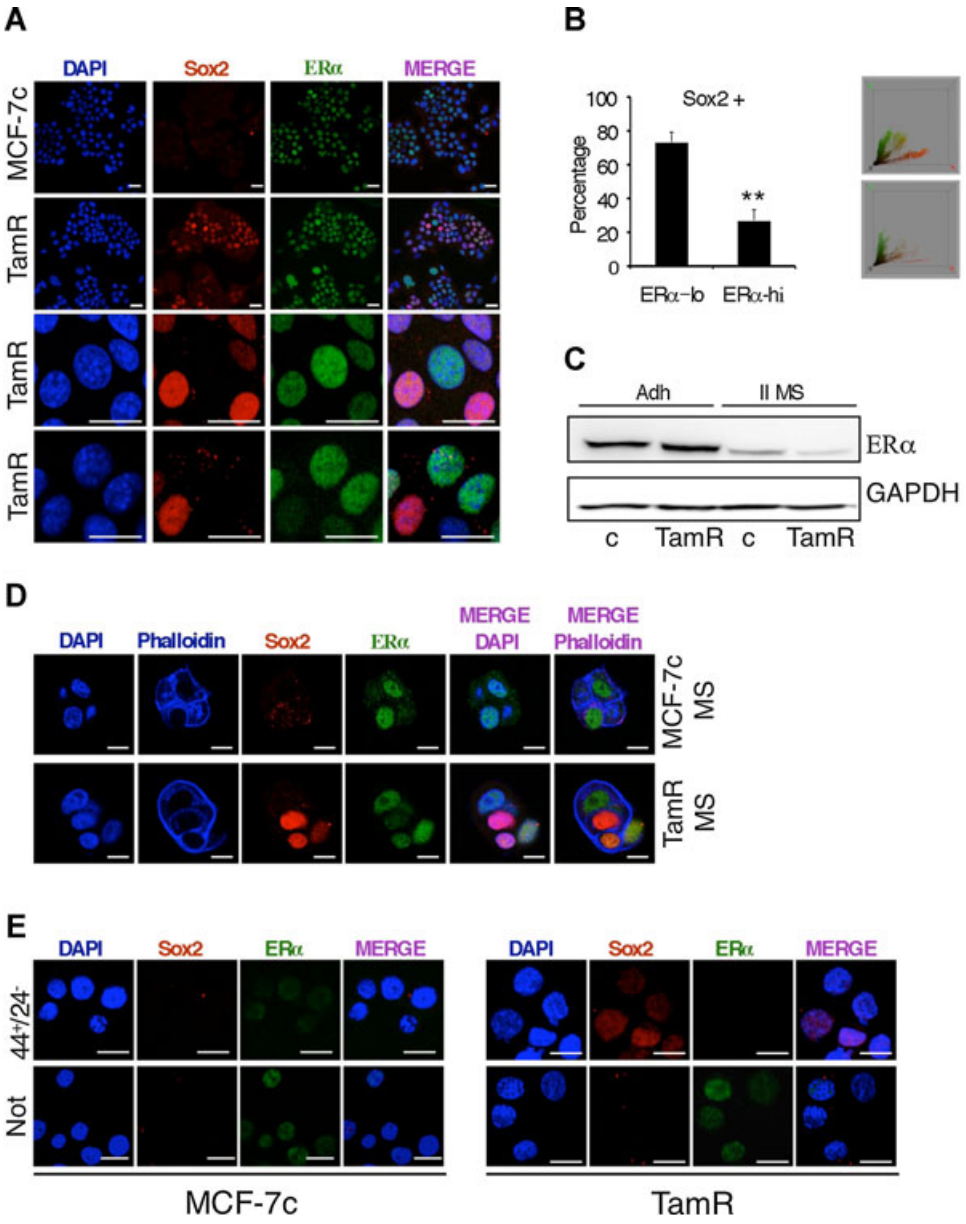

Figure 4. Inverse association between ER and Sox2 expression in MCF-7TamR cells.

A Coexpression of SOX2 and ER was visualized by immunofluorescence in MCF-7c and MCF-7TamR cells grown as adherent cells (scale bar = 40 μm) and,

B as secondary mammospheres at day 4 (Scale bar = 20 μm).

C Left, percentage of adherent MCF-7TamR cells that were Sox2-positive and that expressed low (lo) or high (hi) ER levels (n = 3) $^{**}p$ = 0.0011 by t-test. Right, 2 representative plots obtained with ImageJ 3d colour inspector analysis, in green and in red, ER and Sox2 positivity, respectively.

D Western blot analysis of ER expression levels in MCF-7c and MCF-7TamR cells grown as adherent cells (Adh) or as secondary mammospheres (II MS). GAPDH was used as a loading control.

E Immunofluorescence analysis of Sox2 and ER expression in FACS-sorted $CD44^{+}CD24^{-/low}$ ($44^{+}24^{-}$) stem cells and the rest of the cell population lacking $CD44^{+}CD24^{-/low}$ cells (Not). Scale bar = 30 μm.

expression analysis. Comparison of the expression profiles of Sox2-overexpressing cells with parental MCF-7 cells in adherent and suspension culture conditions highlighted the relevance of the Wnt signalling pathway in Sox2-overexpressing cells (supplementary Fig 6A and B). DKK1 and AXIN2, two known Wnt target genes, were among the most significant differentially expressed genes in Sox2-overexpressing cells. Their increased levels of expression due to Sox2 overexpression were confirmed by qPCR (Fig 7A). Inhibition of Sox2 expression in tamoxifen resistant cells using two different Sox2 shRNAs was sufficient to reduce DKK1 and AXIN2

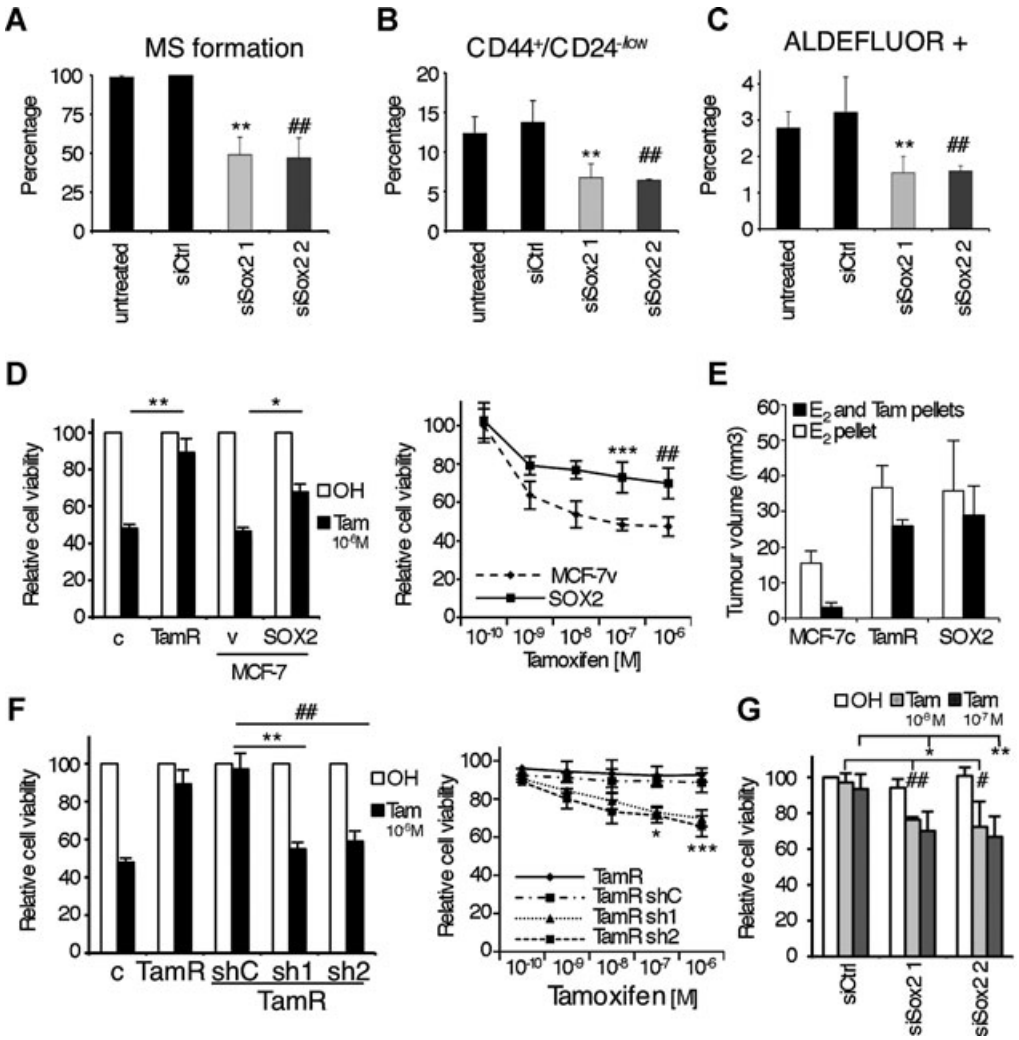

Figure 5. Alteration of Sox2 expression levels affects stem cell properties.

A Mammosphere formation assay of MCF-7TamR cells transfected with siRNA. Values obtained with scramble siRNA are set as 100% (n = 3) $^{**}p$ = 0.01, $^{\#\#}p$ = 0.009 by t-test.

B $CD44^{+}CD24^{-/low}$ stem cell population analysis of primary mammospheres (n = 3) $^{**}p$ = 0.011, $^{\#\#}p$ = 0.01 by t-test and

C ALDEFLUOR assays in adherent cells, were all performed using MCF-7TamR cells transfected with 2 different Sox2 siRNA sequences (siSox2 1 and 2) as well as a control siRNA sequence (siCtrl) (n = 3) $^{**}p$ = 0.002, $^{\#\#}p$ = 0.009 by t-test.

D Viability analysis by crystal violet (left) of MCF-7c (c), MCF-7TamR (TamR) cells and MCF-7 cells stably overexpressing Sox2 (Sox2) and control MCF-7v (v) cells (n = 5) $^{**}p$ = 0.008, $^{*}p$ = 0.02 by t-test and (right) MTT assays of MCF-7SOX2 (SOX2) and control MCF-7v (v) cells growing in presence of increasing concentrations of tamoxifen (from 10^{-1}0 M to 10^{-6} M) (n = 5) $^{***}p$ = 0.008, $^{\#\#}p$ = 0.007 by t-test.

E Tumour size 3 weeks after s.c. implantation of MCF-7c, MCF-7TamR and MCF-7SOX2 cells in athymic female mice in the presence of an exogenous slow oestrogen supplement and with or without a tamoxifen pellet (n = 5 mice/group).

F Viability analysis by (left) crystal violet (n = 5, $^{**}p$ = 0.003, $^{\#\#}p$ = 0.02 by t-test) and (right) MTT assays (n = 5, $^{*}p$ = 0.004, $^{***}p$ = 0.0008 by t-test) of MCF-7c (c), MCF-7TamR (TamR) and MCF-7TamR cells stably transfected with shRNA against Sox2 (sh1 and sh2) and control (shC), growing in the presence of vehicle (ethanol, OH) or tamoxifen.

G Viability analysis by crystal violet and of BT474 cells transfected with a control siRNA sequence (siCtrl) and two different Sox2 siRNA sequences (siSox2 1 and 2) growing in the presence of vehicle (ethanol, OH) or tamoxifen at different concentrations (10^{-8} M, $\#\#p$ = 0.009, $\#p$ = 0.017, 10^{-7} M, $^{*}p$ = 0.044, $^{**}p$ = 0.002 by t-test, as indicated, n = 3).

expression (Fig 7B). Furthermore, Wnt-3a and its receptor FZD4, also identified by microarray analysis, were induced both in tamoxifen resistant cells and in Sox2-overexpressing cells, while expression of WNT4, which inhibits Wnt/β-catenin signalling (Elizalde *et al,* 2011), was reduced (Fig 7C). To determine if activation of the Wnt signalling pathway in these cells was mediated by an autocrine pathway, we used the small-molecule porcupine inhibitor IWP-2, which blocks Wnt secretion (Chen *et al,* 2009). Addition of IWP-2

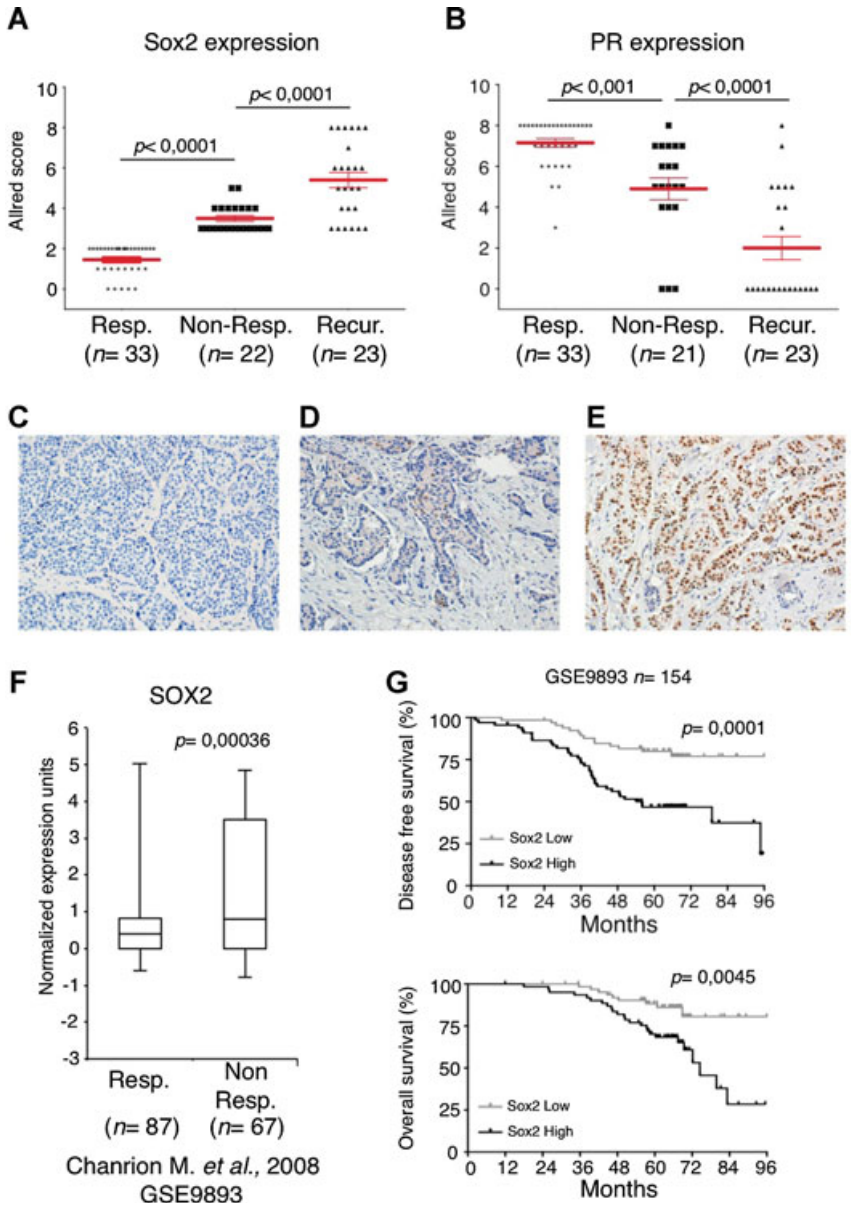

Figure 6. Sox2 expression increases during the development of tamoxifen resistance in breast cancer patients.

A Allred score for Sox2 (A) and PR staining (B). Patients with responder primary tumours (n = 33), namely those that responded to tamoxifen treatment (Resp.); patients with non-responder primary tumours (n = 22) (Non-Resp.) and their recurrent tumours after therapy failure (Recur.). p-values were calculated by Bonferroni multiple comparable test.

C–E Examples of Sox2 staining in (C) a tumour responsive to treatment, (D) a primary tumour not responsive to therapy and (E) a recurrent lesion from the matched primary tumour in (D).

F Correlation between Sox2 expression and recurrence in ER-positive tamoxifen treated breast cancer patients. Box plot from the study indicated (Chanrion et al, 2008) is shown. The y-axis shows normalized expression units. Data are median centered and the 25th–75th percentiles are indicated by the closed box. The numbers of breast carcinoma samples present are shown in parentheses and GEO accession numbers are indicated. Resp and Non Resp. tumours as above.

G The association between Sox2 expression levels and disease free survival (top) and overall survival (bottom) was evaluated by Kaplan–Meier analysis. p-values were calculated by Cox proportional hazards regression analyses. The Sox2 low group was defined by expressing lower Sox2 levels than the median of all patients in the study, and the rest of the patients belonged to the Sox2 high group.

reduced DKK1 and AXIN2 expression in tamoxifen resistant breast cancer cells (Fig 7D). Furthermore, IWP-2 significantly reduced the cancer stem cell population in tamoxifen resistant cells, as confirmed by reduced capacity for mammosphere formation (Fig 7E) and a reduction in the percentage of $CD44^{+}CD24^{-/low}$ cells (Fig 7F). Crucially, IWP-2 restored tamoxifen sensitivity to MCF-7TamR cells (Fig 7G) and this effect of IWP-2 was prevented upon addition of exogenous purified Wnt-3a protein (Fig 7H). These find-

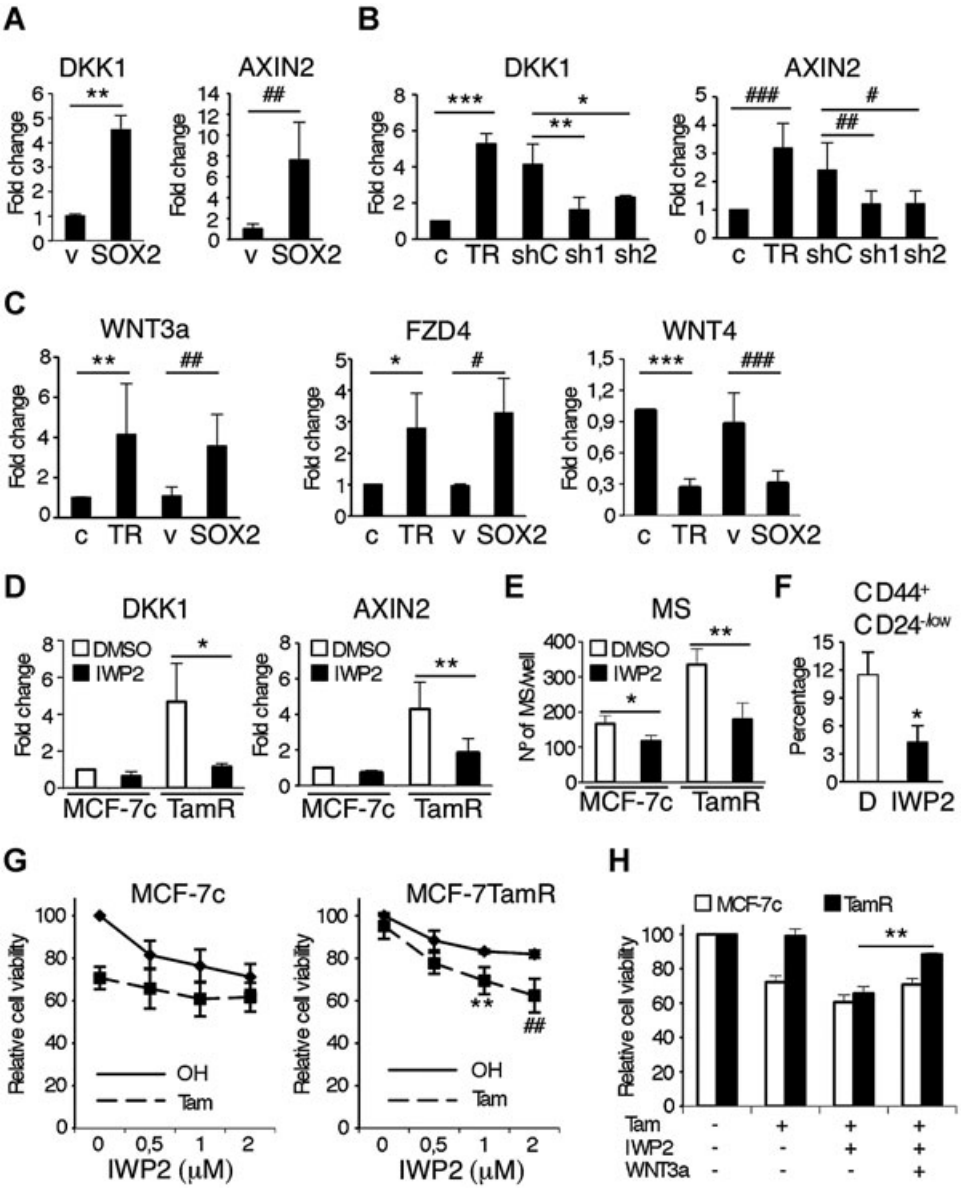

Figure 7. Sox2 overexpression leads to the activation of Wnt signalling.

A DKK1 and AXIN2 mRNA expression levels in MCF-7v (v) and MCF-7SOX2 cells grown in adherent conditions (n = 5) $^{**}p$ = 0.002, $^{\#\#}p$ = 0.002 by t-test.

B DKK1 ($^{***}p$ = 0.0001, $^{**}p$ = 0.009, $^{*}p$ = 0.042 by t-test) and AXIN2 ($^{\#\#\#}p$ = 0.009,$^{\#\#}p$ = 0.043, $^{\#}p$ = 0.029 by t-test) mRNA expression levels in MCF-7c (c) and MCF7TamR (TR) cells and MCF-7TamR cells stably transfected with 2 different Sox2 shRNA sequences (sh1 and sh2) as well as a control shRNA sequence (shC) grown in adherent conditions (n = 5).

C Wnt-3a ($^{**}p$ = 0.008, $^{\#\#}p$ = 0.0056 by t-test), FZD4 ($^{*}p$ = 0.021, $^{\#}p$ = 0.016 by t-test) and WNT4 ($^{***}p$ = 0.0001, $^{\#\#\#}p$ = 0.0015 by t-test) mRNA expression levels in MCF-7c (c), MCF7TamR (TR), MCF-7v (v) and MCF-7SOX2 cells grown in adherent conditions (n = 5).

D DKK1 and AXIN2 mRNA expression levels in MCF-7c (c) and MCF7TamR (TR) cells treated for 48 h with 1 μM of IWP-2 or the vehicle (DMSO) (n = 3) $^{*}p$ = 0.012, $^{**}p$ = 0.017 by t-test.

E Mammosphere formation assay from MCF-7c and MCF-7TamR (TamR) cells growing in presence of 1 μM of IWP-2 or the vehicle (DMSO) (n = 3) $^{*}p$ = 0.036, $^{**}p$ = 0.002 by t-test.

F Flow cytometry analysis of the $CD44^{+}/CD24^{-/low}$ stem cell population in MCF-7TamR cells grown as mammospheres in presence of 1 μM of IWP-2 or the vehicle (D) (n = 3) $^{*}p$ = 0.045 by t-test.

G Cell viability analysis by MTT assay of MCF-7c (left) and MCF-7TamR (right) cells growing in the presence of increasing concentrations of IWP-2 (from 0.5 μM to 2 μM) and in presence or absence of 10^{-7} M tamoxifen (n = 5) $^{**}p$ = 0.002, $^{\#\#}p$ = 0.0011 by t-test.

H Cell viability analysis by MTT assay of MCF-7c and MCF-7TamR cells growing in the presence or absence of 10^{-7} M tamoxifen, 1 μM IWP-2 and 100 ng/ml recombinant Wnt-3a as indicated (n = 3) $^{**}p$ = 0.001.

ings indicate that autocrine Wnt signalling protects breast cancer cells from the anti-proliferative effects of tamoxifen.

Discussion

Development of resistance to tamoxifen remains an important clinical problem. Here we demonstrate that tamoxifen resistant MCF-7 cells express higher levels of Sox2 than parental breast cancer cells. In addition, tamoxifen resistant cells contain a higher proportion of cancer stem/progenitor cells and are more invasive than parental cells. There is an inverse correlation between ER and Sox2 expression in breast cancer cells and an association between the $CD44^{+}CD24^{-/low}$ phenotype of tamoxifen-resistant breast cancer cells and Sox2 expression. Reduction of endogenous Sox2 levels decreases the proportion of the subpopulation of stem/progenitor cells and enhanced Sox2 expression confers tamoxifen resistance to MCF-7 cells *in vitro* and *in vivo*. In addition, Sox2 silencing significantly reversed tamoxifen resistance in both the native (BT474) and another anti-oestrogen resistance model (T47D). Importantly, evidence of the potential clinical relevance was observed in a cohort of ER-positive breast cancer patients who received tamoxifen therapy, where high levels of Sox2 correlated with endocrine treatment failure and poor relapse-free survival. Finally, Sox2 expression leads to Wnt signalling activation and resistance to tamoxifen. Taken together, these findings suggest that Sox2 plays a key role in the development of tamoxifen resistance by maintaining the cells in a more stem cell-like state through increased autocrine Wnt signalling.

Following current anti-cancer treatments a subset of cells, the tumour-initiating cells or cancer stem cells, may reinitiate tumour growth after therapy in many patients. Indeed, radiation-induced enrichment of cancer stem/progenitor cells occurs in MCF-7 breast cancer cells, suggesting that stem/progenitor cells have increased survival mechanisms (Phillips *et al,* 2006; Woodward *et al,* 2007). Further evidence supporting the intrinsic resistance of cancer stem cells to treatment was provided by a study comparing breast cancer core biopsies before and after treatment, which showed that chemotherapy leads to an increase in the proportion of cancer stem cells with the phenotype $CD44^{+}CD24^{-/low}$ and to enhanced mammosphere forming efficiency (Li *et al,* 2008). In addition, high ALDH activity identifies cancer stem cells and is associated with poor prognosis (Ginestier *et al,* 2007). Furthermore, ALDH-positive cells are more invasive than the ALDH-negative cell population and have increased metastatic potential (Charafe-Jauffret *et al,* 2009), in agreement with our findings that MCF-7TamR cells are more invasive and show a higher content of ALDH-positive cells.

Breast stem cells have been reported to lack ER or express it at very low levels (Clayton *et al,* 2004), which may facilitate the resistance of cancer stem cells to the antiproliferative effects of tamoxifen. Consistent with this, we show that the cancer stem cells, which express high levels of Sox2, lack or express very low levels of ER and, therefore, they will be more resistant to tamoxifen. In fact, the impact of reducing Sox2 expression on the proportion of stem cells in MCF-7TamR cells suggests that Sox2 plays a relevant role in conferring a less differentiated phenotype. This observation was corroborated in the clinical samples where increased histological grade significantly correlated with Sox2 expression. Accordingly, it was shown that histologically poorly differentiated breast tumours display preferential overexpression of genes normally enriched in ES cells (Ben-Porath *et al,* 2008) and that they contain a higher proportion of cancer stem cells than well-differentiated cancers (Pece *et al,* 2010), supporting the notion that the cancer stem cell content reflects the malignancy of the tumour (Vivanco, 2010).

The mechanisms that contribute to elevated Sox2 levels in resistant cancers are not fully understood. The previously reported differentiating effect of oestrogen on stem cells (Simoes *et al,* 2011) may be partly due to its capacity to repress Sox2, although this effect is similar in parental MCF-7c and MCF-7TamR cells (supplementary Fig 6C), suggesting that high expression of Sox2 in tamoxifen resistant cells cannot simply be explained by lack of ER activity. We observed that oestrogen reduces Sox2 mRNA expression levels already after 4 h, independently of the presence of actinomycin D (supplementary Fig 6D). ER phosphorylation at Serine 118 was found to be increased in MCF-7TamR cells, consistent with previous studies in other resistance models (Chen *et al,* 2013; Sarwar *et al*, 2006). However, changes in Sox2 expression did not affect Serine 118 phosphorylation (supplementary Fig 6E), indicating that the effects of Sox2 do not involve phosphorylation at this site. Interestingly, Sox2 has been proposed to be a possible driver of the basal-like phenotype in sporadic breast cancer because it is expressed frequently in basal-like breast carcinomas (Rodriguez-Pinilla *et al*, 2007). In addition, the level of Sox2 expression is strongly correlated with tumour grade in breast cancer (Chen *et al*, 2008), and high expression of Sox2 has been proposed to increase metastatic potential (Lengerke *et al*, 2011). Furthermore, a 3q copy number gain (that includes the *SOX2* locus) is a stronger predictor of recurrence than grade and other features in invasive breast carcinoma (Janssen *et al*, 2003). Our results indicate that Sox2 is not just implicated in tumourigenesis but is also involved in the development of resistance to therapy. Ectopic expression of Sox2 in MCF-7 cells is sufficient to render them more resistant to tamoxifen treatment *in vitro* and *in vivo*, in association with increases in the frequency of stem cells and capacity for invasion, suggesting a potential mechanism for the development of resistance to endocrine therapy. In addition, our gene expression analysis highlights the differential expression of several genes involved in the response to drugs (supplementary Fig 6B). Consistent with these findings, Sox2 is also implicated in the cancer stem cell phenotype and development of chemoresistance in glioblastoma (Jeon *et al*, 2011) and prostate cancer (Jia *et al*, 2011). Most importantly, our experimental findings were recapitulated in samples derived from breast cancer patients that had received tamoxifen treatment. Intriguingly, increased Sox2 levels also significantly correlated with lower PR expression than in primary tumours, as observed in the resistance models examined, suggesting that the ER signalling pathway is compromised during development of tamoxifen resistance. The use of a larger cohort of patients is now warranted to explore the predictive power of Sox2 for resistance to endocrine therapy.

Wnt signalling has recently been shown to be implicated in the normal physiology of the mammary gland stem cells (Zeng & Nusse, 2010). Furthermore, altered Wnt/β-catenin pathway has been proposed to be implicated in breast tumour initiating cells (Roarty & Rosen, 2010), and a small molecule inhibitor of Wnt secretion was recently reported to halt tumour growth *in vivo* (Proffitt *et al*,

2013). Gene expression profiling of Sox2 overexpressing cells revealed increased expression of the Wnt target genes DKK1 and Axin2. DKK1 has been found preferentially expressed in hormone resistant breast tumours and tumours with poor prognosis (Forget *et al*, 2007). Axin2 can regulate epithelial-mesenchymal transition by controlling Snail1 activity in breast cancer cells (Yook *et al*, 2006) and its expression has been shown to be upregulated in breast tumours (Ayyanan *et al*, 2006). Furthermore, increased Wnt/β-catenin signalling has been shown to be an early event in a model of breast neoplasia (Khalil *et al*, 2012) and to enhance self-renewal and mediate radiation resistance in mammary gland progenitor cells (Chen *et al*, 2007). Our results suggest that Wnt signalling is activated in tamoxifen resistant cells through an autocrine mechanism, since it is blocked by IWP-2, which inhibits Wnt secretion. Moreover, the block can be rescued by exogenous Wnt-3a, which restored hormone resistance to IWP-2-treated tamoxifen resistant cells. Finally, there is reciprocal regulation of Sox2 and Wnt signalling, since not only does Sox2 regulate Wnt activity, but Wnt signals regulate Sox2, as recently reported by Wang and colleagues, who showed that the Lgr4/Wnt/β-catenin/Lef1 pathway controls Sox2 expression (Wang *et al*, 2013). Consistent with these results and with a positive feedback mechanism, we observed that treatment of MCF-7TamR cells with the Wnt inhibitor IWP-2 reduces Sox2 expression (supplementary Fig 6F). Together these observations highlight the relevance of the Wnt/β-catenin signalling pathway in breast cancer and in resistance to tamoxifen.

In normal breast, the expression levels of stem cell markers are downregulated during the differentiation process to epithelial cells, while their expression appears to be "reawakened" in tumour cells (Simoes *et al*, 2011). Significantly, development of tamoxifen resistance implies loss of ER transcriptional activity and elevated Sox2 expression, leading to Wnt signalling activation and enrichment of the cancer stem cell population (supplementary Fig 7). Targeting the Wnt signalling pathway may favour stem cell differentiation and render tumour cells more sensitive to tamoxifen. The implication of these findings is that a combination of tamoxifen and small molecule inhibitors of Wnt signalling could be developed as a new treatment to prevent recurrence in defined groups of breast cancer patients.

Materials and Methods

Cell culture and establishment of TamR cells

All cells were obtained from American Type Culture Collection (ATTC). MCF-7 cells were cultured in DMEM:F12 medium with GlutaMAX (Gibco) supplemented with 8% foetal bovine serum, FBS, (Sigma) and 1% penicillin/streptomycin (Sigma) at 37°C in 5% CO_2. Cells were grown in the presence of ethanol, as vehicle, and 5×10^{-7} M 4-OH-tamoxifen (Sigma), respectively, in DMEM:F12 with 8% FBS for 6 months. During this time, the medium was replaced every 3 days and the cell cultures were passaged by trypsinization after 70–80% confluency was reached. During the first few weeks cell growth rates were strongly reduced by tamoxifen treatment (no effect was ever detected by the very small dose (<0.01% v/v) of ethanol provided to the MCF-7 control cells. Eventually, cell growth gradually increased, leading to the development of the tamoxifen resistant cell line MCF-7TamR. These cells were maintained in culture with 4-OH-tamoxifen for a further 4 months before characterization. MCF-7c (parental control) and MCF-7TamR have been routinely maintained in the presence of ethanol, as vehicle, and 5×10^{-7} M of 4-OH-tamoxifen, respectively. Their cell growth properties have remained stable since then. BT474 cells were cultured in DMEM:F12 medium with GlutaMAX (Gibco) supplemented with 8% foetal bovine serum, FBS, 5 μg/ml insulin (Sigma) and 1% penicillin/streptomycin (Sigma) at 37°C in 5% CO_2. MCF-7GFP (MCF-7v) and MCF-7SOX2 overexpressing cells (Simoes *et al*, 2011) were generated by infection with lentivirus encoding GFP (pSin-EF2-EGFP-Pur vector) and Sox2 (pSin-EF2-Sox2-Pur vector), respectively. Mammosphere cultures were maintained as in (Dontu *et al*, 2003). More detailed information can be found in supplementary.

Proliferation assay

MCF-7, MCF-7c and MCF-7TamR cells were seeded at 10^5 cells/well in six-well plates in normal medium. Cell numbers were determined by counting with a haemocytometer. The medium was changed after 3 days. MCF-7c and MCF-7TamR cells were seeded in six-well plate at 5×10^4 cells/well in six-well plates and hormone starved in DMEM:F12 containing 8% charcoal-treated FBS for 48 h. Cells were then washed and grown in DMEM:F12 containing 8% charcoal-treated FBS in the presence of 5×10^{-7} M tamoxifen or ethanol.

Mammosphere formation assay

MCF-7c and MCF-7TamR cells were plated in poly-HEMA six-well coated plates at 5000 cells/ml. At day 7, 1 μM of calcein AM (Sigma) was added to each well and incubated for 1 h. After solidification in 0.3% agarose mammospheres bigger than 35 μm diameter were counted using a Metaxpress microscope (Molecular Devices). The mammosphere formation efficiency (shown as percentage) was calculated by dividing the number of mammospheres formed by the original number of single cells seeded.

Invasion assay

In vitro invasion and migration assays were performed as in (Hayashida *et al*, 2010). More detailed information can be found in supplementary.

Transient transfection and luciferase assay

MCF-7, MCF-7c and MCF-7TamR cells were seeded in six-well plate at 2.5×10^5 cells/well and grown in charcoal-treated conditions for 48 h. The cells were transfected with the ERE-TK-luciferase reporter (kindly provided by Prof. M Parker, London) using Lipofectamine 2000 (Invitrogen) following the manufacturer's instructions. Each well also received pRL β-galactosidase to normalize for transfection efficiency (Vivanco *et al*,1995). After transfection, the cells were maintained in phenol red free DMEM:F12 containing 8% charcoal stripped FBS, treated with 10^{-8} M oestrogen or 5×10^{-7} M 4-OH-tamoxifen or ethanol (vehicle) for 48 h. The cell lysates were assayed for luciferase and β-galactosidase activities with the Luciferase Assay Kit (Promega) and the Tropix Galacto-light-plus assay (Applied Biosystems), respectively, using a luminometer (Turner Biosystem). The luciferase results are shown as relative light units of luciferase activity normalized with respect to β-galactosidase activity.

Real-Time Polymerase Chain Reaction (PCR)

RNA was isolated using the TRIzol method (Invitrogen). Real-time PCR was performed on a 7300 Real-Time PCR System (Applied Biosystems). More detailed information can be found in supplementary.

Western blot

Cell lysates were prepared directly with Laemmli sample buffer (Sigma). Primary antibodies included; mouse anti-ERα (6F11, Novocastra), rabbit anti-phospho ER (S118) (2515, Cell Signaling), mouse anti-PR (Novocastra), goat anti-SOX2 (Y17, Santa Cruz), mouse anti-OCT3/4 (H-134, Santa Cruz), goat anti-NANOG (R&D System), mouse anti-GAPDH (Sigma), anti-β-actin and mouse anti-β-tubulin (Sigma). For detection an enhanced chemiluminescence detection kit (Amersham) was used.

Immunofluorescence

Cells were cultured on cover slips, fixed with paraformaldehyde (4% for 10 min at 4°C) and permeabilized for 20 min with PBS supplemented with 0.5% of Triton X-100, followed by blocking for 20 min with TBS supplemented with 0.1% of Triton X-100 (Sigma) and 3% of BSA and incubated for 1 h at room temperature with primary antibody: goat anti-SOX2 and mouse anti-ERα, and with secondary antibodies, anti-mouse Alexa 647 (Molecular Probes), anti-mouse Alexa 488 (Molecular Probes), anti-goat Alexa 568 (Molecular Probes) and phalloidin-FITC (Sigma). Slides were mounted in Vectashield with DAPI (Vector). Immunofluorescence of sorted cells was performed on cytospin preparations (800 g for 5 min) as described above. Mammospheres were collected by centrifugation, fixed in paraformaldehyde 4% overnight at 4°C, permeabilized in PBS supplemented with 1% of Triton X-100 for 1 h at room temperature, blocked and incubated overnight at 4°C with primary antibody (anti-SOX2 and anti-ERα) followed by secondary antibodies (anti-mouse Alexa 647, anti-goat Alexa 568) and phalloidin-FITC. Antibody binding was visualized using a Leica confocal microscope. Digital images were processed using Adobe Photoshop CS2 and analysed with ImageJ image-analysis software (W. Rasband, NIH).

Fluorescence activated cell sorting (FACS)

Human epithelial membrane antigen (EMA) and common acute lymphoblastic leukaemia antigen (CALLA) labelling was performed as previously described (Clayton *et al*, 2004). The mouse PE anti-CD24 antibody (BD, clone ML5) and mouse allophycocyanin (APC) anti-CD44 antibody (BD, clone G44-26) were used to label CD24 and CD44. More detailed information can be found in supplementary.

ALDEFLUOR assay

The ALDEFLUOR assay was carried out according to manufacturer's (Stemcell Technologies) guidelines. More details provided in supplementary.

Small interfering and short hairpin RNA transfection

Small interfering RNA oligonucleotides were transfected using Lipofectamine 2000 (Invitrogen) according to the manufacturer's protocol. siRNA oligos (50 nM) were incubated with the cells for 48 h before analysis. To transfect siRNA in suspension culture, 48 h after the first transfection, cells were transfected again with 50 nM of siRNA and allowed to grow in suspension culture for 96 h. The sequences of each Stealth™ RNAi (Invitrogen) oligonucleotide are as follows:

siSOX2 1, HSS186041 5′ CCUGUGGUUACCUCUUCCUCCCACU 3′
siSOX2 2, HSS186045 5′ GCGUGAACCAGCGCAUGGACAGUUA 3′.

Two pLKO.1 lentivirus shRNAs vector targeted against SOX2 were purchased from Open Biosystem (sh1: TRCN0000085748; sh2: TRCN0000085750). An empty shRNA vector was used as negative control (shC). Lentiviruses were produced as previously described (Simoes *et al*, 2011).

Xenograft analysis

All animal procedures were carried out at the SPF animal facility of CIC bioGUNE (AAALAC-accredited) and conducted in accordance with the*Guide for the Care and Use of Laboratory Animals* (Institute of Laboratory Animal Resources NRC, 1996) and with European policies (European Commission, 1986). Protocols were approved by the CIC bioGUNE Bioethical and Animal Welfare Committee. A total of 1×10^6 cells of MCF7c, MCF7TamR or MCF7SOX2 cells were suspended in 100 μl of PBS/Matrigel (1:1) and injected s.c. into female 3- to 4-week-old BALC/c nu/nu athymic mice (Harlan), which simultaneously received a 60-day slow release pellet containing 0.72 mg of 17β-estradiol with or without 5 mg tamoxifen (Innovative Research of America). Animals were observed once a week.

Cell growth analysis

MTT assays were performed following the manufacturer's instructions. Detailed information for this assay and crystal violet staining can be found in supplementary.

Immunohistochemistry

Immunohistochemical staining on formalin-fixed, paraffin-embedded carcinomas and non-neoplastic breast tissue was performed using the Leica Bond-III stainer. Sox2 staining was scored on the basis of both the percentage of positive cells and the intensity of the staining according to the Allred score (Harvey *et al*, 1999). Detailed information can be found in supplementary.

Gene expression microarray analysis

Gene expression profiles were compared between MCF-7v and MCF-7SOX2 cells cultured in adherent or suspension conditions using the Human HT-12 v1 BeadChips (Affymetrix, Santa Clara, CA). Detailed information can be found in supplementary. Microarray data are available in the ArrayExpress database (www.ebi.ac.uk/arrayexpress) under accession number E-MEXP-3984.

Statistical analysis

Data from at least three independent experiments are expressed as means ± SD. Clinical data were analysed as indicated in the figure legends. Each data point of real-time PCR, MTT, mammosphere formation, luciferase activity assays and proliferation was run at least in triplicates and independent experiments were performed at least three times. Student's *t*-test was used to determine statistically significant differences and $p < 0.05$ was considered to be statistically significant unless otherwise specified.

Supplementary information for this article is available online: http://embomolmed.embopress.org.

The paper explained

Problem
Breast cancer is the most common cancer in women. Hormone therapy is widely used to treat oestrogen receptor (ER)-positive breast tumours, which are the most abundant type. However, development of resistance to treatment continues to be a serious clinical problem. Recent findings suggest that tumours contain a subpopulation of cancer cells that share some properties with stem/progenitor cells. These tumour-initiating or cancer stem cells are relatively resistant to ionizing radiation and chemotherapy. We wished to address the possibility that these cells also play a role in the development of resistance to the ER antagonist tamoxifen, and explore the mechanisms implicated.

Results
In this study, we observe that, compared with control cells, tamoxifen resistant (TamR) cells are more invasive and show increased stem/progenitor cell properties, as measured using mammosphere formation assays, the proportion of $CD44^{+}CD24^{-/low}$cells and aldehyde dehydrogenase (ALDH) activity. Sox2 is highly expressed in TamR cells and in recurrent tumours from patients who have been treated with tamoxifen. *SOX2* gene silencing reduces the cancer stem cell population and increases sensitivity to tamoxifen. In contrast, overexpression of Sox2 is sufficient to render the cells resistant to tamoxifen *in vitro* and *in vivo*. Gene expression profiling highlighted the activation of Wnt signalling in Sox2 overexpressing cells. Since small molecule inhibition of Wnt signalling pathway sensitizes the cells to tamoxifen, an effect that can be rescued by Wnt-3a, we conclude that the development of tamoxifen resistance is driven by Sox2-dependent activation of Wnt signalling in cancer stem/progenitor cells.

Impact
This study indicates the relevance of Sox2 in the development of resistance to tamoxifen. In addition, it suggests Sox2 as a potential prognostic biomarker for tamoxifen resistance. Furthermore, it provides a link between Sox2 expression, cancer stem/progenitor cells and autocrine Wnt signalling in tamoxifen resistant tumours. Consequently, we propose that a combination of hormone therapy and inhibitors of Wnt secretion could provide a novel strategy to treat breast cancer and prevent its recurrence.

Author contributions

MP designed and performed experiments, analysed results and prepared the figures; GD and MR contributed to the characterization of the cell lines with modulated Sox2 levels; OI and MR performed the FACS sorting and analyses; BS analysed factors expression in some breast cancer cell lines; VC contributed to the characterization of the resistant cell lines; IB, JALR and IZ managed the collection of human samples; RK conceived and coordinated the Wnt experiments and contributed to the preparation of the manuscript; MV conceived the project, analysed the data and wrote the paper.

Acknowledgements

We thank the members of the laboratory for helpful discussions, Nora Bengoa for support with qPCR, Jessica Cellot for excellent technical assistance, Juan Rodríguez (Animal Facilities Unit, CIC bioGUNE) for help with the animal experiments, Ana Aransay and the Genome Analysis Platform for help with the microarray analysis. This work was funded by grants from the Spanish Ministry of Science and Innovation (SAF2011-30494 to RK), the Institute of Health Carlos III (PI11/02251 to MV), the Departments of Education (PI2009-7 to MV) and Health (2010-111060 to MV) of the Government of the Autonomous Community of the Basque Country, the Department of Industry, Tourism and Trade (Etortek) and Department of Innovation Technology of the Government of the Autonomous Community of the Basque Country (to MV and RK), and the SES-PM (Spanish Society of Breast Pathology) and Foundation La Caixa (to MV)

Conflict of interest

The authors declare that they have no conflict of interest.

References

Al-Hajj M, Wicha MS, Benito-Hernandez A, Morrison SJ, Clarke MF (2003) Prospective identification of tumorigenic breast cancer cells. *Proc Natl Acad Sci USA* 100: 3983 – 3988

Ali S, Coombes RC (2002) Endocrine-responsive breast cancer and strategies for combating resistance. *Nat Rev Cancer* 2: 101 – 112

Ayyanan A, Civenni G, Ciarloni L, Morel C, Mueller N, Lefort K, Mandinova A, Raffoul W, Fiche M, Dotto GP, *et al* (2006) Increased Wnt signaling triggers oncogenic conversion of human breast epithelial cells by a Notch-dependent mechanism. *Proc Natl Acad Sci USA* 103: 3799 – 3804

Ben-Porath I, Thomson MW, Carey VJ, Ge R, Bell GW, Regev A, Weinberg RA (2008) An embryonic stem cell-like gene expression signature in poorly differentiated aggressive human tumors. *Nat Genet* 40: 499 – 507

Chanrion M, Negre V, Fontaine H, Salvetat N, Bibeau F, Mac Grogan G, Mauriac L, Katsaros D, Molina F, Theillet C, *et al* (2008) A gene expression signature that can predict the recurrence of tamoxifen-treated primary breast cancer. *Clin Cancer Res* 14: 1744 – 1752

Charafe-Jauffret E, Ginestier C, Iovino F, Wicinski J, Cervera N, Finetti P, Hur MH, Diebel ME, Monville F, Dutcher J, *et al* (2009) Breast cancer cell lines contain functional cancer stem cells with metastatic capacity and a distinct molecular signature. *Cancer Res* 69: 1302 – 1313

Chen MS, Woodward WA, Behbod F, Peddibhotla S, Alfaro MP, Buchholz TA, Rosen JM (2007) Wnt/beta-catenin mediates radiation resistance of Sca1+ progenitors in an immortalized mammary gland cell line. *J Cell Sci* 120: 468 – 477

Chen Y, Shi L, Zhang L, Li R, Liang J, Yu W, Sun L, Yang X, Wang Y, Zhang Y, *et al* (2008) The molecular mechanism governing the oncogenic potential of SOX2 in breast cancer. *J Biol Chem* 283: 17969 – 17978

Chen B, Dodge ME, Tang W, Lu J, Ma Z, Fan CW, Wei S, Hao W, Kilgore J, Williams NS, *et al* (2009) Small molecule-mediated disruption of Wnt-dependent signaling in tissue regeneration and cancer. *Nat Chem Biol* 5: 100 – 107

Chen M, Cui YK, Huang WH, Man K, Zhang GJ (2013) Phosphorylation of estrogen receptor alpha at serine 118 is correlated with breast cancer resistance to tamoxifen. *Oncol Lett* 6: 118 – 124

Clayton H, Titley I, Vivanco M (2004) Growth and differentiation of progenitor/stem cells derived from the human mammary gland. *Exp Cell Res* 297: 444 – 460

Diehn M, Cho RW, Clarke MF (2009) Therapeutic implications of the cancer stem cell hypothesis. *Semin Radiat Oncol* 19: 78 – 86

Dontu G, Abdallah WM, Foley JM, Jackson KW, Clarke MF, Kawamura MJ, Wicha MS (2003) In vitro propagation and transcriptional profiling of human mammary stem/progenitor cells. *Genes Dev* 17: 1253 – 1270

Elizalde C, Campa VM, Caro M, Schlangen K, Aransay AM, Vivanco M, Kypta RM (2011) Distinct roles for Wnt-4 and Wnt-11 during retinoic acid-induced neuronal differentiation. *Stem Cells* 29: 141 – 153

Forget MA, Turcotte S, Beauseigle D, Godin-Ethier J, Pelletier S, Martin J, Tanguay S, Lapointe R (2007) The Wnt pathway regulator DKK1 is

preferentially expressed in hormone-resistant breast tumours and in some common cancer types. *Br J Cancer* 96: 646 – 653

Ginestier C, Hur MH, Charafe-Jauffret E, Monville F, Dutcher J, Brown M, Jacquemier J, Viens P, Kleer CG, Liu S, *et al* (2007) ALDH1 is a marker of normal and malignant human mammary stem cells and a predictor of poor clinical outcome. *Cell Stem Cell* 1: 555 – 567

Harvey JM, Clark GM, Osborne CK, Allred DC (1999) Estrogen receptor status by immunohistochemistry is superior to the ligand-binding assay for predicting response to adjuvant endocrine therapy in breast cancer. *J Clin Oncol* 17: 1474 – 1481

Hayashida T, Takahashi F, Chiba N, Brachtel E, Takahashi M, Godin-Heymann N, Gross KW, Vivanco MM, Wijendran V, Shioda T, *et al* (2010) HOXB9, a gene overexpressed in breast cancer, promotes tumorigenicity and lung metastasis. *Proc Natl Acad Sci USA* 107: 1100 – 1105

Janssen EA, Baak JP, Guervos MA, van Diest PJ, Jiwa M, Hermsen MA (2003) In lymph node-negative invasive breast carcinomas, specific chromosomal aberrations are strongly associated with high mitotic activity and predict outcome more accurately than grade, tumour diameter, and oestrogen receptor. *J Pathol* 201: 555 – 561

Jeon HM, Sohn YW, Oh SY, Kim SH, Beck S, Kim S, Kim H (2011) ID4 imparts chemoresistance and cancer stemness to glioma cells by derepressing miR-9*-mediated suppression of SOX2. *Cancer Res* 71: 3410 – 3421

Jia X, Li X, Xu Y, Zhang S, Mou W, Liu Y, Liu Y, Lv D, Liu CH, Tan X, *et al* (2011) SOX2 promotes tumorigenesis and increases the anti-apoptotic property of human prostate cancer cell. *J Mol Cell Biol* 3: 230 – 238

Jordan VC, O'Malley BW (2007) Selective estrogen-receptor modulators and antihormonal resistance in breast cancer. *J Clin Oncol* 25: 5815 – 5824

Khalil S, Tan GA, Giri DD, Zhou XK, Howe LR (2012) Activation status of Wnt/ss-catenin signaling in normal and neoplastic breast tissues: relationship to HER2/neu expression in human and mouse. *PLoS ONE* 7: e33421

Lengerke C, Fehm T, Kurth R, Neubauer H, Scheble V, Muller F, Schneider F, Petersen K, Wallwiener D, Kanz L, *et al* (2011) Expression of the embryonic stem cell marker SOX2 in early-stage breast carcinoma. *BMC Cancer* 11: 42

Li X, Lewis MT, Huang J, Gutierrez C, Osborne CK, Wu MF, Hilsenbeck SG, Pavlick A, Zhang X, Chamness GC, *et al* (2008) Intrinsic resistance of tumorigenic breast cancer cells to chemotherapy. *J Natl Cancer Inst* 100: 672 – 679

Liu S, Ginestier C, Charafe-Jauffret E, Foco H, Kleer CG, Merajver SD, Dontu G, Wicha MS (2008) BRCA1 regulates human mammary stem/progenitor cell fate. *Proc Natl Acad Sci USA* 105: 1680 – 1685

Osborne CK, Shou J, Massarweh S, Schiff R (2005) Crosstalk between estrogen receptor and growth factor receptor pathways as a cause for endocrine therapy resistance in breast cancer. *Clin Cancer Res* 11: 865s – 870s

Pece S, Tosoni D, Confalonieri S, Mazzarol G, Vecchi M, Ronzoni S, Bernard L, Viale G, Pelicci PG, Di Fiore PP (2010) Biological and molecular heterogeneity of breast cancers correlates with their cancer stem cell content. *Cell* 140: 62 – 73

Phillips TM, McBride WH, Pajonk F (2006) The response of $CD24^{(-/low)}$/$CD44^{+}$ breast cancer-initiating cells to radiation. *J Natl Cancer Inst* 98: 1777 – 1785

Proffitt KD, Madan B, Ke Z, Pendharkar V, Ding L, Lee MA, Hannoush RN, Virshup DM (2013) Pharmacological inhibition of the Wnt acyltransferase PORCN prevents growth of WNT-driven mammary cancer. *Cancer Res* 73: 502 – 507

Reya T, Morrison SJ, Clarke MF, Weissman IL (2001) Stem cells, cancer, and cancer stem cells. *Nature* 414: 105 – 111

Roarty K, Rosen JM (2010) Wnt and mammary stem cells: hormones cannot fly wingless. *Curr Opin Pharmacol* 10: 643 – 649

Rodriguez-Pinilla SM, Sarrio D, Moreno-Bueno G, Rodriguez-Gil Y, Martinez MA, Hernandez L, Hardisson D, Reis-Filho JS, Palacios J (2007) Sox2: a possible driver of the basal-like phenotype in sporadic breast cancer. *Mod Pathol* 20: 474 – 481

Sarwar N, Kim JS, Jiang J, Peston D, Sinnett HD, Madden P, Gee JM, Nicholson RI, Lykkesfeldt AE, Shousha S, *et al* (2006) Phosphorylation of ERalpha at serine 118 in primary breast cancer and in tamoxifen-resistant tumours is indicative of a complex role for ERalpha phosphorylation in breast cancer progression. *Endocr Relat Cancer* 13: 851 – 861

Sheridan C, Kishimoto H, Fuchs RK, Mehrotra S, Bhat-Nakshatri P, Turner CH, Goulet R Jr, Badve S, Nakshatri H (2006) $CD44^{+}$/$CD24^{-}$ breast cancer cells exhibit enhanced invasive properties: an early step necessary for metastasis. *Breast Cancer Res* 8: R59

Simoes BM, Piva M, Iriondo O, Comaills V, Lopez-Ruiz JA, Zabalza I, Mieza JA, Acinas O, Vivanco MD (2011) Effects of estrogen on the proportion of stem cells in the breast. *Breast Cancer Res Treat* 129: 23 – 35

Vivanco M (2010) Function follows form: defining mammary stem cells. *Sci Transl Med* 2: 31ps22

Vivanco MD, Johnson R, Galante PE, Hanahan D, Yamamoto KR (1995) A transition in transcriptional activation by the glucocorticoid and retinoic acid receptors at the tumor stage of dermal fibrosarcoma development. *EMBO J* 14: 2217 – 2228

Wang Y, Dong J, Li D, Lai L, Siwko S, Li Y, Liu M (2013) Lgr4 regulates mammary gland development and stem cell activity through the pluripotency transcription factor Sox2. *Stem Cells* 31: 1921 – 1931

Woodward WA, Chen MS, Behbod F, Alfaro MP, Buchholz TA, Rosen JM (2007) WNT/beta-catenin mediates radiation resistance of mouse mammary progenitor cells. *Proc Natl Acad Sci USA* 104: 618 – 623

Yook JI, Li XY, Ota I, Hu C, Kim HS, Kim NH, Cha SY, Ryu JK, Choi YJ, Kim J, *et al* (2006) A Wnt-Axin2-GSK3beta cascade regulates Snail1 activity in breast cancer cells. *Nat Cell Biol* 8: 1398 – 1406

Zeng YA, Nusse R (2010) Wnt proteins are self-renewal factors for mammary stem cells and promote their long-term expansion in culture. *Cell Stem Cell* 6: 568 – 577

Distinct breast cancer stem/progenitor cell populations require either HIF1α or loss of PHD3 to expand under hypoxic conditions

Oihana Iriondo[1], Miriam Rábano[1], Giacomo Domenici[1], Onintza Carlevaris[1], José Antonio López-Ruiz[2], Ignacio Zabalza[3], Edurne Berra[1] and Maria dM Vivanco[1]

[1] Cell Biology and Stem Cells Unit, CIC bioGUNE, Derio, Spain

[2] Servicio de Radiodiagnóstico Preteimagen, Bilbao, Spain

[3] Department of Pathology, Galdakao-Usansolo Hospital, Galdakao, Spain

Correspondence to: *Maria dM Vivanco*, ***email***: *mdmvivanco@cicbiogune.es*

Keywords: breast cancer, estrogen receptor, hypoxia, PHD3, stem cells

Received: *March 16, 2015* ***Accepted***: *August 10, 2015* ***Published***: *September 10, 2015*

ABSTRACT

The heterogeneous nature of breast cancer is a result of intrinsic tumor complexity and also of the tumor microenvironment, which is known to be hypoxic. We found that hypoxia expands different breast stem/progenitor cell populations (cells with increased aldehyde dehydrogenase activity (Aldefluor$^+$), high mammosphere formation capacity and CD44$^+$CD24$^{-/low}$ cells) both in primary normal epithelial and tumor cells. The presence of the estrogen receptor (ER) limits hypoxia-dependent CD44$^+$CD24$^{-/low}$ cell expansion. We further show that the hypoxia-driven cancer stem-like cell enrichment results from a dedifferentiation process. The enhanced mammosphere formation and Aldefluor$^+$ cell content observed in breast cancer cells relies on hypoxia-inducible factor 1α (HIF1α). In contrast, the CD44$^+$CD24$^{-/low}$ population expansion is HIF1α independent and requires prolyl hydroxylase 3 (PHD3) downregulation, which mimics hypoxic conditions, leading to reduced CD24 expression through activation of NFkB signaling. These studies show that hypoxic conditions expand CSC populations through distinct molecular mechanisms. Thus, potential therapies that combine current treatments for breast cancer with drugs that target CSC should take into account the heterogeneity of the CSC subpopulations.

INTRODUCTION

Breast cancer, the most frequent malignancy in the female population in incidence and mortality [1], is a very heterogeneous disease in terms of histology, genetic profile, therapeutic response and patient outcome. Global gene expression studies of breast tumors led to the description of five different breast cancer subtypes -luminal A, luminal B, HER2-positive, basal and normal-like- with distinct clinical outcomes [2-4] and a novel molecular stratification was derived from the association of somatic copy number aberrations with the transcriptome [5, 6], highlighting the molecular heterogeneity of the disease. Approximately 70% of breast tumors express the estrogen receptor (ER) and, in general, ER expression is associated with better prognosis [7].

The tissue expansion and remodeling that occurs in the mammary gland during successive cycles of pregnancy, lactation and involution has been linked to the presence of stem cells and early progenitor cells in the adult mammary epithelium [8]. Similarly, breast tumors are also composed of morphologically and phenotypically heterogeneous cell populations, characterized by varying self-renewal capacities, degrees of differentiation and tumorigenic potentials. In the apex of the hierarchy lie the cancer stem cells (CSCs), also known as tumor initiating cells. In addition to directing tumor onset and metastatic expansion, CSCs have been shown to be resistant to chemo- and radiotherapy and more recently also to endocrine therapy [9], and could therefore be responsible for tumor recurrence. Several methods have been used to identify and isolate human breast epithelial stem cells and cancer stem cells. In the normal breast, cells coexpressing the luminal marker EMA and the myoepithelial marker CALLA [10], CD49f^{high}ESA$^{-/low}$ cells [11, 12], and cells with high ALDH activity [13], have been shown to

be enriched in bipotent progenitors. Furthermore, the phenotype $CD44^{+}CD24^{-/low}ESA^{+}$ and high ALDH activity identify cells with increased tumor initiation capacity [13, 14]. Importantly, $CD44^{+}CD24^{-/low}ESA^{+}$ cells, $ALDH^{+}$ cells and mammosphere-forming cells isolated from breast cancer cell lines are also enriched for self-renewal capacity and tumorigenic potential in xenograft tumor assays [15, 16].

In solid tumors, the combination of rapid cell division and aberrant tumor angiogenesis often leads to the generation of hypoxic sites [17]. Tumor hypoxia has been associated with increased malignancy, poor prognosis and resistance to radiotherapy and chemotherapy [18]. Hypoxia-inducible factors (HIFs) are the main transcriptional regulators of the adaptive responses that are activated when oxygen supply does not reach the metabolic, energetic and redox demands of cells [19]. In well-oxygenated environments, the HIFα subunit (HIF1α or HIF2α) becomes hydroxylated by members of the prolyl hydroxylase domain-containing proteins (PHD) family (PHD1, PHD2 and PHD3, also known as EGLNs), which use oxygen as co-substrate [20], and is targeted for degradation by the proteasome [21, 22]. Under low oxygen availability, PHDs are inactive, HIFα is stabilized, dimerises with HIFβ and regulates the transcription of target genes [23]. Although the role of PHDs in cancer has been less studied, altered levels of PHD1, PHD2 and PHD3 have been correlated with the development of different types of carcinomas [24-26]. Distinct members of the hypoxia-signaling pathway are involved in the regulation of both normal and cancer stem cells. In breast cancer cells, antiangiogenic factors increase the population of CSCs by generating intratumoral hypoxia mediated by HIF1α [27]. Furthermore, HIF factors have also recently been implicated in the enhancement of breast CSCs by chemotherapy [28].

Considering the links of hypoxia with cancer and stem cells, we wished to investigate the molecular mechanisms that underlie the impact of hypoxic conditions on the cancer stem cell compartment. Here, we show that hypoxia increases the proportion of breast CSCs through a dedifferentiation process and limits the differentiation of CSCs. Depending on the stem/progenitor cell subpopulation, this process requires either HIF1α expression or the inactivation of the hydroxylase activity of PHD3. These findings suggest that different therapeutic strategies should be adopted to eliminate hypoxia-induced breast cancer stem cells depending on tumor characteristics.

RESULTS

Hypoxia increases the proportion of primary breast stem cells and tumor initiating cells

Firstly, to investigate whether hypoxia had any effect in the pool of normal stem/progenitor cells of the human mammary gland, different stem cell subpopulations were examined. Cells are routinely cultured in atmospheric oxygen (21% O_2), although this is not physiological. Normal pO_2 in the breast is 8.6% [29], nevertheless, comparable CSC activity has been reported between 21% and 8% oxygen [30]. Hypoxic conditions are usually represented as 1% O_2, despite the fact that the average pO_2 in breast cancer is 3.9%, although in approximately 30-40% of the cases tumors exhibit pO_2 values between 0 and 1% [29]. Thus, breast epithelial cells isolated from reduction mammoplasties (Supplementary Table 1) were cultured in suspension in atmospheric oxygen, which will be referred to as normoxic (21% O_2) or under hypoxic conditions (1% O_2). After 7 days, cells grown in hypoxia formed more mammospheres, which are enriched for stem/progenitor cells, than cells cultured in atmospheric oxygen concentration (Figure 1A). Furthermore, cells cultured under hypoxia were enriched in $CD49f^{high}ESA^{-/low}$ cells (Figure 1B; Supplementary Figure 1A, 1B), independently of whether cells were cultured in adherent or suspension conditions. Similarly, $EMA^{+}CALLA^{+}$ (Figure 1C; Supplementary Figure 1C) and $CD44^{+}CD24^{-/low}$ (Figure 1D; Supplementary Figure 1D) stem cell subpopulations were also enhanced under hypoxia. Moreover, hypoxic conditions increased the ability of primary breast epithelial cells to form colonies in Matrigel at low density (Figure 1E), suggesting that decreased oxygen availability leads to the expansion of the pool of stem/progenitor cells in the normal mammary gland.

To evaluate whether hypoxia also influences the proportion of CSCs, tumor cells isolated from breast cancer patients were grown in suspension in normoxic or hypoxic culture conditions. The effect of hypoxia on breast CSCs was tumor-dependent. The proportion of $CD44^{+}CD24^{-/low}$ cells was not significantly affected by hypoxia in those samples that presented high levels of ER and PR expression (Figure 1F, PR^{high}). In contrast, in tumor samples lacking ER expression or with low ER transcriptional activity (as reflected by low PR expression, PR^{low}), hypoxia promoted the expansion of $CD44^{+}CD24^{-/low}$ cells (Figure 1F; Supplementary Figure 1E; Supplementary Table 2). The differences observed in the response to hypoxia likely reflect the high molecular heterogeneity present in breast tumors. Overall these findings suggest that low oxygen availability increases the normal and cancer stem cell content in the breast.

Hypoxia increases the proportion of cancer stem cells in breast cancer cell lines

In order to investigate how hypoxic conditions influence breast CSCs and the mechanisms implicated, we examined the effects of hypoxia in several breast cancer cell lines. Firstly, using MDA-MB-468 cells, we observed a significant increase in $CD44^{+}CD24^{-/low}ESA^{+}$ cells, which reached a plateau by 48-72 hours treatment (Supplementary Figure 2A) and, therefore, we evaluated the effect of 3-day long hypoxia treatment on the CSC populations in a panel of ER-positive and ER-negative

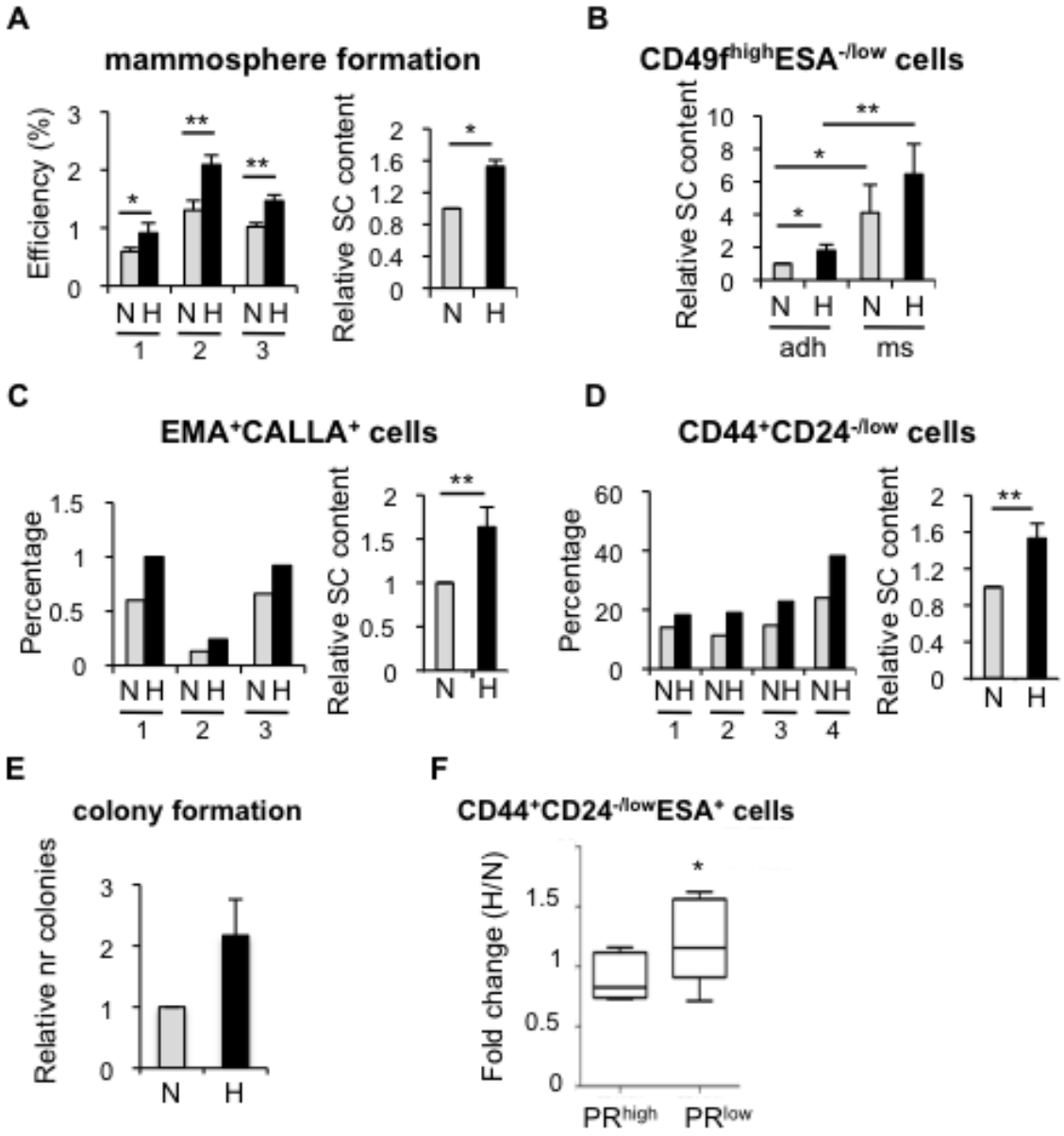

Figure 1: Effect of hypoxia in cells isolated from normal or tumor primary tissue. A. Normal primary epithelial cells cultured in suspension in normoxia or hypoxia for 7 days. Mammosphere formation efficiency of cells from four different breast specimens (left graph) and mean ±SD of three experiments (right graph) are represented as the percentage of mammospheres formed with respect to the number of plated cells, and as fold change between normoxia and hypoxia, respectively. **B.** Percentage of $CD49f^{high}ESA^{-/low}$cells in normal breast epithelial cells cultured in normoxia or hypoxia, in adherent (adh) or suspension (ms) conditions. **C.**, **D.** Percentage of $EMA^{+}CALLA^{+}$ and $CD44^{+}CD24^{-/low}$ cells in normal breast epithelial cells cultured in normoxia or hypoxia. **E.** Relative number of colonies formed in Matrigel by primary normal epithelial cells cultured in normoxic or hypoxic conditions. **F.** Percentage of $CD44^{+}CD24^{-/low}ESA^{+}$ cells found in primary tumor cells cultured as mammospheres in normoxic or hypoxic conditions and represented as fold change between hypoxia and normoxia. The graph shows the mean ±SD of the fold changes grouped based on high or low ER transcriptional activity (PR^{high} or PR^{low}, respectively, low was defined as less than 11% expression) $*P < 0.05$ ($P = 0.031$).

breast cancer cell lines. FACS analysis showed that ER-negative MDA-MB-468, MDA-MB-231 and SKBR3 cells cultured in hypoxic conditions contained a higher proportion of $CD44^+CD24^{-/low}ESA^+$ cells than their normoxic counterparts. In contrast, the $CD44^+CD24^{-/low}ESA^+$ content of ER-positive MCF-7, T47D and ZR75-1 cells was not significantly affected by hypoxia (Figure 2A; Supplementary Figure 2B). The observed expansion of $CD44^+CD24^{-/low}ESA^+$ cells by hypoxia encouraged us to examine whether oxygen levels affected the proportion of different subpopulations of CSCs in breast cancer cells. Hypoxic conditions increased the mammosphere forming capacity of both ER-positive (MCF-7) and ER-negative (MDA-MB-468) cells (Figure 2B; Supplementary Figure 2C). Furthermore, a cell population with ALDH activity, as measured by ALDEFLUOR assay, $ALDH^+$, was also increased in response to hypoxia in both ER-positive and ER-negative cells (Figure 2C; Supplementary Figure 2D). These findings indicate that hypoxic conditions lead to expansion of different types of CSC subpopulations and that the levels of ER expression in breast cancer cells may influence their response.

Hypoxia reduces ER expression and transcriptional activity

The above findings suggest that the presence of ER hampers the expansion of $CD44^+CD24^{-/low}$ cells by hypoxia. To explore this possibility further, ER-positive T47D cells were treated with the ER antagonist fulvestrant

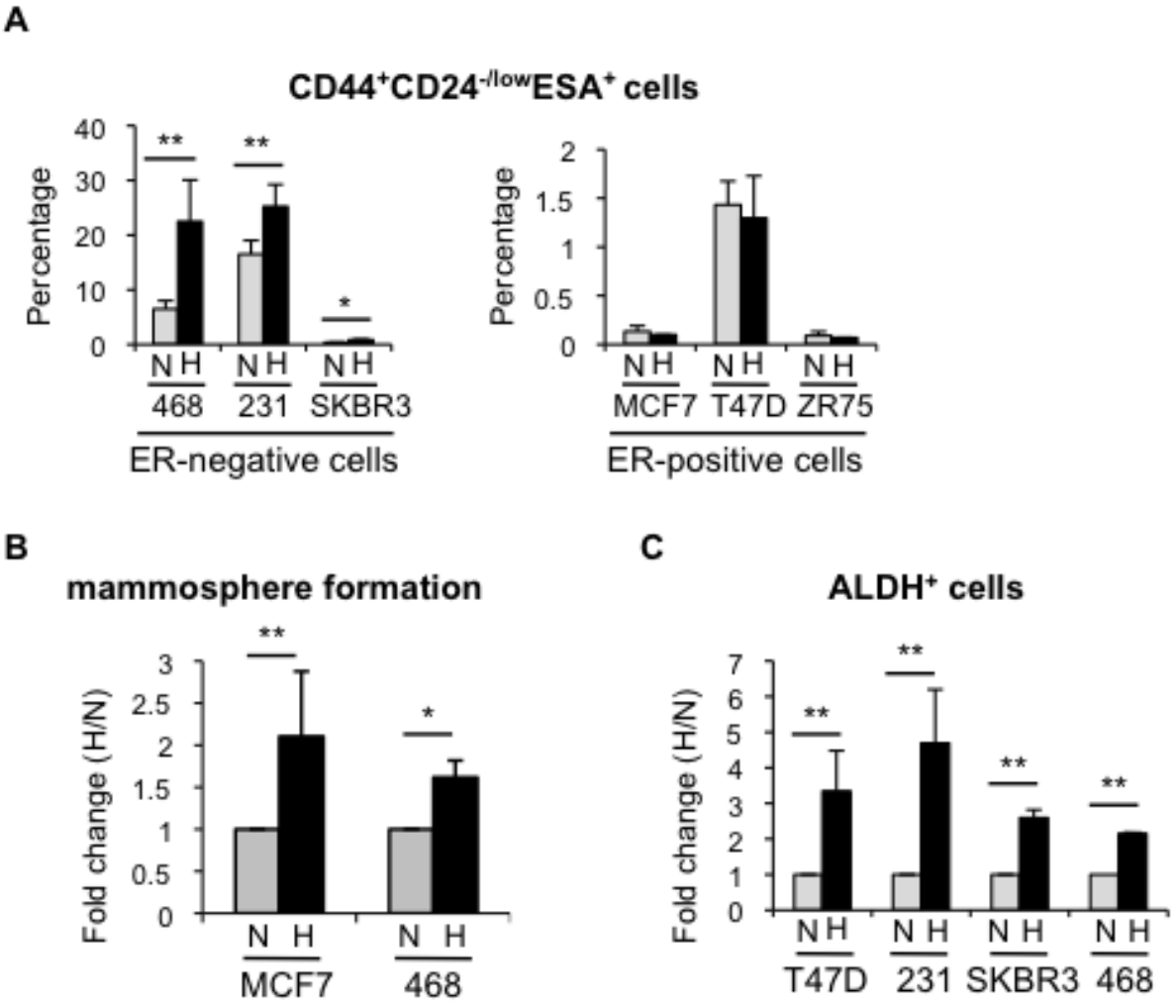

Figure 2: Hypoxia increases the percentage of CSCs in different breast cancer cell lines. A. Percentage of $CD44^+CD24^{-/low}ESA^+$ cells in ER-negative and ER-positive cell lines cultured in normoxia or hypoxia for 3 days. **B.** Number of mammospheres formed by MCF-7 or MDA-MB-468 cells cultured in normoxia or hypoxia and represented as fold change (hypoxia/normoxia). **C.** Percentage of $ALDH^+$ cells in different cell lines cultured in normoxia or hypoxia. In A, B and C, means ±SD of at least three independent experiments are represented. $*P < 0.05$ $**P < 0.01$.

(ICI 182,780), leading to strong ER degradation (Supplementary Figure 3A). Indeed, now in the absence of ER, hypoxia induced a significant increase in the percentage of $CD44^{+}CD24^{-/low}$ cells in T47D cells (Figure 3A), suggesting that loss of ER is required for hypoxia to expand the $CD44^{+}CD24^{-/low}$ cell population.

We have previously shown that normal and CSCs from the mammary gland are characterized by the absence or low expression levels of ER [8]. The finding that ER limits the amplification of $CD44^{+}CD24^{-/low}$ CSC subpopulation under low oxygen conditions prompted us to explore this relationship in more detail. To this end, several ER-positive breast cancer cell lines were cultured in the absence or presence of estrogen, in normoxic or hypoxic conditions. Western blot analysis showed that hypoxia treatment reduced ER expression levels in all cell lines tested, MCF7 (Figure 3B), T47D (Supplementary Figure 3A) and ZR75-1 (data not shown). Furthermore, the decrease in ER levels induced by hypoxia was also detected at the RNA level (Figure 3C; Supplementary Figure 3D, 3E). More importantly, the evaluation of the expression levels of several ER target genes (progesterone receptor, retinoic acid receptor alpha, amphiregulin and *pS2*) (Figure 3B, 3D; Supplementary Figure 3B-3E) and ER activity by transcriptional assays (Figure 3E) clearly showed that hypoxia-dependent decrease in ER expression correlates with reduced estrogen-dependent ER signaling. These findings indicate that hypoxia reduces ER expression and activity in breast cancer cells, thereby enriching for CSCs.

Hypoxia prevents differentiation of CSCs and promotes dedifferentiation of breast cancer cells

Next, we wished to decipher the process by which hypoxia increases the proportion of CSCs. First, we evaluated whether differences in proliferation or apoptosis

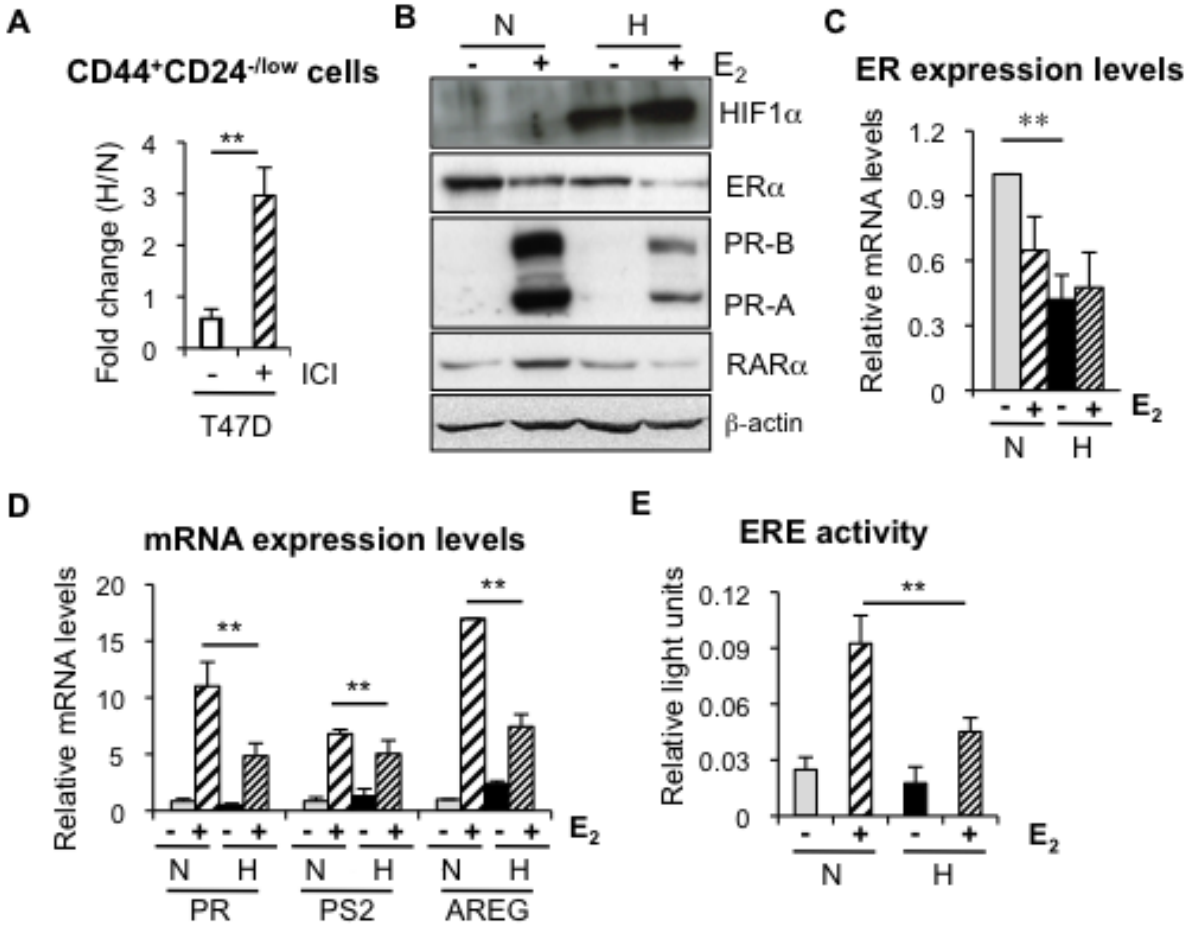

Figure 3: Hypoxia reduces ER expression and transcriptional activity. A. Percentage of $CD44^{+}CD24^{-/low}$ cells in T47D cells treated or not with 0,5 µM fulvestrant (ICI 182,870) and cultured in normoxia or hypoxia. **B.** Representative western blot showing expression of ER and its targets PR and RARα in MCF-7 cells cultured under normoxic or hypoxic conditions, with or without 10 nM estrogen (E_2). **C.** RNA expression levels of ER in MCF-7 cells treated or not with estrogen, in normoxia or hypoxia. **D.** RNA expression levels of PR, PS2 and AREG in MCF-7 cells treated or not with estrogen, in normoxia or hypoxia. In A, C and D, Data are presented as mean ±SD of 3 independent experiments. **E.** ER transcriptional activity in MCF-7 cells grown in normoxia or hypoxia in the presence of ethanol (-) or estrogen. The graph shows the mean ±SEM of 5 experiments done in triplicates. $^{**}P < 0.01$.

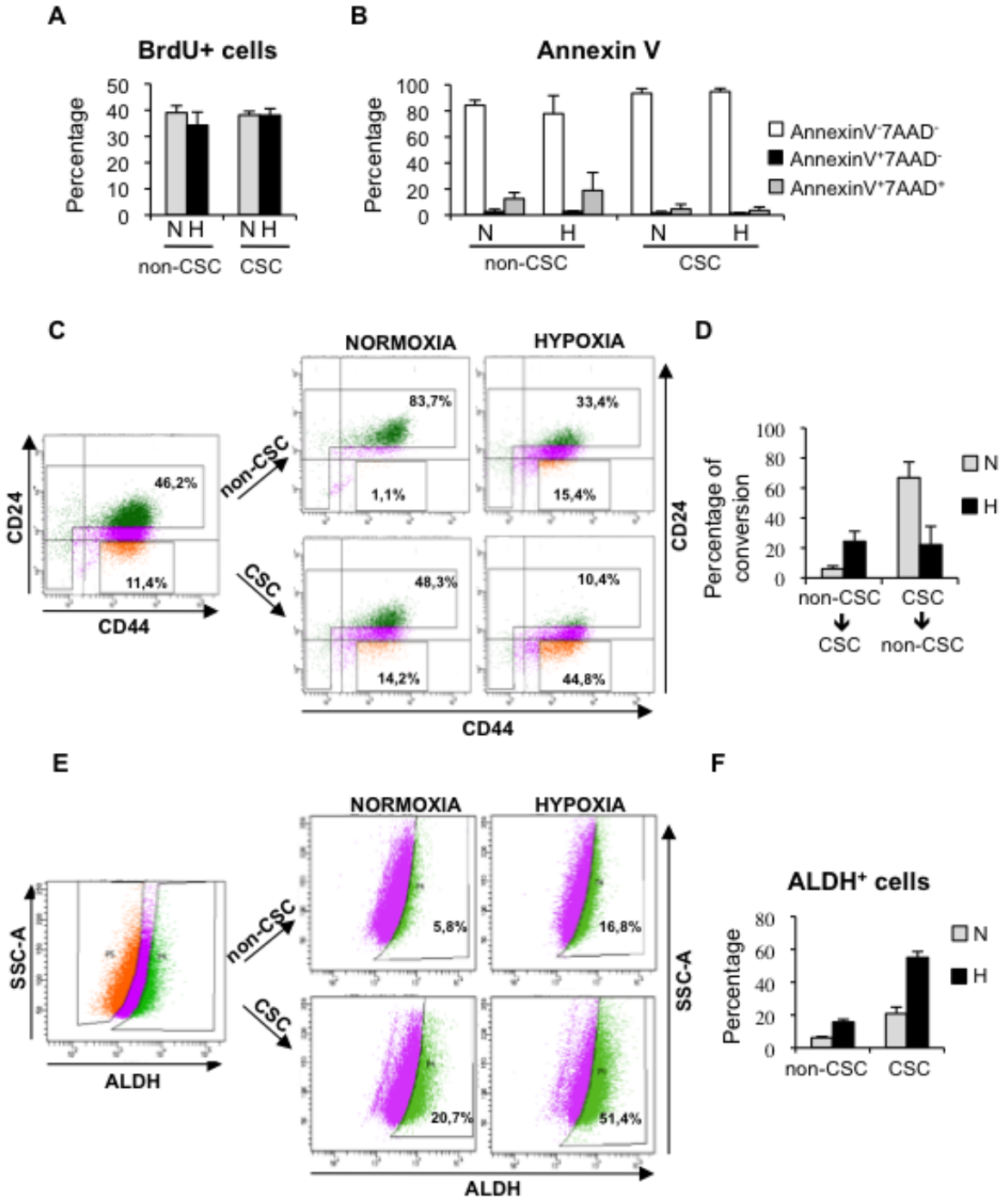

Figure 4: Hypoxia promotes dedifferentiation of breast cancer cells. A. Percentage of BrdU positive MDA-MB-468 cells in sorted cell populations: $CD44^{+}CD24^{-/low}$ CSCs and non-CSCs, grown in normoxia or hypoxia. **B.** Detection of apoptotic cells in CSCs and non-CSCs isolated from MDA-MB-468 cells that were grown in normoxia or hypoxia. The percentages of live cells ($AnnexinV^{-}7AAD^{-}$), early apoptotic ($AnnexinV^{+}7AAD^{-}$) and late apoptotic ($AnnexinV^{+}7AAD^{+}$) cells are shown. **C.** Representative example of a sorting experiment with CD44/CD24-stained MDA-MB-468 cells. On the left, CD44/CD24 staining of MDA-MB-468 cells cultured in hypoxia for 3 days. Gates used to sort $CD44^{+}CD24^{-/low}$ cells (CSC) and the cell population depleted of CSCs (non-CSC) are presented. On the right, CD44/CD24 stainings performed with sorted CSCs and non-CSCs after 3 additional days growing in normoxia or hypoxia. **D.** Graph shows the capacity of $CD44^{+}CD24^{-/low}$ CSCs to produce $CD44^{+}CD24^{high}$ non-CSCs, and vice-versa, in normoxic and hypoxic conditions. **E.** Representative example of a dedifferentiation experiment performed with T47D cells sorted based on their ALDEFLUOR activity. **F.** Percentage of $ALDH^{+}$ cells obtained after culturing $ALDH^{+}$ CSCs and $ALDH^{-}$ non-CSCs in normoxia or hypoxia. A, B, D and F show means ±SD of three independent experiments.

between CSC and non-CSCs cultured in normoxic or hypoxic conditions could contribute to the increase in $CD44^{+}CD24^{-/low}$ cells observed under low oxygen conditions. BrdU incorporation assay and annexin-V staining showed no significant differences in the response of CSC and non-CSCs to hypoxia in terms of proliferation (Figure 4A; Supplementary Figure 4A) or apoptosis (Figure 4B; Supplementary Figure 4B). To assess further the influence of oxygen concentration in CSC content, MDA-MB-468 cells were cultured in hypoxic conditions for 3 days, in order to enrich for CSCs, and $CD44^{+}CD24^{-/low}$ (CSCs) and $CD44^{-/+}CD24^{high}$ (non-CSCs) cells were sorted and cultured again in normoxic or hypoxic conditions for 3 days. The culture of non-CSCs in hypoxic conditions led to the dedifferentiation of a considerable percentage of non-CSC cells into $CD44^{+}CD24^{-/low}$ CSCs, while the non-CSC population remained very high in normoxia (Figure 4C, 4D). On the other hand, $CD44^{+}CD24^{-/low}$ CSCs cultured in normoxic conditions were able to produce both $CD44^{+}CD24^{-/low}$ cells and more differentiated non-CSC cells that expressed high levels of CD24. In contrast, when $CD44^{+}CD24^{-/low}$ cells were kept in hypoxic conditions, a significantly high percentage of cells maintained their CSC phenotype (Figure 4C, 4D). To ascertain whether hypoxic conditions can also lead to the dedifferentiation of other cell subpopulations, $ALDH^{+}$ and $ALDH^{-}$ T47D cells were sorted and cultured under normoxic or hypoxic conditions. Consistent with the results observed with $CD44^{+}CD24^{-/low}$ cells, hypoxia increased the proportion of $ALDH^{+}$ CSCs in a cell population that was originally $ALDH^{-}$ (non-CSCs). In addition, differentiation of sorted $ALDH^{+}$ CSCs into $ALDH^{-}$ cells was lower in hypoxic than in normoxic conditions (Figure 4E, 4F). Among the 19 ALDH isoforms expressed in humans, ALDH1A3 has been shown to correlate best with ALDH activity of patient breast tumor CSCs and cell lines [31]. We therefore examined ALDH1A3 expression in the sorted $ALDH^{+}$ and $ALDH^{-}$ T47D cell subpopulations, which were subsequently cultured under normoxic or hypoxic conditions. Quantitative PCR analyses showed increased ALDH1A3 levels under hypoxia in all cases, even in non-CSC, and furthermore, ALDH1A3 expression levels correlated with ALDH activity (Supplementary Figure 4C), supporting the notion that ALDH activity is primarily due to isoform ALDH1A3 [31]. These findings show that hypoxia expands the pool of CSCs by limiting their differentiation and promoting dedifferentiation of breast cancer cells.

Hypoxia expands the pool of CSCs both through HIF-dependent and independent mechanisms

HIF factors are key mediators of most adaptive changes that occur in response to hypoxia and, indeed, we show induction of HIF1α (Figure 3 and Supplementary Figure 3). Therefore, to determine whether HIF1α and/or HIF2α were implicated in the observed alterations in CSC content under hypoxic conditions, we silenced their expression using specific siRNA sequences. Efficient downregulation of HIF1α (Supplementary Figure 5A, 5C) abrogated the hypoxia-dependent increase in mammosphere formation (Figure 5A) and the percentage of $ALDH^{+}$ cells (Figure 5B), while silencing of HIF2α (Supplementary Figure 5B, 5C) did not affect either of these two subpopulations (Figure 5A, 5B). Surprisingly, silencing of HIF1α and/or HIF2α did not abrogate the increase in $CD44^{+}CD24^{-/low}$ CSCs observed in MDA-MB-468 cells under hypoxic conditions (Figure 5C). Furthermore, $CD44^{+}CD24^{-/low}$ CSCs and non-CSCs expressed similar levels of HIF1α and HIF2α, both at RNA (Figure 5D) and protein (Figure 5E) levels. Taken together, these observations suggest that the increase in mammosphere formation and $ALDH^{+}$ cell content under hypoxic conditions depends on hypoxia-mediated stabilization of HIF1α. In contrast, the finding that HIF silencing did not affect $CD44^{+}CD24^{-/low}$ cell content suggests that some HIF-independent activity is implicated in the regulation of this subpopulation.

Regulation of HIF proteins is the best-known function of prolyl-4-hydroxylases PHD1, PHD2 and PHD3; nevertheless, during the last few years some HIF-independent functions have been described for these proteins. To analyze the potential contribution of the PHDs, all three *PHD* genes were silenced (Supplementary Figure 5D-5F) and alterations in $CD44^{+}CD24^{-/low}$ cell content were evaluated by FACS. While *PHD1* and *PHD2* silencing did not exert any significant effect on CSC content, *PHD3* silencing led to a significant increase in the percentage of $CD44^{+}CD24^{-/low}$ CSCs in normal oxygen conditions, comparable to that observed under hypoxic conditions (Figure 5F). The same result was obtained when the analysis was repeated using an independent PHD3-specific siRNA sequence (Supplementary Figure 5G). Crucially, silencing of *PHD3* did not result in increased HIF1α or HIF2α expression (Figure 5G), confirming that hypoxia-dependent expansion of $CD44^{+}CD24^{-/low}$ CSCs was HIF-independent. Furthermore, PHD3 silencing also increased the $CD44^{+}CD24^{-/low}$ population in BT549 cells, confirming that the effect of PHD3 on CSCs is not cell type specific (Supplementary Figure 5H). Analysis of PHD3 expression in $CD44^{+}CD24^{-/low}$ CSCs and non-CSCs by qPCR (Figure 5H) and western blot (Figure 5I) indicated that PHD3 expression levels were lower in CSCs than in non-CSCs, while expression of PHD1 and PHD2 did not significantly differ between the two populations (Figure 5H, 5I). Interestingly, PHD3 silencing did not influence the proportion of the $CD44^{+}CD24^{-/low}$ cell population in ER-positive MCF7 cells (Supplementary Figure 5I). In conclusion, downregulation of PHD3 increases the proportion of CSCs in ER-negative cells, suggesting that hypoxia can influence the CSC content

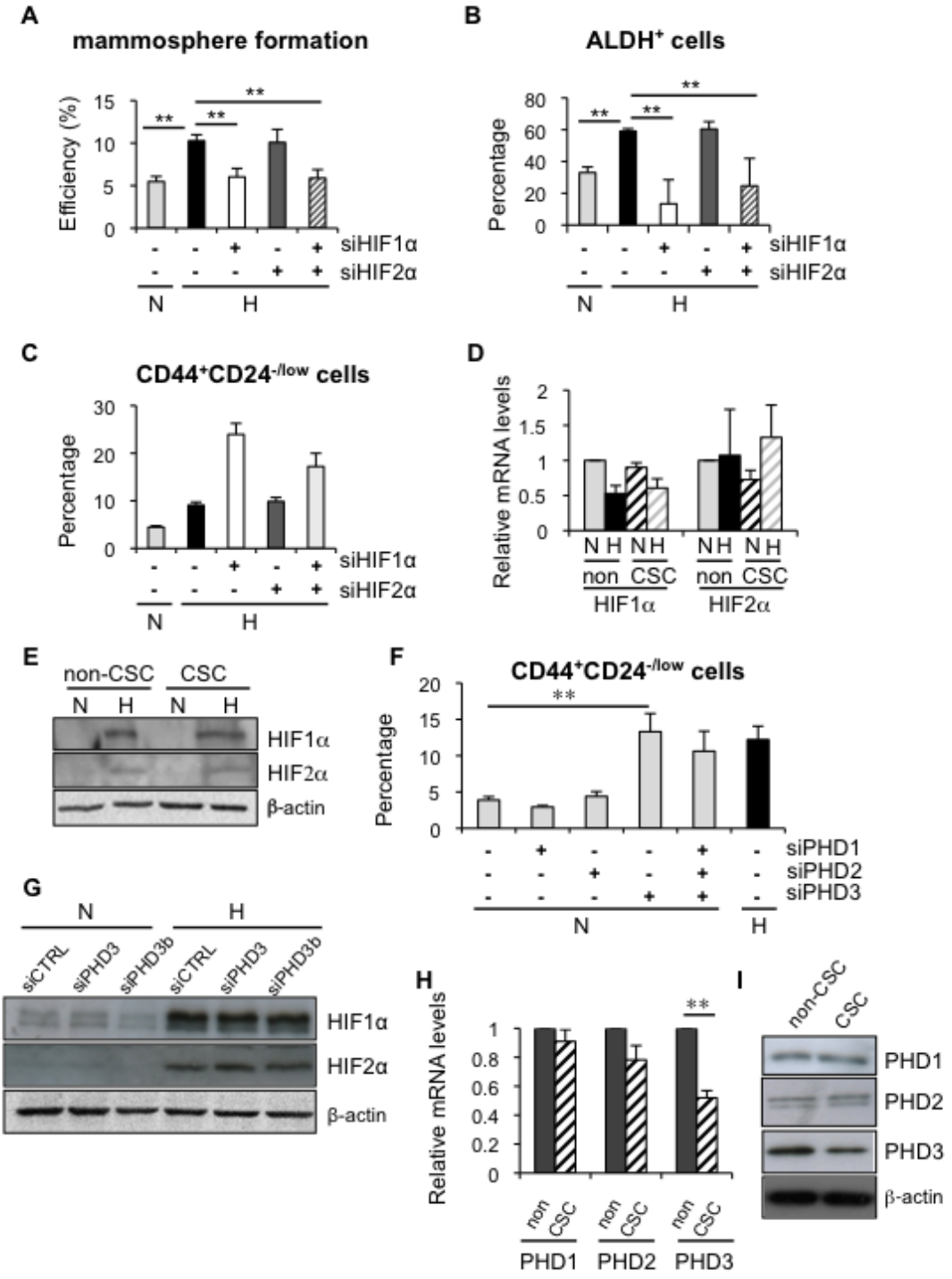

Figure 5: Hypoxia induced dedifferentiation employs both HIF-dependent and independent mechanisms. A. Mammosphere formation efficiency in MCF-7 cells transfected with siHIF1α and/or siHIF2α, and cultured in normoxia or hypoxia for 3 days. **B.** Percentage of ALDH$^+$ cells in T47D cells transfected with siHIF1α and/or siHIF2α, and cultured in normoxia or hypoxia. **C.** Percentage of CD44$^+$CD24$^{-/low}$ cells from MDA-MB-468 cells transfected with siHIF1α and/or siHIF2α, and cultured in normoxia or hypoxia. Data are presented as mean ±SEM of 8 independent experiments. (D, E) HIF1α and HIF2α mRNA **D.** and protein **E.** expression in CSCs and non-CSCs from MDA-MB-468 cells cultured in normoxia or hypoxia. **F.** Percentage of CD44$^+$CD24$^{-/low}$ MDA-MB-468 cells grown in normoxia after silencing all three PHDs individually or collectively or in hypoxia. **G.** Protein expression of HIF1α and HIF2α in MDA-MB-468 cells transfected with a control siRNA or a siRNA directed to PHD3 and cultured in normoxia or hypoxia. **H.**, **I.** PHD1, PHD2 and PHD3 mRNA (**H**) and protein (**I**) expression levels in CSCs and non-CSCs sorted from MDA-MB-468 cells. A, B, D, F and H show means ±SD of three independent experiments.

in a HIF-independent manner through changes in PHD3 expression levels.

PHD3 silencing mimics hypoxia-driven expansion of CSCs by reducing CD24 expression

Next, we wished to determine the mechanism by which PHD3 influences the CSC content in breast cancer cells. PHD3 silencing promoted the dedifferentiation of non-CSCs to $CD44^{+}CD24^{-/low}$ CSCs and prevented the differentiation of the CSCs to non-CSCs ($CD44^{+}CD24^{high}$) in MDA-MB-468 cells (Figure 6A), mimicking the effects observed under hypoxic conditions. In order to examine whether the effect of PHD3 on the pool of CSCs depended on its hydroxylase activity, the proportion of $CD44^{+}CD24^{-/low}$ cells was measured after treating MDA-MB-468 cells with the pan-hydroxylase inhibitor dimethyloxalylglycine (DMOG), which leads to stabilization of HIF1α (Supplementary Figure 6A). Treatment with DMOG increased the proportion of $CD44^{+}CD24^{-/low}$ cells in a dose- and time-dependent manner (Figure 6B), resembling the effect caused by hypoxic conditions. These findings suggest that hypoxia-dependent induction of $CD44^{+}CD24^{-/low}$ CSC population implies inhibition of PHD3 hydroxylation.

FACS analysis showed that hypoxia, PHD3 inactivation and DMOG treatment increased the proportion of $CD44^{+}CD24^{-/low}$ CSCs by reducing the expression of CD24 at the cell surface, while CD44 expression remained unaltered. To gain insight into the effects of hypoxia signaling on CD24, its expression was analyzed by qPCR and immunofluorescence. Hypoxia, PHD3 downregulation and inhibition of the prolyl-hydroxylase activity by DMOG treatment reduced CD24 expression at the RNA level (Figure 6C, 6D) and protein level (Figure 6E, 6F). However, the combination of PHD3 silencing with hypoxic conditions or DMOG treatment did not further affect CD24 expression when compared to each treatment alone (Figure 6C-6E), suggesting that silencing of PHD3, DMOG and hypoxia are working through the same pathway. In conclusion, hypoxia increases the $CD44^{+}CD24^{-/low}$ CSC fraction by reducing CD24 expression levels through the modulation of PHD3 hydroxylase activity.

Hypoxia and PHD3 silencing regulate CD24 expression through activation of NFκB signaling

First, we observed that culturing MDA-MB-468 cells in the presence of actinomycin D reduced *CD24* gene expression, independently of oxygen conditions and CD24 mRNA stability was not differentially affected by normoxic or hypoxic conditions (Figure 7A), suggesting that hypoxia reduces CD24 transcription. We next sought to characterize the mechanism involved in the regulation of CD24 expression in response to hypoxia and reduced PHD3 activity. To this end, we investigated different signaling pathways that have been implicated in the regulation of CSCs. FACS analysis showed that the use of specific inhibitors of Wnt (C59) (Supplementary Figure 7A) or Notch (DAPT) (Supplementary Figure 7B) signaling did not abrogate the hypoxia-induced increase in $CD44^{+}CD24^{-/low}$ CSCs (Supplementary Figure 7C) or the reduction of CD24 expression levels (Figure 7B). Hypoxia and PHD3 have been shown to regulate NFκB signaling in various tissues. Therefore, we examined NFκB transcriptional activity, which was activated by TNFα (Supplementary Figure 7D) and repressed by the small-molecule IKK inhibitor PS1145 (Supplementary Figure 7E), as expected. We confirmed that NFκB transcriptional activity increased in different breast cancer cell lines cultured under hypoxic conditions (Figure 7C). Inhibition of NFκB signaling by PS1145 (Supplementary Figure 7F, 7G) promoted a statistically significant reduction in the hypoxia-driven expansion of $CD44^{+}CD24^{-/low}$ CSCs (Figure 7D), which was due to increased CD24 expression (Figure 7E). In addition, silencing of PHD3, using two different siRNA sequences, also resulted in increased NFκB transcriptional activity (Supplementary Figure 7H, 7I), which could be inhibited by PS1145, leading to reduced $CD44^{+}CD24^{-/low}$ cell content (Figure 7F) by releasing the repression of CD24 expression levels (Figure 7G). To evaluate the implication of NFκB signaling using a different strategy, shRelA/p65, which reduces endogenous RelA/p65 levels and therefore target gene expression (Supplementary Figure 7J), was also tested. Analysis of cells transfected with shRelA/p65 showed that lack of functional NFκB activation impaired hypoxia-dependent repression of CD24 expression (Figure 7H). Furthermore, activation of NFkB with TNFα or inhibition by shRelA/p65, was sufficient to reduce or increase CD24 mRNA expression, respectively, even in normal oxygen conditions (Supplementary Figure 7K). Taken together, these results suggest that silencing of PHD3, similar to hypoxic conditions, increase CSC content by reducing expression of CD24 through the activation of NFκB signaling.

DISCUSSION

In this report we show that hypoxic conditions increase the pool of stem cells both in normal primary epithelial cells and breast cancer cells. The hypoxia-driven increase of CSC populations is a result of limited CSC differentiation and dedifferentiation of breast cancer cells. Hypoxia increases mammosphere formation capacity and the proportion of $ALDH^{+}$ cells through the stabilization of HIF1α, while reducing ER expression and transcriptional activity in ER-positive cells. In contrast, in ER-negative cells, the enrichment in $CD44^{+}CD24^{-/low}$ cells by hypoxia involves reduction of the hydroxylase activity of PHD3

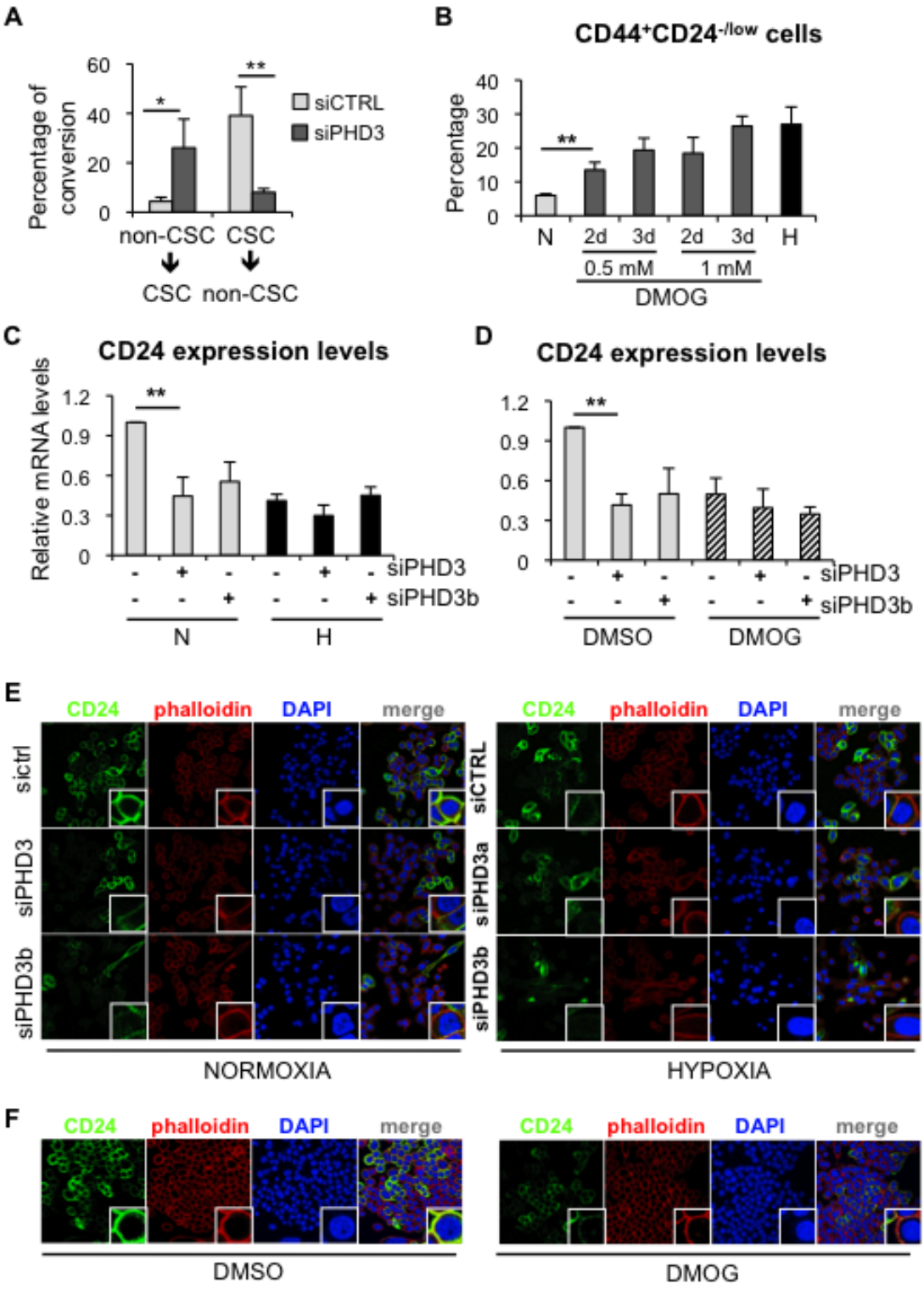

Figure 6: PHD3 silencing promotes dedifferentiation in breast cancer cells through a hydroxylase-dependent mechanism. A. Graph representing the capacity of $CD44^{+}CD24^{-/low}$ CSCs to produce $CD44^{+}CD24^{high}$ non-CSCs, and vice-versa, in MDA-MB-468 cells transfected with a control siRNA or a siRNA directed to PHD3. **B.** Percentage of $CD44^{+}CD24^{-/low}$ CSCs in MDA-MB-468 cells treated with DMOG. **C.** CD24 mRNA expression levels in MDA-MB-468 cells transfected with two specific siRNA sequences against PHD3 and cultured in normoxia or hypoxia. **D.** CD24 mRNA expression levels in MDA-MB-468 cells transfected with two specific siRNA sequences against PHD3 and treated with the carrier DMSO or 1mM DMOG. **E.** immunofluorescence analysis of CD24 expression in MDA-MB-468 cells cultured in normoxia or hypoxia after PHD3 silencing. **F.** CD24 immunostaining in MDA-MB-468 cells treated with DMSO or DMOG. A, B, C, D, show means ±SD of at least 3 independent experiments, $*P < 0.05$, $**P < 0.01$.

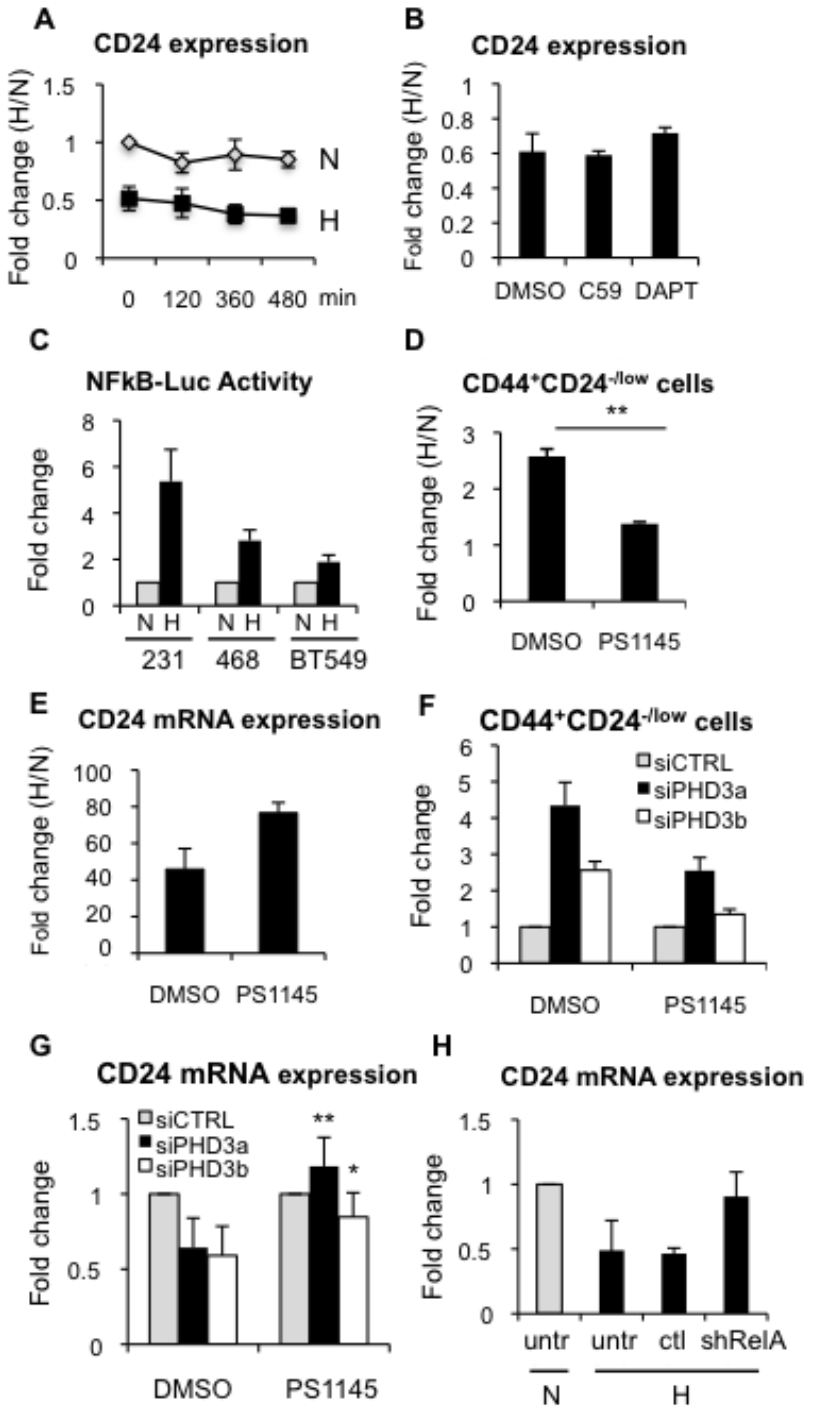

Figure 7: Hypoxia-dependent CD24 downregulation is mediated through NFκB. A. Analysis of CD24 mRNA stability by qPCR in the presence of actinomycin D during 16 h in normoxic or hypoxic conditions. **B.** CD24 mRNA expression levels in the absence or presence of C59 or DAPT, shown as fold change between hypoxia and normoxia. **C.** NFκB transcriptional activity in MDA-MB-231, MDA-MB-468 and BT549 cells transfected with a NFκB-dependent luciferase reporter. Data are represented as fold change activity in hypoxia versus normoxia. **D.** Percentage of $CD44^{+}CD24^{-/low}$ in MDA-MB-468 cells, in the presence or absence of PS1145 (2 μM). Data are presented as fold change between hypoxia and normoxia. **E.** CD24 mRNA expression levels in the absence or presence of PS1145. **F.** Percentage of $CD44^{+}CD24^{-/low}$ in MDA-MB-468 cells transfected with specific siRNA sequences against PHD3 in the presence or absence of PS1145. **G.** CD24 mRNA expression in MDA-MB-468 cells transfected with specific siRNA sequences against PHD3 in the presence or absence of PS1145. **H.** CD24 mRNA expression in BT549 cells transfected or not (untr) with a sh control (ctl) or shRelA/p65.

and CD24 expression through activation of NFκB signaling.

Hypoxic microenvironments have been shown to influence the behavior of both normal and cancer stem cells in several tissues [32, 33]. We demonstrate that hypoxic conditions increase normal mammary stem/progenitor cell content, leading to the enhanced capacity of primary mammary epithelial cells to form colonies in 3D Matrigel cultures. Hypoxia signaling pathway plays a role during mammary gland development and lactation [34]. In fact, it has been shown that deletion of *Hif1a* from the murine mammary epithelium led to defects in mammary gland development and physiology [35]. In addition, increased expression of genes identified in a hypoxia signature has been correlated with poor prognosis in several types of cancer, including breast cancer [36, 37]. In primary mammary carcinomas hypoxia increases the proportion of $CD44^+CD24^{-/low}ESA^+$ CSCs in tumors that have low levels or no active ER signaling [8, 9], according to their ER and PR expression levels detected by immunohistochemistry. However, given the known heterogeneity of breast cancer [5], a more extensive study would be needed to be able to conclude the consequences of hypoxic conditions in different subtypes of breast carcinomas. It has previously been shown that high levels of HIF proteins are implicated in triple negative breast cancer invasiveness and metastasis [38] and that HIF-1α overexpression is observed more often in ER and PR negative carcinomas [39, 40], consistent with our findings that hypoxia reduces ER expression and activity. In fact, the capacity of ER to limit hypoxia-induced expansion of $CD44^+CD24^{-/low}$ CSCs was further confirmed by depleting ER with the antagonist fulvestrant. Several groups have demonstrated increased breast CSC content in response to hypoxia, but the populations of CSCs analyzed differed. Thus, hypoxia-induced expansion of $ALDH^+$ cells was observed both in ER-positive and ER-negative cells [27, 28], and increases in the percentage of $CD44^+CD24^-$ cells and mammosphere formation capacity were shown in ER-negative cells [27, 41, 42], in agreement with our results and in contrast to one report, which detected a decrease in $ALDH^+$ cells and mammosphere formation in ER-negative cancers [30]. We and others have shown that HIF1α stabilization mediates the hypoxia-dependent effects in mammospheres and $ALDH^+$ cells [27, 28, 30]. Using ER-negative cells derived from late stage tumors spontaneously formed in MMTV-PyMT mice, deletion of HIF1α has been shown to reduce tumor growth in allotransplantation experiments, while decreasing mammosphere formation *in vitro* [43]. Furthermore, it was demonstrated that the increase in $ALDH^+$ cells under hypoxic conditions is, at least partly regulated by the Akt/β-catenin signaling pathway in a HIF1α-dependent manner [27], providing a potential mechanism for hypoxia-induced increase in this CSC population. These findings support a correlation between HIF1α expression levels, $ALDH^+$ cells, mammosphere formation capacity and tumorigenicity.

ER expression is considered characteristic of well-differentiated luminal tumors and both normal and breast cancer stem and progenitor cells do not express or express low levels of ER [9, 10, 13, 44, 45]. It has been shown that under hypoxic conditions, ER expression is reduced due to proteasomal degradation, leading to reduced ER transcriptional activity [46-48], although other reports argue that the decrease in ER expression is coupled to an increase in its activity [30, 49]. Our data shows that hypoxia reduces ER expression and transcriptional activity. Using different ER-positive breast cancer cell lines, we demonstrate that hypoxia downregulates ER expression, at least in part, at the RNA level, in agreement with previous data [50], resulting in decreased ER transcriptional activity. These results indicate that hypoxia reduces ER expression and activity, which explains the significant correlation observed between HIF-1α immunoreactivity and the absence of ER and PR [40]. Furthermore, it has been observed that well vascularized intratumoral regions contain larger number of ER-positive cells than areas with low blood flow and necrosis [51].

An important question was how the CSC fraction is altered by hypoxia. Changes in the CSC content due to hypoxic conditions are not related to significant alterations in proliferation or apoptosis, but are rather due to the dedifferentiation of cancer cells. Importantly, hypoxic conditions also prevent the differentiation of sorted CSCs. The observation that hypoxia affects the differentiation status of the cells highlights the plasticity of CSCs. Indeed, recently it has been shown that breast CSCs display a cellular plasticity that enables them to transition between epithelial-like and mesenchymal-like states regulated by the tumor microenvironment [52]. In addition, CSC plasticity has recently been demonstrated by elegant intravital lineage tracing experiments in unperturbed mammary tumors [53]. Furthermore, the capacity of hypoxia to drive a reversible phenotype that increases stem-like properties of cells to favor tumor survival has also been observed in other tumors, such as neuroblastoma [54, 55].

Interestingly, we found that silencing PHD3 mimics hypoxia, preventing differentiation of CSCs and leading to dedifferentiation of breast cancer cells. We present evidence that neither HIF1α nor HIF2α are involved in the hypoxia-induced expansion of $CD44^+CD24^{-/low}$ cells in ER-negative breast cancer cells. This finding was surprising, considering the central role of HIF transcription factors in the regulation of normal and cancer stem cells from several tissues [33, 56-58]. Yet, this result does not necessarily imply that HIFs are not involved in hypoxia-induced increase in stem cell content in ER-negative breast tumors. In fact, we and others have shown that hypoxia increases the percentage of different population of CSCs, $ALDH^+$ cells, as well as cells with

enhanced mammosphere formation capacity, through HIF1α stabilization, both in ER-positive and ER- negative breast cancer cells [27]. However, in ER-negative breast cancer cells, hypoxia can enlarge different subpopulations of CSCs through two different mechanisms. These findings suggest that therapeutic approaches directed to HIF1α inactivation would be insufficient to prevent the expansion of $CD44^{+}CD24^{-/low}$ CSCs. It has been argued that this hypoxia-dependent expansion in CSCs could at least in part explain why patients treated with antiangiogenic factors relapse and present tumors that are more aggressive than the original tumor [27, 59, 60].

The maintenance of $CD44^{+}CD24^{-/low}$ cells implicates PHD3, while it is independent of HIF. Interestingly, PHD3 expression has been found to correlate with lower tumor grade and ER positivity [24], and PHD3 transcription is activated by ER both *in vitro* and *in vivo* [61]. These findings are consistent with our observations that low PHD3 levels are found in ER-negative $CD44^{+}CD24^{-/low}$ cells and that PHD3 silencing results in dedifferentiation of breast cancer cells. In pancreatic tumors it has been observed that undifferentiated tumors express lower PHD3 levels than well-differentiated tumors, while silencing of PHD3 expression accelerated cell growth, independently of HIF-1 activation [62]. Inhibition of NFκB signaling prevented hypoxia-driven enrichment of $CD44^{+}CD24^{-/low}$ cells and reduction of CD24 expression. We propose that down-regulation of PHD3 leads to activation of NFκB, in a HIF-independent manner, which results in the expansion of $CD44^{+}CD24^{-/low}$ cells in ER-negative cells (Supplementary Figure 8). A similar effect has been reported in skeletal muscle, where PHD3 was found to promote myoblast differentiation by downregulating NFκB activity [63]. Importantly, increased NFκB activity has been associated with expansion of CSCs in several types of tumors, including breast cancer [64-67]. Tumor-initiating cells are characterized by low levels of membrane CD24 expression [14, 15]. The observed expansion of $CD44^{+}CD24^{-/low}$ cells appears to be due to the reduction of membrane CD24 expression through the activation of NFκB signaling. Indeed, activation or inhibition of NFkB signaling reduces or increases CD24 expression, respectively, even in normoxic conditions, supporting a role for NFkB in the regulation of CD24. Interestingly, it has also been shown that CD24 expression can attenuate cell viability and NFkB signaling, but only in CD44-expressing cells [68], thus suggesting a regulatory loop between CD24 and NFkB that may be particularly relevant in CSCs.

A decade ago, the isolation of tumorigenic breast cancer cells with the phenotype $CD44^{+}CD24^{-/low}$ represented a first step towards the characterization of breast CSCs [14], which was complemented soon after with the discovery of their capacity to grow as mammospheres [69] and their enhanced aldehyde dehydrogenase activity [13]. Importantly, all these subpopulations of breast CSCs were more efficient at initiating tumors in NOD/SCID mice than non-CSC populations. Nevertheless, genetic profiling has shown that $CD44^{+}CD24^{-/low}$ and $ALDH^{+}$ cells represent distinct breast CSCs that, furthermore, are not static, but instead display a cellular plasticity allowing them to transit between epithelial and mesenchymal states [52] and to respond differentially to γ-secretase inhibitors [70]. These findings suggest that the complexity of breast CSCs is higher than initially anticipated [71, 72]. Furthermore, this also implies that these distinct CSC subpopulations, which are using specific molecular pathways, are likely to present distinct anti-cancer drug responsiveness. This work also has potential clinical implications given that it has been proposed that treatment with antiangiogenic agents should be combined with CSC-targeting drugs, since HIF1α increases breast CSCs [27], and that chemotherapy should be combined with HIF inhibitors in women with triple negative breast cancer [28]. Therefore, we propose that the design of combinatorial therapies targeting CSCs should take into account their intrinsic heterogeneity in order to achieve the wide spectrum required to avoid or limit CSC expansion in the tumor and development of resistance to therapy leading to metastasis.

MATERIALS AND METHODS

Isolation of human breast epithelial cells and Ethics Statement

Normal breast tissue was obtained from women (24 - 43 years old) undergoing reduction mammoplasty with no previous history of breast cancer (clinical data can be found in Supplementary Table 1). Tumor samples were obtained from core biopsies or from women who underwent therapeutic surgery (histopathological information can be found in Supplementary Table 2). Investigation has been conducted in accordance with the ethical standards and according to the Declaration of Helsinki and according to national and international guidelines. All patients provided written informed consent and the procedures were approved by the local Hospital Research Ethics Committee, by the "Ethics Committee of Clinical Investigations of Euskadi" and by the Centre´s review board. Upon arrival, all samples were immediately processed as previously described [44].

Adherent cell culture

MCF-7, T47D, MDA-MB-468, MDA-MB-231, ZR75-1 and SK-BR-3 cell lines were obtained from American Type Culture Collection (ATCC) and cultured in DMEM/F-12 medium with GlutaMAX (Gibco) supplemented with 8% FBS (Sigma) and 1% penicillin/

streptomycin (Gibco) at 37°C in 5% CO_2. BT549 cells (kindly provided by A Carracedo) were cultured in DMEM/F-12 medium with GlutaMAX supplemented with 10% FBS and 1% penicillin/streptomycin. For experiments with hormonal treatments, MCF-7 and T47D cells were hormone-depleted for 2-3 days in phenol-red free (PRF) DMEM/F-12 medium (Gibco) supplemented with 8% charcoal (Sigma) stripped FBS, before adding 17-β-estradiol (estrogen) (Sigma), or fulvestrant (ICI 182,780, kindly provided by AE Wakeling). Primary normal epithelial cells were cultured in DMEM/F-12 with GlutaMax supplemented with 5% FBS, 5 µg/ml insulin (Sigma), 1 µg/ml hydrocortisone (Sigma), 10 ng/ml EGF (Invitrogen), 100 ng/ml cholera toxin (Sigma) and 1% penicillin/streptomycin.

Cells were treated with 2 µM PS1145, 100 nM C59 [80]or 10 µM DAPT (Sigma). Media were changed every 24 h - 36 h to ensure the activity of all compounds. C59 was kindly provided by R Kypta and the other drugs are from Sigma.

Mammosphere culture

Cells were detached with TrypLE™ Select (Invitrogen) and plated in 75 cm^2 in flasks treated with poly(2-hydroxyethylmethacrylate) (poly-HEMA [Sigma]) at a density of 3,000 cells/ml. Alternatively, 500 cells were sorted into poly-HEMA coated 6-well plates. MCF-7 and MDA-MB-468 cells were grown in DMEM/F-12 medium with GlutaMAX, supplemented with B27 (Gibco), 10 ng/ml EGF (Invitrogen), 2 ng/ml bFGF (Millipore) at 37°C in 5% CO_2. When culturing primary cells, medium was enriched with B27, 20 ng/ml EGF, 20 ng/ml bFGF. After 5 to 8 days, mammospheres were stained with crystal violet solution, immobilized in 0,3% agar, and counted.

Hypoxia treatment

Hypoxic cultures were carried out in a humidified hypoxia workstation (*In Vivo* 400, Ruskin) with an atmosphere of 1% oxygen and 5% CO_2 balanced with nitrogen. When used, and unless otherwise stated, cells were treated with the hypoxia mimetic dimethyloxaloylglycine (DMOG) at 1 mM for 3 days, replacing the media every 24h.

Colony formation assay with normal breast epithelial cells

Following cell culture in adherence or suspension conditions for 3-4 days, as described above, dissociated single cells were plated in Millicell EZ SLIDE chamber slides (Millipore) (1000 cells per well) on top of a layer of growth factor reduced Matrigel (BD) that was previously allowed to polymerize. Cells were cultured for 10-12 days in different oxygen conditions in medium supplemented with 5% FBS, 5 µg/ml insulin (Sigma), 1 µg/ml hydrocortisone (Sigma), 10 ng/ml EGF (Invitrogen), 100 ng/ml cholera toxin (Sigma), 5% Matrigel and 1% penicillin/streptomycin.

RNA extraction and qPCR

Total RNA was isolated using TRIzol (Invitrogen). When the cell number was low, RNeasy Micro Kit (Qiagen) was used. In all cases, RNA extraction was performed according to the instructions of the manufacturer. DNAse-treated RNA was used to synthesize cDNA using M-MLV reverse transcriptase (Invitrogen) or Omniscript reverse transcriptase, following the manufacturer's protocol. qPCR was performed on a 7300 Real-Time PCR System (Applied Biosystems) or a ViiA 7™ Real-Time PCR System (Applied Biosystems), using iTaq™ SYBR® Green Supermix with ROX (BioRad) or PerfeCta® SYBR® Green SuperMix with Low Rox (Quanta Biosciences), respectively. Primer sequences used for PCR amplification are summarized in Supplementary Table 3.

Transcription assays

All cells were seeded at 40.000 cells per well in 24-well tissue-culture plates, hormone-depleted for 2-3 days and transfected using Genejuice reagent (Merck), following the indications of the manufacturer. Cells were transfected with the pGL2-ERE TK-luciferase vector containing the thymidine kinase (TK) promoter and three copies of a consensus ERE (Estrogen Responsive Element), driving the expression of the luciferase gene (kindly provided by M Parker). A vector expressing beta-galactosidase was used as control for transfection efficiency [73]. After transfection cells were treated with or without estrogen and cultured in normoxic or hypoxic conditions for 40 h, after which luciferase and beta-galactosidase activities were measured using the Luciferase Assay Kit (Promega) and the Tropix Galacto-Light-Plus Assay (Applied Biosystems), respectively. Luminescence was measured in a Veritas TM Microplate Luminometer (Turner Biosystems).

MDA-MB-468, MDA-MB-231 and BT-549 cells were seeded in 6-well plate at $3x10^5$ cells/well and were transfected with the NFkB-TK-luciferase reporter [74] (kindly provided by R Kypta) using Lipofectamine LTX (Invitrogen) following the manufacturer's instructions. Each well also received *renilla* to normalize for transfection efficiency. After transfection, the cells were maintained in DMEM:F12 containing 8% FBS for 48 h. The cell lysates were assayed for luciferase and renilla activities with a luciferase reporter assay kit (Dual-

Luciferase Reporter Assay System; Promega) using a luminometer (Turner Biosystem).

To assay for NFkB activity BT-549 cells were seeded in 6-well plates at $3x10^5$ cells/well and were transfected with the *shRelA* (p65 shRNA) *plasmid [75],* kindly provided by B Lewis) using Lipofectamine LTX (Invitrogen) following the manufacturer's instructions. After 5 h, cells were maintained in normoxic or hypoxic conditions for 40 h. GFP positive (transfected) or negative (not transfected) cells were sorted using a FACS ARIA and collected to perform total RNA extraction.

Gene silencing

siRNA transfection was performed using Lipofectamine 2000 or Lipofectamine RNAimax (Invitrogen), following the guidelines of the manufacturer for reverse transfection. For the mammosphere formation assays after gene silencing, cells were transfected twice, to ensure efficient silencing during the whole experiment. Following incubations with liposomes, cells were collected by centrifugation (400 x g for 5 minutes). 3000 cells/ml were seeded in 75 cm^2 poly-HEMA coated flasks in order to allow mammosphere formation. The RNAi sequences used in this study are shown in Supplementary Table 4.

Western blotting

Cell lysates were prepared with Laemmli buffer (50 mM tris pH 6,8, 1,25% SDS, 15% glycerol). Protein extracts of cells cultured in hypoxia were made inside the hypoxic chamber to avoid reoxygenation. All extracts were heated at 95ºC for 15 minutes for a complete lysis and denaturalization and Lowry protein assay (BioRad) was used for the quantification of protein extracts, followed by addition of β- mercaptoethanol (Applichem) (5% final concentration) and bromophenol blue (Sigma). Blots were then incubated with the following primary antibodies: ERα (Novocastra, clone 6F11), HIF1α (antiserum 2087 [76]), HIF2α (kindly provided by D Richard), PHD1 (Bethyl, A300-326A), PHD2 (antiserum 804 [77]), PHD3 (Novus Biologicals, NB-100-139), PR (Novocastra, clone 16), RARα (Santa Cruz, sc-6551), β-actin (AC-15/A5441), and β-tubulin (Sigma). Proteins were detected using ECL (Amersham) and visualized on X-ray film or by acquiring digital images with the Molecular Imager ChemiDoc XRS System.

Immunofluorescence

For immunofluorescence experiments, cells were processed as previously described [78]. Briefly, cells grown on cover slides were fixed in 4% paraformaldehyde (Santa Cruz), permeabilised with PBS 0,5% saponin and blocked in blocking buffer (PBS containing 2%BSA, 50 mM Glycine and 0,1% saponin). Cells were then incubated with anti-CD24 antibody (Dianova, T-1358) overnight at 4ºC. After washing with PBS-0,1% saponin, cells were incubated with anti-mouse Alexa 488 (Molecular Probes, A21202) and phalloidin (phalloidin-Tetramethylrhodamine B isothiocyanate, Sigma, P1951). Slides were washed and finally mounted in Vectashield with DAPI (Vector) and visualized on a Leica confocal microscope.

Fluorescence activated cell sorting (FACS)

For CD44/CD24/ESA, CD44/CD24 and CD49f/ESA stainings, PE-conjugated anti-CD24 antibody (BD, 555428), APC-conjugated anti-CD44 antibody (BD, 559942), FITC-conjugated anti-ESA antibody (Biomeda Corp, FM010) and APC-conjugated anti-CD49f antibody (eBioscience, 17-0495-80) were used [79]. EMA/CALLA labeling was performed as previously described [10], using a rat monoclonal antibody against EMA (ICR2 [10]), followed by FITC-conjugated anti-rat antibody (Southern Biotech, 3010-02), and PE-conjugated anti-CALLA antibody (DAKO, R0848). In all cases, control samples were stained with isotype-matched control antibodies, the viability dye 7-aminoactinomycin D (7AAD) (BD) was used for dead cell exclusion, and fluorescence minus one (FMO) controls were used to define the gates [79].

For BrdU incorporation assay, cells were treated with 10 μM bromodeoxyuridine (BrdU) (Amersham) for 1 h. Upon harvesting, cells were fixed in 4% PFA for 15 minutes, permeabilized in 0,1% triton for 20 minutes, and incubated with Fastimmun™ anti-BrdU-FITC antibody with DNAse (BD, 340649) for 30 minutes. Cells not treated with BrdU were used as negative control. Annexin V staining was performed using FITC Annexin V Apoptosis Detection kit (BD, 556547), following the instructions of the manufacturer and using 7AAD instead of Propidium Iodide.

To measure ALDH activity in cells, ALDEFLUOR assay (Stemcell Technologies) was carried out according to manufacturer's guidelines, and as previously described [44].

In all cases, cells were analyzed using FACSCanto II (Becton Dickinson) or FACSAria (Becton Dickinson) flow cytometres. FACSAria was used for sorting cells. Data were analyzed using the FACSDiva software.

Statistical analysis

Data from at least three independent experiments are expressed as means ± SD (or ± SEM, if indicated). Each data point of real-time PCR, mammosphere formation and luciferase activity assays was run at least in triplicate.

Student´s *t*-test was used to determine statistically significant differences and $p < 0.05$ was considered to be significant unless otherwise specified.

Abbreviations

SC, stem cell; CSC, cancer stem cell; ER, estrogen receptor; HIF, hypoxia-inducible factor; PR, progesterone receptor; RAR, retinoic acid receptor; AREG, amphiregulin; pS2, also known as TFF1, trefoil factor 1; DMOG, dimethyloxalylglycine.

ACKNOWLEDGMENTS

The authors would like to thank the women that so generously collaborated with this project and the members of the laboratory for helpful discussions. They also thank Robert Kypta for providing reagents, scientific discussions and critically reading and editing the manuscript. The authors also appreciate the plasmids kindly provided by M Parker and B Lewis. This work was funded by grants from the Institute of Health Carlos III (PI11/02251 to MV), the Departments of Education (PhD grant to OI) and Health (2010-111060 to MV) of the Government of the Autonomous Community of the Basque Country and the Ministry of Science and Innovation (SAF2010-20067 to EB).

Author contributions

O.I. conceived the study, designed and performed experiments, analyzed data and wrote the manuscript. M.R. and G.D. performed and analyzed experiments and edited the manuscript. O.C. provided technical assistance and reagents. J.A.L.R. and I.Z. provided essential normal and tumor biological material and managed the collection of human samples. E.B. provided reagents and scientific support, contributed to the design of experiments and edited the manuscript. M.V. conceived the project, designed experiments, analyzed data and wrote the manuscript.

CONFLICTS OF INTEREST

The authors declare no conflict of interest.

FUNDING

Grants from the Institute of Health Carlos III (PI11/02251 to MV), the Departments of Education (PhD grant to OI) and Health (2010-111060 to MV) of the Government of the Autonomous Community of the Basque Country.

REFERENCES

1. Ferlay J, Soerjomataram I, Dikshit R, Eser S, Mathers C, Rebelo M, Parkin DM, Forman D and Bray F. Cancer incidence and mortality worldwide: Sources, methods and major patterns in GLOBOCAN 2012. Int J Cancer. 2015;136:E359-86.
2. Perou CM, Sorlie T, Eisen MB, van de Rijn M, Jeffrey SS, Rees CA, Pollack JR, Ross DT, Johnsen H, Akslen LA, Fluge O, Pergamenschikov A, Williams C, Zhu SX, Lonning PE, Borresen-Dale AL, et al. Molecular portraits of human breast tumours. Nature. 2000; 406:747-752.
3. Sorlie T, Perou CM, Tibshirani R, Aas T, Geisler S, Johnsen H, Hastie T, Eisen MB, van de Rijn M, Jeffrey SS, Thorsen T, Quist H, Matese JC, Brown PO, Botstein D, Lonning PE, et al. Gene expression patterns of breast carcinomas distinguish tumor subclasses with clinical implications. Proc Natl Acad Sci U S A. 2001; 98:10869-10874.
4. Sorlie T, Tibshirani R, Parker J, Hastie T, Marron JS, Nobel A, Deng S, Johnsen H, Pesich R, Geisler S, Demeter J, Perou CM, Lonning PE, Brown PO, Borresen-Dale AL and Botstein D. Repeated observation of breast tumor subtypes in independent gene expression data sets. Proc Natl Acad Sci U S A. 2003; 100:8418-8423.
5. Curtis C, Shah SP, Chin SF, Turashvili G, Rueda OM, Dunning MJ, Speed D, Lynch AG, Samarajiwa S, Yuan Y, Graf S, Ha G, Haffari G, Bashashati A, Russell R, McKinney S, et al. The genomic and transcriptomic architecture of 2,000 breast tumours reveals novel subgroups. Nature. 2012; 486:346-352.
6. Ali H, Rueda OM, Chin SF, Curtis C, Dunning MJ, Aparicio S and Caldas C. Genome-driven integrated classification of breast cancer validated in over 7,500 samples. Genome biology. 2014; 15:431.
7. Payne SJ, Bowen RL, Jones JL and Wells CA. Predictive markers in breast cancer—the present. Histopathology. 2008; 52:82-90.
8. Simoes BM and Vivanco MD. Cancer stem cells in the human mammary gland and regulation of their differentiation by estrogen. Future Oncol. 2011; 7:995-1006.
9. Piva M, Domenici G, Iriondo O, Rabano M, Simoes BM, Comaills V, Barredo I, Lopez-Ruiz JA, Zabalza I, Kypta R and Vivanco MD. Sox2 promotes tamoxifen resistance in breast cancer cells. EMBO Mol Med. 2014; 6:66-79.
10. Clayton H, Titley I and Vivanco M. Growth and differentiation of progenitor/stem cells derived from the human mammary gland. Exp Cell Res. 2004; 297:444-460.
11. Eirew P, Stingl J, Raouf A, Turashvili G, Aparicio S, Emerman JT and Eaves CJ. A method for quantifying normal human mammary epithelial stem cells with *in vivo* regenerative ability. Nat Med. 2008; 14:1384-1389.
12. Lim E, Vaillant F, Wu D, Forrest NC, Pal B, Hart AH, Asselin-Labat ML, Gyorki DE, Ward T, Partanen A,

Feleppa F, Huschtscha LI, Thorne HJ, Fox SB, Yan M, French JD, et al. Aberrant luminal progenitors as the candidate target population for basal tumor development in BRCA1 mutation carriers. Nat Med. 2009; 15:907-913.

13. Ginestier C, Hur MH, Charafe-Jauffret E, Monville F, Dutcher J, Brown M, Jacquemier J, Viens P, Kleer CG, Liu S, Schott A, Hayes D, Birnbaum D, Wicha MS and Dontu G. ALDH1 is a marker of normal and malignant human mammary stem cells and a predictor of poor clinical outcome. Cell Stem Cell. 2007; 1:555-567.
14. Al-Hajj M, Wicha MS, Benito-Hernandez A, Morrison SJ and Clarke MF. Prospective identification of tumorigenic breast cancer cells. Proc Natl Acad Sci U S A. 2003; 100:3983-3988.
15. Fillmore CM and Kuperwasser C. Human breast cancer cell lines contain stem-like cells that self-renew, give rise to phenotypically diverse progeny and survive chemotherapy. Breast Cancer Res. 2008; 10:R25.
16. Charafe-Jauffret E, Ginestier C, Iovino F, Wicinski J, Cervera N, Finetti P, Hur MH, Diebel ME, Monville F, Dutcher J, Brown M, Viens P, Xerri L, Bertucci F, Stassi G, Dontu G, et al. Breast cancer cell lines contain functional cancer stem cells with metastatic capacity and a distinct molecular signature. Cancer Res. 2009; 69:1302-1313.
17. Semenza GL. Cancer-stromal cell interactions mediated by hypoxia-inducible factors promote angiogenesis, lymphangiogenesis, and metastasis. Oncogene. 2013; 32:4057-4063.
18. Bertout JA, Patel SA and Simon MC. The impact of O2 availability on human cancer. Nature reviews Cancer. 2008; 8:967-975.
19. Semenza GL. HIF-1 mediates metabolic responses to intratumoral hypoxia and oncogenic mutations. The Journal of clinical investigation. 2013; 123:3664-3671.
20. Bruick RK and McKnight SL. A conserved family of prolyl-4-hydroxylases that modify HIF. Science. 2001; 294:1337-1340.
21. Huang LE, Gu J, Schau M and Bunn HF. Regulation of hypoxia-inducible factor 1alpha is mediated by an O2-dependent degradation domain via the ubiquitin-proteasome pathway. Proc Natl Acad Sci U S A. 1998; 95:7987-7992.
22. Salceda S and Caro J. Hypoxia-inducible factor 1alpha (HIF-1alpha) protein is rapidly degraded by the ubiquitin-proteasome system under normoxic conditions. Its stabilization by hypoxia depends on redox-induced changes. The Journal of biological chemistry. 1997; 272:22642-22647.
23. Semenza GL. Hypoxia-inducible factors in physiology and medicine. Cell. 2012; 148:399-408.
24. Peurala E, Koivunen P, Bloigu R, Haapasaari KM and Jukkola-Vuorinen A. Expressions of individual PHDs associate with good prognostic factors and increased proliferation in breast cancer patients. Breast Cancer Res Treat. 2012; 133:179-188.
25. Chan DA, Kawahara TL, Sutphin PD, Chang HY, Chi JT and Giaccia AJ. Tumor vasculature is regulated by PHD2-mediated angiogenesis and bone marrow-derived cell recruitment. Cancer Cell. 2009; 15:527-538.
26. Henze AT, Garvalov BK, Seidel S, Cuesta AM, Ritter M, Filatova A, Foss F, Dopeso H, Essmann CL, Maxwell PH, Reifenberger G, Carmeliet P, Acker-Palmer A and Acker T. Loss of PHD3 allows tumours to overcome hypoxic growth inhibition and sustain proliferation through EGFR. Nature communications. 2014; 5:5582.
27. Conley SJ, Gheordunescu E, Kakarala P, Newman B, Korkaya H, Heath AN, Clouthier SG and Wicha MS. Antiangiogenic agents increase breast cancer stem cells via the generation of tumor hypoxia. Proc Natl Acad Sci U S A. 2012; 109:2784-2789.
28. Samanta D, Gilkes DM, Chaturvedi P, Xiang L and Semenza GL. Hypoxia-inducible factors are required for chemotherapy resistance of breast cancer stem cells. Proc Natl Acad Sci U S A. 2014.
29. Vaupel P, Schlenger K, Knoop C and Hockel M. Oxygenation of human tumors: evaluation of tissue oxygen distribution in breast cancers by computerized O2 tension measurements. Cancer Res. 1991; 51:3316-3322.
30. Harrison H, Rogerson L, Gregson HJ, Brennan KR, Clarke RB and Landberg G. Contrasting hypoxic effects on breast cancer stem cell hierarchy is dependent on ER-alpha status. Cancer Res. 2013; 73:1420-1433.
31. Marcato P, Dean CA, Pan D, Araslanova R, Gillis M, Joshi M, Helyer L, Pan L, Leidal A, Gujar S, Giacomantonio CA and Lee PW. Aldehyde dehydrogenase activity of breast cancer stem cells is primarily due to isoform ALDH1A3 and its expression is predictive of metastasis. Stem cells. 2011; 29:32-45.
32. Mohyeldin A, Garzon-Muvdi T and Quinones-Hinojosa A. Oxygen in stem cell biology: a critical component of the stem cell niche. Cell Stem Cell. 2010; 7:150-161.
33. Li Z, Bao S, Wu Q, Wang H, Eyler C, Sathornsumetee S, Shi Q, Cao Y, Lathia J, McLendon RE, Hjelmeland AB and Rich JN. Hypoxia-inducible factors regulate tumorigenic capacity of glioma stem cells. Cancer Cell. 2009; 15:501-513.
34. Shao Y and Zhao FQ. Emerging evidence of the physiological role of hypoxia in mammary development and lactation. Journal of animal science and biotechnology. 2014; 5:9.
35. Seagroves TN, Hadsell D, McManaman J, Palmer C, Liao D, McNulty W, Welm B, Wagner KU, Neville M and Johnson RS. HIF1alpha is a critical regulator of secretory differentiation and activation, but not vascular expansion, in the mouse mammary gland. Development. 2003; 130:1713-1724.
36. Chi JT, Wang Z, Nuyten DS, Rodriguez EH, Schaner ME, Salim A, Wang Y, Kristensen GB, Helland A, Borresen-Dale AL, Giaccia A, Longaker MT, Hastie T, Yang GP, van

de Vijver MJ and Brown PO. Gene expression programs in response to hypoxia: cell type specificity and prognostic significance in human cancers. PLoS medicine. 2006; 3:e47.

37. Buffa FM, Harris AL, West CM and Miller CJ. Large meta-analysis of multiple cancers reveals a common, compact and highly prognostic hypoxia metagene. British journal of cancer. 2010; 102:428-435.

38. Montagner M, Enzo E, Forcato M, Zanconato F, Parenti A, Rampazzo E, Basso G, Leo G, Rosato A, Bicciato S, Cordenonsi M and Piccolo S. SHARP1 suppresses breast cancer metastasis by promoting degradation of hypoxia-inducible factors. Nature. 2012; 487:380-384.

39. Kaya AO, Gunel N, Benekli M, Akyurek N, Buyukberber S, Tatli H, Coskun U, Yildiz R, Yaman E and Ozturk B. Hypoxia inducible factor-1 alpha and carbonic anhydrase IX overexpression are associated with poor survival in breast cancer patients. Journal of BUON : official journal of the Balkan Union of Oncology. 2012; 17:663-668.

40. Trastour C, Benizri E, Ettore F, Ramaioli A, Chamorey E, Pouyssegur J and Berra E. HIF-1alpha and CA IX staining in invasive breast carcinomas: prognosis and treatment outcome. Int J Cancer. 2007; 120:1451-1458.

41. Louie E, Nik S, Chen JS, Schmidt M, Song B, Pacson C, Chen XF, Park S, Ju J and Chen EI. Identification of a stem-like cell population by exposing metastatic breast cancer cell lines to repetitive cycles of hypoxia and reoxygenation. Breast Cancer Res. 2010; 12:R94.

42. Chen X, Iliopoulos D, Zhang Q, Tang Q, Greenblatt MB, Hatziapostolou M, Lim E, Tam WL, Ni M, Chen Y, Mai J, Shen H, Hu DZ, Adoro S, Hu B, Song M, et al. XBP1 promotes triple-negative breast cancer by controlling the HIF1alpha pathway. Nature. 2014; 508:103-107.

43. Schwab LP, Peacock DL, Majumdar D, Ingels JF, Jensen LC, Smith KD, Cushing RC and Seagroves TN. Hypoxia-inducible factor 1alpha promotes primary tumor growth and tumor-initiating cell activity in breast cancer. Breast cancer research : BCR. 2012; 14:R6.

44. Simoes BM, Piva M, Iriondo O, Comaills V, Lopez-Ruiz JA, Zabalza I, Mieza JA, Acinas O and Vivanco MD. Effects of estrogen on the proportion of stem cells in the breast. Breast Cancer Res Treat. 2011; 129:23-35.

45. Shipitsin M, Campbell LL, Argani P, Weremowicz S, Bloushtain-Qimron N, Yao J, Nikolskaya T, Serebryiskaya T, Beroukhim R, Hu M, Halushka MK, Sukumar S, Parker LM, Anderson KS, Harris LN, Garber JE, et al. Molecular definition of breast tumor heterogeneity. Cancer cell. 2007; 11:259-273.

46. Jung YS, Lee SJ, Yoon MH, Ha NC and Park BJ. Estrogen receptor alpha is a novel target of the Von Hippel-Lindau protein and is responsible for the proliferation of VHL-deficient cells under hypoxic conditions. Cell cycle. 2012; 11:4462-4473.

47. Stoner M, Saville B, Wormke M, Dean D, Burghardt R and Safe S. Hypoxia induces proteasome-dependent degradation of estrogen receptor alpha in ZR-75 breast cancer cells. Molecular endocrinology. 2002; 16:2231-2242.

48. Cooper C, Liu GY, Niu YL, Santos S, Murphy LC and Watson PH. Intermittent hypoxia induces proteasome-dependent down-regulation of estrogen receptor alpha in human breast carcinoma. Clinical cancer research : an official journal of the American Association for Cancer Research. 2004; 10:8720-8727.

49. Yi JM, Kwon HY, Cho JY and Lee YJ. Estrogen and hypoxia regulate estrogen receptor alpha in a synergistic manner. Biochemical and biophysical research communications. 2009; 378:842-846.

50. Ryu K, Park C and Lee Y. Hypoxia-inducible factor 1 alpha represses the transcription of the estrogen receptor alpha gene in human breast cancer cells. Biochemical and biophysical research communications. 2011; 407:831-836.

51. Lloyd MC, Alfarouk KO, Verduzco D, Bui MM, Gillies RJ, Ibrahim ME, Brown JS and Gatenby RA. Vascular measurements correlate with estrogen receptor status. BMC cancer. 2014; 14:279.

52. Liu S, Cong Y, Wang D, Sun Y, Deng L, Liu Y, Martin-Trevino R, Shang L, McDermott SP, Landis MD, Hong S, Adams A, D'Angelo R, Ginestier C, Charafe-Jauffret E, Clouthier SG, et al. Breast cancer stem cells transition between epithelial and mesenchymal states reflective of their normal counterparts. Stem cell reports. 2014; 2:78-91.

53. Zomer A, Ellenbroek SI, Ritsma L, Beerling E, Vrisekoop N and Van Rheenen J. Intravital imaging of cancer stem cell plasticity in mammary tumors. Stem cells. 2013; 31:602-606.

54. Jogi A, Ora I, Nilsson H, Lindeheim A, Makino Y, Poellinger L, Axelson H and Pahlman S. Hypoxia alters gene expression in human neuroblastoma cells toward an immature and neural crest-like phenotype. Proc Natl Acad Sci U S A. 2002; 99:7021-7026.

55. Heddleston JM, Li Z, Lathia JD, Bao S, Hjelmeland AB and Rich JN. Hypoxia inducible factors in cancer stem cells. British journal of cancer. 2010; 102:789-795.

56. Mazumdar J, Hickey MM, Pant DK, Durham AC, Sweet-Cordero A, Vachani A, Jacks T, Chodosh LA, Kissil JL, Simon MC and Keith B. HIF-2alpha deletion promotes Kras-driven lung tumor development. Proc Natl Acad Sci U S A. 2010; 107:14182-14187.

57. Takubo K, Goda N, Yamada W, Iriuchishima H, Ikeda E, Kubota Y, Shima H, Johnson RS, Hirao A, Suematsu M and Suda T. Regulation of the HIF-1alpha level is essential for hematopoietic stem cells. Cell Stem Cell. 2010; 7:391-402.

58. Zhang H, Li H, Xi HS and Li S. HIF1alpha is required for survival maintenance of chronic myeloid leukemia stem cells. Blood. 2012; 119:2595-2607.

59. Casanovas O, Hicklin DJ, Bergers G and Hanahan D. Drug resistance by evasion of antiangiogenic targeting of VEGF signaling in late-stage pancreatic islet tumors. Cancer Cell. 2005; 8:299-309.

60. Paez-Ribes M, Allen E, Hudock J, Takeda T, Okuyama H, Vinals F, Inoue M, Bergers G, Hanahan D and Casanovas O. Antiangiogenic therapy elicits malignant progression of tumors to increased local invasion and distant metastasis. Cancer Cell. 2009; 15:220-231.

61. Kim M, Neinast MD, Frank AP, Sun K, Park J, Zehr JA, Vishvanath L, Morselli E, Amelotte M, Palmer BF, Gupta RK, Scherer PE and Clegg DJ. ERalpha upregulates Phd3 to ameliorate HIF-1 induced fibrosis and inflammation in adipose tissue. Molecular metabolism. 2014; 3:642-651.

62. Su Y, Loos M, Giese N, Hines OJ, Diebold I, Gorlach A, Metzen E, Pastorekova S, Friess H and Buchler P. PHD3 regulates differentiation, tumour growth and angiogenesis in pancreatic cancer. British journal of cancer. 2010; 103:1571-1579.

63. Fu J and Taubman MB. Prolyl hydroxylase EGLN3 regulates skeletal myoblast differentiation through an NF-kappaB-dependent pathway. The Journal of biological chemistry. 2010; 285:8927-8935.

64. Liu M, Sakamaki T, Casimiro MC, Willmarth NE, Quong AA, Ju X, Ojeifo J, Jiao X, Yeow WS, Katiyar S, Shirley LA, Joyce D, Lisanti MP, Albanese C and Pestell RG. The canonical NF-kappaB pathway governs mammary tumorigenesis in transgenic mice and tumor stem cell expansion. Cancer Res. 2010; 70:10464-10473.

65. Yamamoto M, Taguchi Y, Ito-Kureha T, Semba K, Yamaguchi N and Inoue J. NF-kappaB non-cell-autonomously regulates cancer stem cell populations in the basal-like breast cancer subtype. Nature communications. 2013; 4:2299.

66. Kendellen MF, Bradford JW, Lawrence CL, Clark KS and Baldwin AS. Canonical and non-canonical NF-kappaB signaling promotes breast cancer tumor-initiating cells. Oncogene. 2014; 33:1297-1305.

67. Wei L, Liu TT, Wang HH, Hong HM, Yu AL, Feng HP and Chang WW. Hsp27 participates in the maintenance of breast cancer stem cells through regulation of epithelial-mesenchymal transition and nuclear factor-kappaB. Breast Cancer Res. 2011; 13:R101.

68. Ju JH, Jang K, Lee KM, Kim M, Kim J, Yi JY, Noh DY and Shin I. CD24 enhances DNA damage-induced apoptosis by modulating NF-kappaB signaling in CD44-expressing breast cancer cells. Carcinogenesis. 2011; 32:1474-1483.

69. Dontu G, Abdallah WM, Foley JM, Jackson KW, Clarke MF, Kawamura MJ and Wicha MS. *In vitro* propagation and transcriptional profiling of human mammary stem/progenitor cells. Genes Dev. 2003; 17:1253-1270.

70. Azzam DJ, Zhao D, Sun J, Minn AJ, Ranganathan P, Drews-Elger K, Han X, Picon-Ruiz M, Gilbert CA, Wander SA, Capobianco AJ, El-Ashry D and Slingerland JM. Triple negative breast cancer initiating cell subsets differ in functional and molecular characteristics and in gamma-secretase inhibitor drug responses. EMBO Mol Med. 2013; 5:1502-1522.

71. Vivanco M. Function follows form: defining mammary stem cells. Sci Transl Med. 2010; 2:31ps22.

72. Liu Y, Nenutil R, Appleyard MV, Murray K, Boylan M, Thompson AM and Coates PJ. Lack of correlation of stem cell markers in breast cancer stem cells. British journal of cancer. 2014; 110:2063-2071.

73. Vivanco MD, Johnson R, Galante PE, Hanahan D and Yamamoto KR. A transition in transcriptional activation by the glucocorticoid and retinoic acid receptors at the tumor stage of dermal fibrosarcoma development. Embo J. 1995; 14:2217-2228.

74. Campa VM, Baltziskueta E, Bengoa-Vergniory N, Gorrono-Etxebarria I, Wesolowski R, Waxman J and Kypta RM. A screen for transcription factor targets of glycogen synthase kinase-3 highlights an inverse correlation of NFkappaB and androgen receptor signaling in prostate cancer. Oncotarget. 2014; 5:8173-8187.

75. Ranuncolo SM, Pittaluga S, Evbuomwan MO, Jaffe ES and Lewis BA. Hodgkin lymphoma requires stabilized NIK and constitutive RelB expression for survival. Blood. 2012; 120:3756-3763.

76. Richard DE, Berra E, Gothie E, Roux D and Pouyssegur J. p42/p44 mitogen-activated protein kinases phosphorylate hypoxia-inducible factor 1alpha (HIF-1alpha) and enhance the transcriptional activity of HIF-1. The Journal of biological chemistry. 1999; 274:32631-32637.

77. Berra E, Benizri E, Ginouves A, Volmat V, Roux D and Pouyssegur J. HIF prolyl-hydroxylase 2 is the key oxygen sensor setting low steady-state levels of HIF-1alpha in normoxia. EMBO J. 2003; 22:4082-4090.

78. Elizalde C, Campa VM, Caro M, Schlangen K, Aransay AM, Vivanco M and Kypta RM. Distinct roles for Wnt-4 and Wnt-11 during retinoic acid-induced neuronal differentiation. Stem cells. 2011; 29:141-153.

79. Iriondo O, Rabano M and Vivanco MD. FACS Sorting Mammary Stem Cells. Methods in molecular biology. 2015; 1293:63-72.

80. Bengoa-Vergniory N, Gorroño-Etxebarria I, González-Salazar I and Kypta RM. A switch from canonical to noncanonical Wnt signaling mediates early differentiation of human neural stem cells. Stem Cells. 2014; 32:3196-208.

Rev Senol Patol Mamar. 2014;27(4):149–156

Revista de Senología y Patología Mamaria

www.elsevier.es/senologia

ORIGINAL

Respuesta hormonal de las células madre de mama y resistencia a tamoxifeno

Giacomo Domenici[a], **Miriam Rábano**[a], **Marco Piva**[a], **Oihana Iriondo**[a], **Ignacio Zabalza**[b], **José Antonio López-Ruiz**[c] y **María del Mar Vivanco**[a,*]

[a] *CIC bioGUNE, Derio, Vizcaya, España*
[b] *Servicio de Anatomía Patológica, Hospital Galdakao-Usansolo, Galdakao, Vizcaya, España*
[c] *Pretelmagen, Bilbao, España*

Recibido el 3 de mayo de 2014; aceptado el 23 de julio de 2014
Disponible en Internet el 27 de septiembre de 2014

PALABRAS CLAVE
Estrógeno;
Tamoxifeno;
Fulvestrant;
Células madre;
Células madre cancerosas;
Resistencia a terapia;
Sox2;
Biomarcador

Resumen
Objetivo: Determinar la influencia a nivel celular y molecular de varios tratamientos hormonales (estrógeno, tamoxifeno y fulvestrant) sobre las células epiteliales y las células madre de la mama sana y tumoral.
Métodos: Se emplearon muestras de tejido mamario sano y tumoral, así como líneas celulares de cáncer de mama y células resistentes a tamoxifeno, para analizar los efectos de las hormonas sobre la proliferación y diferenciación celular.
Resultados: Las células epiteliales y las células madre de la mama respondieron de forma diferente a los tratamientos hormonales. Las células resistentes a tamoxifeno presentaban un mayor contenido de células madre cancerosas y expresaban niveles de Sox2 más elevados, mientras que los niveles de expresión del receptor de progesterona eran muy bajos. Las células resistentes a tamoxifeno eran, además, más resistentes al tratamiento con fulvestrant.
Conclusiones: El desarrollo de resistencia a tamoxifeno está asociado con un incremento en el contenido de células madre cancerosas. El tratamiento con fulvestrant no parece disminuir la población de células madre cancerosas. Sox2 podría ser un biomarcador de resistencia a tamoxifeno en el cáncer de mama.

KEYWORDS
Estrogen;
Tamoxifen;
Fulvestrant;
Stem cells;

Hormone response of breast stem cells and tamoxifen resistance

Abstract
Objective: To determine the influence of various hormones (estrogen, tamoxifen and fulvestrant) on cell proliferation and differentiation in normal and cancer breast stem cells.

* Autor para correspondencia.
Correo electrónico: mdmvivanco@cicbiogune.es (M.d.M. Vivanco).

http://dx.doi.org/10.1016/j.senol.2014.07.006

Cancer stem cells;
Resistance;
Sox2;
Biomarker

Methods: Primary tissue samples, breast cancer cell lines and tamoxifen-resistant cells were used to analyze the effects of hormones on cell proliferation and differentiation.
Results: Breast epithelial cells and stem cells responded differentially to hormone treatments. Tamoxifen-resistant cells showed increased cancer stem cell content and expressed higher Sox2 levels, while progesterone receptor levels were very low. Tamoxifen-resistant cells were resistant to fulvestrant treatment.
Conclusions: The development of tamoxifen resistance is associated with an increase in cancer stem cell content. Treatment with fulvestrant does not appear to reduce the cancer stem cell population. Sox2 could represent a biomarker of tamoxifen resistance in breast cancer.

Introducción

La glándula mamaria es un órgano altamente regenerativo que puede experimentar múltiples ciclos de proliferación, diferenciación y apoptosis durante diferentes etapas de la vida, como la pubertad, el embarazo o la lactancia. Esta capacidad evidenció la presencia en la mama de células con características de células madre, es decir, con capacidad de autorrenovación (dar lugar a células iguales a ellas mismas) y de diferenciación (en la mama, a células luminales y células mioepiteliales)[1]. Debido a su larga vida, las células madre tienen el potencial de sufrir mayor número de mutaciones y, por lo tanto, perder el control de sus propiedades y dar origen a un tumor.

El cáncer de mama es una enfermedad muy heterogénea a nivel histológico y, sobre todo, a nivel molecular. Esta heterogeneidad se ve reflejada también a nivel celular con la identificación, en los carcinomas de mama, de una pequeña subpoblación de células con características de células madre, las células madre cancerosas (CSC).

Hoy en día es un hecho aceptado que las vías de señalización que controlan el destino y la función de las células madre se encuentran con frecuencia alteradas en el cáncer de mama y otros tipos de cáncer[2]. En consecuencia, se ha postulado la hipótesis de que las CSC son las células responsables de la iniciación de los tumores y, además, son más resistentes a las terapias actuales como la radioterapia[3], la quimioterapia[4] o la terapia hormonal[5]. Por otra parte, se ha demostrado que los tumores de alto grado contienen un mayor número de células con fenotipo de células madre que los tumores más diferenciados[6,7].

Se han empleado diferentes estrategias para identificar y caracterizar las células madre de la mama sana y tumoral, incluyendo la capacidad de formar mamoesferas[8], la presencia de células con fenotipo doble positivo (DP, es decir que expresan ambos antígenos de superficie, EMA^+ y $CALLA^+$)[9], con la expresión de los marcadores de superficie $CD44^+CD24^{-/low}$ [10], *side population* (SP, con mayor capacidad de expulsar la tinción Hoechst 33342)[11] o la elevada actividad aldehído deshigrogenasa[12]. En este estudio analizamos la respuesta de las células madre de la mama, empleando varios de estos fenotipos, para investigar la influencia de los estrógenos, tamoxifeno y fulvestrant sobre las células madre en la mama sana y en cáncer de mama, con especial énfasis en su implicación en la resistencia a la terapia hormonal.

Pacientes y métodos

Pacientes

El tejido de mama sano (n = 15) fue obtenido de mujeres premenopáusicas sin historia previa de cáncer de mama, que se sometieron a mamoplastia de reducción. Las muestras de tumores (n = 10) fueron obtenidas de mujeres con cáncer de mama (rango de edad de 42 a 80 años, sin criterios de inclusión ni exclusión, las muestras incluían diferentes tipos de carcinomas mamarios). En todos los casos las pacientes ofrecieron su consentimiento informado y firmado, y todos los procedimientos fueron aprobados por el Comité Ético de Investigación Clínica de Euskadi y del Hospital de Galdakao-Usansolo.

Materiales y métodos

Procesamiento del tejido mamario

El tejido mamario fue procesado inmediatamente para su estudio, como se ha descrito previamente[13]. El tejido fue cortado y digerido con colagenasa a 37 °C. Después de varios lavados, los organoides (fragmentos muy pequeños de epitelio mamario, ductales y lobuloalveolares, obtenidos directamente tras la digestión del tejido mamario) fueron separados, filtrados y disgregados para dar lugar a una suspensión celular. Las células tumorales fueron aisladas empleando el mismo procedimiento.

Cultivo celular

Las líneas MCF-7 y T47D se obtuvieron de la *American Type Culture Collection*, y las células resistentes a tamoxifeno de estas líneas celulares (MCF-7-TamR y T47D-TamR) fueron desarrolladas manteniendo las células en presencia de una concentración de 5×10^{-7} M de 4-OH-tamoxifeno durante más de 6 meses. Las líneas fueron mantenidas en medio DMEM/F-12 con GlutaMAX™ suplementado al 10% con suero fetal bovino y con 1% penicilina/estreptomicina a 37 °C y atmósfera del 5% de CO_2. Las mamosferas se cultivaron durante una semana en medio DMEM/F-12 con GlutaMAX™,

suplementado con 0,5X de B27 (Gibco), 10 ng/ml EGF (Invitrogen), 2 ng/ml bFGF (Invitrogen) y 1% penicilina-estreptomicina a 37 °C y atmósfera del 5% de CO_2.

Preparación y análisis de ácido ribonucleico y proteínas

El ARN total se extrajo siguiendo las recomendaciones del fabricante (Illustra™ RNAspin Mini Isolation Kit, GE Healthcare). La síntesis de ARN y su análisis cuantitativo por reacción en cadena de la polimerasa se llevó a cabo en un equipo 7300 Real-Time PCR System de 96 pocillos (Applied Biosystems), según se ha detallado previamente[14]. Los *primers* utilizados fueron: Sox2, *forward primer* (5'-3'): GCACATGAACGGCTGGAGCAACG, *reverse:* TGCTGCGAGTAGGACATGCTGTAGG; receptor de progesterona (PR), *forward:* CGCGCTCTACCCTGCACTC, *reverse:* TGAATCCGGCCTCAGGTAGTT; control 36B4, *forward:* GTGTTCGACAATGGCAGCAT, *reverse:* GACACCCTCCAGGAAGCGA. Las condiciones fueron 5 min a 95 °C, 15 s a 95 °C y 60 s a 65 °C. Así mismo, en ese trabajo se podrán encontrar detalles del análisis de proteínas por *western blotting* e inmunohistoquímica. Para el análisis por *western blotting* las células fueron extraídas directamente en solución Laemmli (Sigma). Los anticuerpos empleados fueron los siguientes: beta-actina (Sigma, AC-15/A5441), PR (Novocastra, PGR-312), Sox2 (Santa Cruz, sc-17320), HER2 (Cell Signaling, 2165). Para el estudio inmunohistoquímico, las muestras de carcinomas, fijadas en formalina y embebidas en parafina, fueron procesadas empleando el sistema Leica Bond-III y los tampones de Novocastra. Se siguió un paso de precalentamiento para el desenmascaramiento (20 min, 100 °C), y las secciones fueron lavadas e incubadas con el anticuerpo contra Sox2 (Stem Cells Technologies) durante 20 min a temperatura ambiente. La peroxidasa fue bloqueada durante 10 min, seguida de HRP y DAB con hematoxilina para el contraste. Los controles negativos incluyeron la omisión del primer anticuerpo y el uso de un anticuerpo control IgG.

Cuantificación y aislamiento de las poblaciones de células madre

Para medir la actividad enzimática de aldehído deshidrogenasa en las células se llevó a cabo el ensayo ALDEFLUOR™ de acuerdo con el protocolo de la compañía (Stemcell Technologies). Para el fenotipo SP y las tinciones con anticuerpos de superficie contra EMA (BD, 559774) y CALLA (Dako, SS2/36) (DP) se siguieron los protocolos empleados previamente[9]. Para la tinción del fenotipo CD44/CD24 se emplearon los anticuerpos: CD44-APC (BD, G44-26) y CD24-PE (BD, ML5)[5]. Todas las muestras se examinaron en un citómetro de flujo FACSAria™. Los resultados se analizaron utilizando el programa FACSDiva™.

Ensayo de proliferación

Las células MCF-7 y T47D fueron sembradas por triplicado en placa de 96 pocillos y tratadas con crecientes concentraciones de ICI 182,720 (Fulvestrant) y etanol como vehículo del fármaco. Después de 5 días, las células fueron lavadas y fijadas con una solución de cristal violeta y metanol, y la concentración de cristal violeta retenida fue cuantificada en un espectrofotómetro a 595 nm. Los resultados son mostrados como *fold change proliferation*, es decir, el cambio en la proliferación celular producido como consecuencia del tratamiento hormonal con respecto al efecto en las células tratadas con el vehículo solo (MCF-7, n = 7, T47D, n = 5; $p < 0{,}05$).

Análisis estadístico

Datos de por lo menos 3 experimentos independientes fueron expresados como media ± DE. El test de la t de Student

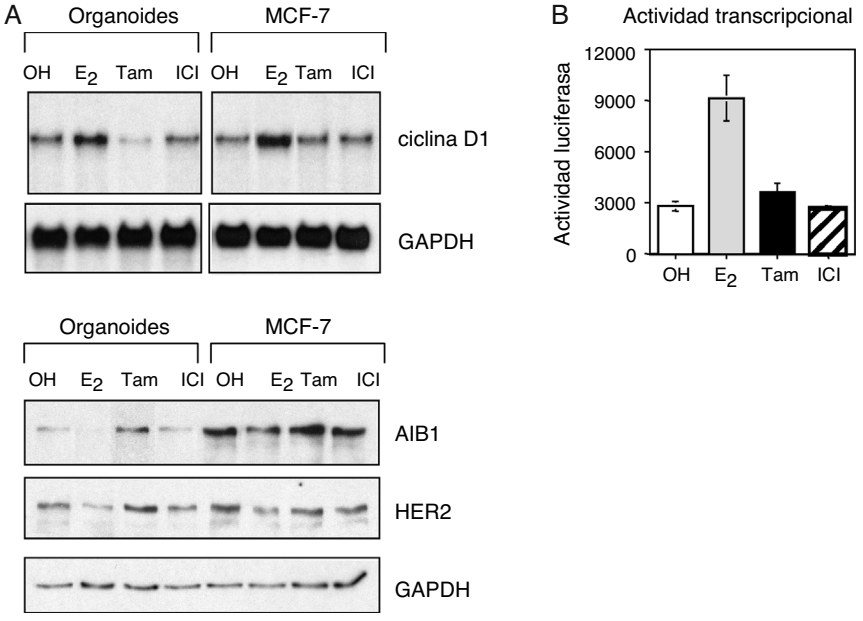

Figura 1 Las células epiteliales de la mama responden al tratamiento hormonal. A. Análisis por Western blot de los niveles de expresión de ciclina D1, AIB1 y HER2 en organoides aislados de tejido mamario sano y en células de cáncer de mama MCF-7. B. Actividad transcripcional del receptor de estrógeno en células epiteliales de mama transfectadas con un gen reportero de luciferasa y tratadas con 10^{-8} M estrógeno (E_2), 10^{-7} M tamoxifeno (Tam) o 10^{-7} M fulvestrant (ICI 182,780, ICI).

fue empleado para determinar las diferencias estadísticamente significativas, y $p < 0{,}05$ fue considerado significativo.

Resultados

Las células epiteliales de mama responden a los tratamientos hormonales

Para estudiar la respuesta de la mama a los tratamientos hormonales se determinó la actividad transcripcional del receptor de estrógeno (ER) en células de mama sana. Las células epiteliales fueron tratadas con diferentes hormonas: 17-beta-estradiol (estrógeno), 4-hidroxitamoxifeno (tamoxifeno), el antagonista completo ICI 182,780 (Faslodex®, nombre genérico: fulvestrant), o el control (etanol) durante un periodo de 24 h. La activación del receptor por el estrógeno dio lugar a niveles de expresión más elevados de genes diana dependientes de estrógeno, como la ciclina D1, y redujo la expresión de AIB1 y HER2 (fig. 1A). Por otra parte, los antagonistas tamoxifeno y fulvestrant ejercieron el efecto contrario, dando lugar a una reducción de los niveles de ciclina D1 y un incremento en los niveles de AIB1 y HER2. Es interesante destacar que en las células de cáncer de mama MCF-7, empleadas como control positivo y estudiadas con frecuencia en los laboratorios como modelo de cáncer de mama ER-positivo, se obtuvo la misma respuesta. Además, se analizó la actividad transcripcional de ER empleando el ensayo de la actividad luciferasa. Estos ensayos mostraron una mayor actividad de ER en respuesta al estrógeno, mientras que los antagonistas no tuvieron ningún efecto (fig. 1B). En conjunto, estas observaciones demuestran que las células epiteliales de la mama sana responden a través del receptor de estrógeno a los tratamientos hormonales.

La población de células madre cancerosas se enriquece con los tratamientos antiestrogénicos

Para examinar los niveles de expresión de ER en los diferentes tipos celulares en la mama sana, las células epiteliales fueron separadas por *fluorescence activated cell sorting*, lo que permite aislar los diferentes tipos celulares basándose en el marcaje celular diferencial con un marcador de fluorescencia. En este caso, se aislaron las células diferenciadas en base a la expresión de proteínas de superficie específicas: EMA^+, que identifica las células luminales, y CD10 o $CALLA^+$, a las células mioepiteliales; por otro lado, se sortearon las células madre con fenotipo SP[9]. Se observó que aproximadamente el 25% de las células luminales (EMA^+) expresaban ER (fig. 2A). Sin embargo, las células madre con fenotipo SP no expresaban ER, así como tampoco las células mioepiteliales ($CALLA^+$). Estos resultados confirman la ausencia de ER en las células madre de mama sana.

A continuación se investigó la influencia de las hormonas sobre diferentes poblaciones de células madre. El tratamiento con estrógeno redujo de forma significativa el porcentaje de células madre en la mama sana, mientras que tamoxifeno ejercía el efecto contrario, y estos efectos se observaron con varios fenotipos diferentes, incluyendo formación de mamoesferas (fig. 2B) y porcentaje de células DP

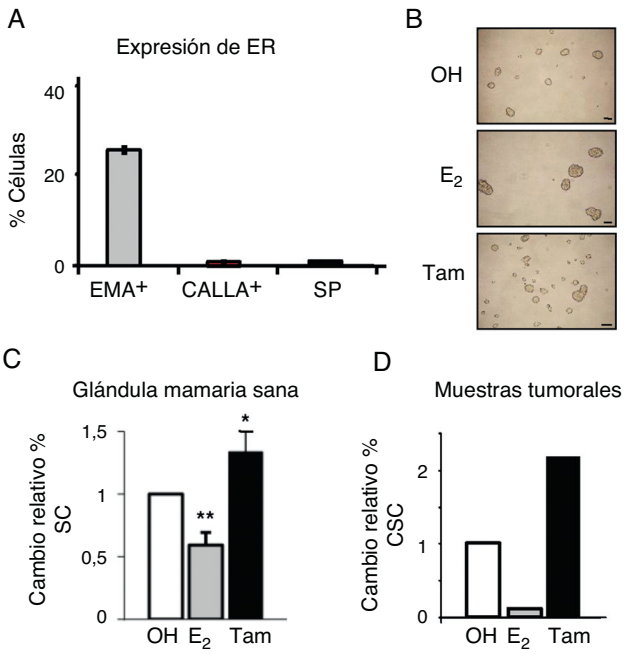

Figura 2 La población de células madre se enriquece en respuesta al tratamiento con tamoxifeno. A. Expresión de ER (mARN) en células epiteliales de mama sana a nivel unicelular, representado como el porcentaje de cada tipo de células que expresa ER, EMA^+ (luminales), $CALLA^+$ (mioepiteliales) y SP *(stem cells)*. B. Fotografía representativa de las mamoesferas formadas por células MCF-7 tratadas con estrógeno (E_2), tamoxifeno (Tam) o el control (OH). C. Porcentaje de células madre (SC) con fenotipo DP en células de mama sana tratadas con estrógeno o tamoxifeno. D. Porcentaje de células madre cancerosas (CSC) con fenotipo $CD44^+CD24^{-/low}$ en células de cáncer de mama tratadas con estrógeno o tamoxifeno.

(EMA^+, $CALLA^+$) (fig. 2C). Igualmente, en las células de cáncer de mama aisladas de tumores primarios, el estrógeno reducía de forma significativa el porcentaje de CSC, mientras que se observaba un enriquecimiento de la población de CSC en respuesta a tamoxifeno (fig. 2D). Estas observaciones indican que el estrógeno reduce la población de células madre sanas y cancerosas en la mama.

Los tumores resistentes a tamoxifeno contienen más células madre cancerosas, y expresan niveles más elevados de Sox2 y más reducidos de receptor de progesterona

La observación de que la población de células madre se enriquece en respuesta a tamoxifeno daba lugar a la pregunta sobre sus consecuencias en el contexto del desarrollo de resistencia al mismo. Para examinar el papel de las CSC en este proceso se empleó un modelo de resistencia a tamoxifeno desarrollado a partir de 2 líneas celulares de cáncer de mama, MCF-7 y T47D, que desarrollaron resistencia a tamoxifeno tras varios meses de exposición a la terapia[5]. Estas células expresan ER, pero el receptor es menos activo a nivel transcripcional, como se puede inferir por los niveles muy reducidos de expresión de uno de sus genes diana más

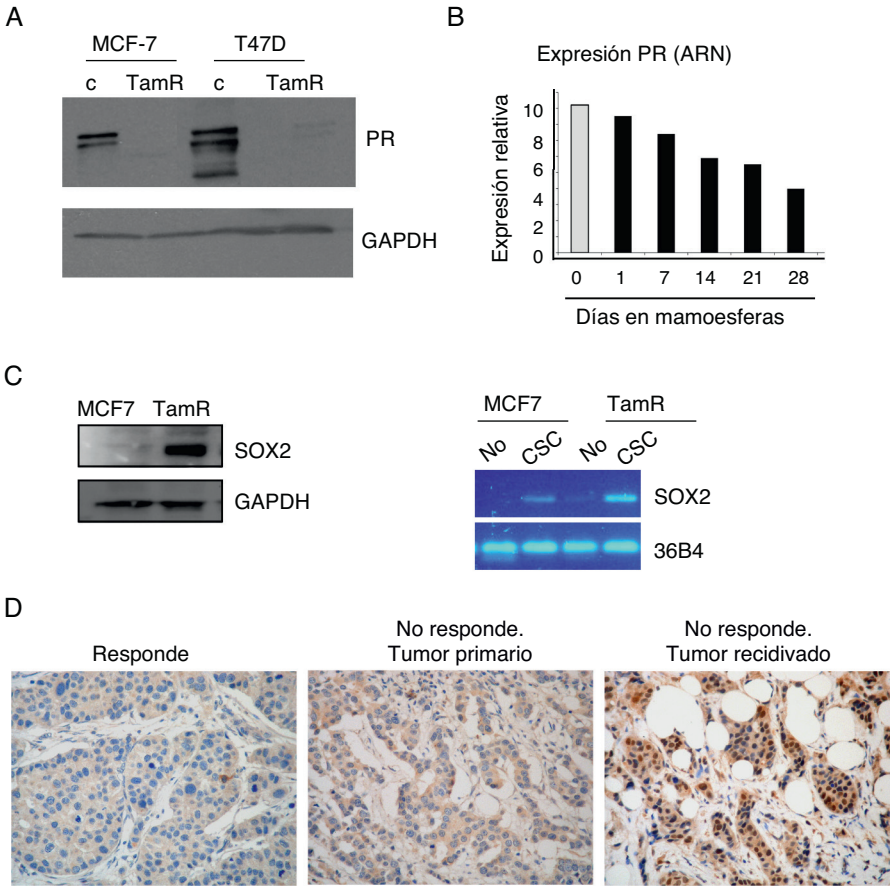

Figura 3 Mayor contenido de CSC en células resistentes a tamoxifeno. A. Análisis por Western blot de los niveles de expresión del receptor de progesterona (PR) en células MCF-7 y T47D parentales (c) o resistentes a tamoxifeno (TamR). GAPDH es el control de carga. B. Niveles de expresión de PR a nivel de ARN en células adherentes (barra gris) o en mamoesferas durante varios días en cultivo (barras negras). C. Análisis de los niveles de Sox2 por Western blot (izquierda) o ARN (derecha) en células CSC con fenotipo $CD44^{+}CD24^{-/low}$ o no *stem*. GAPDH y 36B4 se emplearon como controles en cada caso. D. Estudio por inmunohistoquímica de la expresión de Sox2 en muestras de cáncer de mama ER-positivo. Izquierda, ejemplo representativo de muestra de tumor que respondió al tratamiento hormonal («Responde»); centro, ejemplo de muestra del tumor primario de una paciente que no respondió a tamoxifeno («No responde. Tumor primario); derecha, ejemplo de muestra de la recidiva desarrollada después del fallo de la terapia hormonal («No responde. Tumor recidivado»).

empleado en la clínica, el PR (fig. 3A). De hecho, observamos que el cultivo de las células de cáncer MCF-7 en mamoesferas, es decir, en condiciones de enriquecimiento de CSC, es suficiente para reducir considerablemente los niveles de expresión de PR (fig. 3B).

Para examinar el contenido de CSC se analizaron los niveles de expresión de Sox2, un marcador de células madre, y se observó que las células resistentes a tamoxifeno expresan niveles más altos de Sox2 que las células de cáncer parentales. Además, cuando las CSC fueron separadas del resto de las células tumorales, se observó que Sox2 se expresa de forma claramente mayoritaria en las CSC con respecto al resto de las células (fig. 3C). Estos resultados alentaron el análisis retrospectivo de los niveles de Sox2 en muestras tisulares de 55 pacientes con cáncer de mama. Los niveles de Sox2 eran apenas detectables en los tumores de aquellas pacientes que respondieron al tratamiento con tamoxifeno (un ejemplo representativo lo observamos en la figura 3D, como «Responde»). Sin embargo, los tumores primarios de pacientes que, más tarde, desarrollaron resistencia a tamoxifeno ya presentaban niveles significativos de Sox2 (fig. 3D, «No responde. Tumor primario»). Además, las recidivas de estas pacientes presentaban niveles de Sox2 aún más elevados (fig. 3D, «No responde. Tumor recidiva»). Estas observaciones confirman que los tumores resistentes a tamoxifeno presentan un mayor contenido de CSC, niveles reducidos de PR y elevada expresión de Sox2, lo cual sugiere que Sox2 podría ser un marcador de resistencia a tamoxifeno.

Las células madre cancerosas resistentes a tamoxifeno también lo son a fulvestrant

Se ha planteado el uso de fulvestrant como tratamiento alternativo a tamoxifeno cuando este falla como terapia endocrina. En primer lugar, se trataron células de cáncer de mama T47D con fulvestrant y se examinó el porcentaje de CSC con fenotipo positivo para aldehído deshidrogenasa. Como resultado de este tratamiento el porcentaje de CSC

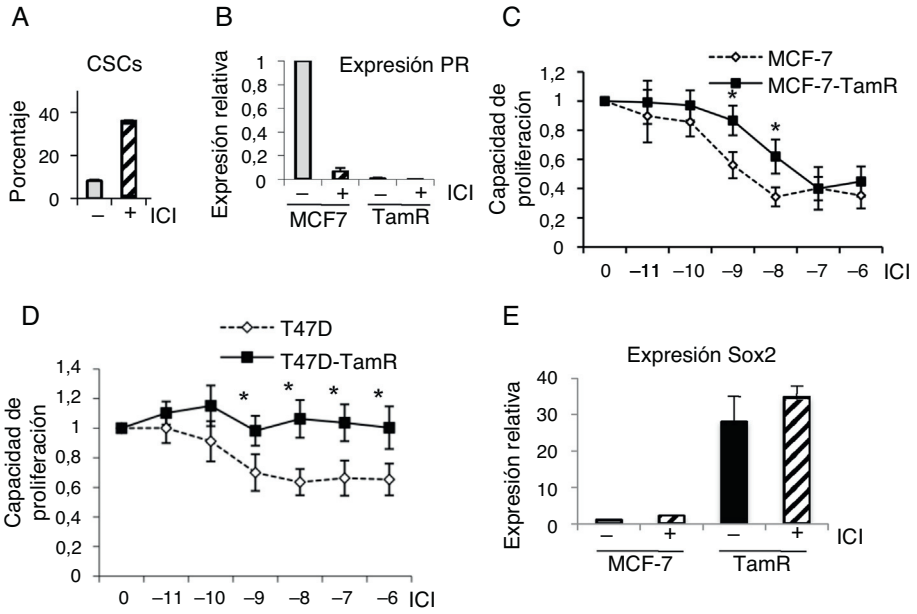

Figura 4 Células resistentes a tamoxifeno son resistentes a fulvestrant. A. Porcentaje de CSC (con fenotipo $ALDH^+$) en células T47D, con fenotipo ALDH-positivas, en presencia o ausencia de fulvestrant (ICI). B. Análisis de expresión de PR (ARN) en células MCF-7 y resistentes a tamoxifeno (TamR) en presencia o ausencia de fulvestrant. C y D. Ensayo de proliferación de células MCF-7 y MCF-7-TamR (C) y células T47D y T47D-TamR (D) tratadas con concentraciones crecientes de fulvestrant ($p < 0,05$). E. Niveles de expresión de Sox2 en células MCF-7 y resistentes a tamoxifeno en presencia o ausencia de fulvestrant.

se incrementó (fig. 4A). Por otra parte, el tratamiento con fulvestrant de células MCF-7 parentales y MCF-7 resistentes a tamoxifeno resultó en una fuerte reducción de los niveles de PR, indicando que el antagonista destruye el ER (fig. 4B y datos no mostrados). Para determinar la respuesta a fulvestrant de las células resistentes a tamoxifeno se realizaron ensayos de viabilidad celular en presencia de concentraciones crecientes de fulvestrant. Ambos modelos celulares de resistencia a tamoxifeno, bien derivados de las células MCF-7 (fig. 4C), bien de las T47D (fig. 4D), mostraron que las células resistentes a tamoxifeno también lo son a fulvestrant.

Finalmente, los análisis del marcador Sox2 demostraron que los niveles de expresión de Sox2 se mantienen incrementados en las células resistentes a tamoxifeno tratadas con fulvestrant (fig. 4E), indicando que el contenido de CSC es muy alto en estas condiciones. Estos resultados evidencian que el tratamiento con fulvestrant mantiene el elevado porcentaje de CSC en las células resistentes a tamoxifeno, razón por la cual estos tumores son también resistentes a fulvestrant.

Discusión

Tamoxifeno ha sido empleado como tratamiento contra tumores ER-positivos durante muchos años. Sin embargo, la resistencia a tamoxifeno se desarrolla en un gran número de pacientes[15,16]. Con este trabajo hemos evaluado la respuesta de las células madre de la mama a los tratamientos hormonales y su implicación en la resistencia a tamoxifeno. Observamos que a pesar de que las células epiteliales de mama responden al tratamiento hormonal, las células madre pueden eludir sus efectos debido a la ausencia de ER. El estrógeno reduce la población de células madre, mientras que tamoxifeno la incrementa, lo que puede explicar el elevado contenido de Sox2, un marcador de CSC, y la notable reducción de los niveles de expresión de PR. Por otra parte, el tratamiento de las células resistentes a tamoxifeno con fulvestrant no elimina la población de CSC, lo que explica la resistencia a sus efectos antiproliferativos.

Tamoxifeno funciona como un antagonista de ER en la mama, uniéndose a dicho receptor y bloqueando su actividad transcripcional, mientras que fulvestrant degrada al receptor. Fulvestrant se puede emplear cuando el tratamiento con tamoxifeno, o con inhibidores de aromatasa, ha fallado. La posible utilidad de combinar fulvestrant con otros tratamientos está siendo investigada en ensayos clínicos, aunque algunos resultados preliminares son controvertidos, con frecuentes recidivas y pronósticos pobres[17–19]. Es posible que algunos de estos resultados poco prometedores puedan ser explicados por la observada capacidad de las células de resistir a los efectos de fulvestrant y el mantenimiento de la población de CSC, a pesar del tratamiento.

Se ha especulado que con los tratamientos anticancerosos actuales, una subpoblación de células, las CSC o células iniciadoras del tumor, pueden reiniciar el crecimiento de este después de la terapia en un considerable número de pacientes. Nuestros resultados coinciden con las observaciones obtenidas en varios laboratorios, que muestran que los tratamientos actuales eliminan la mayoría de la masa tumoral, resultando en un enriquecimiento del contenido de CSC, debido al hecho de que estas células pueden ignorar sus efectos y no verse afectadas por estos tratamientos[1,20].

Las células madre en la mama sana son las responsables de la formación de nuevas células epiteliales depen-

diendo de las necesidades del organismo. Varios grupos de investigación, incluyendo el nuestro, han demostrado previamente que las células madre no expresan ER, o lo hacen a niveles muy bajos[9,21]. En el caso de las células tumorales tratadas con tamoxifeno, la ausencia de ER en las células madre facilita que las CSC se vuelvan insensibles a los efectos antiproliferativos de tamoxifeno (o de fulvestrant) y seguir creciendo, mientras las células más diferenciadas, que expresan ER, desaparecen, dando lugar a un tumor con mayor contenido de CSC y, por lo tanto, más agresivo[5]. En consonancia con estas observaciones, Sox2 también ha sido implicado en el mantenimiento de la población de CSC y en la resistencia a terapia en varios tipos de carcinomas, incluyendo glioblastoma[22], cáncer de próstata[23] y melanomas[24]. La elevada expresión de Sox2 en las muestras clínicas de pacientes con recidivas confirma observaciones previas, que mostraban tumores de mama pobremente diferenciados con una incrementada expresión de genes normalmente enriquecidos en células madre embrionarias[25] y con una mayor proporción de CSC que los tumores bien diferenciados[7], apoyando la noción de que el contenido de CSC refleja la malignidad del tumor[6].

La correlación detectada entre los niveles de Sox2 y el desarrollo de resistencia a la terapia garantiza una sólida base para un estudio más detallado y amplio sobre el uso de Sox2 como marcador de resistencia a tamoxifeno, en los carcinomas de mama. La posible aplicación práctica de nuestros resultados es que la combinación de terapia endocrina para eliminar las células ER-positivas, junto con un inhibidor de Sox2 para atacar a las células madre, podría suponer una nueva estrategia terapéutica para prevenir la recurrencia en determinados grupos de pacientes con cáncer de mama.

En conclusión, el desarrollo de resistencia a tamoxifeno en cáncer de mama implica un incremento en el contenido de células madre cancerosas. El tratamiento con el antagonista fulvestrant no disminuye de forma significativa la población de células madre cancerosas. Sox2 podría ser un biomarcador de resistencia a tamoxifeno en el cáncer de mama.

Responsabilidades éticas

Protección de personas y animales. Los autores declaran que para esta investigación no se han realizado experimentos en seres humanos ni en animales.

Confidencialidad de los datos. Los autores declaran que en este artículo no aparecen datos de pacientes.

Derecho a la privacidad y consentimiento informado. Los autores declaran que en este artículo no aparecen datos de pacientes.

Conflicto de intereses

Los autores declaran no tener ningún conflicto de intereses.

Agradecimientos

Los autores expresan su gratitud a todas las pacientes por su interés en cooperar con este estudio. M.M. Vivanco agradece especialmente el apoyo otorgado por varios proyectos: FIS del Instituto de Salud Carlos III (PI11/02251), del Departamento de Sanidad del Gobierno de la Comunidad Autónoma del País Vasco (PI2009-7) y de la Sociedad Española de Senología y Patología Mamaria.

Bibliografía

1. Simões BM, Vivanco MD. Cancer stem cells in the human mammary gland and regulation of their differentiation by estrogen. Future Oncol. 2011;7:995–1006.
2. Visvader JE, Lindeman GJ. Cancer stem cells: Current status and evolving complexities. Cell Stem Cell. 2012;10:717–28.
3. Woodward WA, Chen MS, Behbod F, Alfaro MP, Buchholz TA, Rosen JM. WNT/beta-catenin mediates radiation resistance of mouse mammary progenitor cells. Proc Natl Acad Sci U S A. 2007;104:618–23.
4. Li X, Lewis MT, Huang J, Gutierrez C, Osborne CK, Wu MF, et al. Intrinsic resistance of tumorigenic breast cancer cells to chemotherapy. J Natl Cancer Inst. 2008;100:672–9.
5. Piva M, Domenici G, Iriondo O, Rábano M, Simões BM, Comaills V, et al. Sox2 promotes tamoxifen resistance in breast cancer cells. EMBO Mol Med. 2014;6:66–79.
6. Vivanco M. Function follows form: Defining mammary stem cells. Sci Transl Med. 2010;2, 31ps22.
7. Pece S, Tosoni D, Confalonieri S, Mazzarol G, Vecchi M, Ronzoni S, et al. Biological and molecular heterogeneity of breast cancers correlates with their cancer stem cell content. Cell. 2010;140:62–73.
8. Dontu G, Abdallah WM, Foley JM, Jackson KW, Clarke MF, Kawamura MJ, et al. In vitro propagation and transcriptional profiling of human mammary stem/progenitor cells. Genes Dev. 2003;17:1253–70.
9. Clayton H, Titley I, Vivanco M. Growth and differentiation of progenitor/stem cells derived from the human mammary gland. Exp Cell Res. 2004;297:444–60.
10. Al-Hajj M, Wicha MS, Benito-Hernandez A, Morrison SJ, Clarke MF. Prospective identification of tumorigenic breast cancer cells. Proc Natl Acad Sci U S A. 2003;100:3983–8.
11. Alvi AJ, Clayton H, Joshi C, Enver T, Ashworth A, Vivanco M, et al. Functional and molecular characterisation of mammary side population cells. Breast Cancer Res. 2003;5:R1–8.
12. Ginestier C, Hur MH, Charafe-Jauffret E, Monville F, Dutcher J, Brown M, et al. ALDH1 is a marker of normal and malignant human mammary stem cells and a predictor of poor clinical outcome. Cell Stem Cell. 2007;1:555–67.
13. Simões BM, Piva M, Iriondo O, Comaills V, López-Ruiz JA, Zabalza I, et al. Effects of estrogen on the proportion of stem cells in the breast. Breast Cancer Res Treat. 2011;129:23–35.
14. Gonzalez E, Piva M, Rodriguez-Suarez E, Gil D, Royo F, Elortza F, et al. Human mammospheres secrete hormone-regulated active extracellular vesicles. PLoS One. 2014;9:e83955.
15. Ali S, Coombes RC. Endocrine-responsive breast cancer and strategies for combating resistance. Nat Rev Cancer. 2002;2:101–12.
16. Schiavon G, Smith IE. Endocrine therapy for advanced/metastatic breast cancer. Hematol Oncol Clin North Am. 2013;27:715–36, viii.
17. Johnston SR, Kilburn LS, Ellis P, Dodwell D, Cameron D, Hayward L, et al. Fulvestrant plus anastrozole or placebo versus exemestane alone after progression on non-steroidal aromatase inhibitors in postmenopausal patients with hormone-receptor-positive locally advanced or metastatic breast cancer (SoFEA): A composite, multicentre, phase 3 randomised trial. Lancet Oncol. 2013;14:989–98.

18. Feng Q, Zhang Z, Shea MJ, Creighton CJ, Coarfa C, Hilsenbeck SG, et al. An epigenomic approach to therapy for tamoxifen-resistant breast cancer. Cell Res. 2014;24:809–19.
19. Malorni L, Biagioni C, Thirlwell J, Guarducci C, Bonechi M, Rukazenkov Y, et al. Efficacy of fulvestrant according to duration and type of adjuvant endocrine treatment, in metastatic breast cancer patients enrolled in the CONFIRM trial. Ann Oncol. 2014;25 Suppl 1:i11.
20. McDermott SP, Wicha MS. Targeting breast cancer stem cells. Mol Oncol. 2010;4:404–19.
21. Liu S, Ginestier C, Charafe-Jauffret E, Foco H, Kleer CG, Merajver SD, et al. BRCA1 regulates human mammary stem/progenitor cell fate. Proc Natl Acad Sci U S A. 2008;105:1680–5.
22. Jeon HM, Sohn YW, Oh SY, Kim SH, Beck S, Kim S, et al. ID4 imparts chemoresistance and cancer stemness to glioma cells by derepressing miR-9*-mediated suppression of SOX2. Cancer Res. 2011;71:3410–21.
23. Jia X, Li X, Xu Y, Zhang S, Mou W, Liu Y, et al. SOX2 promotes tumorigenesis and increases the anti-apoptotic property of human prostate cancer cell. J Mol Cell Biol. 2011;3:230–8.
24. Santini R, Pietrobono S, Pandolfi S, Montagnani V, D'Amico M, Penachioni JY, et al. SOX2 regulates self-renewal and tumorigenicity of human melanoma-initiating cells. Oncogene. 2014;31:0.
25. Ben-Porath I, Thomson MW, Carey VJ, Ge R, Bell GW, Regev A, et al. An embryonic stem cell-like gene expression signature in poorly differentiated aggressive human tumors. Nat Genet. 2008;40:499–507.

nature COMMUNICATIONS

ARTICLE

Received 27 Oct 2015 | Accepted 12 Jul 2016 | Published 24 Aug 2016

DOI: 10.1038/ncomms12595 OPEN

Stratification and therapeutic potential of PML in metastatic breast cancer

Natalia Martín-Martín[1,*], Marco Piva[1,*], Jelena Urosevic[2], Paula Aldaz[3], James D. Sutherland[1], Sonia Fernández-Ruiz[1], Leire Arreal[1], Verónica Torrano[1], Ana R. Cortazar[1], Evarist Planet[4,5], Marc Guiu[2], Nina Radosevic-Robin[6,7], Stephane Garcia[8], Iratxe Macías[1], Fernando Salvador[2], Giacomo Domenici[1], Oscar M. Rueda[9], Amaia Zabala-Letona[1], Amaia Arruabarrena-Aristorena[1], Patricia Zúñiga-García[1], Alfredo Caro-Maldonado[1], Lorea Valcárcel-Jiménez[1], Pilar Sánchez-Mosquera[1], Marta Varela-Rey[1,10], Maria Luz Martínez-Chantar[1,10], Juan Anguita[1,11], Yasir H. Ibrahim[12,13], Maurizio Scaltriti[14], Charles H. Lawrie[3,11], Ana M. Aransay[1,10], Juan L. Iovanna[8], Jose Baselga[15], Carlos Caldas[9], Rosa Barrio[1], Violeta Serra[12], Maria dM Vivanco[1], Ander Matheu[3,11,**], Roger R. Gomis[2,16,**] & Arkaitz Carracedo[1,11,17]

Patient stratification has been instrumental for the success of targeted therapies in breast cancer. However, the molecular basis of metastatic breast cancer and its therapeutic vulnerabilities remain poorly understood. Here we show that PML is a novel target in aggressive breast cancer. The acquisition of aggressiveness and metastatic features in breast tumours is accompanied by the elevated PML expression and enhanced sensitivity to its inhibition. Interestingly, we find that STAT3 is responsible, at least in part, for the transcriptional upregulation of PML in breast cancer. Moreover, PML targeting hampers breast cancer initiation and metastatic seeding. Mechanistically, this biological activity relies on the regulation of the stem cell gene *SOX9* through interaction of PML with its promoter region. Altogether, we identify a novel pathway sustaining breast cancer aggressiveness that can be therapeutically exploited in combination with PML-based stratification.

[1] CIC bioGUNE, Bizkaia Technology Park, Bulding 801a, 48160 Derio, Spain. [2] Oncology Programme, Institute for Research in Biomedicine (IRB-Barcelona), 08028 Barcelona, Spain. [3] Oncology Area, Biodonostia Institute, 20014 San Sebastian, Spain. [4] Biostatistics and Bioinformatics Unit, Institute for Research in Biomedicine (IRB-Barcelona), 08028 Barcelona, Spain. [5] School of Life Sciences, Ecole Polytechnique Fédérale de Lausanne (EPFL), 1015 Lausanne, Switzerland. [6] ERTICa Research Group, University of Auvergne EA4677, Clermont-Ferrand, France. [7] Biodiagnostics Laboratory OncoGenAuvergne, Pathology Unit, Jean Perrin Comprehensive Cancer Center, 63000 Clermont-Ferrand, France. [8] Centre de Recherche en Cancérologie de Marseille (CRCM), INSERM UMR 1068, CNRS UMR 7258, Aix-Marseille University and Institut Paoli-Calmettes, Parc Scientifique et Technologique de Luminy, 13288 Marseille, France. [9] Cancer Research UK Cambridge Institute, University of Cambridge, Li Ka Shing Centre, Robinson Way, Cambridge CB2 0RE, UK. [10] Centro de Investigación Biomédica en Red de Enfermedades Hepáticas y Digestivas (CIBERehd). [11] IKERBASQUE, Basque foundation for science, 48013 Bilbao, Spain. [12] Experimental Therapeutics Group, Vall d'Hebron University Hospital, 08035 Barcelona, Spain. [13] Weill Cornell Medicine, New York 10021, USA. [14] Human Oncology and Pathogenesis Program, Department of Pathology, Memorial Sloan-Kettering Cancer Center, 10065 New York, USA. [15] Human Oncology and Pathogenesis Program, Department of Medicine, Memorial Sloan-Kettering Cancer Center, 10065 New York, USA. [16] Institució Catalana de Recerca i Estudis Avançats (ICREA), 08010 Barcelona, Spain. [17] Biochemistry and Molecular Biology Department, University of the Basque Country (UPV/EHU), 48949 Leioa, Spain. * These authors contributed equally to this work. ** These authors jointly supervised this work. Correspondence and requests for materials should be addressed to A.C. (email: acarracedo@cicbiogune.es).

Patient stratification for cancer therapy is an excellent illustration of precision medicine, and biomarker-based treatment selection has tremendously aided in the success of current cancer therapies[1]. In this sense, the current ability to molecularly define and differentiate breast cancer (BCa) into molecular subtypes[2,3] has allowed the identification of patients at risk of relapse[4] and has led to biomarker signatures used to spare low-risk patients from aggressive chemotherapy[5].

Tumours are heterogeneous entities and most cancers retain a differential fraction of cells with increased self-renewal capability (cancer stem or initiating cells)[6]. Cancer-initiating cells (CICs) exhibit a unique spectrum of biological, biochemical and molecular features that have granted them an important role in disease recurrence and metastatic dissemination in BCa[7,8]. Despite the accepted relevance of CICs in cancer progression, the molecular cues governing their activity and function remain largely unknown. The sex determining region Y Box 9 (SOX9) is a recently described regulator of cell differentiation and self-renewal[9–11] and is found upregulated in BCa[12–14].

The promyelocytic leukaemia (PML) protein negatively regulates survival and proliferation pathways in cancer, functions that have established it as a classical pro-apoptotic and growth inhibitory tumour suppressor[15,16]. PML is the essential component of multi-protein sub-nuclear structures commonly referred to as the PML nuclear bodies. PML multimerizes to function as a scaffold critical for the composition and assembly of the entire complex, a process that is regulated by Small Ubiquitin-like Modifier (SUMO)-mediated modifications and interactions[15,16]. Despite the general perception of being PML a bona fide tumour suppressor in cancer, a series of recent studies have demonstrated that PML exhibits activities in cancer that go far and beyond tumour suppression[17]. The work in chronic myeloid leukaemia has evidenced that PML expression can be promoted in certain cancers, providing a selective advantage to tumour cells[18,19]. Moreover, PML is found upregulated in a subset of BCa[20]. However, to which extent PML targeting could be a valuable therapeutic approach in solid cancers remains obscure.

In this study, we reveal the therapeutic and stratification potential of PML in BCa and the molecular cues, underlying the therapeutic response unleashed by PML inhibition.

Results

PML silencing hampers BCa-initiating cell capacity. The elevated expression of PML in a subset of BCa[17,20] strongly suggests that it could represent an attractive target for therapy. To ascertain the molecular and biological processes controlled by PML in BCa, we carried out short hairpin RNA (shRNA) lentiviral delivery-mediated *PML* silencing in different cellular systems. Four constitutively expressed shRNAs exhibited activity against *PML* (Fig. 1a; Supplementary Fig. 1a–d). *PML* knockdown elicited a potent reduction in the number of ALDH1-positive cells and in oncosphere formation (OS, readout of self-renewal potential[7,21]), in up to three PML-high-expressing basal-like BCa (BT549 and MDA-MB-231) or immortalized (HBL100) cell lines tested (Fig. 1b–d; Supplementary Fig. 1e–g). This phenotype was recapitulated with a doxycycline-inducible lentiviral shRNA system targeting *PML* (sh4; Fig. 1e,f; Supplementary Fig. 1h).

Self-renewal capacity is a core feature of CICs[7]. On the basis of this notion, we hypothesized that PML could regulate tumour initiation in BCa. We performed tumour formation assays in immunocompromised mice, using MDA-MB-231 cells (PML-high-expressing triple-negative breast cancer (TNBC)) transduced with non-targeting (shRNA Scramble: shC) or *PML*-targeting shRNAs. *PML* silencing exhibited a profound defect in tumour formation capacity, resulting in a decrease in the frequency of tumour-initiating cells from 1/218 (shC) to 1/825 (sh5) and completely abolished (1/infinite) in sh4 (Fig. 1g; Supplementary Fig. 1i).

To extrapolate these observations to the complexity of human BCa, we characterized a series of patient-derived xenografts (PDXs; Table 1; Supplementary Fig. 1j). The distribution of PML expression in the different subtypes of engrafted tumours was reminiscent of patient data, with a higher proportion of PML-high-expressing tumours in basal-like/triple-negative subtype[20]. Taking advantage of the establishment of a PML-high-expressing PDX-derived cell line (PDX44), we sought to corroborate the results obtained in the PML-high-expressing cell lines. As with MDA-MB-231 cells, *PML* silencing was effective in the PDX44-derived cell line (Fig. 1h) and resulted in a significant decrease in OS formation (Fig. 1i). *In vivo*, *PML* silencing decreased tumour-forming capacity of PDX44 cells (tumour-initiating cell frequency was estimated of 1/39.6 in shC, 1/100 in sh5 and 1/185 in sh4; Fig. 1j; Supplementary Fig. 1k).

These data demonstrate that PML expression is required for BCa-initiating cell function in TNBC cells.

PML sustains metastatic potential in BCa. CIC activity is associated with tumour initiation and recurrence[7,22]. We have previously shown that PML expression is associated to early recurrence[20], which we validated in an independent data set[23] (Supplementary Fig. 2a). The development of metastatic lesions is based on the acquisition of novel features by cancer cells[24]. On the basis of our data, we surmised that the activity of PML on CICs could impact on the survival and growth in distant organs. To test this hypothesis, we measured metastasis-free survival (MFS) in two well-annotated large messenger RNA (mRNA) data sets[3,25,26]. First, we evaluated the impact of high *PML* expression in MFS in the MSK/EMC (Memorial Sloan Kettering Cancer Center-Erasmus Medical Center) data set[25,26]. As predicted, *PML* expression above the mean was associated with reduced MFS (Fig. 2a). Second, we validated this observation in the METABRIC data set, focusing on early metastasis (up to 5 years)[3]. On the one hand, we confirmed the MSK/EMC data (Fig. 2b; hazard ratio (HR) = 1.31, log-rank test $P = 0.006$). On the other hand, a Cox continuous model demonstrated an association of PML expression with the increased risk of metastasis (HR = 2.305, $P = 0.002$). Of note, we tested the expression of PML in patients with complete pathological response or residual disease after therapy[27], but could not find a significant association of these parameters in two data sets (Supplementary Fig. 2b).

The molecular alterations associated to metastatic capacity can be studied using BCa cell lines, in which metastatic cell sub-clones have been selected through the sequential enrichment in immunocompromised mice[28]. If PML is a causal event in the acquisition of metastatic capacity, then changes in its expression should be observed in this cellular system. As predicted, PML mRNA and protein expression were elevated in three distinct metastatic sub-clones compared with their parental counterparts[25,26] (Fig. 2c; Supplementary Fig. 2c).

Metastasis surrogate assays provide valuable information about the capacity of cancer cells to home and colonize secondary organs[29]. TNBC cells exhibit metastatic tropism to the lung[30], and the molecular requirements of this process have begun to be clarified through the generation of highly metastatic sub-clones[31]. Our patient analysis suggests that PML expression is favoured in primary tumours, with higher capacity to disseminate. Moreover, cell sub-clone analysis further reveals that PML expression is selected for in the process of metastatic selection. With this data

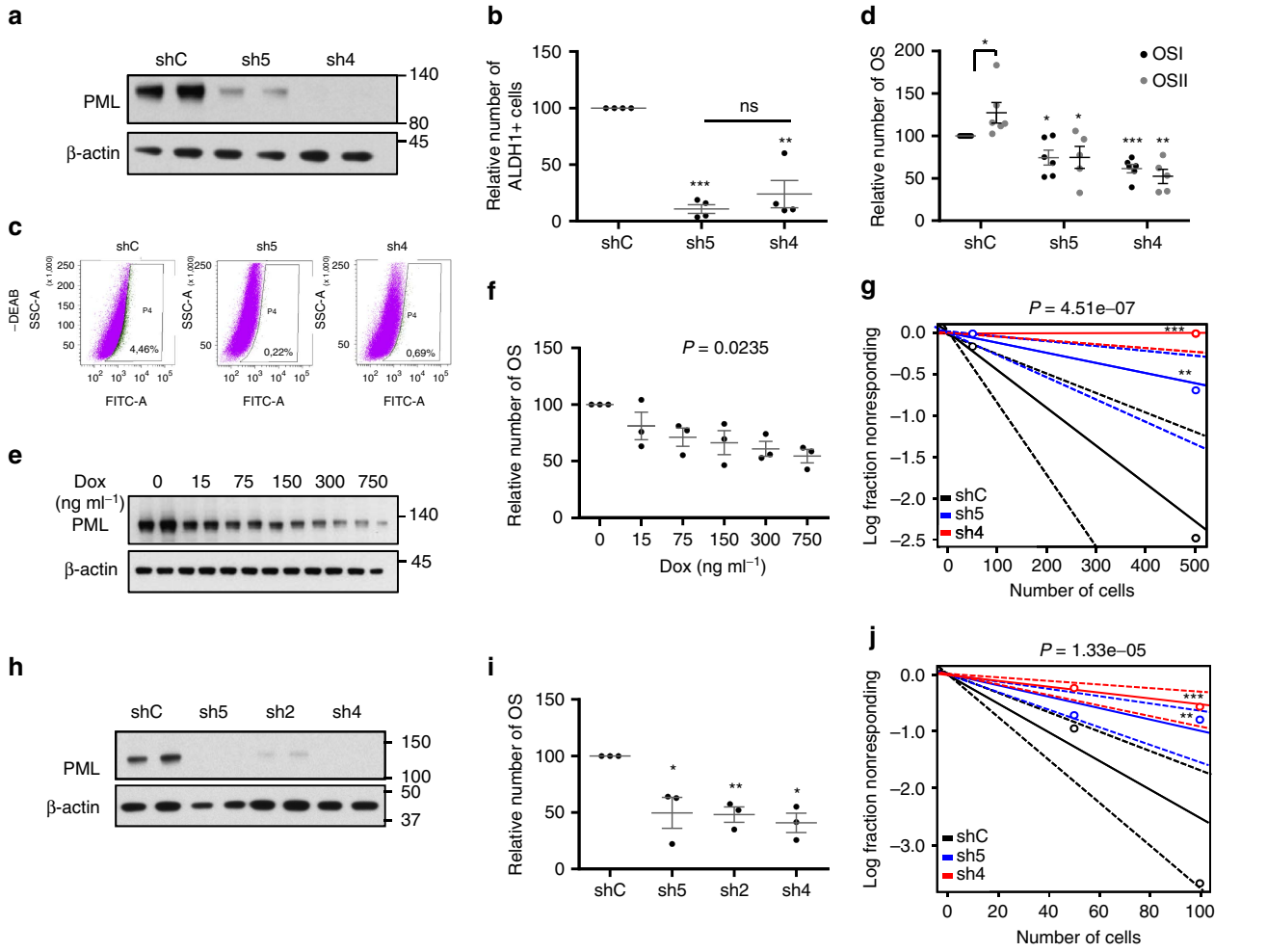

Figure 1 | Genetic targeting of *PML* hampers breast cancer initiation potential. (**a**) PML levels (representative western blot out of four independent experiments) upon *PML* silencing with two shRNAs (sh) in MDA-MB-231 cells. (**b**) Percentage of ALDH1+ cells upon *PML* silencing with two shRNAs in MDA-MB-231 cells ($n=4$). (**c**) Representative flow cytometry analysis out of three independent experiments of the ALDH1+ population in shC or shPML-transduced MDA-MB-231 cells (FITC: fluorescein-isothiocyanate, SSC-A: side-scatter). (**d**) Effect of *PML* silencing on primary (OSI) and secondary (OSII) OS formation in MDA-MB-231 cells ($n=5$ for OSII in shPML cells and $n=6$ for shC and OSI in shPML cells). (**e**,**f**) PML levels (representative western blot out of three independent experiments) (**e**) and OS formation ($n=3$) (**f**) upon *PML* inducible silencing (shPML#4) with the indicated doses of doxycycline in MDA-MB-231 cells. (**g**) Limiting dilution experiment after xenotransplantation. Nude mice were inoculated with 500,000 or 50,000 MDA-MB-231 cells ($n=12$ injections per experimental condition). Tumour-initiating cell number was calculated using the ELDA platform. A log-fraction plot of the limiting dilution model fitted to the data is presented. The slope of the line is the log-active cell fraction (solid lines: mean; dotted lines: 95% confidence interval; circles: values obtained in each cell dilution). (**h**) PML levels (representative western blot out of four independent experiments) upon *PML* silencing in the PDX44-derived cell line. (**i**) OSI formation upon *PML* silencing in PDX44 cells ($n=3$). (**j**) Limiting dilution experiment after xenotransplantation. Nude mice were inoculated either with 100,000 or 10,000 PDX44 cells ($n=20$ injections per experimental condition). Tumour-initiating cell number was calculated using the ELDA platform as in **g**. Error bars represent s.e.m., *P* value (*$P<0.05$; **$P<0.01$; ***$P<0.001$ compared with shC or as indicated). Statistics test: one-tail unpaired *t*-test (**b**,**d**,**i**), analysis of variance (**f**) and χ^2-test (**g**,**j**). dox, doxycycline; OS, oncospheres; shC, Scramble shRNA; sh2, sh4 and sh5, shRNA against *PML*.

in mind, we asked to which extent PML would be responsible for the enhanced metastatic capacity. To address this question, we silenced *PML* in a highly metastatic sub-clone derived from MDA-MB-231 and injected these cells in the tail vein of nude mice. We chose tail vein injection due to the fact that other metastasis models based on the orthotopic implantation of cells in the mammary fat pad[25] are influenced by primary tumour formation, which we reported to be altered by PML (Fig. 1). The reduction of PML was confirmed in the injected cells (Fig. 2d). Strikingly, *PML* silencing led to a significant reduction in lung metastatic foci formation (Fig. 2e). When evaluating the immunoreactivity of PML in the metastatic lesions (Fig. 2e–g), we observed a direct association between PML silencing at the time of injection (Fig. 2d) and the immunoreactivity of PML in metastatic foci (Fig. 2g). We evaluated whether the lack of PML could be limiting metastatic growth capacity by eliciting an apoptotic response, rather than CIC capacity. However, no differential apoptosis was detected by the means of cleaved caspase-3 staining (Supplementary Fig. 2d–e).

These data demonstrate that the genetic targeting of *PML* results in a tumour-suppressive response, characterized by decreased BCa-initiating cell function and consequently, reduced tumour initiation and metastasis.

STAT3 participates in the regulation of PML expression. Our data demonstrate that *PML* is transcriptionally regulated in BCa. *PML* gene expression is regulated upon various external stimuli,

Table 1 | PDX characterization based on BCa subtype (intrinsic subtype is presented in brackets).

PDX	Subtype	PML
31	TNBC (HER2 enriched)	−
102	ER + (basal like)	−
131	ER + (luminal B)	−
156	ER + (basal like)	−
197	TNBC (basal like)	−
4	ER + (luminal B)	+
6	ER + (luminal A)	+
10	HER2 + (HER2 enriched)	+
39	ER + (luminal B)	+
60	ER + (basal like)	+
98	ER + (basal like)	+
136	TNBC (basal like)	+
137	TNBC (basal like)	+
161	ER + (luminal B)	+
93	TNBC (NA)	+ +
179	TNBC (NA)	+ +
44	TNBC (basal like)	+ + +
88	TNBC (basal like)	+ + +
89	TNBC (NA)	+ + +
94	TNBC (basal like)	+ + +
124	TNBC (basal like)	+ + +
127	TNBC (basal like)	+ + +
167	TNBC (basal like)	+ + +

ER, oestrogen receptor; NA, not applicable; TNBC, triple-negative breast cancer.

including type I and II interferons and interleukin 6, which are mediated by interferon regulatory factors and signal transducers and activators of transcription (STATs), respectively[32–35]. Specifically, it has been reported that activated STAT3 but not STAT1 correlates with *PML* mRNA and protein levels in fibroblasts, HeLa and U2OS cell lines[34]. Since, STAT3 is activated in oestrogen receptor (ER)-negative BCa[36], we hypothesized that this transcription factor may be responsible for the transcriptional activation of *PML* in this tumour type. We silenced *STAT3* with two different short hairpins (sh41 and sh43), and showed that this approach led to the decrease in PML protein and gene expression in the different cell lines tested (Fig. 3a; Supplementary Fig. 3a–b). Moreover, pharmacological inhibition of the Janus kinase/signal transducers and activators of transcription (JAK/STAT) pathway at two different levels (SI3-201, an inhibitor of STAT3 phosphorylation and activation; TG1013148, a potent and highly selective ATP-competitive inhibitor of JAK2) decreased PML levels (Fig. 3b,c). In coherence with the activity of PML, genetic and pharmacological inhibition of STAT3 in MDA-MB-231 cells reduced the primary OS formation capacity (Fig. 3d–f). Importantly, *PML* gene expression levels in a cohort of 448 patients (MSK/EMC) correlated with the activity of STAT3, as confirmed with two different STAT3 signatures (Fig. 3g; ref. 37; http://software.broadinstitute.org/gsea/msigdb/cards/V$STAT3_01). In addition, immunohistochemical analysis confirmed an association between the PML immunoreactivity and phosphorylated STAT3 levels in the Marseille cohort (Fig. 3h). Our results provide strong support for the role of STAT3 as an upstream regulator of PML in BCa.

Elevated PML expression predicts response to arsenic trioxide. PML can be pharmacologically inhibited with arsenic trioxide (Trisenox, ATO), which induces SUMO-dependent ubiquitylation and proteasome-mediated degradation of the protein[38,39]. Similar to our results obtained by knocking down *PML* via shRNA, low doses of ATO decreased PML levels and exerted a negative effect on the OS formation capacity both in MDA-MB-231 and PDX44 cells (Fig. 4a,b). Moreover, ATO reduced the tumour formation capacity in a xenograft model derived from MDA-MB-231 cells in full coherence with the genetic approach (tumour-initiating cell frequency was estimated of 1/279 in vehicle and 1/703 in ATO; Fig. 4c; Supplementary Fig. 4a).

We hypothesized that cells with elevated PML would be 'addicted'[40] to the expression of the protein and hence be more sensitive to the action of PML inhibitors. To prove this notion, we studied additional cell lines with high (BT549, HBL100) or low (MCF7, T47D) PML expression. With this approach, we could demonstrate that the effect of *PML* silencing on the OS formation was exquisitely restricted to PML-high-expressing cells (Fig. 4d). This effect was recapitulated with ATO (Fig. 4e), where PML-low cells remained refractory to the drug in terms of the OS formation capacity.

Our results open a new avenue for the treatment of tumours that exhibit elevation in PML expression. *PML* elevation is predominant in ER-negative tumours (Supplementary Fig. 4b), which also present worse prognosis than ER-positive BCa[2,41]. Whereas luminal subtypes present better overall prognosis, there is a subset of patients within this subtype that exhibits aggressive disease[42]. We hypothesized that within this PML-low-expressing subtypes, the worse prognosis subgroup would exhibit increased PML levels. Indeed, MFS analysis within each intrinsic subtype confirmed that ER-positive BCa (luminal A and luminal B) contained a subset of patients with higher *PML* and worse prognosis (Supplementary Fig. 4c–g).

Our results in ER-positive tumours indicate that the PML expression is enriched in patients harbouring tumours of poor prognosis[2,3]. These results are coherent with our data in metastatic clone selection (Fig. 2c), suggesting that the acquisition of aggressive features is accompanied by the elevation of PML expression and 'addiction' to the protein. We therefore sought to study whether metastatic ER-positive cell sub-clones, which present elevated PML expression, would exhibit sensitivity to PML inhibition, in contrast to the parental cells. Indeed, ATO reduced the OS formation selectively in PML-high-expressing metastatic cells derived from MCF7, whereas the parental cells remained refractory to the drug (Fig. 4f,g). Our results strongly suggest that PML elevation in BCa is associated to a dependence on its expression and hence enforces the need for patient stratification based on PML levels before the establishment of PML-directed therapies.

PML regulates BCa-initiating cell function through SOX9. To ascertain the molecular mechanism by which PML regulates BCa-initiating cell function, we first evaluated the expression levels of this gene in a sorted population of ALDH1-positive versus -negative MDA-MB-231 cells (Fig. 5a,b), and in adherent cultures versus OS (CIC-enriched cultures) (Fig. 5c). Strikingly, *PML* expression increased in both experimental approaches (Fig. 5b,c), together with the levels of well-established stem cell regulators (Fig. 5c). On this basis, we hypothesized that PML might control the expression of stem cell factors, as a mean to regulate BCa-initiating cell function. SOX9 is a recently described regulator of cell differentiation and self-renewal[9,10,11] and is upregulated in BCa[12–14]. Constitutive (Fig. 5d; Supplementary Fig. 5a–b) and inducible (Fig. 5e) *PML* silencing exerted an inhibitory effect on SOX9 expression that correlated with the OS formation capacity (Fig. 5f). PML pharmacological inhibition also induced a decrease on SOX9 expression (Fig. 5g; Supplementary Fig. 5c–d). This regulatory activity was corroborated in the PDX44 cell line (Fig. 5h,i; Supplementary Fig. 5e), and in a

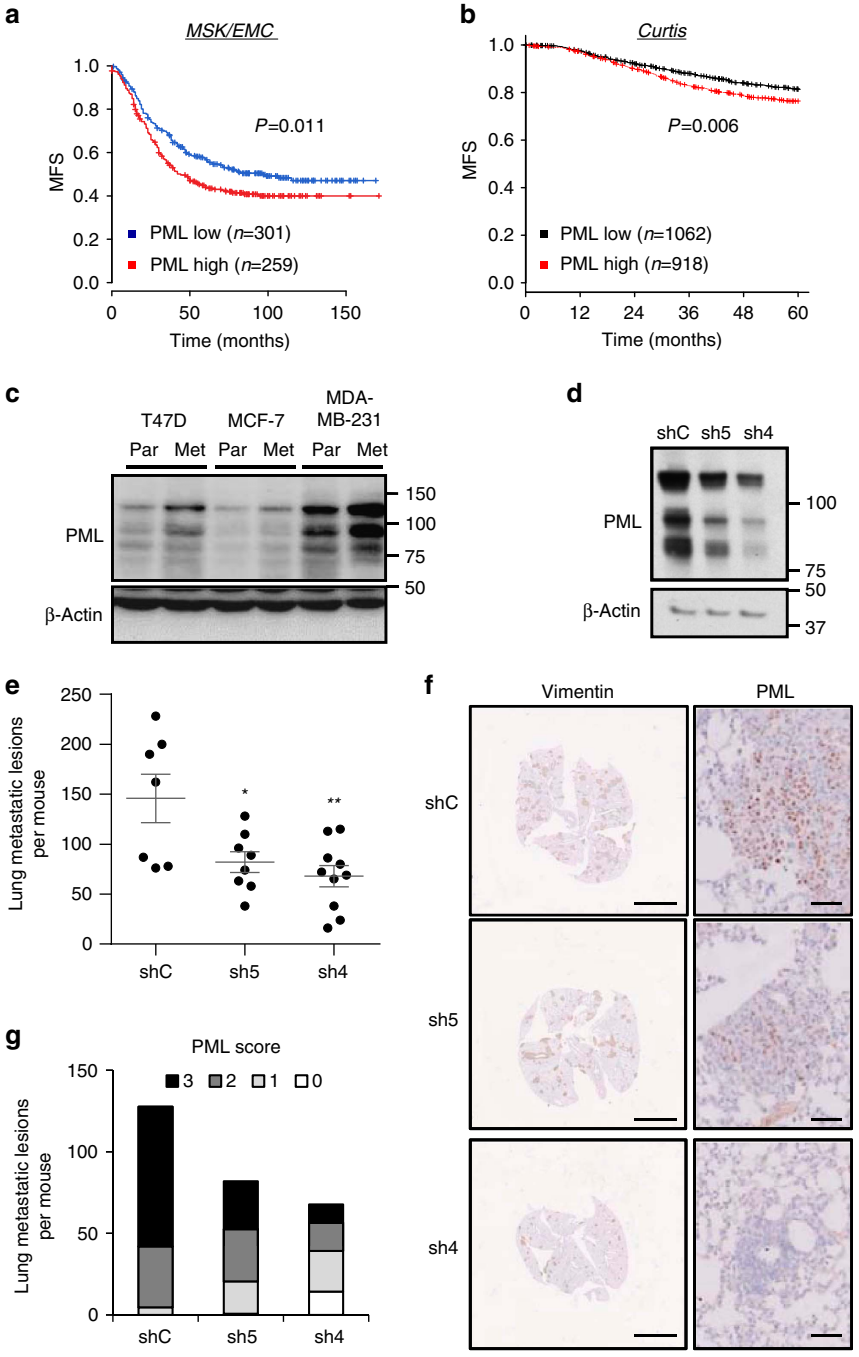

Figure 2 | PML is associated to breast cancer metastatic dissemination. (**a**,**b**) Kaplan–Meier representations of MFS based on *PML* RNA expression. (**a**) MSK/EMC data set, $n=560$. (**b**) Curtis data set (MFS before 60 months), $n=1980$. PML high: above the mean expression; PML low: below the mean expression. (**c**) Representative western blot out of three independent experiments, showing PML protein expression in cell line sub-clones selected for high metastatic potential (Par = parental and Met = metastatic). (**d–g**) Effect of PML silencing on metastatic capacity of intravenously injected metastatic MDA-MB-231 sub-clones ($n=10$ mice per condition): Western blot showing PML silencing in cells at the time of injection (**d**), number of metastatic lesions (**e**), representative immunostaining of Vimentin (scale bar, 3 mm) and PML (scale bar, 50μm) as indicator of metastatic lesions (**f**), and number of metastatic lesions for each PML immunoreactivity score (22 metastatic foci were scored and extrapolated to the number of total metastatic foci in each lung) (**g**). Error bars represent s.e.m., *P* value (*$P<0.05$; **$P<0.01$ compared with shC). Statistical test: Gehan–Breslow–Wilcoxon test (**a**,**b**) and one-tail unpaired *t*-test (**e**). MFS, metastasis-free survival; shC: Scramble shRNA; sh4 and sh5, shRNA against *PML*.

correlative manner in the PDX data set (Fig. 5j), as well as in the aforementioned Marseille data set (Fig. 5k).

We next ascertained the molecular cues regulating *SOX9* expression downstream PML. Since the regulation was observed at the mRNA level, we interrogated *SOX9* promoter *in silico* and in public datasets. The ENCODE project has provided a vast amount of information about regulators and binding sites[43]. *SOX9* promoter exhibited a 2 kb region of acetylated H3K27 (H3K27Ac), which would indicate the proximal regulatory region. To our surprise, we found PML among the 10 proteins with highest confidence DNA-binding score in *SOX9* promoter region (Fig. 5l; cluster score = 527 (refs 44–46)). There is limited

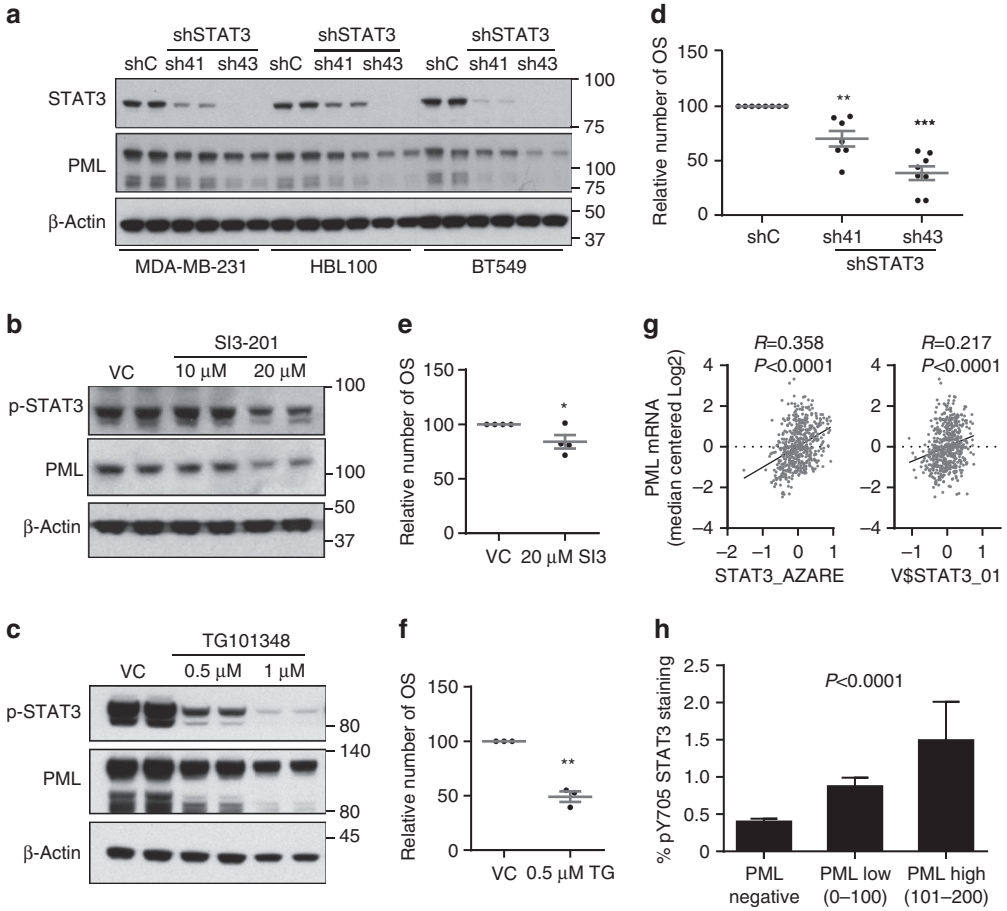

Figure 3 | STAT3 regulates PML expression in breast cancer. (**a**) Representative western blot out of three independent experiments showing STAT3 and PML protein expression upon *STAT3* silencing with two different shRNA (sh41 and sh43). (**b**,**c**) Representative western blot out of three independent experiments, showing STAT3 and PML protein expression upon STAT3 inhibition using SI3-201 (**b**) and TG101314 (**c**) in MDA-MB-231 cells. (**d–f**) Effect of STAT3 inhibition on primary OS formation using sh41 and sh43 against *STAT3* ($n=7$) (**d**), SI3-201 (SI3; $n=4$) (**e**) and TG101314 (TG; $n=3$) (**f**) in MDA-MB-231 cells. (**g**) Correlation of two different STAT3 gene signatures with *PML* gene expression in the MSK/EMC data set. (**h**) Immunoreactivity of pY705 STAT3 protein in patient biopsies with varying expression of PML in the Marseille cohort ($n=737$). Error bars represent s.e.m., *P* value (*$P<0.05$; **$P<0.01$; ***$P<0.001$ compared with shC or VC as indicated). Statistics test: one-tail unpaired *t*-test (**d**,**e**,**f**), Pearson correlation (**g**) and analysis of variance (**h**). OSI, primary oncospheres; shC, Scramble shRNA; sh41 and sh43, shRNA against *STAT3*; VC, vehicle control.

evidence of the capacity of PML to regulate gene expression in concordance with transcription factors through association with DNA[47–49]. We performed chromatin immunoprecipitation (ChIP) analysis of ectopically expressed and endogenous PML, as well as SOX9 expression analysis in these conditions. We confirmed that PML is in close proximity to *SOX9* promoter region and that its ectopic expression upregulates *SOX9* transcript and protein levels (Fig. 5m; Supplementary Fig. 5f–j). It is worth noting that PML does not present a canonical DNA-binding domain, and it is therefore plausible that it lies in close proximity to *SOX9* promoter through the interaction with intermediary DNA-binding proteins.

The regulation of *SOX9* led us to hypothesize that this transcription factor mediated the effects of PML on the regulation of CIC function. On the one hand, we ascertained whether *SOX9* silencing would recapitulate the effects of PML inhibition. We set up two shRNAs targeting *SOX9* (Fig. 6a) that exhibited a potent effect on primary (Fig. 6b) and secondary (Supplementary Fig. 6a) OS formation. Moreover, *SOX9* silencing in MDA-MB-231 cells reduced the tumour formation capacity *in vivo* (tumour-initiating cell frequency was estimated of 1/71.7 in shC, completely abolished (1/infinite) in sh9.1 and 1/4145.5 in sh9.2; Fig. 6c; Supplementary Fig. 6b–c), in agreement with other reports[12].

On the other hand, we evaluated the capacity of ectopically expressed SOX9 to bypass the effects of PML silencing on CIC function. Ectopic SOX9-expressing BCa cells were refractory to *PML* genetic inhibition in terms of the OS formation (Fig. 6d,e) and tumour formation (tumour-initiating cell frequency was estimated of 1/139.8 in shC/Mock, 1/57.5 in shC/SOX9, 1/1506 in sh4/Mock and 1/270.8 in sh4/SOX9; Fig. 6f; Supplementary Fig. 6d). Importantly, the *in vitro* observation was recapitulated in ATO-treated cells (Fig. 6g).

These data reveal a novel molecular mechanism by which PML controls the expression of the stem cell factor SOX9 to regulate BCa-initiating cell function (Fig. 6h). It is worth noting that we found PML at the promoter region of other stem cell genes, such as *LGR5* (Supplementary Fig. 6e–g), indicating that the capacity of this protein to regulate CIC function could involve a larger and more complex transcriptional program.

Discussion

Finding successful targeted treatment strategies for women at risk of metastatic BCa is of outstanding clinical interest. Our data unveil the therapeutic potential of targeting PML in combination

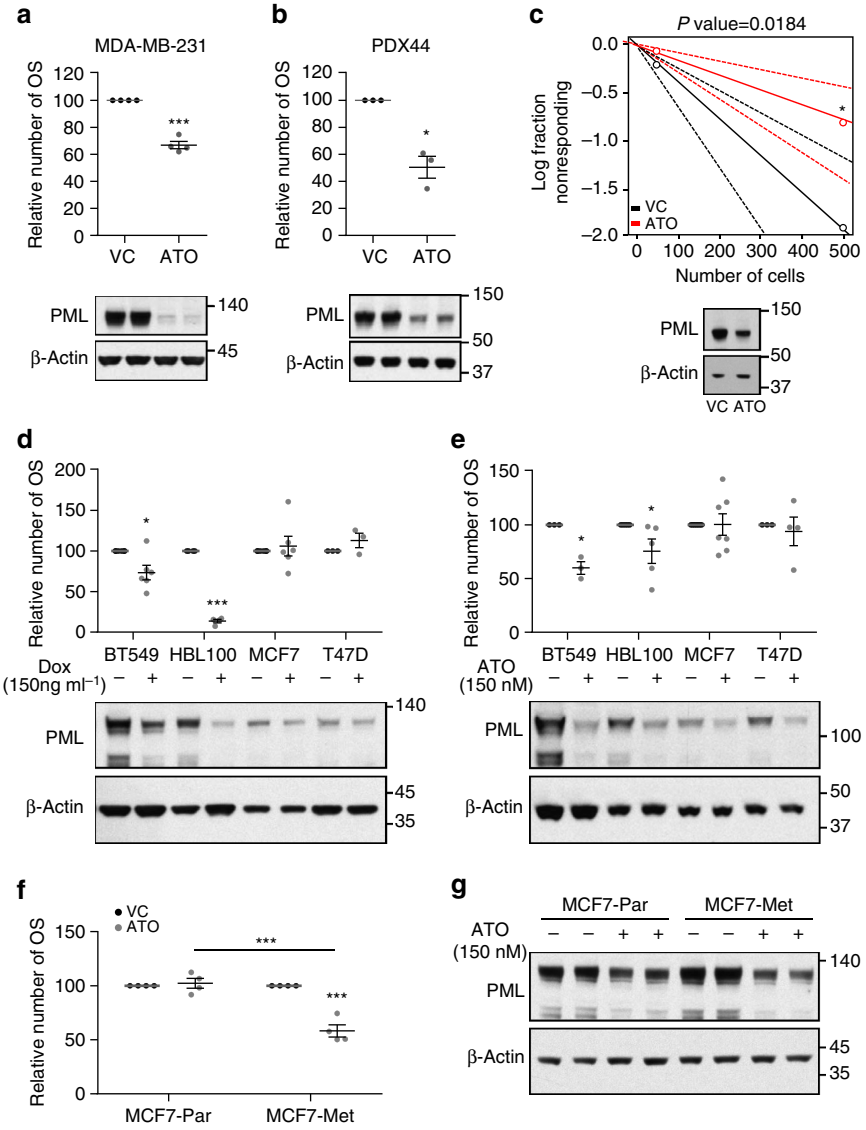

Figure 4 | PML inhibition selectively targets PML-high-expressing breast cancer cells. (**a**,**b**) Effect of 150 nM ATO treatment on OSI formation (top panels) in MDA-MB-231 ($n=4$) (**a**) and PDX44 cells ($n=3$) (**b**) and PML protein expression (3-day treatment, lower panels, representative western blot out of four—MDA-MB-231—or three—PDX44—independent experiments). (**c**) Limiting dilution experiment after xenotransplantation. Nude mice were inoculated with 500,000 or 50,000 MDA-MB-231 cells ($n=20$ injections per experimental condition). ATO cells were pre-treated with 150 nM ATO 2 days before injection. Tumour-initiating cell number was calculated using the ELDA platform. A log-fraction plot of the limiting dilution model fitted to the data is presented. The slope of the line is the log-active cell fraction (solid lines: mean; dotted lines: 95% confidence interval; circles: values obtained in each cell dilution). A PML western blot from cells at the time of injection is presented in lower panel. (**d**,**e**) OSI formation in cell lines with high (BT549 and HBL100) and low (MCF7 and T47D) PML expression upon *PML* genetic silencing (MCF7 and T47D $n=3$, and BT549 and HBL100 $n=6$) (**d**) and 150 nM ATO (BT549 $n=3$, HBL100 $n=5$, MCF7 $n=7$ and T47D $n=4$) (**e**). A representative PML western blot out of three independent experiments is presented in lower panels. (**f**,**g**) Effect of 150 nM ATO on OSI formation ($n=4$) (**f**) and on PML levels (a representative western blot is presented out of four independent experiments) (**g**) in MCF7 parental cells and MCF7 metastatic sub-clone. Error bars represent s.e.m., *P* value (*$P<0.05$; ***$P<0.001$ compared with each control). Statistics test: one-tail unpaired *t*-test (**a**,**b**,**d**,**e**,**f**), χ^2-test (**c**). ATO, arsenic trioxide; Met, metastatic; OSI, primary oncospheres; Par, parental; VC, vehicle control.

with a stratification companion that identifies patients harbouring PML-high-expressing BCa.

We demonstrate that PML targeting impacts on BCa-initiating cell function, and hence on cancer initiation and dissemination. In addition, we observed that PML expression is increased in BCa-initiating cells, highly metastatic sub-clones and in BCa patients at risk of metastasis. These data suggest that, in a subset of BCas, PML sustains the function of BCa-initiating cells and in turn supports the metastatic dissemination capacity[6].

We show that PML-directed therapies are efficient in BCa cells with elevated expression of the protein. Such phenomenon has been defined as 'addiction'[40,50,51], and it represents an exciting avenue in the establishment of novel therapeutic initiatives. Importantly, targeted therapies have been particularly successful when combined with a predictive biomarker. The availability of a clinically validated protocol to detect PML immunoreactivity[52] offers a unique opportunity to define the patients that would benefit from therapies based on PML inhibition. In addition, our

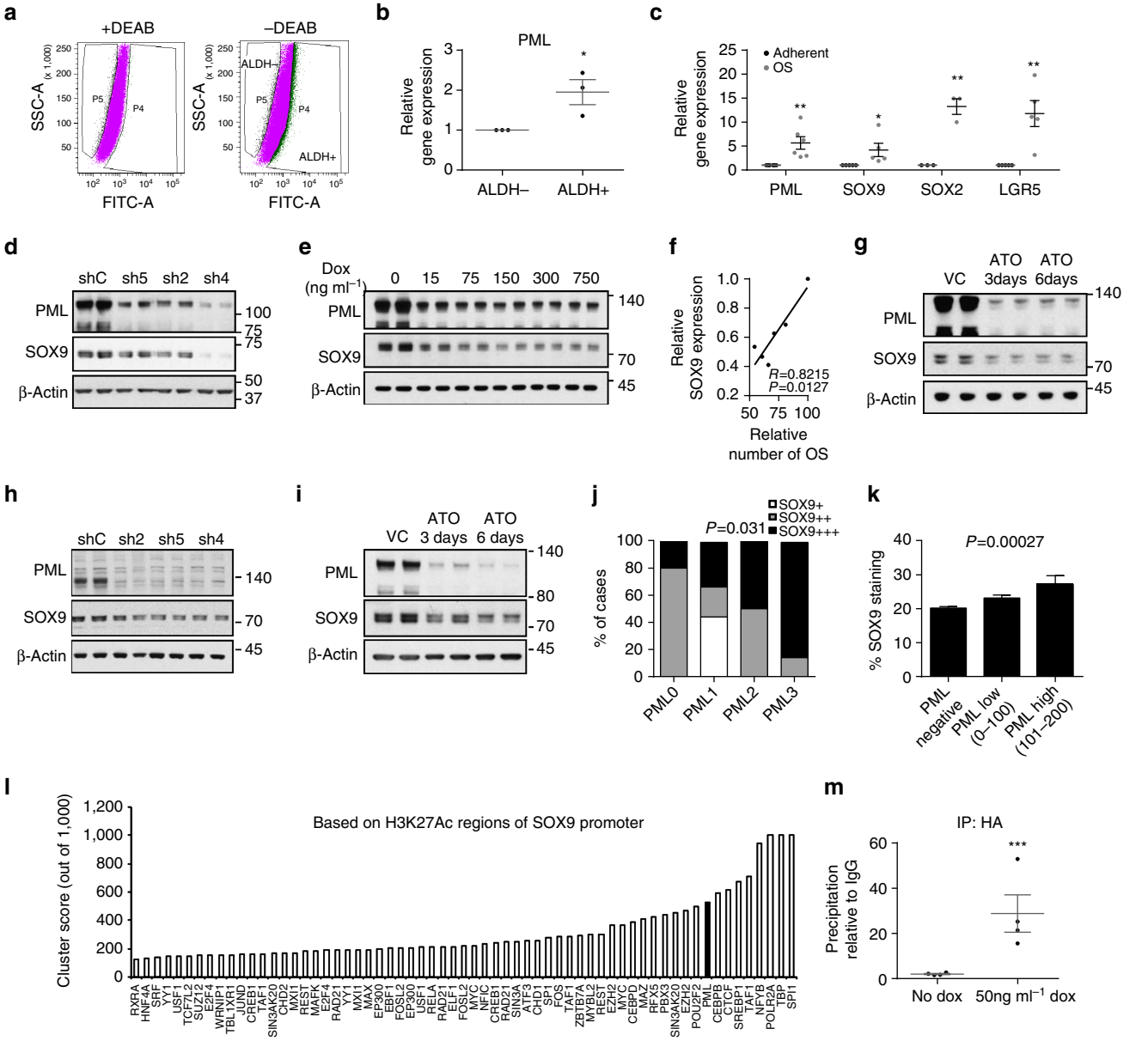

Figure 5 | PML regulates SOX9 expression in breast cancer. (**a**) Flow cytometry analysis of MDA-MB-231 cells based on ALDH1 activity. (**b**) *PML* gene expression in the two populations sorted in a ($n=3$). (**c**) Expression of self-renewal-associated genes in OSI compared with adherent MDA-MB-231 cells (*PML* $n=6$, *SOX9* and *LGR5* $n=5$ and *SOX2* $n=3$). (**d**,**e**) Representative western blot out of four independent experiments depicting the downregulation of SOX9 protein upon constitutive (**d**) and inducible (**e**) *PML* silencing in MDA-MB-231 cells. (**f**) Correlation analysis of SOX9 protein densitometry from (**e**) and OSI formation in MDA-MB-231 cells ($n=3$). (**g**) Representative western blot out of four independent experiments depicting the downregulation of SOX9 protein upon 150 nM ATO treatment in MDA-MB-231 cells. (**h**,**i**) Representative western blot out of three independent experiments depicting the downregulation of SOX9 protein upon *PML* silencing (**h**) and 150 nM ATO treatment (**i**) in PDX44 cells. (**j**) PML and SOX9 immunoreactivity assed by immunohistochemistry in a panel of PDX samples (Table 1). (**k**) SOX9 immunoreactivity in patient biopsies with varying expression of PML in the Marseille cohort ($n=737$). (**l**) Cluster score of DNA-binding proteins in *SOX9* promoter region using ENCODE database. (**m**) SOX9 promoter region abundance in chromatin immunoprecipitation (ChIP) of exogenous HA-PMLIV using HA-tag antibody in MDA-MB-231 cells after induction with 50 ng ml^{-1} doxycycline for 3 days ($n=4$). Data were normalized to IgG (negative-binding control). Error bars represent s.e.m., *P* value (*$P<0.05$, **$P<0.01$, ***$P<0.001$ compared with control). Statistic test: one-tail unpaired *t*-test (**b**,**c**,**m**), Pearson correlation (**f**), χ^2-test (**j**) and analysis of variance (**k**). ATO, arsenic trioxide; DEAB, diethylaminobenzaldehyde; dox, doxycycline; OSI, primary oncospheres; shC, Scramble shRNA; sh2, sh4 and sh5, shRNA against *PML*; VC, vehicle control.

proof-of-concept demonstration of the therapeutic efficacy of PML pharmacological inhibition with ATO indicates that (1) repositioning of ATO (that is currently used in the treatment of acute PML) for BCa therapy is a viable approach, (2) there is strong support for the development of novel and more effective PML inhibitors and (3) the identification of combined therapies with PML inhibitors in BCa is a novel and exciting area of investigation.

Mechanistically, our data demonstrate that PML is in close proximity to the promoter region of *SOX9*, and positively regulates the expression of the gene. SOX9 has been recently established as a central regulator of normal and cancer stem

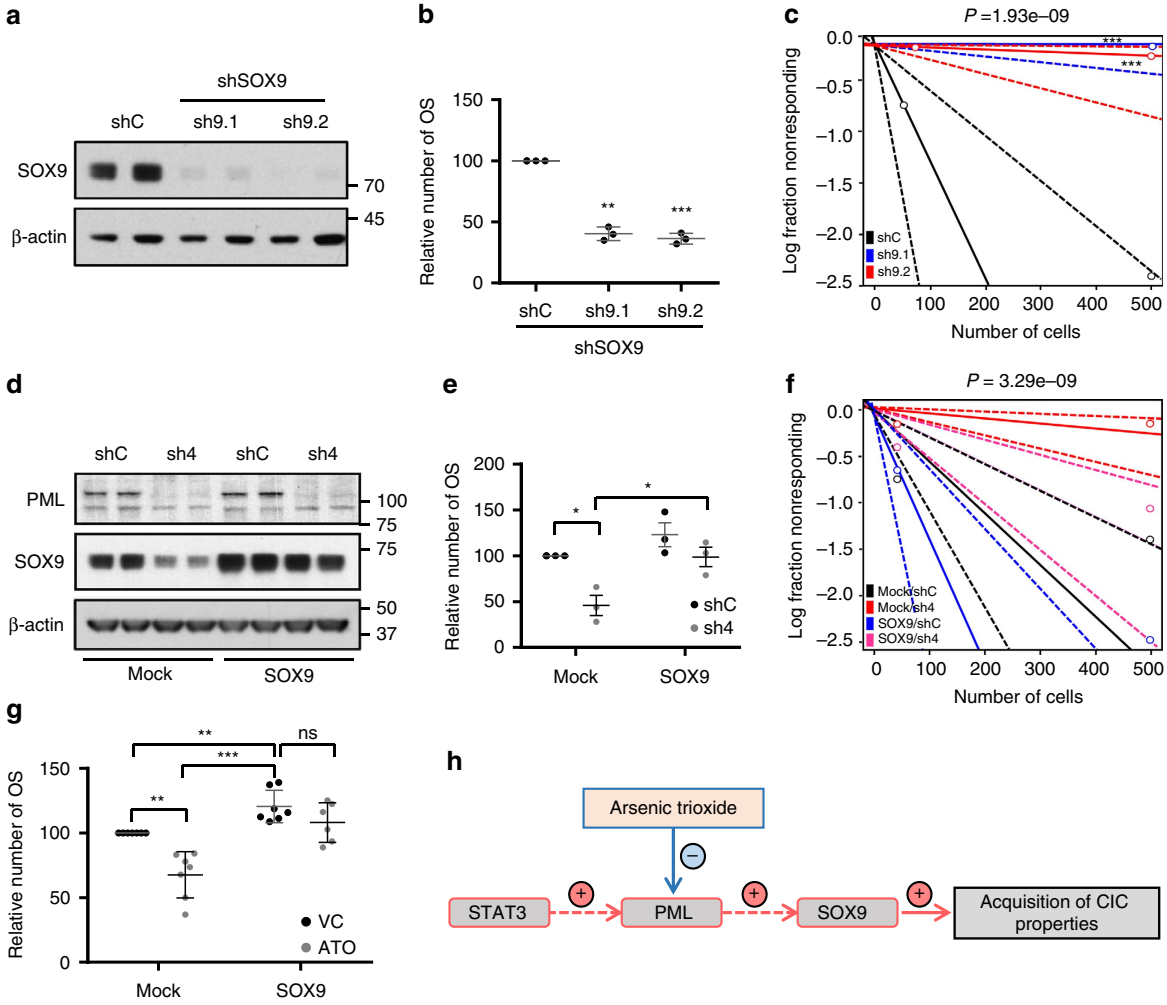

Figure 6 | SOX9 is critical for the regulation of breast cancer-initiating capacity downstream PML. (**a**,**b**) Effect of *SOX9* silencing with two shRNA (sh9.1 and sh9.2) on SOX9 protein expression (representative western blot out of three independent experiments) (**a**) and on OSI formation ($n=3$) (**b**) in MDA-MB-231 cells. (**c**) Limiting dilution experiment after xenotransplantation. Nude mice were inoculated with 500,000 or 50,000 MDA-MB-231 cells ($n=8$ injections per experimental condition). Tumour-initiating cell number was calculated using the ELDA platform. A log-fraction plot of the limiting dilution model fitted to the data is presented. The slope of the line is the log-active cell fraction (solid lines: mean; dotted lines: 95% confidence interval; circles: values obtained in each cell dilution). (**d**,**e**) Effect of ectopic SOX9 expression on the consequences of *PML* silencing. Representative western blot (out of three independent experiments) depicting expression of PML and SOX9 (endogenous and ectopic protein are detected) (**d**) and OSI formation ($n=3$) (**e**) in the different experimental conditions in MDA-MB-231 cells. (**f**) Limiting dilution experiment to assess frequency of tumour-initiating cells after xenotransplantation. Nude mice were inoculated either with 500,000 or 50,000 MDA-MB-231 cells ($n=12$ per experimental condition, except in shC/Mock and sh4/SOX9, $n=16$). Tumour-initiating cell number was calculated using the ELDA platform as in **c**. (**g**) OSI formation in MDA-MB-231 cells transduced with the indicated constructs (mock, *SOX9*) and treated with vehicle or 150 nM ATO ($n=6$). (**h**) Diagram of the molecular mechanism by which PML controls the expression of the stem cell factor SOX9 to regulate BCa-initiating cell function. Error bars represent s.e.m., *P* value (*$P<0.05$; **$P<0.01$; ***$P<0.001$ compared with its control or as indicated). Statistic test: one-tail unpaired *t*-test (**b**,**e**,**g**) and χ^2-test (**c**,**f**). ATO, arsenic trioxide; OSI, primary oncospheres; shC, Scramble shRNA; sh9.1 and sh9.2, shRNA against *SOX9*; sh4, shRNA against *PML*; VC, vehicle control.

cells[9–13,53–61]. This activity is executed in part through the functional interplay with epithelial-to-mesenchymal transition regulators such as SLUG[12,53,56]. In BCa, SOX9 is found overexpressed in the TNBC subtype, and regulates the WNT/beta-catenin pathway[14]. In addition, this transcription factor is a main driver of the transcriptional signature of this subtype of BCa[62]. All these features make SOX9 an ideal target for BCa therapy. However, development of small molecules targeting transcription factors has been an outstanding challenge with limited success[63]. Our data demonstrating that PML sustains SOX9 expression in aggressive BCa opens the possibility to bypass this limitation and inhibit the function of the transcription factor through upstream PML targeting.

In summary, our data provide proof-of-concept demonstration of the fact that PML-inhibiting compounds could exhibit strong potential for BCa therapy upon PML-based stratification.

Methods

Cell culture. MDA-MB-231, BT594, HBL100, MCF7 and T47D cell lines were obtained from the American Type Culture Collection (Manassas, VA, USA) or from Leibniz-Institut—Deutsche Sammlung von Mikroorganismen und Zellkulturen GmbH (DMSZ, Germany), who provided an authentication certificate. None of the cell lines used in this study was found in the database of commonly misidentified cell lines maintained by ICLAC and NCBI biosample. PDX44-derived cell line was generated by Dr Ibrahim and Dr Serra starting from xenograft tumours. Cell lines were routinely monitored for mycoplasma contamination and quarantined, while treated if positive. All cell lines were

maintained in DMEM media supplemented with 10% (v/v) foetal bovine serum and 1% (v/v) penicillin–streptomycin. OS formation assays were carried out as previously described[64]. In brief, single-cell suspensions were plated in six-well tissue culture plates covered with poly-2-hydroxyethyl-methacrylate (Sigma, St Louis, MO) to prevent cell attachment, at a density of 3,000 cells per ml in serum-free DMEM supplemented with 1% penicillin/streptomycin, 1% B27 (Invitrogen, Carlsbad, CA, USA), 10 ng ml^{-1} epidermal growth factor (EGF) (Sigma, St. Louis, MO) and 2 ng ml^{-1} fibroblast Growth Factor, basic (FGFb) (Invitrogen, Carlsbad, CA, USA). After 6 days in culture, OS were counted using a light microscope. For secondary OS formation, following the same protocol, 100,000 cells were plated in 100 mm dishes and collected by gentle centrifugation (200*g*) and dissociated enzymatically (5 min in 1:1 TrypLE solution at 37 °C, Life Technologies, cat: 12604013) and single cells were re-plated at a density of 3,000 cells per ml in six-well tissue culture plates for 6 days.

Generation of stable cell lines. 293FT cells were used for lentiviral production. Lentiviral vectors expressing shRNAs against human *PML*, *STAT3* and *SOX9* from the Mission shRNA Library were purchased from Sigma-Aldrich or Addgene. Cells were transfected with lentiviral vectors following standard procedures, and viral supernatant was used to infect cells. Selection was done using puromycin (2 µg ml^{-1}) for 48 h. As a control, a lentivirus with scrambled shRNA (shC) was used. Short hairpins sequence: sh1PML (TRCN0000003865): CCGGCAATACAA CGACAGCCCAGAACTCGAGTTCTGGGCTGTCGTTGTATTGTTTTT, sh2PML (TRCN0000003865): CCGGCAATACAACGACAGCCCAGAACTC GAGTTCTGGGCTGTCGTTGTATTGTTTTT; sh4PML (TRCN 0000003867): CCGGGCCAGTGTACGCCTTCTCCATCTCGAGATGGAGAAGGCGTACACT GGCTTTTT; sh5PML (TRCN 0000003867): CCGGGTGTACCGGCAGATTGT GGATCTCGAGATCCACAATCTGCCGGTACACTTTTT; shC: CCGGCAACAA GATGAAGAGCACCAACTCGAGTTGGTGCTCTTCATCTTGTTG. sh41STAT3 (TRCN0000020841): CCGGGCTGAAATCATCATGGGCTATCTCGAGATAGC CCATGATGATTTCAGCTTTTT; sh43STAT3 (TRCN0000020843): CCGGGCAA AGAATCACATGCCACTTCTCGAGAAGTGGCATGTGATTCTTTGCTTTTT. sh1SOX9 (Addgene, GenBank ID: RHS3979-9587792; GCATCCTTCAATTTCTG TATA); sh2SOX9 (TRCN0000342824): CCGGCTCCACCTTCACCTACATGAAC TCGAGTTCATGTAGGTGAAGGTGGAGTTTTTG. Sub-cloning of shC and sh4PML into pLKO-Tet-On vector was done introducing AgeI and EcoRI in the 5′-end of top and bottom shRNA oligos, respectively (following the strategy provided by Dr Dmitri Wiederschain[65], Addgene plasmid: 21915). HA-PMLIV was sub-cloned into a TRIPZ vector using Age1–Mlu1 sites.

Immunoassays. Western blot analysis was carried out as previously described[20]. Uncropped scans are provided as part of the Supplementary Information (Supplementary Fig. 7). In brief, cells were seeded on six-well plates and 4 days (unless otherwise specified) after seeding cell lysates were prepared with RIPA buffer (50 mM TrisHCl pH 7.5, 150 mM NaCl, 1 mM EDTA, 0.1% SDS, 1% Nonidet P40, 1% sodium deoxycholate, 1 mM sodium fluoride, 1 mM sodium orthovanadate, 1 mM beta-glycerophosphate and protease inhibitor cocktail; Roche). The following antibodies were used for western blotting: rabbit polyclonal anti-PML, 1:1,000 dilution (cat: A301-167A; Bethyl laboratories), rabbit polyclonal anti-phospho-STAT3 (Tyr705) 1:1,000 dilution and total STAT3 1:1,000 dilution (cat: 9145, 9132 respectively; Cell Signaling), rabbit polyclonal anti-SOX9 1:2,000 dilution (cat: AB5535; CHEMICON International), HA-Tag polyclonal antibody 1:2,000 dilution (cat: C29F4, Cell Signaling Technology, Inc) and mouse monoclonal anti-beta-ACTIN 1:2,000 dilution (clone: AC-74, catalogue: A5316, Sigma-Aldrich). After standard SDS–polyacrylamide gel electrophoresis and western blotting techniques, proteins were visualized using the enhanced chemiluminescence (ECL) system.

For immunofluorescence, cells were seeded on glass cover slips in 24-well plates and 4 days after seeding, cells were fixed with 4% paraformaldehyde (15 min), PBS (three times wash), 1% Triton X-100 (5 min), PBS (three times wash), 10% goat serum (1 h) and anti-PML antibody 1:100 ditution (catalogue A301-167A; Bethyl laboratories) was added overnight (4°C) in goat serum. Cover slips were washed with PBS three times and incubated with secondary antibody (anti-rabbit Alexa488; Invitrogen-Molecular Probes) for 1 h (room temperature). Cover slips were washed with PBS three times, and 4,6-diamidino-2-phenylindole added to stain nuclei (10 min), followed by mounting with Mowiol. Immunofluorescence images were obtained with an AxioImager D1 microscope.

For immunohistochemistry, tissues were fixed in 10% neutral-buffered formalin and embedded in paraffin according to standard procedures. Three to four µm-thick sections were stained for PML (clone PG-M3 Santa Cruz Biotechnology Inc, sc-966, 1:200 dilution), and vimentin (1:1,000, NCL-L-VIM-V9, Novocastra). Antigen retrieval was performed with citrate buffer (pH 6). Detection was performed with the ABC Kit from Vector Laboratories and 3,3′-diaminobenzidine (DAB)-based development. Sections were counterstained with haematoxylin. The PML general immunoreactivity scoring system (used in Fig. 1h) is described in ref. 20. For the Marseille data set, PML (1:200), SOX9 (1:400, Millipore) and phospho-STAT3 (Tyr705) (1:100, Cell Signalling: M9C6) immunostaining was performed as reported[11,20]. The percentage of PML-high (Ph) and -low (Pl) immunoreactive tumour cells in the Marseille data set was quantified separately and the *h*-score was calculated, attributing a relative value of 1 × to Pl and 2 × to Ph intensity nuclear signal ($h = (1 \times \mathrm{Pl}) + (2 \times \mathrm{Ph})$). For SOX9 automated quantification and construction of tissue microarrays (TMAs) in the Marseille data set was carried out as reported[23]. In brief, cores were punched from the selected paraffin blocks, and distributed in new blocks including two cores of 0.6 mm diameter for each tumour. All the TMA blocks were stored at 4 °C. TMA serial tissue sections were prepared 24 h before immunohistochemistry processing and stored at 4 °C. The immunoperoxidase procedures were performed using an automated Ventana Benchmark XT auto-stainer. This device allowed identical well-controlled procedures for antigen retrieval and Ventana kits.

Quantitative real-time PCR. Cells were seeded as for western blot. Total RNA was extracted from cells using NucleoSpin RNA isolation kit from Macherey-Nagel (ref: 740955.240C). Complementary DNA was produced from 1 µg of RNA using qScript cDNA SuperMixt (Quanta Bioscience, ref: 95048). Taqman probes were obtained from Applied Biosystems. Amplifications were run in a Viia7 Real-Time PCR System (Applied Biosystems) using the following probes: *PML* (Hs00971694_m1, cat: 4331182) and *SOX9* (Hs01001343_g1, cat: 4331182). For *STAT3*, *SOX2* and *LGR5* amplification, Universal Probe Library (Roche) primers and probes were employed (*STAT3*, For: cccttggattgagagtcaaga, Rev: aagcggctatac tgctggtc; probe: 14; *SOX2*, For: gggggaatggaccttgtatag, Rev: gcaaagctcctaccgtacca; probe: 65; *LGR5*, For: accagactatgcctttggaaac, Rev: ttcccagggagtggattctat; probe: 78). *ß-actin* (Hs99999903_m1, cat: 4331182) and *GAPDH* (Hs02758991_g1, cat: 4331182) housekeeping assays from Applied Biosystems showed similar results (all quantitative PCR with reverse transcription data presented were normalized using *GAPDH*).

ALDH1 activity by FACS. To measure the ALDH1 activity present in the cells, the ALDEFLUOR assay was carried out according to manufacturer's (Stemcell Technologies) guidelines. In brief, dissociated MDA-MB-231 cells were resuspended in ALDEFLUOR assay buffer at a final concentration of 1.10^{6} ml^{-1}. ALDH substrate, bodipyaminoacetaldehyde was added to the cells at a final concentration of 1.5 mM. Immediately, half of the cells were transferred to an Eppendorf tube containing a two fold molar excess of the ALDH inhibitor, diethylaminobenzaldehyde. Both tubes were incubated for 45 min at 37 °C, and after this incubation cells were centrifuged at 250*g* for 5 min at 4 °C and resuspended in ice-cold ALDEFLUOR assay buffer. Cells were analysed using a FACSAria1 (Becton Dickinson) flow cytometer. DRAQ7 (BiostatuS) was added prior analysis to each tube for dead cell exclusion. FACSAria1 was also used for sorting cells. Data were analysed using the FACSDiva software.

Reagents. For *in vitro* experiments, SI3-201 (Sigma-Aldrich, SML0330) was prepared at 10 mg ml^{-1} in dimethylsulfoxide and used at the indicated concentrations. TG101348 (Santa Cruz, sc-364740) was prepared 100 mg ml^{-1} in dimethylsulfoxide and used at the indicated concentrations. ATO (Sigma-Aldrich) was prepared at a concentration of 100 mM in NaOH 1 N and subsequently diluted to 0.1 mM in PBS for a 1,000 × working solution. ATO was used at 150 nM either 3 or 6 days as indicated in figure legends. For *in vivo* experiments a dose of 5 mg kg^{-1} per day was intraperitoneally administered.

Mice. Xenograft experiments were carried out following the ethical guidelines established by the Biosafety and Welfare Committee at CIC bioGUNE and Biodonostia Institute. The procedures employed were carried out following the recommendations from AAALAC. Xenograft experiments were performed as previously described[66], injecting either 5.10^{5} or 5.10^{4} cells per condition (unless otherwise specified), four injections per mouse. Metastasis experiment was approved by the institutional animal care and use committee of IRB-Barcelona. For tail vein injections, cells were resuspended in PBS and injected into tail vein of mice using a 26 G needle (1.2 × 10^{5} cells per mouse), as previously described[25]. Cell lung colonization capacity was scored 21 days post inoculation by human vimentin. PML expression was scored as undetectable (PML 0) and detectable (PML 1+, 2+ and 3+). All mice (female Hsd:Athymic Nude-Foxn1 nu/nu) were inoculated at 8–12 weeks of age.

ChIP. ChIP was performed using the SimpleChIP Enzymatic Chromatin IP Kit (cat: 9003, Cell Signaling Technology, Inc). MDA-MB-231 cells were grown in 150 mm dishes either with or without 50 ng ml^{-1} doxycycline during 3 days. Cells from three 150 mm dishes (2.5 × 10^{7} cells) were cross-linked with 35% formaldehyde for 10 min at room temperature. Glycine was added to dishes, and cells incubated for 5 min at room temperature. Cells were then washed twice with ice-cold PBS, and scraped into PBS + PMSF. Pelleted cells were lysed and nuclei were collected following manufacturer's instructions. Nuclear lysates were digested with micrococcal nuclease for 20 min at 37 °C and then sonicated in 500 µl aliquots on ice for three pulses of 15 s using a Branson sonicator. Cells were held on ice for at least 1 min between sonications. Lysates were clarified at 11,000*g* for 10 min at 4 °C, and chromatin was stored at −80 °C. HA-Tag polyclonal antibody (cat: C29F4, Cell Signaling Technology), rabbit polyclonal anti-PML (cat: A301-167A; Bethyl laboratories) and IgG antibody (cat: 2729, Cell Signaling Technology, Inc), were incubated overnight (4 °C) with rotation and protein G magnetic beads were

incubated 2 h (4 °C). Washes and elution of chromatin were performed following manufacturer's instructions. DNA quantification was carried out using a Viia7 Real-Time PCR System (Applied Biosystems) with SybrGreen reagents and primers that amplify the predicted PML binding region to *SOX9* promoter (chr17:70117013-70117409) as follows: left primer: ccggaaacttttctttgcag and right primer: cggcgagcacttaggaag.

Patient data sets, bioinformatics and statistical analysis. All studies involving human subjects were approved by the corresponding committees with informed consent as stated in the original publications[3,23,25]. The use of MSK/EMC and Marseille cohorts were previously described[23,25]. For MSK/EMC, MFS curves were plotted using Kaplan–Meier estimates and compared using the Gehan–Breslow–Wilcoxon test. Two groups were compared using mean *PML* expression values as the cutoff between PML high and low. Kaplan–Meier survival and correlation analysis in patient samples: publicly available and clinically annotated BCa cohorts with gene expression profiles (GSE2603, GSE2034, GSE5327 and GSE12276) were pooled as described above. To remove systematic biases, before merging the expression measurements were converted to *z* scores for all genes. For intrinsic subtype classification, we carried out the following analysis: for luminal genes, *ESR1* and *PGR1* presented a bimodal distribution. We used package mclust to fit a mixture of normal distributions with two components and obtain the posterior probability that each patient belongs to the luminal low and luminal high components. A patient was considered luminal low if the posterior probability of belonging to this group was $>80\%$. The same criterion was used for luminal high. When a patient was neither luminal high nor luminal low, it was considered luminal intermediate. Proliferation status (Prol) and *ERBB2* expression did not present a bimodal distribution. Therefore, half of the patients with lowest mean values were considered proliferation low. The rest were considered proliferation high. After defining high and low populations for each parameter, the subtypes were constructed as follows: luminal A: Prol low, *ESR1* intermediate or high, luminal intermediate or high; luminal B: Prol high, *ESR1* intermediate or high, luminal intermediate or high; *HER2* enriched: Prol high, *ESR1* intermediate or low, luminal intermediate or low; *ERBB2* high; basal like: Prol high, *ESR1* low, luminal low; *ERBB2* low, *PGR1* low. Sixty-four patients could not be assigned to any subtype according to PAM50's classification. A Cox proportional hazards model was fitted to compute HR. Likelihood ratio tests were performed to compute *P* values. The HR was checked for constancy over time, fulfilling Cox model assumptions.

For Curtis data set patients, RNA was extracted from 1,980 tumours as described[3]. RNA hybridizations were performed using Illumina HT-12 v3 platform and analysed using the bioconductor bead array package[67]. The BASH algorithm[68] was applied to correct for spatial artefacts in the arrays. Bead-level data were summarized and re-annotated as described in ref. 3. Log-intensity values for *PML* expression were scaled to *z* scores. Probe selection was performed on the basis of probe quality, 3′-position, no other genomic matches and no single-nucleotide polymorphisms in the region. On the basis of these criteria, PML probe ILMN_1731299 was selected for analysis. Survival analysis was done using as endpoints MFS at 5 years (distant metastasis as event). Two groups were compared using mean *PML* expression values as the cutoff between PML high and low. We used the log-rank test as implemented in the survival R package[69].

For therapy response analysis, publicly available data sets (GSE22093 and GSE23988) were downloaded from Gene Expression Omnibus (GEO), and subjected to background correction, $\log_2$ transformation and quartile normalization.

For correlation analysis with *STAT3* signatures, gene sets were extracted (ref. 37, and http://software.broadinstitute.org/gsea/msigdb/cards/V$STAT3_01) and average signal value in the MSK/EMC data set was calculated. These values were used to perform the correlation analysis with PML signal values (Pearson correlation).

No statistics were applied to determine sample size. The experiments were not randomized. The investigators were not blinded to allocation during experiments and outcome assessment. Data analysed by parametric tests are represented by the mean ± s.e.m. of pooled experiments unless otherwise stated. *n* values represent the number of independent experiments performed or the number of individual mice or patient specimens. For each independent *in vitro* experiment, at least three technical replicates were used and a minimum number of three experiments were performed to ensure adequate statistical power. Analysis of variance test was used for multi-component comparisons and Student's *t*-test for two-component comparisons. In the *in vitro* experiments, normal distribution was confirmed or assumed (for $n<5$) and Student's *t*-test was applied for two-component comparisons. Two-tailed statistical analysis was applied for experimental design without predicted result, and one tail for validation or hypothesis-driven experiments. The confidence level used for all the statistical analyses was of 0.95 (alpha value = 0.05). Tumour-initiating cell frequency was estimated using ELDA software as previously described[70].

Data availability. Data from public repositories analysed throughout this manuscript (see the 'Patient data sets, bioinformatics and statistical analysis' section) is available as indicated in the referenced publications.

References

1. Haber, D. A., Gray, N. S. & Baselga, J. The evolving war on cancer. *Cell* **145,** 19–24 (2011).
2. Sorlie, T. *et al.* Gene expression patterns of breast carcinomas distinguish tumor subclasses with clinical implications. *Proc. Natl Acad. Sci. USA* **98,** 10869–10874 (2001).
3. Curtis, C. *et al.* The genomic and transcriptomic architecture of 2,000 breast tumours reveals novel subgroups. *Nature* **486,** 346–352 (2012).
4. Normanno, N. *et al.* Prognostic applications of gene expression signatures in breast cancer. *Oncology (Williston Park)* **77**(Suppl 1): 2–8 (2009).
5. van de Vijver, M. J. *et al.* A gene-expression signature as a predictor of survival in breast cancer. *N. Engl. J. Med.* **347,** 1999–2009 (2002).
6. Stingl, J. & Caldas, C. Molecular heterogeneity of breast carcinomas and the cancer stem cell hypothesis. *Nat. Rev. Cancer* **7,** 791–799 (2007).
7. Valent, P. *et al.* Cancer stem cell definitions and terminology: the devil is in the details. *Nat. Rev. Cancer* **12,** 767–775 (2012).
8. Li, F., Tiede, B., Massague, J. & Kang, Y. Beyond tumorigenesis: cancer stem cells in metastasis. *Cell Res.* **17,** 3–14 (2007).
9. Jo, A. *et al.* The versatile functions of Sox9 in development, stem cells, and human diseases. *Genes Dis.* **1,** 149–161 (2014).
10. Larsimont, J. C. *et al.* Sox9 controls self-renewal of oncogene targeted cells and links tumor initiation and invasion. *Cell Stem Cell* **17,** 60–73 (2015).
11. Matheu, A. *et al.* Oncogenicity of the developmental transcription factor Sox9. *Cancer Res.* **72,** 1301–1315 (2012).
12. Guo, W. *et al.* Slug and Sox9 cooperatively determine the mammary stem cell state. *Cell* **148,** 1015–1028 (2012).
13. Malhotra, G. K. *et al.* The role of Sox9 in mouse mammary gland development and maintenance of mammary stem and luminal progenitor cells. *BMC Dev. Biol.* **14,** 47 (2014).
14. Wang, H. *et al.* SOX9 regulates low density lipoprotein receptor-related protein 6 (LRP6) and T-cell factor 4 (TCF4) expression and Wnt/beta-catenin activation in breast cancer. *J. Biol. Chem.* **288,** 6478–6487 (2013).
15. Bernardi, R. & Pandolfi, P. P. Structure, dynamics and functions of promyelocytic leukaemia nuclear bodies. *Nat. Rev. Mol. Cell. Biol.* **8,** 1006–1016 (2007).
16. Carracedo, A., Ito, K. & Pandolfi, P. P. The nuclear bodies inside out: PML conquers the cytoplasm. *Curr. Opin. Cell. Biol.* **23,** 360–366 (2011).
17. Martin-Martin, N., Sutherland, J. D. & Carracedo, A. PML: not all about tumor suppression. *Front. Oncol.* **3,** 200 (2013).
18. Ito, K. *et al.* PML targeting eradicates quiescent leukaemia-initiating cells. *Nature* **453,** 1072–1078 (2008).
19. Ito, K. *et al.* A PML–PPAR-δ pathway for fatty acid oxidation regulates hematopoietic stem cell maintenance. *Nat. Med.* **18,** 1350–1358 (2012).
20. Carracedo, A. *et al.* A metabolic prosurvival role for PML in breast cancer. *J. Clin. Invest.* **122,** 3088–3100 (2012).
21. Li, H. *et al.* Stem cell marker aldehyde dehydrogenase 1 (ALDH1)-expressing cells are enriched in triple-negative breast cancer. *Int. J. Biol. Markers* **28,** e357–e364 (2013).
22. Baccelli, I. & Trumpp, A. The evolving concept of cancer and metastasis stem cells. *J. Cell Biol.* **198,** 281–293 (2012).
23. Charpin, C. *et al.* Validation of an immunohistochemical signature predictive of 8-year outcome for patients with breast carcinoma. *Int. J. Cancer* **131,** E236–E243 (2012).
24. Chiang, A. C. & Massague, J. Molecular basis of metastasis. *N. Engl. J. Med.* **359,** 2814–2823 (2008).
25. Morales, M. *et al.* RARRES3 suppresses breast cancer lung metastasis by regulating adhesion and differentiation. *EMBO Mol. Med.* **6,** 865–881 (2014).
26. Pavlovic, M. *et al.* Enhanced MAF Oncogene Expression and Breast Cancer Bone Metastasis. *J. Natl Cancer Ins.t* **107,** djv256 (2015).
27. Iwamoto, T. *et al.* Gene pathways associated with prognosis and chemotherapy sensitivity in molecular subtypes of breast cancer. *J. Natl Cancer Inst.* **103,** 264–272 (2011).
28. Minn, A. J. *et al.* Genes that mediate breast cancer metastasis to lung. *Nature* **436,** 518–524 (2005).
29. Bos, P. D., Nguyen, D. X. & Massague, J. Modeling metastasis in the mouse. *Curr. Opin. Pharmacol.* **10,** 571–577 (2010).
30. Gupta, G. P. *et al.* ID genes mediate tumor reinitiation during breast cancer lung metastasis. *Proc. Natl Acad. Sci. USA* **104,** 19506–19511 (2007).
31. Bos, P. D. *et al.* Genes that mediate breast cancer metastasis to the brain. *Nature* **459,** 1005–1009 (2009).
32. Dror, N. *et al.* Interferon regulatory factor-8 is indispensable for the expression of promyelocytic leukemia and the formation of nuclear bodies in myeloid cells. *J. Biol. Chem.* **282,** 5633–5640 (2007).

33. Stadler, M. *et al.* Transcriptional induction of the PML growth suppressor gene by interferons is mediated through an ISRE and a GAS element. *Oncogene* **11,** 2565–2573 (1995).
34. Hubackova, S., Krejcikova, K., Bartek, J. & Hodny, Z. Interleukin 6 signaling regulates promyelocytic leukemia protein gene expression in human normal and cancer cells. *J. Biol. Chem.* **287,** 26702–26714 (2012).
35. Lavau, C. *et al.* The acute promyelocytic leukaemia-associated PML gene is induced by interferon. *Oncogene* **11,** 871–876 (1995).
36. Yeh, Y. T. *et al.* STAT3 ser727 phosphorylation and its association with negative estrogen receptor status in breast infiltrating ductal carcinoma. *Int. J. Cancer* **118,** 2943–2947 (2006).
37. Azare, J. *et al.* Constitutively activated Stat3 induces tumorigenesis and enhances cell motility of prostate epithelial cells through integrin beta 6. *Mol. Cell. Biol.* **27,** 4444–4453 (2007).
38. Tatham, M. H. *et al.* RNF4 is a poly-SUMO-specific E3 ubiquitin ligase required for arsenic-induced PML degradation. *Nat. Cell. Biol.* **10,** 538–546 (2008).
39. Lallemand-Breitenbach, V. *et al.* Arsenic degrades PML or PML-RARalpha through a SUMO-triggered RNF4/ubiquitin-mediated pathway. *Nat. Cell. Biol.* **10,** 547–555 (2008).
40. Weinstein, I. B. Cancer. Addiction to oncogenes--the Achilles heal of cancer. *Science* **297,** 63–64 (2002).
41. Perou, C. M., Parker, J. S., Prat, A., Ellis, M. J. & Bernard, P. S. Clinical implementation of the intrinsic subtypes of breast cancer. *Lancet Oncol.* **11,** 718–719 (2010).
42. Perou, C. M. *et al.* Molecular portraits of human breast tumours. *Nature* **406,** 747–752 (2000).
43. Consortium EP. The ENCODE (ENCyclopedia Of DNA Elements) Project. *Science* **306,** 636–640 (2004).
44. Gerstein, M. B. *et al.* Architecture of the human regulatory network derived from ENCODE data. *Nature* **489,** 91–100 (2012).
45. Wang, J. *et al.* Sequence features and chromatin structure around the genomic regions bound by 119 human transcription factors. *Genome Res.* **22,** 1798–1812 (2012).
46. Wang, J. *et al.* Factorbook.org: a Wiki-based database for transcription factor-binding data generated by the ENCODE consortium. *Nucleic Acids Res.* **41,** D171–D176 (2013).
47. Vernier, M. *et al.* Regulation of E2Fs and senescence by PML nuclear bodies. *Genes Dev.* **25,** 41–50 (2011).
48. von Mikecz, A., Zhang, S., Montminy, M., Tan, E. M. & Hemmerich, P. CREB-binding protein (CBP)/p300 and RNA polymerase II colocalize in transcriptionally active domains in the nucleus. *J. Cell Biol.* **150,** 265–273 (2000).
49. Kuo, H. Y. *et al.* PML represses lung cancer metastasis by suppressing the nuclear EGFR-mediated transcriptional activation of MMP2. *Cell Cycle* **13,** 3132–3142 (2014).
50. Weinstein, B. Relevance of the concept of oncogene addiction to hormonal carcinogenesis and molecular targeting in cancer prevention and therapy. *Adv. Exp. Med. Biol.* **617,** 3–13 (2008).
51. Weinstein, I. B. & Joe, A. Oncogene addiction. *Cancer Res.* **68,** 3077–3080 discussion 3080 (2008).
52. Lo-Coco, F. & Ammatuna, E. The biology of acute promyelocytic leukemia and its impact on diagnosis and treatment. *Hematology. Am. Soc. Hematol. Educ. Program* **156-161,** 514 (2006).
53. Fazilaty, H., Gardaneh, M., Akbari, P., Zekri, A. & SLUG, Behnam B. and SOX9 Cooperatively Regulate Tumor Initiating Niche Factors in Breast Cancer. *Cancer Microenviron.* **9,** 71–74 (2016).
54. Hiraoka, K. *et al.* SOX9-mediated upregulation of LGR5 is important for glioblastoma tumorigenicity. *Biochem. Biophys. Res. Commun.* **460,** 216–221 (2015).
55. Hong, Y. *et al.* Upregulation of sex-determining region Y-box 9 (SOX9) promotes cell proliferation and tumorigenicity in esophageal squamous cell carcinoma. *Oncotarget* **6,** 31241–31254 (2015).
56. Luanpitpong, S. *et al.* SLUG is required for SOX9 stabilization and functions to promote cancer stem cells and metastasis in human lung carcinoma. *Oncogene* **35,** 2824–2833 (2016).
57. Roche, K. C. *et al.* SOX9 maintains reserve stem cells and preserves radioresistance in mouse small intestine. *Gastroenterology* **149,** 1553–1563 e1510 (2015).
58. Scott, C. E. *et al.* SOX9 induces and maintains neural stem cells. *Nat. Neurosci.* **13,** 1181–1189 (2010).
59. Furuyama, K. *et al.* Continuous cell supply from a Sox9-expressing progenitor zone in adult liver, exocrine pancreas and intestine. *Nat. Genet.* **43,** 34–41 (2011).
60. Adam, R. C. *et al.* Pioneer factors govern super-enhancer dynamics in stem cell plasticity and lineage choice. *Nature* **521,** 366–370 (2015).
61. Garros-Regulez, L. *et al.* mTOR inhibition decreases SOX2-SOX9 mediated glioma stem cell activity and temozolomide resistance. *Expert. Opin. Ther. Targets* **20,** 393–405 (2016).
62. Willis, S. *et al.* Enriched transcription factor signatures in triple negative breast cancer indicates possible targeted therapies with existing drugs. *Meta Gene* **4,** 129–141 (2015).
63. Johnston, S. J. & Carroll, J. S. Transcription factors and chromatin proteins as therapeutic targets in cancer. *Biochim. Biophys. Acta.* **1855,** 183–192 (2015).
64. Piva, M. *et al.* Sox2 promotes tamoxifen resistance in breast cancer cells. *EMBO Mol. Med.* **6,** 66–79 (2014).
65. Wiederschain, D. *et al.* Single-vector inducible lentiviral RNAi system for oncology target validation. *Cell Cycle* **8,** 498–504 (2009).
66. Carracedo, A. *et al.* Inhibition of mTORC1 leads to MAPK pathway activation through a PI3K-dependent feedback loop in human cancer. *J. Clin. Invest.* **118,** 3065–3074 (2008).
67. Dunning, M. J., Smith, M. L., Ritchie, M. E. & Tavare, S. beadarray: R classes and methods for Illumina bead-based data. *Bioinformatics* **23,** 2183–2184 (2007).
68. Cairns, J. M., Dunning, M. J., Ritchie, M. E., Russell, R. & Lynch, A. G. BASH: a tool for managing BeadArray spatial artefacts. *Bioinformatics* **24,** 2921–2922 (2008).
69. Therneau, T. M. & Grambsch, P. M. *Statistics for Biology and Health* (Springer, 2000).
70. Hu, Y. & Smyth, G. K. ELDA: extreme limiting dilution analysis for comparing depleted and enriched populations in stem cell and other assays. *J. Immunol. Methods* **347,** 70–78 (2009).

Acknowledgements

Apologies to those whose related publications were not cited due to space limitations. We thank Dr Miquel Angel Pujana for insightful discussions, Dr Monika González for technical help, Dr Miriam Rábano for technical help with flow cytometry cell sorting and Dr Aleix Prat for the evaluation of the intrinsic subtypes in PDX. The work of A.C. is supported by the Ramón y Cajal award, the Basque Department of Industry, Tourism and Trade (Etortek), Health (2012111086) and Education (PI2012-03), Marie Curie (277043), Movember Foundation (GAP1), ISCIII (PI10/01484, PI13/00031), FERO (VIII Fellowship) and ERC (336343). N.M.-M. and P.A. are supported by the Spanish Association Against Cancer (AECC), AECC JP Vizcaya and Guipuzcoa, respectively. J.U. and F.S. are Juan de la Cierva Researchers (MINECO). L.A., A.A.-A. and L.V.-J. are supported by the Basque Government of education. M.L.-M.C. acknowledges SAF2014-54658-R and Asociación Española contra el Cancer. R.B. acknowledges Spanish MINECO (BFU2014-52282-P, Consolider BFU2014-57703-REDC), the Departments of Education and Industry of the Basque Government (PI2012/42) and the Bizkaia County. M.S., V.S. and J.B. acknowledge Banco Bilbao Vizcaya Argentaria (BBVA) Foundation (Tumour Biomarker Research Program). M.S. and J.B. are supported by NIH grant P30 CA008748. M.dM.V. is supported by the Institute of Health Carlos III (PI11/02251, PI14/01328) and Basque Government, Health Department (2014111145). A.M. is supported by ISCIII (CP10/00539, PI13/02277) and Marie Curie CIG 2012/712404. V.S. is supported by the SCIII (PI13/01714, CP14/00228), the FERO Foundation and the Catalan Agency AGAUR (2014 SGR 1331). R.R.G. research support is provided by the Spanish Ministry of Science and Innovation grant SAF2013-46196, BBVA Foundation, the Generalitat de Catalunya (2014 SGR 535), Institució Catalana de Recerca i Estudis Avançats, the Spanish Ministerio de Economia y Competitividad (MINECO) and FEDER funds (SAF2013-46196).

Authors contributions

N.M.-M. and M.P. performed all the *in vitro* and *in vivo* experiments, unless specified otherwise. P.A., J.U., M.G., F.S., A.M. and R.R.G. performed or coordinated (A.M. and R.R.G.) *in vivo* tumour formation and metastasis assays. J.D.S. and R.B. generated PML inducible overexpressing and silencing lentiviral vectors. S.F.-R. performed the histochemical stainings and contributed to *in vitro* analyses. L.A. and I.M. contributed to *in vitro* analyses. V.T. contributed to the SOX9 promoter analysis. N.R.-R., S.G. and J.L.I. performed or coordinated (J.L.I.) the immunohistochemical scoring in patient specimens. A.R.C., E.P., O.M.R., A.M.A. and C.C. performed or coordinated (A.M.A. and C.C.) the bioinformatic and biostatistical analysis. G.D. performed ALDH1 analysis. Y.I., M.S., J.B. and V.S. generated the PDX. A.Z.-L., A.A.-A., P.Z., A.C.-M., L.V.-J., P.S.-M., M.V.-R., M.L.-M.C., J.A. and C.H.L. contributed to the experimental design and discussion. M.dM.V., A.M. and R.R.G. contributed to the experimental design, data analysis and discussion. A.C. directed the project, contributed to data analysis and wrote the manuscript.

Additional information

Supplementary Information accompanies this paper at http://www.nature.com/naturecommunications

Competing financial interests: The authors declare no competing financial interests.

Reprints and permission information is available online at http://npg.nature.com/reprintsandpermissions/

How to cite this article: Martín-Martín, N. *et al.* Stratification and therapeutic potential of PML in metastatic breast cancer. *Nat. Commun.* 7:12595 doi: 10.1038/ncomms12595 (2016).